



Neurotrophin Receptor p75 as a target for gene delivery to motor neurons

Kevin Sean Smith

BMSc, BSc (Hons)

A thesis submitted for the degree of
Doctor of Philosophy on September 14, 2015

Centre for Neuroscience
Department of Human Physiology
School of Medicine
Flinders University, South Australia

“I have no special talent. I am only passionately curious”

Albert Einstein (1879-1955)

This thesis is dedicated to the memory of Kevin Charles Smith (1948-2008)

Table of Contents

Chapter 1: Introduction	1
1 Introduction.....	2
1.1 Motor Neurons	2
1.2 Motor Neuron Disease	3
1.3 Genetics in Motor Neuron Disease	6
1.3.1 <i>SOD1</i>	6
1.3.2 <i>TDP-43</i>	8
1.3.3 <i>FUS/TLS</i>	9
1.3.4 <i>C9ORF72</i>	9
1.3.5 <i>Ubiquilin-2</i>	10
1.3.6 <i>Valosin-containing protein</i>	10
1.3.7 <i>Optineurin</i>	11
1.3.8 <i>Other mutant genes</i>	11
1.4 Cellular Pathology	13
1.4.1 <i>Defects in RNA/DNA processing</i>	13
1.4.2 <i>Defects in Proteosomal processing</i>	16
1.4.3 <i>Mitochondrial dysfunction</i>	18
1.4.4 <i>Excitotoxicity</i>	19
1.4.5 <i>Defects in Axonal Transport</i>	20
1.5 Neurotrophins and Neurotrophic Factors	22
1.5.1 <i>Neurotrophins</i>	22
1.5.2 <i>Neurotrophic Factors</i>	23
1.6 Neurotrophin Receptors	27
1.6.1 <i>Tropomyosin receptor kinase</i>	27
1.6.1.1 <i>Structure</i>	27
1.6.1.2 <i>Signalling</i>	28
1.6.2 <i>pan 75 Neurotrophin Receptor (p75NTR)</i>	28
1.6.2.1 <i>Structure</i>	29
1.6.2.2 <i>Signalling</i>	30
1.6.2.3 <i>Expression and disease</i>	36
1.7 Models for Motor Neuron Disease.....	38

1.7.1 NSC-34 cell line	38
1.7.2 E12.5 murine motor neurons	38
1.7.3 Animal models.....	39
1.8 Treatments for Motor Neuron Disease	41
1.9 Gene Therapy	43
1.9.1 Viral gene delivery.....	43
1.9.1.1 Adeno-associated virus (AAV)	45
1.9.1.2 Retrovirus.....	45
1.9.1.3 Adenovirus	46
1.9.2 Non-viral gene delivery.....	47
1.9.2.1 Gene guns.....	47
1.9.2.2 Electroporation	48
1.9.2.3 Pressure	49
1.9.2.4 Lasers and Magnets	49
1.9.2.5 Polycations.....	50
1.9.2.6 Liposomes	53
1.9.2.7 Carbon and silica complexes	54
1.9.2.8 Chitosan	54
1.9.2.9 Toxins	55
1.10 The Immunogene	55
Chapter 2: Materials and Methods	65
2.1 Materials	66
2.1.1 Cell Culture.....	66
2.1.2 Antibodies	67
2.1.3 Immunohistochemistry	67
2.1.4 Immunoporter	67
2.1.5 Plasmid DNA	68
2.2 Methods.....	69
2.2.1 Animals	69
2.2.2 Spinal cord, DRG, eye and mesentery extraction	70
2.2.3 Immunohistochemistry	71
2.2.4 Data Analysis.....	72
2.2.5 Cell culturing	72
2.2.6 Isolation and purification of embryonic motor neurons	73

2.2.7 Immunocytochemistry	78
2.2.8 Purification of antibodies	79
2.2.9 Conjugation of antibodies	79
2.2.10 FACS	80
2.2.11 Immunoporter creation	81
2.2.11.1 BioRad DC-Assay	81
2.2.11.2 TNBS assay	86
2.2.11.3 Preparation of PEI – dissolving and de-protonating PEI.....	86
2.2.11.4 Preparation of PEI-PEG – addition of 12 molecules of PEG to 1 molecule of PEI.....	87
2.2.11.5 Preparation of PEI-PEG-SPDP and mAb-SPDP conjugation	87
2.2.11.6 Purification of MLR2-PEI-PEG immunoporter and desalting	89
2.2.12 Bacterial growth and DNA purification.....	90
2.2.13 Immunogene N/P ratio	91
2.2.14 Gel retardation Assay	92
2.2.15 Neonate injections.....	93
2.2.16 Lipofectamine 2000 methods	93
Chapter 3: Expression levels and targeting of p75NTR positive motor neurons in neonatal mice.....	95
3.1 Introduction.....	96
3.2 Results	99
3.2.1 MLR2 and MLR2-ATTO-488 bind specifically to p75NTR expressing cells	99
3.2.2 Labelled MLR2 is able to bind to p75NTR on neurons of fresh mouse mesentery	100
3.2.3 p75NTR expression in neonatal motor neurons decreases over 7 days and is absent by 14 days	101
3.2.4 MLR2-ATTO-488 is retrogradely transported to motor neurons in the spinal cord of neonatal mice	107
3.2.5 MLR2-ATTO-488 is transported to p75NTR expressing DRG neurons	110
3.3 Discussion.....	113
Chapter 4: Construction of the MLR2-immunogene and its use for <i>in vitro</i> transfection	115
4.1 Introduction.....	116
4.2 Results	119
4.2.1 MLR2 immunogene gel retardation 1	119

4.2.2	<i>Transfection of cell lines (NSC-34 and BSR) with the MLR2 immunogene and PEI polyplexes</i>	121
4.2.3	<i>MLR2 immunogene is able to transfect primary embryonic murine motor neurons</i>	124
4.3	Discussion	130
Chapter 5: Delivery of pDNA to neonatal p75NTR expressing motor neurons via the MLR2 immunogene		133
5.1	Introduction	134
5.2	Results	139
5.2.1	<i>MLR2-PEI-PEG12 immunogene is able to bind pgWiz DNA and tested in vivo</i>	139
5.2.2	<i>MLR2-PEI-PEG12-pVIVO2 immunogene gel retardation</i>	141
5.2.3	<i>MLR2-PEI-PEG12-pVIVO2 immunogene was able to transfect lumbar motor neurons of neonatal mice</i>	141
5.2.4	<i>MLR2-PEI-PEG12-pVIVO2 injected intraperitoneally results in GFP expression at all levels of the spinal cord</i>	144
5.2.5	<i>Motor neurons transfected with GFP delivered by MLR2-PEI-PEG12-pVIVO2 immunogene also express p75NTR</i>	147
5.2.6	<i>GFP expression peaks at 144 hours after injection of MLR2-PEI-PEG12-pVIVO2</i>	147
5.2.7	<i>PEI-PEG12 alone is unable to deliver pDNA to spinal motor neurons</i>	151
5.2.8	<i>Glucose (5%) buffer does not increase transfection efficiency</i>	151
5.2.9	<i>GFP expression was found in Dorsal Root Ganglion Neurons after MLR2-PEI-PEG12-pVIVO2 in vivo injections</i>	154
5.3	Discussion	156
Chapter 6: Characterisation of p75NTR positive motor neurons in SOD1^{G93A} mice		161
6.1	Introduction	162
6.2	Results	166
6.2.1	<i>SOD1^{G93A} mice express p75NTR in lumbar motor neurons</i>	166
6.2.2	<i>Intraperitoneally injected MLR2-ATTO-488 is retrogradely transported to p75NTR positive motor neurons in SOD1^{G93A} mice</i>	166
6.2.3	<i>MLR2-ATTO-488 is transported to p75NTR positive DRG neuronal cell bodies</i>	173
6.2.4	<i>Loss of ChAT positive motor neurons in the lumbar region of SOD1^{G93A} mice</i>	173
6.2.5	<i>Motor neuron number declines to 50% by end stage in SOD1^{G93A} mice</i>	175
6.2.6	<i>The percentage of motor neurons that express p75NTR increases with age in SOD1^{G93A} mice</i>	175
6.2.7	<i>The number of p75NTR positive motor neurons is influenced by total motor neuron number</i>	177

6.2.8 Motor neurons expressing p75NTR are larger than motor neurons that are p75NTR negative	180
6.2.9 p75NTR expressing motor neuron size verified by dual fluorescent channel measurements and retrograde transport in-vivo	183
6.2.10 p75NTR and ATF-3 are rarely co-expressed in SOD1 ^{G93A} motor neurons	183
6.2.11 Cleaved caspase-3 is expressed in a majority of p75NTR positive motor neurons	187
6.2.12 Motor neuron diameter decreases during disease in the SOD1 ^{G93A} mouse	191
6.2.13 Motor neuron area decreases during disease in the SOD1 ^{G93A} mouse	194
6.2.14 Motor neuron diameter and area decline are correlated in SOD1 ^{G93A} mice	196
6.2.15 Frequency distribution of soma area in SOD1 ^{G93A} mice indicates motor neuron shrinkage over time	196
6.2.16 Primary processes on p75NTR positive motor neurons are not affected by age	200
6.3 Discussion.....	203
6.3.1 Targeting of p75NTR positive motor neurons after peripheral injections.....	204
6.3.2 Anti-p75NTR MLR2 is transported to p75NTR positive DRG neurons	205
6.3.3 Neuronal loss and p75NTR expression	206
6.3.4 Motor neurons are larger when they re-express p75NTR	209
6.3.5 p75NTR expressing motor neurons rarely co-express ATF-3, but co-express cleaved caspase-3	210
6.3.6 Motor neurons that are p75NTR negative shrink in size over time in SOD1 ^{G93A} mice	212
Chapter 7: Quantification of the V0_C interneurons.....	215
in SOD1^{G93A} mice	215
7.1 Introduction.....	216
7.2 Results	219
7.2.1 V0 _C interneuron number are decreased in SOD1 ^{G93A} mice.....	219
7.3 Discussion.....	222
Chapter 8: Conclusions and Future Directions.....	224
Chapter 8	225
8.1 Increasing transfection efficiency of the immunogene	226
8.2.1 Changing the cargo carrier	227
8.2.2 Altering the MLR2 antibody.....	228
8.2.3 Changing the antibody for different receptor targets	229
8.3 Potential for Spinal Muscular Atrophy treatment.....	230
8.4 p75NTR short time frame expression	230

8.3 Targeting other cell types that express p75NTR.....	232
8.4 Concluding remarks	233
Appendix.....	236
Appendix I	237
References	240

Table of Tables

Table 1.1- Rare mutations which have been shown to cause, or be involved in, MND.....	12
Table 2.1- Physical attributes of E12.5 murine embryos	72-73
Table 6.1- Counts of MLR2-ATTO-488/p75NTR positive motor neurons in 110d SOD1 ^{G93A} mice.....	170
Table 6.2- Number of ATF3/p75NTR positive motor neurons in SOD1 ^{G93A} mice.....	188
Table 6.3- Number of cleaved caspase 3/p75NTR positive motor neurons in SOD1 ^{G93A} mice	192

Table of Figures

Figure 1.1- Mutations in familial MND	7
Figure 1.2- Cellular Pathology in MND.....	14-15
Figure 1.3- Structure and binding of Trk receptors and p75NTR.....	24-25
Figure 1.4- Signalling of Neurotrophin receptors.....	32-33
Figure 1.5- Mechanism of the Immunogene.....	61-62
Figure 1.6- Overall plan of the Immunogene.....	63-64
Figure 2.1- E12.5 murine embryo.....	74
Figure 2.2- Schematic of polyethylenamine and polyethylene glycol.....	82-83
Figure 2.3- Schematic of Immunoporter synthesis.....	84-85
Figure 3.2.1- Conjugated and unconjugated MLR2 binds specifically to p75NTR expressing cells.....	102
Figure 3.2.2- MLR2-ATTO-488 binds to fresh mouse mesentery tissue.....	103
Figure 3.2.3a- p75NTR expression in PND 1-4 neonatal spinal cords.....	104
Figure 3.2.3b- p75NTR expression in PND 5-7 and PND 14 neonatal spinal cords.....	105
Figure 3.2.4- p75NTR expression does not change in the dorsal horn in PND 1-7 and 14 neonatal lumbar spinal cords.....	106
Figure 3.2.5- Expression of p75NTR in lumbar motor neurons in PND 1-7 and PND 14 neonatal mice.....	108
Figure 3.2.6a- Retrograde transport of MLR2-ATTO-488 to the spinal cord of neonatal mice.....	109
Figure 3.2.6b- Quantification of retrogradely transported MLR2-ATTO-488 to neonatal spinal motor neurons.....	111
Figure 3.2.7- MLR2-ATTO-488 is retrogradely transported to neonatal DRGs.....	112

Figure 4.2.1- MLR2-PEI-PEG12 immunogene is able to bind pDNA and neutralise charge.....	120
Figure 4.2.2a- MLR2 immunogene is able to transfect p75NTR expressing NSC34 cells.....	122
Figure 4.2.2b- The average percentage of NSC34 and BSR cells transfected by the MLR2-PEI-PEG12 immunogene.....	123
Figure 4.2.3- MLR2 immunogene is unable to transfect p75NTR negative BSR cells.....	125
Figure 4.2.4- MLR2 immunogene and PEI polyplexes transfection of embryonic motor neuron mixed cultures.....	126-127
Figure 4.2.5- Anti-GFP antibody detects GFP expressing primary motor neuron cell cultures.....	129
Figure 5.1.1- gWiz GFP Mammalian Expression Vector.....	136
Figure 5.1.2- pVIVO2-GFP/LacZ plasmid.....	137
Figure 5.2.1- MLR2-PEI-PEG12 immunogene is able to bind pgWiz DNA.....	140
Figure 5.2.2- MLR2-PEI-PEG12 immunogene is able to bind pDNA pVIVO2-GFP/LacZ and be charge neutralised at N/P 12.....	142
Figure 5.2.3- MLR2-PEI-PEG12 is able to deliver pDNA to motor neurons in the lumbar region of neonatal mice.....	143
Figure 5.2.4- MLR2-PEI-PEG12 is able to deliver pDNA to motor neurons in the cervical and thoracic spinal regions of neonatal mice.....	145
Figure 5.2.5- Approximately 20% of motor neurons express GFP after immunogene injections.....	146
Figure 5.2.6- MLR2-PEI-PEG12 GFP positive motor neurons are p75NTR positive	148-149
Figure 5.2.7- Motor neuron GFP expression after MLR2 immunogene injection time course.....	150

Figure 5.2.8- PEI-PEG alone is unable to transport pDNA to spinal motor neurons.....	152
Figure 5.2.9- MLR2-PEI-PEG12 buffered with 5% glucose does not increase transfection efficiency.....	153
Figure 5.2.10- GFP expression in MLR2 immunogene injected neonatal mice DRGs.....	155
Figure 6.2.1- p75NTR is expressed in SOD1 ^{G93A} mouse motor neurons, but not B6 controls.....	167
Figure 6.2.2- Fluorescently tagged antibodies are retrogradely transported to spinal motor neurons in SOD1 ^{G93A} mice after intraperitoneal injection.....	169
Figure 6.2.3- Not all MLR2-ATTO-488 positive motor neurons are p75NTR positive and not all p75NTR positive motor neurons show ATTO-488 fluorescence.....	171-172
Figure 6.2.4a- MLR2-ATTO-488 is transported to DRG neurons.....	174
Figure 6.2.4b- MLR2-ATTO-488 is transported to p75NTR+ve DRG neurons.....	174
Figure 6.2.5a- The number of motor neurons in the lumber region of SOD1 ^{G93A} mice declines compared to B6 aged matched controls.....	176
Figure 6.2.5b- SOD1 ^{G93A} motor neurons as a percentage of aged matched controls.....	176
Figure 6.2.6- The percentage of motor neurons that express p75NTR increases with age in SOD1 ^{G93A} mice, but is under 5%.....	178
Figure 6.2.7- The average number of p75NTR positive motor neurons in SOD1 ^{G93A} mice peaks between 100-120 days.....	179
Figure 6.2.8- p75NTR positive motor neurons appear larger than p75NTR negative motor neurons.....	181
Figure 6.2.9- p75NTR positive motor neurons are larger than p75NTR negative motor neurons in SOD1 ^{G93A} mice.....	182

Figure 6.2.10a- Diameter measurements are not affected by staining profiles of p75NTR and ChAT.....	184
Figure 6.2.10b- Area measurements are not affected by staining profiles of p75NTR and ChAT.....	184
Figure 6.2.11- p75NTR motor neurons tagged by intraperitoneal injected MLR2-ATTO-488 are the same size as counterstained p75NTR motor neurons.....	185
Figure 6.2.12- Expression of ATF3 and p75NTR in the ventral horn of the lumbar spinal cord of a 100 day old SOD1 ^{G93A} mice.....	186
Figure 6.2.13- p75NTR and cleaved caspase-3 co-express in majority of motor neurons in SOD1 ^{G93A} mice.....	189-190
Figure 6.2.14a- SOD1 ^{G93A} mouse motor neurons decrease in diameter over time compared to B6 age matched controls.....	193
Figure 6.2.14b- Example of measuring the soma width of a motor neuron.....	193
Figure 6.2.15a- SOD1 ^{G93A} mouse motor neurons decrease in area over time compared to B6 age matched controls.....	195
Figure 6.2.15b- Example of measuring the area of a motor neuron.....	195
Figure 6.2.16- Soma area decline is highly correlated with diameter decline in lumbar motor neurons of SOD1 ^{G93A} mice.....	197
Figure 6.2.17- Frequency distribution as a percentage of soma area in SOD1 ^{G93A} mice and B6 age matched controls.....	198-199
Figure 6.2.18a- Number of primary processers on p75NTR positive neurons in SOD1 ^{G93A} mice do not change with age.....	202
Figure 6.2.18b- Example of primary processer on a p75NTR positive motor neuron.....	202
Figure 7.2.1- V0 _C interneurons strongly express ChAT.....	220
Figure 7.2.2a- Comparison of V0 _C interneuron counts between SOD1 ^{G93A} and B6 age matched controls.....	221

Figure 7.2.2b- V0_C interneurons from SOD1^{G93A} mice as a percentage of B6 age matched controls.....221

Figure 8.1- p75NTR expressing motor neuron hypothesis.....234-235

Figure A1- Injected MLR2-ATTO-488 is transported to p75NTR positive retinal neurons.....238

Figure A2- p75NTR is expressed across all layers of the mouse retina.....239

Abstract

Motor neuron disease (MND) is a relentlessly progressive neurodegenerative disease, which is typically fatal within 3 years. The only FDA approved treatment for MND is Riluzole, which increases life by approximately 3 months, with little to no increase in quality of life. Due to the heterogeneity of the disease and the blood brain barrier, developing treatments for MND is difficult. This study used a novel non-viral gene delivery agent (called the ‘immunogene’) to bypass the blood brain barrier and deliver pDNA to neonatal mouse motor neurons, which has potential to be used as a therapeutic for MND. An immunogene consists of a monoclonal antibody that targets a receptor that is conjugated to a PEGylated polycation allowing it to carry a cargo of pDNA or siRNA.

In this study we used a monoclonal antibody (MLR2) that targets the neurotrophin receptor p75 (p75NTR) that is able to be retrogradely transported in motor neurons with the receptor. We also used polyethylenamine (PEI) as the cation that electrostatically binds and condenses pDNA. PEGylation (polyethylene glycol) of the PEI was used to stealth and shield the complex from the immune system and blood components (full complex; MLR2-PEI-PEG12).

The common neurotrophin receptor p75 (p75NTR) binds all neurotrophins and is highly expressed in motor neurons during development and down-regulated following birth. However, p75NTR is re-expressed in motor neurons of the SOD1^{G93A} MND mouse model and motor neurons of MND patients.

The aim of this study was to use p75NTR expression on motor neurons in neonatal mice and re-expression of p75NTR on symptomatic SOD1^{G93A} mice that model MND to deliver pDNA via the immunoportor MLR2-PEI-PEG12. Motor

neurons re-expressing p75NTR in SOD1^{G93A} mice were characterised for expression time, apoptotic markers and morphology. This was to determine if the MLR2 immunogene would be feasible as a gene therapy agent in SOD1^{G93A} mice. The study first addressed the ability for the MLR2-immunogene to specifically transfect p75NTR expressing cells and primary motor neurons. Motor neuron-like NSC34 cells and primary motor neurons from E12.5 control C57BL/6J mice were able to be transfected with the MLR2-immunogene (~23 and ~8%, respectively), while p75NTR-ve cell lines (including glial cells) were unable to be transfected. Removing the MLR2 from the immunogene (i.e. PEI-PEG12) abolishes the p75NTR+ve cell specificity.

p75NTR was found to be highly expressed on ~92% of all motor neurons in PND1 C57BL/6J mice. This was reduced to ~50% of motor neurons at PND7, and was completely absent at PND14. PND1 mice were injected intraperitoneally with the MLR2-immunogene which resulted in the transfection of ~20% of all motor neurons at all levels of the spinal cord, assessed by the presence of the pDNA expressing green fluorescent protein (GFP). Transfection levels peaked 10 days after injection. Targeting of p75NTR is integral for the immunogene to properly transfect motor neurons as injection of PEI-PEG12 carrying pDNA (MLR2 antibody) resulted in no transfection.

Only a small number (0-5%) of motor neurons in SOD1^{G93A} adult mice (60-140 days of age) expressed p75NTR at any one time. These p75NTR+ve motor neurons were larger than p75NTR-ve neurons, and the majority (~ 80%) co-expressed the apoptotic marker cleaved caspase 3.

The results from this study show that the MLR2-immunogene is able to deliver pDNA to p75NTR expressing motor neurons in neonatal mice after systemic (intraperitoneal) injection. Targeting motor neurons in adult SOD1^{G93A} mice via p75NTR may be difficult as the percentage of neurons expressing the receptor at any specific time is low (<5%) and appear destined to die due to the presence of cleaved caspase 3.

Declaration

I certify that this thesis does not incorporate without acknowledgement any material previously submitted for a degree or diploma in any university; and that to the best of my knowledge or belief it does not contain any material previously published or written by another person except where due reference is made in the text.

.....

Kevin Sean Smith

Acknowledgements

First and foremost I must thank my primary supervisor, Dr. Mary-Louise Rogers. Without her attention to detail, rigorous work ethic and teaching, I would not have been able to complete my thesis nor have become the young scientist I am. Her ability to selflessly support and help myself and other lab members, even when it put her at a detriment, is truly inspiring, and I hope to be able to one day reach her level of both intellect and capability.

For too many reasons to list here, I must thank my secondary supervisor Emeritus Professor Robert Rush. His constant mentoring, both in and out the lab, has allowed me to get a better understanding of the scientific world. He originally took the risk and offered me the opportunity to undertake a PhD in the Neurotrophic lab, for which I am truly forever grateful.

A huge thanks must go to my fellow PhD student in the lab, (soon to be Dr.) Stephanie Shephard. I have been able to keep my sanity with her support and, in her words, our “intellectual and not-so-intellectual” conversations. I wish her all the best in wherever her science takes her.

I owe a debt of gratitude to the Centre for Neuroscience and the many labs in Human Physiology, Medical Biochemistry, and Anatomy and Histology for all the support, help and advice that has been given to me over the last 4 years. A special thanks goes to Yvette and Pat from Anatomy and Histology/Microscopy for the uncountable amount of times they have offered their expertise and/or reagents.

From the bottom of my heart, I thank my partners that have loved and supported me throughout my candidature, particularly my girlfriend Jessica Tapp, but also

my past partner, Aneta Szumny. The number of times ‘time spent together’ has turned into ‘time spent in the lab’ is too many, and my gratitude for unconditionally understanding and accepting this cannot be put into words.

Above all I thank my brother Daniel Smith. Without his love, support, guidance, and most importantly mateship, I would not have completed this thesis, nor survived in this world.

Lastly, I thank my parents, Dianne Smith (1960-2004) and Kevin Charles Smith (1948-2008). They always supported me in whatever I wanted to do in life, even if it meant they had to struggle themselves. Particularly, I thank my father Kevin Charles Smith. He was the reason I originally became interested in science. From watching countless documentaries with me to star gazing for hours while talking about the universe, he constantly stimulated the curiosity in me. Because of this, I dedicate this thesis to him.

Publications arising from this work

-Secret, E., **Smith, K.**, Dubljevic, V., Moore, E., Macardle, P., Delalat, B., Rogers, M.L., Johns, T.G., Durand, J.O., Cunin, F. & Voelcker, N.H. (2013). Antibody-Functionalized Porous Silicon Nanoparticles for Vectorization of Hydrophobic Drugs. *Advanced Healthcare Materials* 2, 718–727.

- Rogers, M.-L., **Smith, K.S.**, Matusica, D., Fenech, M., Hoffman, L., Rush, R. a. & Voelcker, N.H. (2014). Non-viral gene therapy that targets motor neurons in vivo. *Frontiers in Molecular Neuroscience* 7, 1–12.

- **Smith, K.S.**, Rush, R. a. & Rogers, M.-L. (2015). Characterization and changes in neurotrophin receptor p75N-expressing motor neurons in SOD1 G93A G1H mice. *Journal of Comparative Neurology* 523, 1664–1682.

List of Abbreviations

AAV - adeno-associated virus

ADRS – Antibody diluent reagent solution

ANG - Angiogenin

ARTN - Artemin

ATF-3 – Activating transcription factor 3

ATP – Adenosine triphosphate

ATXN2 – Ataxin 2

BBB - blood brain barrier

BBB – Blood Brain Barrier

BDNF – Brain-derived neurotrophic factor

BMAA – beta-methylamino-L-alanine

C9ORF72 – Chromosome 9 open reading frame 72

ChAT – Choline acetyltransferase

CHMP2B – Charged multivesicular body protein 2b

CHOP - C/EBP homologous protein

CMV – Cytomegalovirus

CNS – Central nervous system

CpG's – cytosine-phosphate-guanine

DAO – D-aminio-acid oxidase

DCTN1 – Dynactin 1

DMEM - Dulbecco's Modified Eagle Medium

DMF - Dimethylformamide, anhydrous

DNA – Deoxyribonucleic acid

DRG – Dorsal root ganglion

DTS - DNA Targeting Sequence

ER – Endoplasmic reticulum

ERK - Extracellular signal-related kinase

EWSR1 – Ewing sarcoma breakpoint region 1

Fab - antibody-binding fragments

FACS – Fluorescent activated cell sorting/flow cytometry

FDA – United States Food and Drug Administration

FF – Fast fatigable motor neurons

FIG4 – Phosphatidylinositol 3,5-bisphosphate 5-phosphate

FR – Fatigue resistant motor neurons

FTD – Frontal Temporal Dementia

FUS/TLS – Fused in sarcoma/translocated in sarcoma

GDNF – Glial cell line-derived neurotrophic factor

GFL – GDNF Family of ligands

GT1b -lipid raft-associated ganglioside

GX - Glutamax I

HBS – HEPES buffered saline

HBSS - Hank's Buffered Salt Solution

HCFS - Hybridoma Fusion and Cloning Supplement

HEPES - 4-(2-hydroxyethyl)piperazin-1-ethanesulfonic acid

HGF – Hepatocyte growth factor

HT - Hypoxanthine and Thymidine supplement

JNK - c-Jun N-terminal kinases

JNK - Jun amino-terminal kinase

kDa – kilo Daltons

LBHIs – Lewy body-like hyaline inclusions

MATR3 – Matrin 3

MEM - Minimum Essential Media

MND/ALS – Motor Neuron Disease/ Amyotrophic Lateral Sclerosis

mRNA – messenger ribonucleic acid

N/P – Nitrogen/Phosphate ratio

NADE - p75^{NTR}-associated cell death executor

NFH – Neurofilament heavy chain

NGF – Nerve growth factor

NLS - Nuclear localisation signals

NO – Nitric Oxide

NPC - Nuclear Pore Complexes

NRAGE - Neurotrophin receptor-interacting melanoma antigen (MAGE)
homolog

NRIF - Neurotrophin Receptor Interacting Factor

NRTN - Neurturin

NSC34 – Neuroblastoma x spinal cord motor neuron cell line

NT - Neurotrophin

NT3 – Neurotrophin-3

NT4 – Neurotrophin-4/5

O/N – overnight

OPTN - Optineurin

P13K - Phosphoinositide 3-kinase

p75NTR – pan Neurotrophin Receptor 75

PBS – Phosphate buffered saline

pDNA – plasmid DNA

PEG – Polyethylene glycol

PEG – Polyethylene glycol

PEI - Polyethylenamine

PEI - Polyethyleneimine

PFN1 – Profilin 1

PLL - Poly-L-lysine

PND – post natal day

PORN - Poly-L-Ornithine

PRPH - Peripherin

PSG - Penicillin/Streptomycin/Glutamine

PSPN - Persephin

RET – Rearranged during transfection

RHI – Round Hyaline inclusions

RIP - Regulated intramembrane proteolysis

RISC - RNA-induced silencing complex

RNA – Ribonucleic acid

RPMI - Roswell Park Memorial Institute 1640 media

RT – room temperature

S – Slow motor neurons

scFv - single chain variable fragments

SETX - Senataxin

SLI – Skein-like inclusions

SMA – Spinal Muscular Atrophy

SMN - Survival Motor Neuron

SOD1 – Cu, Zn Superoxide Dismutase 1

SPDP - succinimidyl 3-(2-pyridyldithio) propionate

SQSTM1 – Sequestosome 1

TACE/ADAM17 - disintegrin metalloproteinase tumour necrosis factor- α -
converting enzyme

TAF15 – TATA-binding protein-associated factor 15

TDP43 – Trans-active DNA binding protein 43

TNBS - Picrylsulfonic acid

TNFR – Tumour necrosis family receptors

Trk – Tropomyosin receptor kinase

VACHT - Vesicular acetylcholine transporter

VAPB – Vesicle-associated membrane protein B

VCP – Valosin-containing protein

X-SCID - X-linked severe combined immunodeficiency disease

Chapter 1: Introduction

1 Introduction

Delivery of therapeutic compounds to neurons in the central nervous system (CNS) is very difficult due to the restrictive nature of the blood brain barrier. This inability to access CNS neurons limits treatments for neurodegenerative disorders, such as Motor Neuron Disease (MND). However, the blood brain barrier can be bypassed by taking advantage of cellular receptor trafficking. For example, receptors at the peripheral axonal synapse of motor neurons are activated and retrogradely transported along the axon to the soma for signalling. One such receptor, the pan75 neurotrophic receptor (p75NTR), is retrogradely transported from synapse to soma and can be exploited by the use of a functional antibody. With the addition of plasmid DNA and a carrier to the antibody, there is a potential for an effective gene delivery system. For MND, a genetically and pathologically diverse disorder, a gene delivery agent that provides motor neurons with potent trophic factors to counteract cellular death is of great interest.

1.1 Motor Neurons

The cell bodies of motor neurons are located in the CNS and are responsible for the activation, recruitment and contraction of muscle fibers in the periphery, which allows an organism to perform tasks, both complex and simple. There are two main types of motor neurons; lower motor neurons which have axonal projections that leave the CNS and innervate peripheral muscles, and upper motor neurons that have projections that synapse with, and regulate lower motor neurons entirely within the CNS. Motor neurons control non-conscious rudimentary actions, such as breathing as well as controlled voluntary movement. In the

human body, there are over 600 skeletal muscles, all of which are controlled by motor neurons. Motor neurons can be classified into three different classes; alpha (α), beta (β) and the smaller gamma (γ). Alpha motor neurons are large and innervate extrafusal skeletal muscle, allowing muscle contraction and movement. They can be further split into 3 subclasses; fast-twitch fatigable (FF), fast-twitch fatigue resistant (FR) and slow-twitch fatigue resistant (S), depending on the type of muscle fibre they innervate. The smaller gamma motor neurons have a more complex role, as they innervate the intrafusal muscle spindles inside skeletal muscles. These spindles act as proprioceptors for the muscle and must be kept taut to detect muscle stretch properly. However, when a muscle contracts, the spindles inside will start to slacken. The gamma motor neurons counteract this slackening and keep the spindles taut, and only relax when a muscle is stretched. Beta motor neurons are experimentally difficult to study and as a result are the least studied and least understood. They innervate both intra- and extrafusal fibres and have similar properties to that of alpha motor neurons. (Burke *et al.*, 1973; Kanning, Kaplan & Henderson, 2010; Karpati, 2010; Stifani, 2014).

Motor neurons are some of the largest, longest, most complex and energy hungry cells, which can make them highly susceptible to damage and disease. The most prominent and disabling of motor neuron disorders is Motor Neuron Disease.

1.2 Motor Neuron Disease

Motor Neuron Disease (MND; also known as Amyotrophic Lateral Sclerosis (ALS) or Lou Gehrig's disease) is a debilitating and incurable neurodegenerative disorder. The pathology of MND is characterised by motor neuron cell death in

the primary motor cortex, brainstem (upper motor neurons), spinal cord (lower motor neurons) and degeneration of projecting axons (Swash & Fox, 1974; Saito, Tomonaga & Narabayashi, 1978; Swash *et al.*, 1986). The death of motor neurons causes a loss of connectivity at the neuromuscular junction, resulting in paralysis. The onset of paralysis is usually limb (extremities) or bulbar (tongue/mouth), which spreads or ‘creeps’ towards the trunk, eventually causing death through respiratory failure (Gil *et al.*, 2008; Spataro *et al.*, 2010). The three subclasses of alpha motor neurons denervate and die at different rates; FF being most susceptible, then FR, with S being the most resistant (Frey *et al.*, 2000). The average life expectancy after diagnosis of MND is approximately 3-5 years, however some patients have been known to live for over 10 years with the disease (Turner *et al.*, 2003).

MND was first described clinically and pathologically in medical literature in 1869 by the French neurologist Jean-Martin Charcot (Charcot, 1869). Disease phenotypes display heterogeneity and because of this, there are complications regarding classification, especially when there is overlap with other diseases such as frontal temporal dementia (FTD) (Lomen-Hoerth, Anderson & Miller, 2002). However, the universal commonality with any phenotype is the loss of upper and lower motor neurons. Approximately 90-95% of MND cases are sporadic (sALS, sporadic Amyotrophic Lateral Sclerosis) and 5-10% are familial (fALS, Familial Amyotrophic Lateral Sclerosis) (Byrne *et al.*, 2011), with an ever increasing number of mutations related to the disease (such as SOD1, TDP-43, FUS, C9orf72; discussed later). These mutations have led to the creation of transgenic rodent models, such as the SOD1^{G93A} mouse which overexpresses a mutated form (glycine to alanine substitution) of the *SOD1* gene and mimic MND pathology

(Gurney, Pu, & Chiu, 1994). The initial onset of the disease can also vary greatly between patients. Intriguingly, after onset the spread of the disease to other parts of the body follow a similar pattern, suggesting a common underlying mechanism of propagation (Ravits & La Spada, 2009). The rate of disease progression also differs from patient to patient, with prognosis after diagnosis ranging from months to years (Turner *et al.*, 2003; Kanning *et al.*, 2010).

Currently, the only US Food and Drug Administration (FDA) approved treatment for MND is Riluzole. The drug has been shown to influence cell currents by inhibiting sodium, calcium, potassium and glutamate channels (Bellingham, 2011; Gibson & Bromberg, 2012). Particular focus is on its anti-glutamate properties, as excitotoxicity via glutamate release has been shown to be linked with MND (Plaitakis & Carosco, 1987; Rothstein *et al.*, 1990) and that clinical trials using Riluzole with MND patients slowed disease progression slightly (approximately 2-3 months) (Bensimon, Lacomblez & Meininger, 1994; Lacomblez *et al.*, 1996; Miller, Mitchell & Moore, 2012). Several studies have shown that Riluzole treated SOD1^{G93A} mice have an extension of life by approximately 10%, however, many of these studies have differing dosing criteria and uncontrolled variables (such as detecting mutant SOD1 copy number), which has thrown doubt on the drug's effectiveness (Gurney, Cutting & Zhai, 1996; Gurney *et al.*, 1998; Kriz, Gowing & Julien, 2003; Snow *et al.*, 2003; Waibel *et al.*, 2004; Bellingham, 2011). More doubt was raised after a rigorous assessment of 5,429 SOD1^{G93A} mice showed that no compound (including Riluzole) had any therapeutic effect on the disease when proper parameters are put in place to control critical biological variables (Scott *et al.*, 2008).

1.3 Genetics in Motor Neuron Disease

As previously mentioned, 90-95% of MND is sporadic while 5-10% is familial, owing its pathology to a particular genetic abnormality (Byrne *et al.*, 2011).

Currently, there are over 25 mutated genes associated with MND, with some also involved with Frontal Temporal Dementia (FTD), however 30-40% of familial cases have no known genetic origin (Figure 1.1) (Ince *et al.*, 2011; Robberecht & Philips, 2013). The most well-known, studied and first discovered mutation that causes MND is in Cu/Zn Superoxide Dismutase-1 (SOD1) (Rosen *et al.*, 1993).

1.3.1 SOD1

SOD1 is a ubiquitously expressed protein homodimer, which reduces superoxide free radicals to hydrogen peroxide, before they are further reduced to water via glutathione peroxidase (Andersen, 2006). Generally, the literature quotes that mutations in the *SOD1* gene account for approximately 20% (Cudkowicz *et al.*, 1997; Robberecht & Philips, 2013; Ajroud-driss & Siddique, 2014) of FALS cases, but can range from 12-23.5%, and interestingly from 0-7.3% in SALS cases (Andersen, 2006). Currently, over 150 mutations in the *SOD1* gene have been identified to cause some form of MND (Robberecht & Philips, 2013) with one particular mutation, a glycine to alanine substitution at codon 93, resulting in the creation of a MND mouse model (SOD1^{G93A}) (Gurney *et al.*, 1994). The pathology of SOD1-MND is not caused by a loss of dismutase function. Instead, the disease is thought to be a toxic gain of function, as SOD1 deficient mice show no MND pathologies (Reaume *et al.*, 1996). Mutations in the *SOD1*

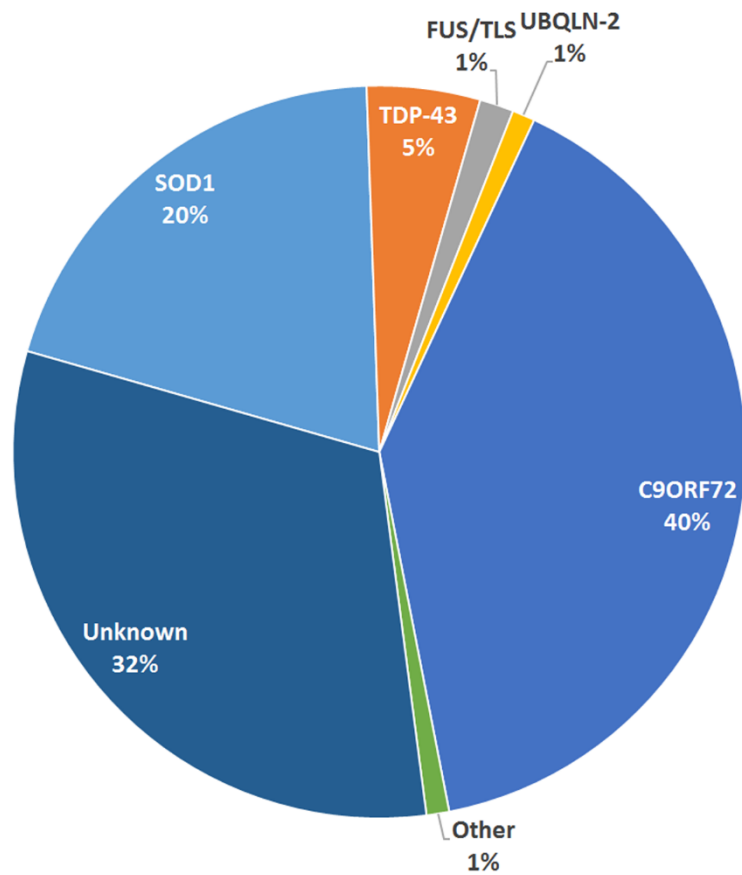


Figure 1.1 Mutations in familial MND

There are currently over 25 known mutations that can cause MND. The recently discovered mutation in C9ORF72 has the highest percentage of familial cases, accounting for ~40%, overtaking the heavily studied SOD1 mutations. Majority of the known mutated genes make up ~1% of all cases, with ~30% of familial cases still having an unknown genetic origin (Robberecht & Philips, 2013).

gene produce misfolded SOD1 proteins which are ubiquitinated for degradation. However, in many of these ubiquitin-tagged proteins are not degraded, but instead aggregate intracellularly (Basso *et al.*, 2006). Protein aggregates are hallmarks of many neurodegenerative diseases such as Alzheimer's Disease, Huntington's Disease, Parkinson's disease and MND, with SOD1 aggregates appearing in many human spinal motor neurons and SOD1 mouse models (Bruijn *et al.*, 1997; Johnston *et al.*, 2000; Watanabe *et al.*, 2001; Deng *et al.*, 2006; Furukawa *et al.*, 2006).

1.3.2 TDP-43

Following the discovery of SOD1, another MND related gene/protein was found; Trans Active Response DNA-binding protein 43 (TDP-43, *TARDBP*). TDP-43 mutations account for approximately 1-5% of fALS and interestingly, are found in ubiquitinated aggregates in MND and FTD (Neumann *et al.*, 2006; Rutherford *et al.*, 2008; Sreedharan *et al.*, 2008; Robberecht & Philips, 2013). TDP-43 is a predominately nuclear protein that has many cellular functions. It is involved in DNA/RNA binding and regulatory functions including; transcription and exon splicing regulation, pre-mRNA and mRNA stability, mRNA translation and microRNA processing, (Ayala *et al.*, 2005; Buratti & Baralle, 2010) and is shuttled in and out of the nucleus during normal cellular metabolism (Ayala *et al.*, 2008). The role of TDP-43 in MND stretches further than mutations, as TDP-43 is found in motor neuron inclusions in all non-SOD1 forms of MND (Mackenzie *et al.*, 2007), implying that TDP-43 and DNA/RNA processing may be intrinsically linked with MND.

1.3.3 *FUS/TLS*

Another nuclear RNA binding protein, Fused in Sarcoma/Translocated in Liposarcoma (*FUS/TLS*) which binds over 5,500 genes (Lagier-Tourenne *et al.*, 2012), has been linked with MND, in both sporadic and familial forms (Belzil *et al.*, 2009; Kwiatkowski *et al.*, 2009; Vance, Rogelj & Hortobágyi, 2009; Corrado *et al.*, 2010; Groen *et al.*, 2010; Tateishi *et al.*, 2010; Drepper *et al.*, 2011) and accounts for about 1-5% of FALS cases (Robberecht & Philips, 2013). Similar to SOD1 and TDP-43, *FUS/TLS* has been found in aggregates in MND patient ventral motor neurons (Deng *et al.*, 2010). Majority of mutations in *FUS/TLS* gene are in the NLS (Nuclear Localisation Sequence) domain which allow the protein to enter/exit the nucleus. It has been proposed that the inability to re-enter the nucleus, due to the location of the mutation and form stress granules/aggregates in the cytoplasm is the main pathology of *FUS/TLS* (Dormann *et al.*, 2010).

1.3.4 *C9ORF72*

The most recent genetic cause linked to MND is a hexanucleotide repeat expansion in the non-coding region of *C9ORF72* (Chromosome 9 Open Reading Frame 72), which can also cause FTD/MND-FTD (DeJesus-Hernandez *et al.*, 2011; Renton *et al.*, 2011). This mutation has surpassed SOD1 in having the highest percentage of familial cases, with approximately 40% of all FALS having the hexanucleotide repeat and 5% SALS (Majounie *et al.*, 2012). Most healthy people have two to five repeats of the hexanucleotide (GGGGCC) in the non-coding first intron of the gene, yet patients with *C9ORF72*-MND can have

hundreds or even thousands of the hexanucleotide repeats. It is still unknown as to the function of the C9ORF72 protein, yet patients with the mutation have similar pathology to other MND variants, such as TDP-43 inclusions in motor neurons of the cortex and hippocampus (DeJesus-Hernandez *et al.*, 2011; Renton *et al.*, 2011; Robberecht & Philips, 2013).

1.3.5 Ubiquilin-2

Protein aggregation and defects in protein ubiquitination/degradation are common in MND, which led to the discovery of a mutation in ubiquilin 2 (UBQLN2), that accounts for <1% of familial cases. The ubiquilin 2 protein is involved with ubiquitination of proteins for degradation and found in aggregates of both ubiquilin 2 and non-ubiquilin 2 MND (Deng *et al.*, 2011b). Interestingly, ubiquilin 2 mutations also overlap with FTD, and ubiquilin 1 (UBQLN1) has been implicated in Alzheimer's Disease, suggesting common mechanisms of protein degradation in neurodegenerative diseases (Bertram *et al.*, 2005; Deng *et al.*, 2011a; Robberecht & Philips, 2013).

1.3.6 Valosin-containing protein

Mutations in Valosin-containing protein (VCP), another protein involved in protein degradation, can cause MND (Johnson *et al.*, 2010). Interestingly, VCP mutations were originally found in Inclusion body myopathy associated with Paget disease of bone and frontotemporal dementia (IBMPFD), a disease which

has both muscle weakness/atrophy and frontotemporal dementia, similar to MND (Watts *et al.*, 2004).

1.3.7 Optineurin

Mutations in Optineurin (OPTN) were originally implicated in causing primary open-angle glaucoma (Rezaie *et al.*, 2002) but have also been found to cause MND (Maruyama *et al.*, 2010). Optineurin has been shown to suppress NF- κ B mediated cell death, which is upregulated in the spinal cords of patients with MND (Swarup *et al.*, 2011). Mutations in Optineurin are thought to cause an improper regulation of NF- κ B signalling, subsequently resulting in motor neuron cell death (Maruyama *et al.*, 2010; Akizuki *et al.*, 2013).

1.3.8 Other mutant genes

SOD1, TDP-43, FUS/TLS and C9ORF72 mutations account for the bulk of familial MND cases, ranging from 60-80%. The remaining 20-40% are unknown genetic causes with a very small percentage made up of rare mutations. Discovery of the rarer mutations have been accomplished by investigating similarities with the common mutations in specific protein domains/motifs and mechanism of action. These mutations are summarised in Table 1.1. The abundance and diversity of genetic abnormalities in MND leads to a more diverse set of cellular pathologies seen within motor neurons.

Table 1.1 Rare mutations which have been shown to cause, or be involved in, MND.

Gene	Role	Reference
TATA-binding protein associated factor 15 (TAF15)	Both have similar binding properties and prion domains to TDP-43 and FUS/TLS	(Couthouis <i>et al.</i> , 2011, 2012)
Ewing sarcoma breakpoint region 1 (EWSR1)		
Matrin 3 (MATR3)	A DNA/RNA binding protein which interacts with TDP-43	(Johnson <i>et al.</i> , 2014)
Senataxin (SETX)	A DNA helicase and involved in RNA processing	(Chen <i>et al.</i> , 2004)
Angiogenin (ANG)	Involved in angiogenesis but is lacking in understanding with its role in motor neurons	(Greenway <i>et al.</i> , 2006)
Ataxin 2 (ATXN2)	A TDP-43 interacting protein	(Elden <i>et al.</i> , 2010)
Sequestosome (SQSTM1)	Involved with protein ubiquitination	(Fecto <i>et al.</i> , 2011)
Charged multivesicular body protein 2b (CHMP2B)	Has been linked to FTD	(Skibinski <i>et al.</i> , 2005; Parkinson <i>et al.</i> , 2006)
Phosphatidylinositol 3,5-bisphosphate 5-phosphatase (FIG4)	Involved in retrograde endosome to <i>trans</i> -golgi network trafficking and signalling	(Rutherford <i>et al.</i> , 2006; Chow <i>et al.</i> , 2009)
D-amino-acid oxidase (DAO)	Mediates excitotoxic D-serine which has been shown to accumulate in MND and mouse model spinal cords	(Sasabe <i>et al.</i> , 2007; Mitchell <i>et al.</i> , 2010)
Vesicle-associated membrane protein B (VAPB)	Involved in intracellular trafficking and signalling	(Nishimura <i>et al.</i> , 2004)
Peripherin (PRPH)	An intermediate filament which has been found in inclusion bodies of MND	(Gros-Louis <i>et al.</i> , 2004)
Neurofilament heavy chain (NFH)	A cytoskeletal protein causing aggregations	(Figlewicz <i>et al.</i> , 1994)
Profilin 1 (PFN1)	A cytoskeletal protein involved in proper actin/microfilament creation and restructuring	(Wu <i>et al.</i> , 2012)
Dynactin 1 (DCTN1)	A critical component of retrograde transport	(Münch <i>et al.</i> , 2004)

1.4 Cellular Pathology

Within the motor neurons in MND and animal models, there are an array of cellular pathologies which occur concurrently during disease (Figure 1.2). Some of the defects stem directly from genetic mutations previously mentioned, while others have unknown origins. However, whether the disease is a product of a known genetic mutation or is sporadic with no known cause, the two are clinically indistinguishable and share many pathophysiologies, which may ultimately elucidate the underlying mechanism.

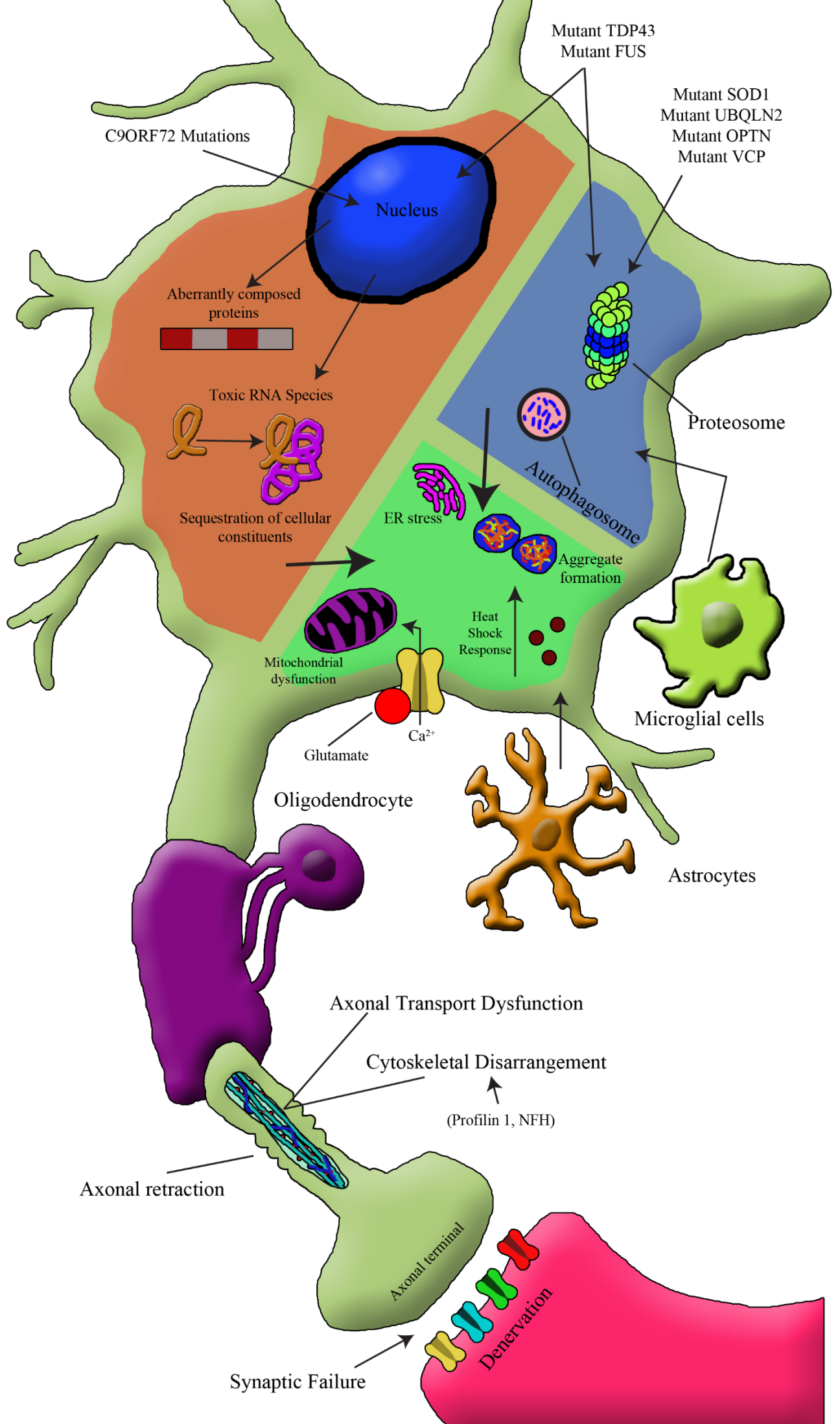
1.4.1 *Defects in RNA/DNA processing*

Since the discovery of TDP-43, there has been extensive research into RNA/DNA processing proteins in MND. TDP-43 has been shown to aggregate in cytoplasmic inclusions and loss of nuclear localisation in over 90% of all non-SOD1 MND cases (indistinguishable in both familial and sporadic (Pamphlett *et al.*, 2009)) (Arai *et al.*, 2006; Mackenzie *et al.*, 2007; Ling, Polymenidou & Cleveland, 2013). Additional RNA-binding proteins similar in function or structure to TDP-43 (and also FUS/TLS), including angiogenin (Greenway *et al.*, 2006), senataxin (Chen *et al.*, 2004) and ataxin-2 have implicated that disruption in RNA homeostasis plays an important role in MND. The loss of RNA/DNA processing in the nucleus and formation of aggregates in the cytoplasm has been speculated in causing disease in both a loss-of-function property (nuclear loss) and gain-of-function toxicity (aggregates).

Figure 1.2 Cellular pathology in MND

While the root cause of MND has yet to be discovered, many of the cellular pathologies that cause dysfunction and death within motor neurons have been described. These pathologies include defects in DNA/RNA processing, defects in proteosomal processing, mitochondrial dysfunction, excitotoxicity and extends to defects in axonal/cellular transport and trafficking.

Due to the heterogeneity of the cellular pathologies in MND and motor neuron location (in the CNS behind the blood brain barrier), it is very difficult to deliver therapeutics to motor neurons and prevent cell death (adapted from Robberecht & Philips, 2013),



1.4.2 Defects in Proteosomal processing

Many neurodegenerative diseases such as Alzheimer's Disease, Parkinson's Disease and MND all share a common characteristic of protein processing defects, which leads to protein aggregation. MND is often referred to as a proteinopathy. Within MND, there are different types of aggregates containing different proteins. Protein aggregates are classified into skein-like inclusions (SLIs), round hyaline inclusions (RHIs), Lewy body-like hyaline inclusions (LBHIs) or Bunina bodies. All four of these aggregate types have been found in MND, however RHIs and LBHIs are also found in other diseases/disorders (Bendotti *et al.*, 2012).

The major aggregate hallmark of MND is ubiquitin positive SLIs, which usually have TDP-43 immunoreactivity, but not SOD1 (Lowe *et al.*, 1988; Leigh *et al.*, 1991; Watanabe *et al.*, 2001; Mackenzie *et al.*, 2007). TDP-43 is naturally shuttled in and out of the nucleus (Ayala *et al.*, 2008), however under cell stress, TDP-43 can completely abandon the nucleus and form cytoplasmic stress granules *in vitro* and in MND/FTD brain tissue (Colombrita *et al.*, 2009; Liu-Yesucevitz *et al.*, 2010; Meyerowitz *et al.*, 2011). Stress granules are impermanent aggregations of mRNA, and thought to be an aggregation site for non-essential proteins during cellular stress to allow the cell to shift energy expenditure to critical repair or survival pathways (Buchan & Parker, 2009). Interestingly, extended cellular stress (e.g. paraquat induced stress) can cause stress granules to form irreversible aggregates of endogenous TDP-43 within the cytoplasm (Parker *et al.*, 2012). TDP-43 has a natural tendency to aggregate,

which is exacerbated in mutated/truncated forms (Johnson *et al.*, 2009) and stress granules may create a pro-aggregate environment.

As ubiquitination of proteins is involved with rapid degradation of proteins and ubiquitin is a major component of inclusions in diseased motor neurons, defects in the ubiquitin-proteasome system (UPS) has been implicated in being a cause or consequence of aggregate formation, due to alterations in proteasome components (Urushitani *et al.*, 2002; Kabashi *et al.*, 2004; Cheroni *et al.*, 2005, 2009).

Recently, mutations in the gene coding ubiquilin 2 have been found in people with MND (Deng *et al.*, 2011b; Williams *et al.*, 2012). Ubiquilin 2 is a ubiquitin-like protein which aids in chaperoning ubiquitinated proteins to the proteasome for degradation and has been shown to bind and regulate TDP-43 levels (Warraich & Yang, 2012; Cassel & Reitz, 2013; Zhang *et al.*, 2014), indicating that defects in the UPS play a major role in MND pathology.

The endoplasmic reticulum (ER), integral in the proper folding and maturation of proteins, has been shown to be affected in MND. Misfolded proteins that aggregate in the ER cause the unfolded protein response (UPR) (Kaufman, 2002), which when prolonged, can cause cell death by signalling via C/EBP homologous protein (CHOP), caspase-12 (human caspase-4) and c-Jun amino-terminal kinase (JNK) (Nakagawa *et al.*, 2000; Urano *et al.*, 2000; Hitomi *et al.*, 2004). Evidence of the UPR and ER changes have been found in cell lines expressing mutant SOD1 (Soo *et al.*, 2012) or mutant FUS (Farg *et al.*, 2012) mouse models of MND (Atkin *et al.*, 2006) and in the motor neurons of patients with sporadic MND (Atkin *et al.*, 2008).

Bunina bodies are small, eosinophilic granular cytoplasmic ubiquitin-negative inclusions, immunoreactive for cystatin-C and transferrin, that are specific to MND, although not all cases appear to have them (Okamoto *et al.*, 1993; Okamoto, Mizuno & Fujita, 2008; Mizuno *et al.*, 2006; Kato, 2008). However, unlike SKIs, Bunina bodies have no correlation with disease severity (van Welsem *et al.*, 2002) and have not been found in SOD1 mouse models or SOD1 patients (Kato, 2008).

1.4.3 Mitochondrial dysfunction

Motor neurons have a high demand for energy, both in the soma and at the distal axon, and as such, mitochondria have been investigated in regards to disease pathology. Mitochondrial defects in motor neurons are one of the earliest pathologies seen in MND model mice. As early as E13, defects in mitochondria are seen in cultured motor neurons from SOD1^{G93A} mice (De Vos *et al.*, 2007). Morphological changes in mitochondria are apparent at around 2 weeks of age in SOD1^{G93A} mice, where they appear slightly swollen (Bendotti *et al.*, 2001). Swelling of mitochondria progresses with age, so that between 60-70 days of age approximately 90% of mitochondria in SOD1^{G93A} motor neurons are swollen (even slightly), and by 100 days, nearly half (40%) of mitochondria are twice the normal size. Interestingly, swollen mitochondria are able to keep their structural integrity and not burst (Martin *et al.*, 2007). It has been shown that wild type SOD1 is located in both the cytosol and mitochondria where it protects mitochondria from oxidative stress (Weisiger & Fridovich, 1973; Sturtz *et al.*, 2001). The mutant SOD1 protein in SOD1^{G93A} mice is also present in

mitochondria in substantial amounts (Jaarsma *et al.*, 2001; Higgins *et al.*, 2002; Mattiazzi *et al.*, 2002) and it is primarily localised, like wild type SOD1, in the intermembrane space (Sturtz *et al.*, 2001; Magrané *et al.*, 2009), but also on the cytoplasmic face of the outer membrane (Vande Velde *et al.*, 2008). Respiration, ATP synthesis and electron transport chain defects coincide with symptom onset in SOD1 mouse mitochondria (Mattiazzi *et al.*, 2002). Interestingly, mice overexpressing human TDP-43 show similar impairment in mitochondria (Shan *et al.*, 2010; Xu *et al.*, 2010). In rat motor neurons, it has been shown that TDP-43 co-localises with mitochondria and impairment is exacerbated in cultured neurons when mutated TDP-43 is expressed (Wang *et al.*, 2013).

1.4.4 Excitotoxicity

Currently, the only Food and Drug Administration (FDA) approved treatment for MND is Riluzole. Riluzole is an anti-glutamatergic drug that has been shown to, at best, extend the life of someone with MND by approximately 2-3 months (Bensimon *et al.*, 1994; Miller *et al.*, 2012). Excitotoxicity was investigated as a link to MND since glutamate, the major excitatory and excitotoxic neurotransmitter in the CNS, metabolism and quantity were altered in MND patients (Plaitakis & Carosco, 1987). Excitability by glutamate causes the influx of Ca²⁺ ions, which normally elicit an action potential. However, cell death occurs when too much Ca²⁺ enters the cell (excitotoxicity) (Van Den Bosch *et al.*, 2006). The abundance of Ca²⁺ can cause cell death by the production of toxic oxygen free radicals produced by mitochondria (Dykens, 1994; Carriedo *et al.*, 2000; Urushitani *et al.*, 2001), as well as activation of phospholipases, proteases,

endonucleases, protein phosphatases, protein kinase C, xanthine oxidase and NO synthase (Van Den Bosch *et al.*, 2006). Intriguingly, motor neurons susceptible in MND lack expression of Ca²⁺ buffering proteins parvalbumin and calbindin D-28k (Ince *et al.*, 1993). However, motor neuron pools resistant in the disease, such as Onuf's nucleus, oculomotor, trochlear and abducens motor neurons, express parvalbumin and/or calbindin D-28 (Alexianu *et al.*, 1994). Excitotoxicity has also been implicated to cause motor neuron disease (with Alzheimer's Disease- and Parkinson's Disease-like symptoms) in Guam by the excitotoxic BMAA (β -methylamino-L-alanine) which is found in the false sago plant *Cycas circinalis* (Spencer *et al.*, 1986). It is thought however, that direct consumption of the plant does not cause Guam MND, but is most likely due to the consumption of flying foxes in the region, which have a diet including the toxic plant seeds that store and concentrate the toxin (Cox & Sacks, 2002).

1.4.5 Defects in Axonal Transport

Functioning axonal transport, both anterograde and retrograde, is vital in neuronal health. This is particularly true for motor neurons, as their very long axons (some >1m in humans) constitute over 99% of their total cytoplasmic volume, yet almost all protein synthesis occurs in the soma so that proper transport of cargo to the axonal synapse is crucial (Holzbaur, 2004). Mutations in *DCTN1* gene, which produces the dynactin protein - a linker between transported cargo, microtubule and dynein - has been shown to cause MND, implicating a possibility that axonal transport is an underlying defective mechanism in the disease (Waterman-storer, Karki & Holzbaur, 1995; Münch *et al.*, 2004). In cultured motor neurons

expressing mutant SOD1^{G93A}, defects of both retrograde and anterograde axonal transport of mitochondria and membrane bound organelles is seen as early as E13 (De Vos *et al.*, 2007). In SOD1^{G93A} mice, and mice expressing mutant TDP-43, retrograde transport of mitochondria was decreased at 45 days of age and by 90 days, with anterograde transport also affected (Magrané *et al.*, 2014).

Interestingly, there is a decrease in retrogradely transported survival factors including; phosphorylated-Trk receptors, -Erk1/2 and -Erk5 and neurotrophins NGF and BDNF. Conversely, there is an increase in the retrograde transport of stress and injury related proteins such as; phosphorylated c-Jun N-terminal kinase, caspase-8 and the intracellular signalling cleavage fragment p75NTR (Perlson *et al.*, 2009).

There are two hypotheses that may explain the general aetiology and origins of MND. The first is the ‘dying forward’ hypothesis. This hypothesis suggests that the disease originates in cortico-motor neurons (upper motor neurons) which synapse onto lower motor neurons, where they mediate anterograde degeneration by means of glutamate excitotoxicity (Kiernan *et al.*, 2011). The second is the ‘dying back’ hypothesis. This suggests that the origin of the disease at the neuromuscular junction of the lower motor neurons, due to the degradation of the synapse and/or loss of target-derived trophic support (Dadon-Nachum, Melamed & Offen, 2011). Neurotrophins and neurotrophic factors are potent target-derived pro-survival molecules which play many roles in the adult and developing nervous system. While no genetic abnormalities have been found in neurotrophins/neurotrophic factors and MND, the retrograde transport of pro-

survival trophic factors is impaired in SOD1^{G93A} mice motor neurons (Perlson *et al.*, 2009).

1.5 Neurotrophins and Neurotrophic Factors

1.5.1 Neurotrophins

The overly complex nature of the nervous system relies heavily on a particular family of proteins called neurotrophins (NT), which influence and guide neuronal cells. The four classic neurotrophins include NGF (Nerve Growth Factor), BDNF (Brain Derived Neurotrophic Factor), NT-3 (Neurotrophin-3) and NT-4/5 (Neurotrophin-4/5). These four neurotrophic factors have cognate receptors in which they can bind and cause intracellular messaging signals. The neurotrophic receptors that neurotrophins bind to are p75NTR and the Trk receptors. NGF binds to TrkA with high affinity (Cordon-Cardo *et al.*, 1991; Kaplan *et al.*, 1991; Klein *et al.*, 1991a); BDNF and NT-4/5 bind to TrkB with high affinity (Berkemeier *et al.*, 1991; Klein *et al.*, 1991b; Soppet *et al.*, 1991; Ip *et al.*, 1992), NT-3 binds to TrkC with high affinity and can bind to TrkA/TrkB with low affinity (Klein *et al.*, 1991b; Lamballe, Klein & Barbacid, 1991; Soppet *et al.*, 1991). All NTs can bind to p75NTR with equal affinity. p75NTR also has the ability of binding with pro-neurotrophins with a much higher affinity than the mature forms (Lee *et al.*, 2001) (Figure 1.3).

The neurotrophins are structurally homologous proteins and have very similar gene sequences (Hallböök, 1999; Skaper, 2008). All NTs are first synthesised as full length pro-neurotrophins (approximately 30kDa). Pro-neurotrophins form homodimers, are biologically active, and can have profound effects on cellular

function (Lee *et al.*, 2001). Following synthesis and modification in the ER, pro-neurotrophins have one of two pathways to follow; either cleavage by furin and proconvertases, or transported out of the cell uncleaved. The uncleaved pro-neurotrophins are then either extracellularly cleaved by metalloproteases or plasmin, or rarely uncleaved (Schweigreiter, 2006). After cleavage of the pro-domain, they are known as mature NTs which continue to exist as homodimers of approximately 26kDa (Lee *et al.*, 2001).

1.5.2 Neurotrophic Factors

Apart from the ‘classic neurotrophins’ (NGF, BDNF, NT-3 and NT-4/5), there are other potent neuronal molecules called ‘neurotrophic factors’. Many neurotrophic factors were originally discovered in non-neural tissue, but have shown to have a vast array of actions in neurons including, survival, proliferation, differentiation and arborisation.

For example, GDNF (Glial cell-line Derived Neurotrophic Factor) is a neurotrophic factor that in motor neuron cultures is 75x more potent than any of the classic neurotrophins in supporting cell survival (Henderson *et al.*, 1994).

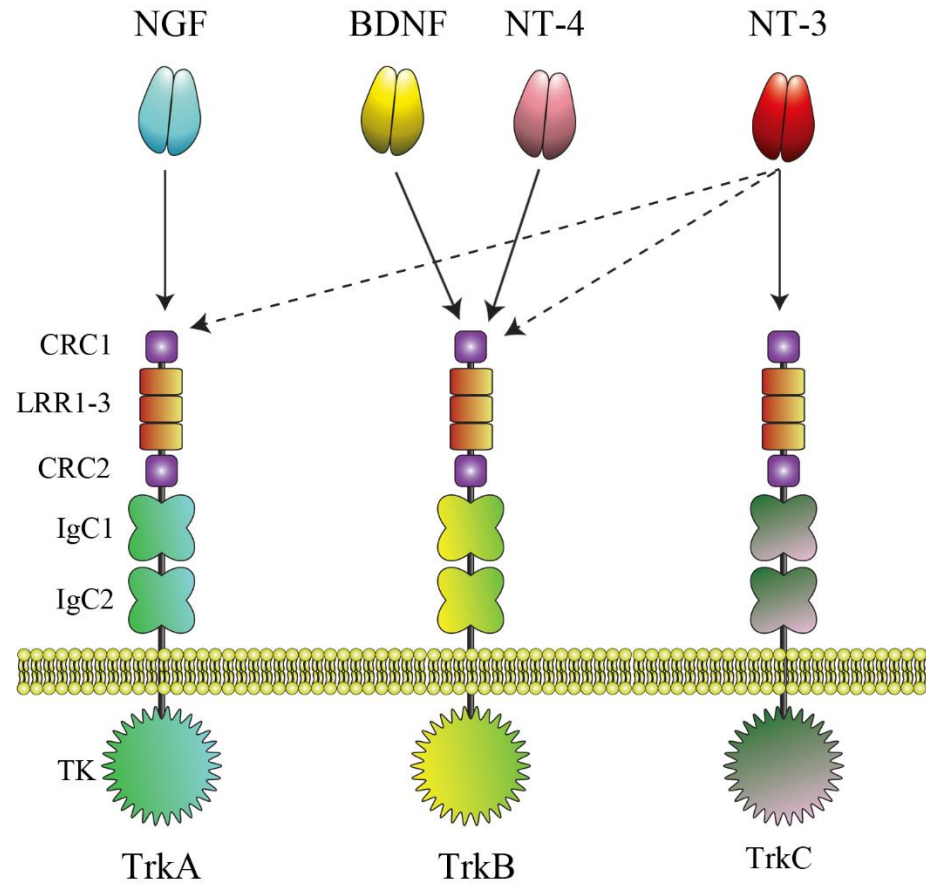
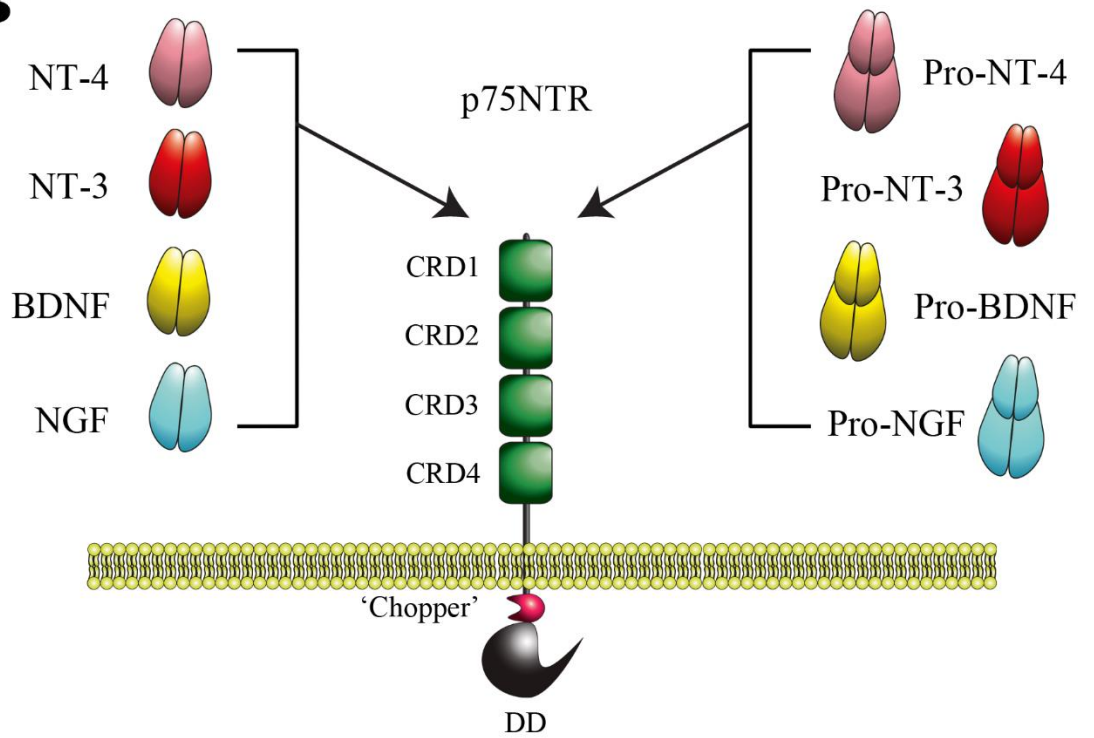
GDNF belongs to the GFL (GDNF-Family of Ligands), along with artemin (ARTN), neurturin (NRTN) and persephin (PSPN), which bind to their cognate co-receptors GFR α 1-4 (GDNF family-receptor α) (Airaksinen & Saarma, 2002).

Similar to neurotrophins, the GFLs exist as a

Figure 1.3 Structure and binding of Trk receptors and p75NTR

(A) the three Trk receptors (TrkA, TrkB and TrkC) all share a structural homology, containing, from the N-terminus extracellular domain; a cysteine rich cluster (CRC1), three leucine rich repeats (LRR 1-3), a second cysteine rich cluster (CRC2), two immunoglobulin-like domains (IgC1, IgC2), a single transmembrane region and a tyrosine kinase domain at the in the intracellular COOH end (TK). The second immunoglobulin-like domain is where each neurotrophin binds to their respective receptor.

(B) the structure of p75NTR is well conserved across many vertebrate species (including human, mouse, rat, cat, quail and to some extent frog). The receptor has an extracellular domain made up of four sets of six cysteine repeat residues (CRD1-4), with the second, third and fourth being important for neurotrophin binding, an juxtamembrane region (Chopper) linked to death signalling, and an intracellular death domain (DD), which is similar to the death domains of other tumour necrosis family receptor (TNFR) members.

A**B**

homodimer and upon binding to GFR α 1-4, causes dimerisation of the co-receptor. The GFL-GFR α then binds to two RET (rearranged during transfection; a receptor tyrosine kinase for the GFLs) receptors causing auto-phosphorylation, and subsequent downstream pro-survival signalling (Jing *et al.*, 1996; Trupp *et al.*, 1996; Airaksinen, Titievsky & Saarma, 1999; Takahashi, 2001). Through its receptors (GFR α and RET), GDNF has been shown to support the survival of cultured motor neurons and rescue over 90% of lesioned facial motor neurons after direct application of GDNF (compared to 29% non-treated) (Henderson *et al.*, 1994). GDNF expression via pDNA delivery has also been shown to rescue over 90% of axotomised hypoglossal nerves in rats, compared to non-treated controls (Barati *et al.*, 2006).

HGF (Hepatocyte Growth Factor) is another neurotrophic factor that has neuro-protective properties. Similar to GDNF, HGF promotes survival of embryonic motor neurons *in vitro* (Ebens *et al.*, 1996) and also *in vivo* after direct application to axotomised hypoglossal neurons (Okura *et al.*, 1999). HGF signals through its receptor c-met, a proto-oncogene linked with a variety of cancers, and activation can initiate potent survival mechanisms (e.g. P13K) (Bottaro *et al.*, 1991; Trusolino & Comoglio, 2002). Interestingly, overexpression of HGF in SOD1^{G93A} mice attenuated motor neuron death, reduced axonal degeneration and increased life span (Sun, Funakoshi & Nakamura, 2002). In spinal cord injury models in primates, intrathecally administered rhHGF preserved corticospinal fibers and promoted recovery in motor actions (Kitamura *et al.*, 2011)

1.6 Neurotrophin Receptors

1.6.1 *Tropomyosin receptor kinase*

As previously mentioned, the classic neurotrophins have cognate receptors called tropomyosin receptor kinases (Trk). The three Trk receptors include; TrkA, TrkB and TrkC. The Trk receptors, along with their neurotrophins, are part of the ‘Neurotrophin Hypothesis’, in which during development, multiple neurons compete for target derived trophic factors, allowing for selective cell survival and cell death (Hamburger, 1934; Hamburger & Levi-Montalcini, 1949; Levi-Montalcini, 1987; Bennett, Gibson & Lemon, 2002; Deinhardt & Chao, 2014).

1.6.1.1 *Structure*

The three Trk receptors; TrkA (Martin-zanca *et al.*, 1989), TrkB (Klein *et al.*, 1989) and TrkC (Lamballe *et al.*, 1991) share a structural homology containing, from the N-terminus extracellular domain, a cysteine rich cluster, three leucine rich repeats, a second cysteine rich cluster, two immunoglobulin-like domains, a single transmembrane region and a tyrosine kinase domain at the intracellular COOH end (Schneider & Schweiger, 1991) (Figure 1.1A). The second immunoglobulin-like domain is where each neurotrophin binds to their respective receptor (Ultsch *et al.*, 1999).

All Trk receptors have alternative splicing variants. These variants are naturally occurring and result in different isoforms of the receptors, which can change their signalling within a cell (Skaper, 2012; Deinhardt & Chao, 2014).

1.6.1.2 Signalling

Ligand binding and subsequent signalling of Trk receptors requires mature neurotrophin homodimers. It has been proposed, although never clearly demonstrated, the binding of ligand to Trk causes the receptor to homodimerise, bringing together the intracellular tyrosine kinase regions, forcing autophosphorylation of the two Trk receptors and driving intracellular messaging (Jing, Tapley & Barbacid, 1992; Stephens, 1997). In general, activation of Trk receptors usually has a positive effect on the cell. Effects of Trk receptor activation include, cell survival signalling, cell differentiation, precursor growth and arborization, synapse formation and synaptic plasticity (Deinhardt & Chao, 2014). Activation of Trk receptors triggers downstream signalling pathways such as, phospholipase C- γ (PLC- γ), Ras-mitogen-activated protein kinase/extracellular signal-related kinase (MAPK/ERK) and phosphatidylinositol 3-kinase (PI3K) (Huang & Reichardt, 2003; Skaper, 2012; Deinhardt & Chao, 2014).

1.6.2 pan 75 Neurotrophin Receptor (p75NTR)

The common neurotrophin receptor, pan 75 neurotrophin receptor (p75NTR), can cause the full spectrum of functional outcomes within a cell. First described as a receptor for NGF (Herrup & Shooter, 1973), over the years it has been shown to be able to bind all mature neurotrophins (Rodriguez-Tebar, Dechant & Barde, 1990; Squinto *et al.*, 1991; Rydén & Ibáñez, 1996) and their proform (pro-

neurotrophins) with high affinity (Lee *et al.*, 2001). The signalling pathway activated by the binding of neurotrophins to p75NTR is altered in the presence or absence of the tropomyosin receptor kinase (Trk) family of tyrosine kinase receptors. p75NTR is able to interact with Trk receptors to allow neurotrophins to bind with a higher affinity, as first demonstrated with NGF (Hempstead *et al.*, 1991). p75NTR is expressed in a wide variety of cells, both neuronal and non-neuronal, during embryonic development and is heavily reduced postnatally. However, it can be re-expressed after trauma and disease, again in neuronal and non-neuronal tissue (Roux & Barker, 2002), but most interestingly in motor neurons in MND and MND model mice (Lowry *et al.*, 2001; Copray *et al.*, 2003).

1.6.2.1 Structure

p75NTR is a type I transmembrane receptor with a molecular weight of approximately 75kDa (Grob *et al.*, 1985; Johnson *et al.*, 1986). The structure is well conserved across many vertebrate species (including human, mouse, rat, cat, quail and frog). The receptor has an extracellular domain made up of four sets of cysteine rich domains, with the second, third and fourth being important for neurotrophin binding (Yan & Chao, 1991; Baldwin & Shooter, 1995) (Figure 1.3B). These cysteine rich domains are conserved in the tumour necrosis family receptor (TNFR), a superfamily of over 20 receptors, in which p75NTR is the 16th member of (Itoh *et al.*, 1991; Smith, Farrah & Goodwin, 1994). Another similar domain that p75NTR shares with the TNFR family is the intracellular 'death domain' (Feinstein *et al.*, 1995). Deletion of the death domain has no effect on p75NTR's ability to cause cell death (Coulson, 1999), which is primarily

mediated by the cytoplasmic juxtamembrane region. The juxtamembrane region, named 'Chopper', is a 29 amino acid sequence that is able to cause caspase and calpain mediated cell death. This domain also has a palmitoylation site at cysteine 279 which can direct it to membrane lipid rafts essential for p75NTR mediated cell death (Barker *et al.*, 1994; Coulson *et al.*, 2000; Underwood *et al.*, 2008)

1.6.2.2 Signalling

The many biological outcomes that a cell undergoes after p75NTR activation are complex, diverse and conflicting. These outcomes rely on many different factors, such as co-expression with other receptors (such as the Trk receptors or Sortilin), cell type, time and age of expression (e.g. embryonic or adult organisms), the ligands present and the isoform of p75NTR expressed. Another level of complexity is added to this receptor's function when different combinations of the above factors cause an array of different physiological outcomes. The two most studied functions of p75NTR however have given it its brand of being a 'death receptor' and as a co-receptor to the Trk receptor family (Figure 1.4).

p75NTR's involvement in cell death was found in the early 90's in transfected neural cell lines (Rabizadeh *et al.*, 1993) but since then it's role in mediating cell death has expanded to primary cells *in vitro* and *in vivo*. Some of these findings include p75NTR mediated cell death in, cultured neonatal sympathetic neurons; a study which also showed that p75NTR is involved in naturally occurring cell death *in vivo* (Bamji *et al.*, 1998). Cultured sensory neurons have been found to be affected by p75NTR expression at particular perinatal periods, causing cell

survival during the earlier period of embryogenesis but switching to a cell death inducer at later stages, and even in the post-natal period (Barrett & Bartlett, 1994).

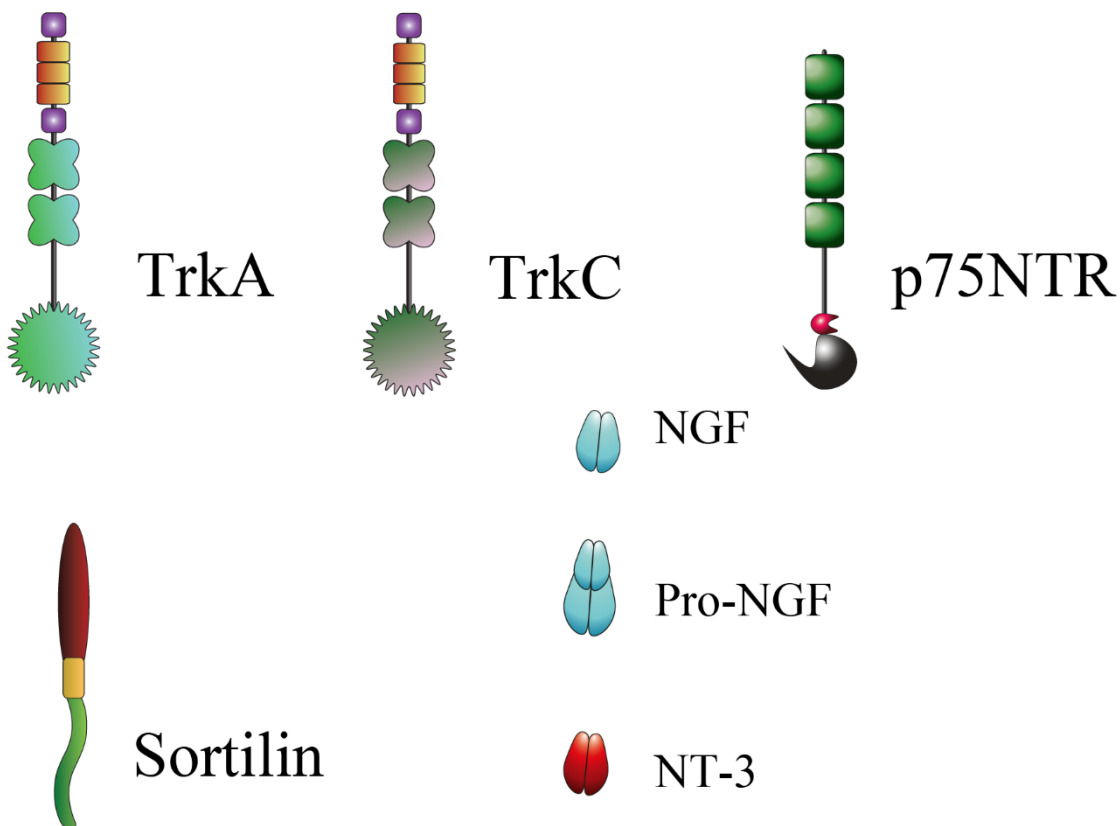
p75NTR can also influence motor neurons. Previous experiments have shown that the addition of NGF to cultured mouse embryonic motor neurons and rat embryonic spinal cord explants caused an increase in p75NTR mediated cell death, which is blocked by p75NTR antibodies (Sedel, Béchade & Triller, 1999; Wiese *et al.*, 1999). The addition of NGF to injured facial motor neurons in mice, which re-express p75NTR, caused an increase in cell death which was ablated in p75NTR KO mice (Wiese *et al.*, 1999). p75NTR driven cell death is not only confined to neurons, as it can also mediate cell death in both oligodendrocytes (Casaccia-Bonofil *et al.*, 1996) and Schwann cells (Soilu-Hänninen *et al.*, 1999). In the 2000 review by Kaplan and Miller, three prerequisites for p75NTR mediated cell death were proposed. The first is that cell death via p75NTR is ligand-mediated and its signal can be abolished if blocked. Second, the cell death is signalled in a Trk-survival-independent manner, with p75NTR causing death even in environments enriched in trophic molecules that work independently of Trk, such as CNTF (Davey & Davies, 1998). Finally the third, p75NTR mediated cell death occurs when Trk receptors are inactive or sub-optimally active. This led them to the conclusion that Trk activation silences p75NTR apoptotic signalling (Kaplan & Miller, 2000).

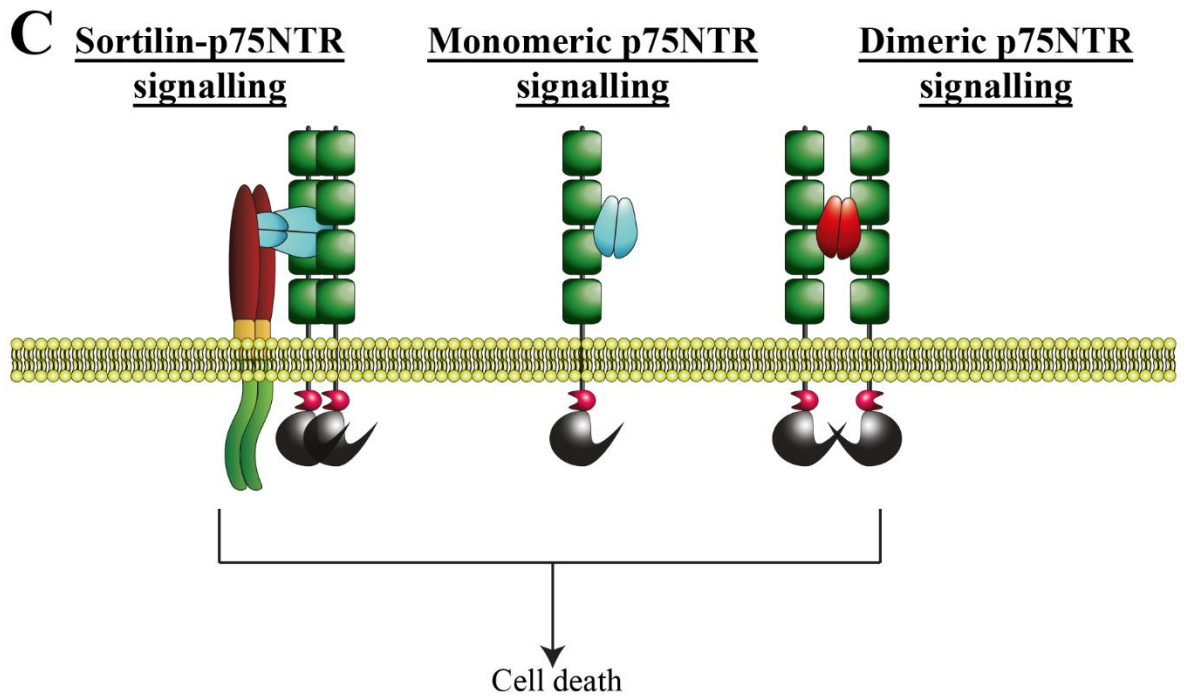
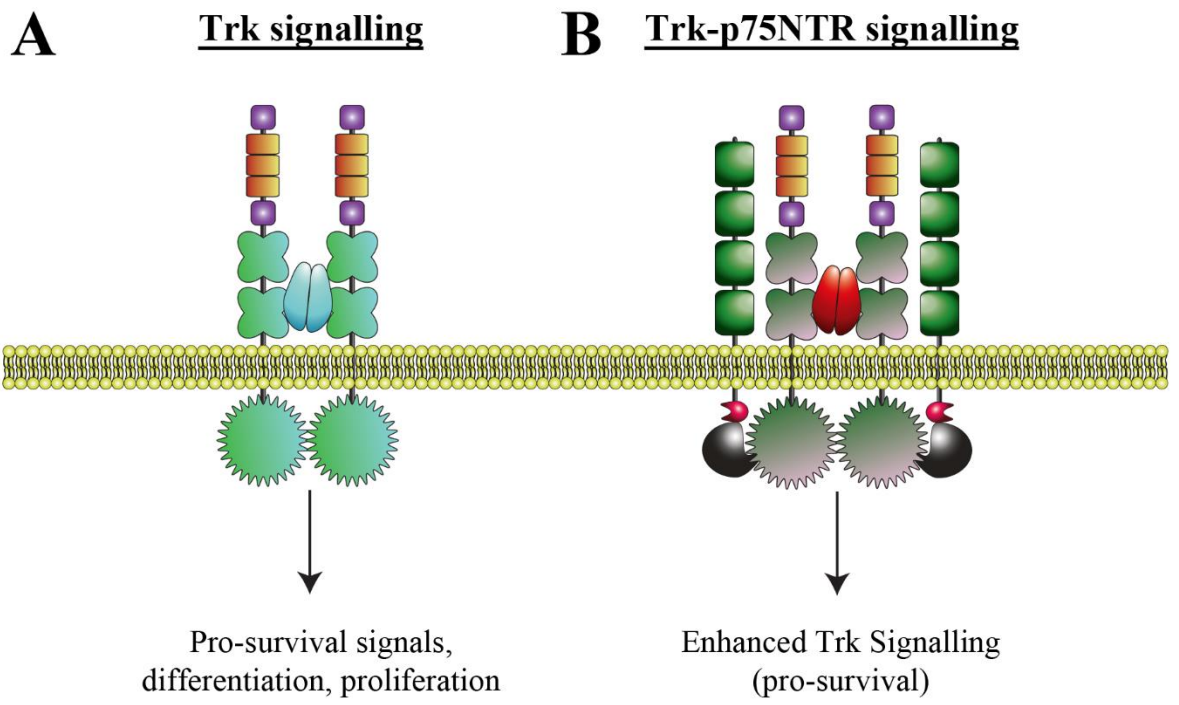
Figure 1.4 Signalling of Neurotrophin receptors

(A) Trk signalling requires a dimerised neurotrophin (such as NGF) to bind to a dimer of its cognate Trk receptor (such as TrkA). This causes the intracellular tyrosine kinase regions on the Trk receptors to interact and signal. Trk activation usually produces pro-survival, proliferation and/or differentiation signalling.

(B) Trk-p75NTR signalling also requires a dimerised neurotrophin and Trk receptor, as well as a p75NTR dimer. The addition of p75NTR to the structure causes the Trk signalling to be enhanced, having a more potent effect

(C) When p75NTR is activated by pro-neurotrophins (such as pro-NGF), it can form a double-dimer structure with sortilin, causing potent apoptotic signalling. Cell death signalling through p75NTR can also occur when the receptor binds to a neurotrophin as both a monomer and dimer.





p75NTR mediated cell death can be activated via several different p75NTR-interacting molecules. After ligand activation and subsequent cleavage of the p75NTR extracellular domain, the intracellular domain interacts with neurotrophin receptor interacting factor (NRIF) which is translocated to the nucleus causing cell death (Casademunt *et al.*, 1999; Kenchappa *et al.*, 2006). NRIF also increases Jun amino-terminal kinase (JNK) activation (Kenchappa *et al.*, 2010), which can be independently activated by ligand-p75NTR interaction causing cell death (Casaccia-Bonofil *et al.*, 1996; Yoon *et al.*, 1998). The neurotrophin receptor-interacting melanoma antigen (MAGE) homolog (NRAGE) is another p75NTR interacting molecule. This NRAGE/p75NTR interaction is mediated by, and competes with, Trk expression and binding, causing cell cycle arrest and death (Salehi *et al.*, 2000). p75NTR-associated cell death executor (NADE) is another p75NTR cell death initiator, however, it appears that this mechanism of cell death relies on NGF binding to p75NTR and is not activated by any other p75NTR/neurotrophin binding (BDNF, NT-3, NT-4/5) (Mukai *et al.*, 2000).

Regardless of the downstream mechanisms of p75NTR mediated cell death, the cleavage of the p75NTR extracellular domain (p75NTR^{ECD}) and release of the intracellular domain in the cytoplasm (p75NTR^{ICD}) is required to trigger apoptosis (Underwood *et al.*, 2008). However, in studies which have overexpressed p75NTR *in vitro*, increased cell death was seen, indicating unnaturally high levels of p75NTR expression is able to cause apoptosis (Roux *et al.*, 2001; Bhakar *et al.*, 2003). Of particular importance is the juxtamembrane region of p75NTR named 'Chopper'; a contributing factor to p75NTR mediated death (Coulson *et al.*, 2000). A specific series of events must take place before the death signals, such as

JNK and caspases, are activated. Firstly, a ligand (pro-neurotrophin, NGF, etc.) must bind to p75NTR^{ECD}. Following this, the receptor undergoes regulated intramembrane proteolysis (RIP), by the disintegrin metalloproteinase tumour necrosis factor- α -converting enzyme (TACE/ADAM17) (Weskamp *et al.*, 2004). This cleavage releases the extracellular domain into the circulation, leaving a membrane bound C-terminal fragment, which is further cleaved by presenilin-dependant γ -secretase, releasing the intracellular domain (Jung *et al.*, 2003; Kanning *et al.*, 2003). As mentioned earlier, activation of Trk receptors can override the cell death signalling of p75NTR (Kaplan & Miller, 2000). This may be because activation of the Trk receptors (specifically TrkA) is able to prevent membrane bound C-terminal fragments from being translocated to the lipid rafts, therefore inhibiting cell death (Underwood *et al.*, 2008).

Cell death is not the only signalling pathway for p75NTR. In conjunction with the Trk receptors, p75NTR can enhance pro-survival signals. This is because the p75NTR and Trk receptors (TrkA, B and C) form a complex (Bibel, Hoppe & Barde, 1999), and this p75NTR-Trk complex enhances affinity for neurotrophins to bind to their cognate receptors (i.e. NGF to TrkA) and diminishes affinity of other neurotrophins from binding and signalling (i.e. NT-3 to TrkA) (Esposito *et al.*, 2001; Mischel *et al.*, 2001). Interestingly, activation of p75NTR with NGF causes apoptotic signalling, however if p75NTR-NGF binding is disrupted in the presence of TrkA expression, binding and signalling of TrkA-NGF is diminished (Barker & Shooter, 1994).

The fate of the extracellular domain of p75NTR after ligand binding is not limited to receptor cleavage and release, but it can also be endocytosed and retrogradely transported to the cell body when bound to neurotrophins (e.g. NGF) (Saxena *et*

al., 2004). The destination of p75NTR after endocytosis and retrograde transport is dependent on the presence of neurotrophins. Motor neurons expressing p75NTR, bound to NGF, are retrogradely transported in motor neurons and escape lysosomal degradation (Lalli & Schiavo, 2002). Interestingly, motor neuron-like cell line, NSC-34 cells, show that the 'default' pathway for p75NTR after functional antibody activation is lysosomal degradation (55-80% of p75NTR vesicles co-localise with lysotracker, a marker of lysosomes), however in the presence of neurotrophins, p75NTR vesicles had a much lower co-localisation with lysotracker (NGF 5-20%, NT-3 20-30%, BDNF 30%, NT-4 50% colocalisation, unpublished data from our lab). Neurotrophins also have an effect on p75NTR receptor endocytosis dynamics, with NGF increasing the speed and amount of p75NTR internalised, while BDNF decreases speed and amount of p75NTR internalised (Matusica *et al.*, 2008).

1.6.2.3 *Expression and disease*

During development, p75NTR expression is highly prevalent in many areas of the nervous system; such as spinal motor neurons, thalamic nuclei, amygdala, sensory neurons, etc. In the adult brain, the expression is reduced to a few areas, including the basal forebrain and lower levels in the caudate and putamen. p75NTR is also expressed in the peripheral nervous system, in DRGs, some sympathetic, parasympathetic and enteric neurons. Non-neural mesenchymal cells within developing limb buds and some organs (lungs, kidneys and testes) express high levels of p75NTR during development, yet adult p75NTR expression is more

limited to some endothelial cells, perivascular fibroblasts and dental pulp cells (see; P A Barker 1998 for review).

p75NTR is re-expressed in both the brain (Gage *et al.*, 1989) and the spinal cord motor neurons (Ernfors *et al.*, 1989a; Rende *et al.*, 1995) after insult. Motor neurons also express p75NTR in high levels during development and post-natally, before being down-regulated by PND 10 (in rats, (Yan & Johnson, 1987, 1988; Ernfors *et al.*, 1989b)). p75NTR expression has also been linked to some neurodegenerative diseases. It has been shown that anti-psychotic drugs used to treat schizophrenia can not only down regulate the expression of p75NTR, but also increase SOD1 in PC12 cells, prolonging their survival (Bai *et al.*, 2002). In Alzheimer's Disease, basal forebrain neurons have been shown to not only have an increase in p75NTR expression (Mufson & Kordower, 1992), but p75NTR interacts with both the toxic A β peptide and its precursor (APP), which in turn has an apoptotic affect (Yu *et al.*, 2012).

Interestingly, p75NTR retrograde transport is hindered in SOD1^{G93A} MND sensory neurons (Bilsland *et al.*, 2010), but some receptor components, including most likely the intracellular domain, are increased in motor neurons (Perlson *et al.*, 2009).

1.7 Models for Motor Neuron Disease

1.7.1 NSC-34 cell line

The murine NSC-34 (neuroblastoma x spinal cord) cell line is used extensively as a cell culture substitute for primary motor neurons. It was created by fusing a neuroblastoma (N18TG2) cell line with embryonic spinal cord motor neuron cells (Cashman *et al.*, 1992). The NSC-34 cell line shares many properties with motor neurons, including, processer-like extensions similar to neurons, the ability to induce muscle twitching when co-cultured with myotubes, the generation of action potentials and the synthesis, storage and release of acetylcholine (Cashman *et al.*, 1992). Further analysis of this cell line revealed that there is expression of TrkB, TrkC, p75NTR, sortilin, VACHT (vesicular acetylcholine transporter) and GT1b (lipid raft-associated ganglioside) (Turner *et al.*, 2004; Matusica *et al.*, 2008). Because the NSC-34 cell line shares many characteristics with motor neurons, it is the most used cell model for studying MND, and can be easily and stably transfected with disease causing genes (e.g. SOD1^{G93A}) (Turner *et al.*, 2009).

1.7.2 E12.5 murine motor neurons

Primary motor neurons are the most appropriate *in vitro* models to use for investigating the properties of motor neurons. Isolating and culturing primary motor neurons however, is problematic in adult animals due to the difficulty of isolating them from the CNS after they have synapsed to their muscle targets. Embryonic motor neurons are easier to culture as they are present in larger

numbers, can be more easily isolated from the tissue and have not begun to penetrate peripheral tissue from the CNS. During E11-13, embryonic motor neurons express high levels of p75NTR (Ernfors *et al.*, 1989a). The expression of p75NTR on embryonic motor neurons allows them to be isolated, purified and cultured using an immunopanning technique (Wiese *et al.*, 2010). Briefly, this technique uses p75NTR antibody coated plates to capture p75NTR expressing motor neurons, which can then be removed from other cell types and cultured into pure motor neuron cultures.

1.7.3 Animal models

The discovery of mutations in SOD1 that cause MND led to the creation of an animal model, the SOD1^{G93A} mouse (Gurney *et al.*, 1994). The SOD1^{G93A} transgenic mouse model has become the most commonly used animal model to study MND. It is currently the only accepted model for pre-clinical testing. The SOD1^{G93A} mouse mimics many human MND pathologies, however the mice have been known to be highly variable which can lead to spurious results (Scott *et al.*, 2008; Kanning *et al.*, 2010; Peviani *et al.*, 2010; Perrin, 2014). The SOD1^{G93A} mouse has been genetically modified to express multiple copies of the human SOD1^{G93A} mutation. The two main strains of the SOD1^{G93A} mouse are known as the G1L strain and the G1H strain. The G1L strain has a low copy of the mutant human SOD1^{G93A} gene (8 ± 1.5 copies), whereas the more commonly used SOD1^{G93A} G1H line has a higher copy number of the mutant gene (25 ± 1.5 copies) (Gurney *et al.*, 1996). The G1L strain has less variability than the G1H strain, however, the G1L strain disease end-stage is ~260 days, where the G1H

stain end-stage is much earlier at ~150 days (Gurney, 1997; Kanning *et al.*, 2010). Methods and guidelines have been developed to reduce variability in the SOD1^{G93A} G1H strain, such as reducing gender variation by having a stable breeding background (Heiman-Patterson *et al.*, 2005), increasing sample sizes to reduce background statistical noise and being stringent with constantly monitoring of transgene copy number within a colony (Scott *et al.*, 2008; Perrin, 2014; Shepherd *et al.*, 2014). Other single point substitution variants of the SOD1 gene have produced additional MND mouse models with similar pathologies, such as the SOD1^{G85R} model, which causes rapid clinical symptoms in these mice (Bruijn *et al.*, 1997) and the SOD1^{G37R} (Wong *et al.*, 1995). However, these models have less transgene stability and are less well characterised by pathology and symptom timelines.

Separate to the SOD1 animal models is a TDP-43 MND mouse model (Prp-TDP43^{A315T}). These mice have shown similar clinical symptoms (e.g. abnormal gait, muscle weakness, weight loss) and pathologies (e.g. loss of descending motor neurons, large motor neuron ubiquitin aggregates, motor neuron loss) (Wegorzewska *et al.*, 2009) to MND/SOD1^{G93A} mice. However, these mutant-TDP-43-expressing mice show no TDP-43 motor neuron aggregates (a common hallmark for MND), in both the brain or spinal cord (Wegorzewska *et al.*, 2009) and the mice die prematurely from gastroenterological complications, which questions the suitability of this model for the study of MND (Hatzipetros *et al.*, 2014).

1.8 Treatments for Motor Neuron Disease

Currently, the only available approved treatment for MND is Riluzole, an anti-glutamate drug which prevents the release of glutamate from the pre-synapse, potentially alleviating cell death-causing excitotoxicity (Bensimon *et al.*, 1994). However, Riluzole has only been shown at best to prolong the life of an MND patient by 2-3 months, with little to no increase in quality of life or prevention of motor neuron death or muscle degradation (Miller *et al.*, 2012). All other treatments for MND are palliative care options. Palliative care extends to specialist wheelchairs and equipment, advice and intervention by specialists including, occupational therapists, nurses, physiotherapists, nutritionists and/or percutaneous endoscopic gastronomy and speech pathology, respiratory monitoring and non-invasive or invasive ventilation and general social work (Mitsumoto & Rabkin, 2007; Miller *et al.*, 2009). Multidisciplinary clinics which offer many or all of the high quality directed care options available to patients with MND have been shown to not only increase mental health of those with the disease, but also to extend life expectancy (Van Den Berg *et al.*, 2005; Rooney *et al.*, 2014).

There are currently many different therapeutic treatments using a wide variety of compounds in various pre-clinical and clinical phases targeting many different factors that are being assessed for use in MND. Some of these targets include mitochondria, immune system modulation, autophagy, glial cells (astrocytes and microglia), motor neurons, the neuromuscular junction and motor neuron innervated muscles (Bucchia *et al.*, 2015). Unfortunately, many treatments that have shown promise in pre-clinical animal testing (particularly with the

SOD1^{G93A} mouse model) have failed in human trials (Perrin, 2014). Many of the problems with translation of treatments into humans are likely to have been due to the variability inherent in the SOD1^{G93A} mouse, both between laboratories and within colonies. These inconsistencies have caused the creation of strict guidelines for pre-clinical testing within this model (Scott *et al.*, 2008; Ludolph *et al.*, 2010). Practically all previously positive published treatments showed no improvement to life span in these mice (with some having a negative effect) when applied within the guidelines (Perrin, 2014). There are however, a few treatments currently underway in phase 2-3 clinical trials showing promise.

For example, Rasagiline is an anti-apoptotic drug targeted at mitochondrial permeability and survival, has achieved an increase of life span of 20% in SOD1^{G93A} mice when given in combination with Riluzole (Waibel *et al.*, 2004) (ClinicalTrials.gov identifier: NCT0123273).

A drug targeting the NMJ, the monoclonal antibody Ozanezumab, targets Nogo-A which is an inhibitor of neural outgrowth and is increased in expression in MND muscle. Ozanezumab has shown decreased neurite growth inhibition and is safe in humans (Weinmann *et al.*, 2006; Meininger *et al.*, 2014) (ClinicalTrials.gov identifier: NCT01753076).

However, the overall consensus is that MND pathology is multifactorial and that a single treatment targeting a specific aspect of the disease will not be a 'cure-all'. Treating MND is made more difficult, as motor neuron cell bodies are protected by the blood brain barrier. One way to address the multiple facets of the disease is to prevent motor neuron cell death completely, by initiation or activation of pro-survival pathways, such as with potent neurotrophic factors (GDNF, IGF, HGF,

etc.). This can be accomplished with the delivery of pDNA that over expresses these trophic factors or for familial cases, silences toxic/mutated protein synthesis. Gene therapy is therefore a potentially powerful therapeutic approach for MND and many other neurodegenerative diseases.

1.9 Gene Therapy

Gene therapy is the introduction of exogenous genes to a host system as a method for disease treatment. Gene therapy has the potential to be a treatment for both genetic and non-genetic diseases. Gene therapy has two mechanisms in which it can influence host DNA; increasing or decreasing specific gene expression, and introducing or silencing specific gene expression. With the already aforementioned mutations involved with MND, gene therapy has the potential to treat this disease. However, the safe and successful mode of administration and transfection of the exogenous nucleotides is still a difficult process to overcome. Currently, gene therapy is split into only two delivery mechanisms; viral and non-viral.

1.9.1 Viral gene delivery

Viruses, in most cases, have the natural ability to avoid the immune system, cross the blood brain barrier (BBB) and insert DNA into a host genome. These traits have evolved and been refined over millions of years of evolution so that taking advantage of these traits is one of the strengths of using viral gene therapy. A

study in Parkinson's Disease model primates showed that delivery of adeno-associated virus (AAV) was able to stably transfect large populations of neurons in the brain with L-amino acid decarboxylase (L-dopa to dopamine enzyme). The transfection persisted for eight years, did not cause neuro inflammation and increased clinical behaviour scores when treated with L-dopa (Hadaczek *et al.*, 2010). In relation to MND, several studies using virus vectors have been used to deliver the growth and survival factors IGF-1 (Kaspar *et al.*, 2003; Dodge *et al.*, 2008), GDNF (Acsadi *et al.*, 2002; Wang *et al.*, 2002) and VEGF (Azzouz *et al.*, 2004; Dodge *et al.*, 2010) to SOD1^{G93A} mice which rescued motor neurons and delayed symptom onset. Other studies delivered interfering RNA (iRNA) to SOD1^{G93A} mice to down regulate toxic SOD1 production, which extended life and reduced neurodegeneration (Ding *et al.*, 2003; Ralph *et al.*, 2005; Raoul *et al.*, 2005; Xia *et al.*, 2006). These studies showed promise in MND animal models. However, applying viral gene therapy to humans has the risk of unwanted immunogenicity and more importantly, genotoxicity.

Viral vectors can cause adverse immune responses and the dependence on immunosuppressors (Wu & Ertl, 2009), and more severely, genotoxicity via oncogenesis (Kustikova, Brugman & Baum, 2010). One unfortunate study outcome after viral gene therapy caused five children who had X-linked severe combined immunodeficiency disease (X-SCID) to develop lymphoma (Woods *et al.*, 2006). Before *in vivo* use, viral vectors have their pathogenic and replication genes removed (Wu & Ertl, 2009), yet there is still a chance of long term oncogenesis due to accidental insertional mutagenesis, as lymphomas in the X-SCID study did not appear until 2-3 years after treatment (Woods *et al.*, 2006).

1.9.1.1 Adeno-associated virus (AAV)

Adeno-associated virus is a small (~20nm), low plasmid size (4.7kb max loading) virus that requires co-infection with another virus (such as adenovirus) in order to replicate (Lentz, Gray & Samulski, 2012). The virus is currently the most used viral vector in gene therapy. It has been shown that recombinant viral vectors from AAV are able to stably transfect rat cortical neurons for up to six months after systemic injection, and for even greater than 6 years in primates (Klein *et al.*, 1999; Hadaczek *et al.*, 2010). As a vector, AAV can be rapidly taken up by neurons in the brain within minutes (Bartlett, Samulski & McCown, 1998). The AAV has been shown to be very safe in terms of tumorigenesis. In a study which used over 600 mice that were subjected to several serotypes of the AAV, only one tumour was found, which had almost no expression of the associated transgene (Bell *et al.*, 2005). These attributes, along with the ease of mass production of this vector, make it the clear leader for viral gene therapy. The major detriment however is the small loading capacity and the non-specific nature of cells transfected (Lentz *et al.*, 2012).

1.9.1.2 Retrovirus

Retroviruses are a family of viruses that are about 100nm which can be split into two different categories; simple and complex - with vectors being created from both. Simple variants require the cell to undergo mitosis for replication, while complex variants are able to replicate in quiescent cells, which makes them

attractive for neural gene therapy (Lewis & Emerman, 1994; Lentz *et al.*, 2012). Even though gutted retroviruses have been created with only the delivery mechanism still in place, which allows up to ~8kb of space for exogenous cargo, retroviruses potentially insert themselves into host genomes (Zufferey *et al.*, 1998). In one respect, this is a positive attribute, as it allows for longer transcription. However, it also runs the risk of mutagenesis. The lymphomas created in the X-SCID case mentioned above were due to a retrovirus (lentivirus) insertional mutagenesis of the viral vector (Woods *et al.*, 2006). This has led to the slowing of progress in using these vectors in clinical settings.

1.9.1.3 Adenovirus

Adenoviruses are a lesser used viral vector, but are still viable for viral gene therapy. They are between 70-100nm in size and have a genome of ~36kb. Adenoviral vectors made from gutted viruses have been shown to transfect liver cells of baboons for up to two years (Morrall *et al.*, 1999). However, adenoviral vectors are notorious for having high immunogenicity and toxicity. Gutted adenovirus vectors have a propensity to activate the innate immune system, particularly macrophages, which clear the viral particles. They can also activate the adaptive immune system, causing cytotoxic T-cell response and potentially destroying transfected cells, as they are recognised as ‘not-self’. This may actually have benefits in treating cancers with adenoviruses, as they can direct the

immune system to destroy unwanted cells (Bessis, GarciaCozar & Boissier, 2004; Lentz *et al.*, 2012)

1.9.2 *Non-viral gene delivery*

Non-viral gene delivery encompasses every other type of gene therapy that does not involve a virus as a vector. Non-viral gene delivery is considered much safer and more specific than viral gene delivery, however the transfection rate is significantly lower (Pérez-Martínez *et al.*, 2011). The difficulty with non-viral gene therapy is that the technology must be completely synthesised from non-viral components, while viral gene therapy is already equipped with the ability to transfect cells. The delivery of genetic material can be broadly classified into two classes; physical (where the cargo is forced into the cell) and chemical (where the cargo is actively brought into the cell).

1.9.2.1 *Gene guns*

Gene guns are machines that ‘shoot’ genetic material into cells. Gold particles are coated in DNA (usually a plasmid) and shot out of a helium propelled ‘gun’. The gold particles containing the DNA bombard the cells and penetrate the cytoplasm and/or the nucleus, delivering a payload of genetic material. They are primarily used in plant-based transfection, where blasting the leaves is adequate for transfection. The ‘guns’ themselves are expensive to run, take special training to use and the gold particles do not degrade, which may lead to undesired side

effects. Gold particle substitutes that are biodegradable are currently being tested, such as the cationic polysaccharide chitosan. The ballistic nature of gene guns, while able to penetrate into nuclei of cells, does cause a significant damage (including death) to cells that are at the epicentre of the blast. Also, due to transfection being limited to the ‘shotgun effect’ delivery method, there is no specificity to the target and, since most of this work is used on the skin, there is a strong immune response, due to the large number of immune cells (e.g. dendritic cells) in the skin (Huang *et al.*, 2009).

1.9.2.2 Electroporation

Electroporation uses electric pulses to cause holes, called pores, in the cell membrane. The pores caused by the electric stimulation allow large molecules such as DNA, to enter the cell. After stimulation and incubation with DNA, cells are left to recover. Depending on the voltage that the cells are subjected to, the membrane may or may not heal. This is split into ‘reversible’ and ‘irreversible’ electroporation. Each cell and cell type has a different electroporation threshold, which determines whether or not the cell can recover (Neumann, Schaefer-Ridder & Wang, 1982). Electroporation was originally only used *in vitro*, but has had successful transfections in skin, kidney, lung, liver, skeletal muscle, cardiac muscle, brain, retina cornea and vasculature systems *in vivo* (Wells, 2004). Due to the ability to kill cells, electroporation can also be used for other applications such as a treatment for killing cancers and tumours with irreversible electroporation (Miller, Leor & Rubinsky, 2005; Al-Sakere *et al.*, 2007). This technology has a

high risk when used in humans, as the voltages needed must be at a level which can prevent permanent damage, yet still deliver a payload.

1.9.2.3 Pressure

Forcing particles, such as genetic material, into cells can be achieved using high pressure. This has been shown to be successful in transfecting liver cells. High volumes of plasmid can be rapidly injected into the tails of mice, causing high transfection efficiency (hydroporation). The large injection causes irregular heart function, sharply increasing venous pressure. The increase in pressure forces the fenestrae in the liver sinusoids to enlarge, increasing hydrostatic pressure in the liver and causing pores to form on cell membranes (Zhang *et al.*, 2004). This method has been refined further with the use of catheter balloons. These balloons have been inserted into the veins of rabbit livers and primate arms concurrently with injections of naked plasmid. The balloons inflate causing a local increase in hydrostatic pressure, allowing the entry of plasmid DNA into the affected cells, with minimal discomfort (Zhang *et al.*, 2001; Eastman *et al.*, 2002).

1.9.2.4 Lasers and Magnets

Laser pulses are another tool that can increase the uptake of DNA plasmids into cells. It is proposed that infrared lasers are able to disrupt cell membranes, allowing the entry of exogenous cargo. Zeria and colleagues demonstrated this by injecting a mouse hind limb with naked DNA and subjected the injection to pulses of an infrared laser aimed 2mm under the skin. Compared to un-lasered

contralateral injections, which showed no transfection, the lasered injection sites showed a high transfection level (Zeira *et al.*, 2003).

Coupling DNA to magnetic particles and using magnetic fields to transfect cells is known as magnetofection. The physical force of magnetism is able to draw the DNA-magnetic particles into cells. Intriguingly, this can also be used *in vivo*. Rats and mice have been injected with the magnetofection agent DNA-transMAG^{PEI} into the ileo-caecal and stomach regions. Following injection, small magnets were placed under the injection sites for approximately 20 minutes. Histological analysis showed that injected animals that were exposed to the magnet treatment had high transfection, while non-magnetised animals had almost none (Scherer *et al.*, 2002). This technology, while efficient at transfection, is invasive and non-specific. The specificity of the magnetofection is limited to where the magnets are placed, which could lead to transfection of non-targeted cells.

The above techniques for physical transfection lack both cell specificity and are risky, due to the damage they can cause to cells (by forcing cargo through the cell membrane) or by inadvertently allowing unwanted or dangerous materials into the cells after pores are made in the membrane.

1.9.2.5 Polycations

Polycation polymers, such as polyethyleneimine (PEI) or poly-L-lysine (PLL) are very attractive non-viral vectors for gene delivery, due to their ability to condense DNA, conjugation readiness and the ability to escape degradation in cells. Since the discovery of PLL as an effective DNA binding agent, other successful cations

have been investigated, with the gold standard being that of polyethyleneimine (PEI) (Morille *et al.*, 2008).

The advantage of using cations are their ability to escape the endosome via the 'proton-sponge' hypothesis. Once the polyplex has been endocytosed, protons (H^+) are pumped into the endosome for acidification and subsequent degradation of cargo. However, the amine groups on polycations such as PEI buffer the protons, keeping the pH environment stable. With the high concentration of protons within the endosome, negatively charged ions (Cl^-) flow in to balance the charge. With the high ionic concentration within the endosome, osmosis causes it to swell and eventually burst, releasing the contents into the cytoplasm (Boussif *et al.*, 1995; Morille *et al.*, 2008).

Polycations are also able to condense and bind DNA easily, due to the negative charge of DNA and polycations positive charge. The smaller the DNA complex is, the increased mobility and decreased degradation it has (Morille *et al.*, 2008). Once the complex has entered the cell and escaped the endosome, the final step is penetrating the nucleus, which is difficult as it must pass through the Nuclear Pore Complexes (NPC), in the nuclear membrane. Neutrally charged molecules that are approximately less than or equal to 9nm in diameter can passively flow in and out of the nucleus, but larger molecules must be actively transported through the NPC. To date, approximately 39nm is the maximum size that has been found that can be transported through the NPC (Panté & Kann, 2002). Active entrance into the nucleus requires a nuclear translocator, such as karyopherins, a sequence of proteins that binds with several cytoplasmic proteins that chaperone molecules through the NPC (Won, Lim & Kim, 2011).

While PEI's high positive charge allows it to carry genetic cargo and act as a transfection agent, it is also a liability. The charge causes it to have high toxicity both *in vitro* (Boussif *et al.*, 1995) and *in vivo* (Ogris *et al.*, 1999).

The high positive charge makes it a target for proteins in the circulation. Serum proteins can bind to the cation complex and cause a charge change from positive to negative or neutral (Li *et al.*, 1998), which will in turn affect the endosomal escape if the complex made it to the target cells. More specifically, the PEI can bind fibronectin (ECM protein), fibrinogen (blood coagulate protein), erythrocytes and serum albumin (McLean *et al.*, 1997; Ogris *et al.*, 1999), which all form aggregates. Not only can these proteins alter the confirmation of the cation complex (exposing degradation sensitive cargo), but they can promote clearance, and worse yet, these clot-like aggregations can cause lethal embolisms especially in the small capillaries in the lungs (Litzinger *et al.*, 1996; Kircheis, Wightman & Wagner, 2001). The body's natural defence against foreign particles, the immune system, must also be avoided. Polycation complexes have been found to bind to complement system factors and activate the complement cascade (Plank, Mechtler & Jr, 1996; Ogris *et al.*, 1999). The complement system and/or immunoglobulins (IgG, IgM) can also stimulate the activation of the MPS (mononuclear phagocyte system) after binding to the cation complexes in circulation (Chonn, Semple & Cullis, 1992; Ogris *et al.*, 1999). The MPS can also passively clear particles that are greater than 100nm or particle aggregations (Li & Szoka, 2007).

1.9.2.6 Liposomes

Liposomes are artificial vesicles that are able to bind and store cargo in their lumen, and subsequently deliver the cargo to cells. Liposomes are made up of a bilayer of cationic lipids, which contain a positive charged head, a linker and a hydrophobic tail. The positively charged head interacts spontaneously with negatively charged cargo, such as DNA. The phospholipid bilayer then forms around the cargo, encapsulating it in this vesicle shape. This leaves a positively charged surface, which allows it to interact with cell membranes and be endocytosed (Felgner *et al.*, 1987; Pérez-Martínez *et al.*, 2011).

The positive charge on the cationic head of the liposomes allows it to readily interact with anionic receptors, such as glycosaminoglycans, and enter the cell. This attribute allows it to easily transfect cells *in vitro*, but is difficult *in vivo*, much like that of the polycations discussed above. The particle must be less than 100nm and have a neutral or protected surface charge to survive the circulation. The positive charge of the liposomes has the same problems as that of the polycations; targeted by the immune system, interaction and subsequent aggregation with serum proteins which are cleared by the MPS or cause blood clots in small capillaries. Serum proteins are also able to bind to the liposomes and disrupt its bilayer structure and stability (Opanasopit, Nishikawa & Hashida, 2002).

1.9.2.7 Carbon and silica complexes

New research using carbon nanotubes have revealed that they have potential as a genetic delivery agent as they are very malleable in their ability as a base, meaning other molecules can be anchored or incorporated in the structure. Unfortunately, knowledge of biological reactions with the nanotubes is still in its infancy and many properties of the tubes still need to be investigated, such as their potential high toxicity and insolubility (Pérez-Martínez *et al.*, 2011).

1.9.2.8 Chitosan

Chitosan is a polysaccharide that is derived from crustacean shells made up of randomly distributed *N*-acetyl-D- glucosamine and D-glucosamine monomers. It has tissue compatibility, is non-toxic and due to the high number of amines on the complex, it is able to bind and condense DNA (Hu *et al.*, 2012). Chitosan also has the added ability of being able to deliver cargo to cells when given orally. Mice fed a chitosan-plasmid complex in their diet, led to the transfection of cells that line the gut (Kai & Ochiya, 2004). Modifications to chitosan complexes can be achieved via the abundance of amine groups present. These amine groups allow simple conjugation, some of which include PEGylation, the addition of cell penetrating peptides and even nuclear localisation signals (NLS) to improve their nuclear penetration (Opanasopit *et al.*, 2009; Hu *et al.*, 2012). However, chitosan complexes can be large (greater than 100nm), which is not ideal for gene delivery and lack cell specificity, which leads them to have a generally low transfection rate. These issues are currently being addressed by biotinylating and conjugating

polycations to the chitosan, which seems to significantly increase transfection, while still keeping cytotoxicity low (Chung *et al.*, 2010; Hu *et al.*, 2012).

1.9.2.9 Toxins

Toxins, such as tetanus toxin, from the bacterium *Clostridium tetani* have been shown to bind to motor and sensory neurons, and utilise cell machinery to retrogradely transport back to the spinal cord (Stockel, Schwab & Thoenen, 1975) and escape the lysosome, without the need of a cation. The toxin is made of a light chain, responsible for intracellular activity, and a heavy chain, being responsible for the binding and internalisation aspects of the toxin. The toxin has been modified and made non-toxic by removing all but the C-terminal of the heavy chain, which is suitable for retrograde transport (Schiavo, Matteoli & Montecucco, 2000; Lalli & Schiavo, 2002). Due to its ability of being able to bind, endocytose, avoid degradation and be transported retrogradely, tetanus toxin C fragment (TTC) has been conjugated to neurotrophins and neurotrophic factors for the treatment of neurodegenerative diseases (Rogers & Rush, 2011).

1.10 The Immunogene

Several key issues have been mentioned within this review, including the following; MND causes the death of motor neurons either through a known genetic mutation or sporadically, neurotrophins/neurotrophic factors and their receptors can have profound effects on motor neurons, and finally that gene

therapy has great promise in the treatment of diseases. A potentially proficient way to bring all these ideas together is to use a technology called 'immunogenes'. This technology conjugates a monoclonal antibody to a PEGylated polycation, creating an immunoportor, which in turn electrostatically binds and condenses genetic cargo (DNA or RNA) creating an immunogene. The immunogene satisfies three of the four 'barriers for successful gene delivery'; electrostatically binds DNA via the positively charged polycation, has cellular and tissue specificity via the antibody, and disruption and escape from the endosome via the polycation. The only barrier the immunogene fails to overcome is nuclear translocation (Morris *et al.*, 2000), which can be achieved with special nuclear localisation signals on plasmid DNA cargo.

This technology has its roots in cancer treatment, by conjugation of an antibody to a toxin, referred to as an 'immunotoxin' (Vitetta *et al.*, 1983). However, to translate this into a therapeutic, such as attaching a genetic cargo, direct conjugation of DNA/RNA to an antibody will alter the genetic integrity and subsequently diminish or modify gene expression. Polycations, such as Poly-L-lysine (PLL) have been used to overcome this problem. PLL was used in the first ever targeted gene therapy study. A hepatocyte receptor ligand was coupled with PLL and then mixed with DNA to form a polyplex, which successfully delivered its cargo (Wu & Wu, 1987). This study showed the viability of polycations such as PLL, to bind to gene cargo, while not disrupting its ability to transfect.

The mechanism in which the immunogene complex, without any nuclear translocators, makes its way to the nucleus is not well understood. Currently, the leading hypothesis is that after endosomal escape, the complex diffuses to the nucleus and enters either passively or actively through the Nuclear Pore

Complexes. It has also been shown that the complex can and will break apart (immunoprotein from genetic cargo) during endosomal escape, leaving naked cargo free floating (Itaka *et al.*, 2004; Mishra, Webster & Davis, 2004; Konishi *et al.*, 2008). This system severely lacks specificity and if the complex does indeed break apart, then the nuclear penetration is even lower, as naked DNA diffuses a lot slower than when it is bound to a cation (Konishi *et al.*, 2008; Shim & Kwon, 2009). However, there are several ways in which entrance into the nucleus can be targeted, such as with the use of karyopherins.

Karyopherins are importins and exportins of the nucleus. The karyopherin importin beta translocates cargo into the nucleus by firstly binding to importin alpha which binds to nuclear localisation signals (NLS). NLS are one (monopartite) or two (bipartite) clusters of four or more lysine or arginine residues that allow proteins in/out of the nucleus (Morris *et al.*, 2000). By adding NLS to immunoprotein complexes, the transfection efficiency can be increased. However, the addition of the NLS must be done in a way that does not hinder the transfection efficiency. If the cargo is a drug, then the NLS should be non-covalently bound directly to it, or if the cargo is genetic in nature (e.g. plasmid DNA) the genetic NLS equivalent, a DTS (DNA Targeting Sequence) should be incorporated. A single NLS/DTS is all that is required on the cargo, as multiples will increase the nuclear import but interact with other cellular factors, overall decreasing the plasmids activity (Morris *et al.*, 2000; Won *et al.*, 2011; Rogers & Rush, 2012). The two most studied and used NLS are the monopartite SV40 large t-antigen NLS (PKKKRKV) and the bipartite nucleoplasm NLS (KRPAATKKAGQAKKKK) (Lange *et al.*, 2007; Duvshani-Eshet *et al.*, 2008). The SV40 NLS is a small, very simple five amino acid chain peptide that is easy

to use, has been shown to be adept at increasing nuclear entry and elicits a very low immune response (Ciolina *et al.*, 1999; Zheng *et al.*, 2006; Duvshani-Eshet *et al.*, 2008).

DNA targeting sequences (DTS) are a way for plasmids to be actively transported into the nucleus. The DTS, most commonly the SV40 enhancer, is a sequence on the plasmid that binds to cytoplasmic transcription factors. These transcription factors contain NLS (as they are active in the nucleus) and then transport the whole DNA complex into the nucleus. DTS has been shown to increase the transfection of many cell types including oligodendrocytes (Lam & Dean, 2010).

The immunogene has been used *in vivo* and shown to be successful at treating injured motor neurons. Barati and colleagues applied an immunogene directly to axotomised motor neurons in both neonate and adults, and showed almost complete ablation of cell death. The immunogene consisted of an p75NTR antibody conjugated to a PLL cation carrying a GDNF plasmid, as p75NTR is expressed on motor neurons after insult (Ernfors *et al.*, 1989a; Rende *et al.*, 1995), and GDNF has potent survival properties for motor neurons (Henderson *et al.*, 1994). This study showed that the non-viral immunogene is able to be as successful as a viral vector. A similar motor neuron injury study using a viral vector showed approximately 50% recovery after application (Baumgartner & Shine, 1998), while the immunogene study showed a 95% recovery. This shows that non-viral vectors for gene delivery, especially the immunogene technology, can be equal to viral gene therapy.

There are four main barriers to overcome, from injection into the system to target cells that a polycation complex must pass in order to deliver its genetic cargo.

Fortunately, the immunogene technology developed has almost overcome all these barriers. The circulation is the first obstacle that immunogenes must overcome after injection in order to deliver their payload. They must avoid the immune system and other serum proteins, to overcome both degradation and aggregation. These problems have been addressed by conjugating the polycation with PEG (polyethylene glycol). This acts as a stealth agent by masking the high positive charge resulting in extending the half-life of the complex in the circulation (Allen & Hansen, 1991; Ogris *et al.*, 1999). It must also be small enough to pass through the extracellular matrix to avoid phagocytes (less than 100nm), which is accomplished by the PEI condensation process (<90nm is size). Secondly, it must be able to bind and endocytose into its specific target, which is accomplished by the attached antibody (Rogers *et al.*, 2006). Thirdly, the complex needs to escape the endosome after endocytosis, achieved through the PEI and its ‘proton sponge’ effect, and finally make its way to the nucleus (Morris *et al.*, 2000; Kircheis *et al.*, 2001). Figure 1.5 illustrates the entire mechanism of the immunogene. What is advantageous about the immunogene is the function of the antibody attached. Upon specific binding, the antibody-directed immunogene is endocytosed into the cell. Considering that motor neurons re-express p75NTR during MND and the immunogene uses an internalising p75NTR antibody, the immunogene can bind and be endocytosed (Rogers *et al.* 2006). This allows the immunogene to be injected into systemic circulation, bind to axonal projections of the motor neurons in the periphery at the NMJ and be endocytosed into the cell body. This effectively uses the axon as a ‘tunnel’ to the somas in the CNS, bypassing the blood brain barrier. However, forcing the cargo to be trafficked to the nucleus is the last barrier that needs to be overcome. By using a plasmid that

has a DTS incorporated into the construct, the four barriers of gene delivery can be overcome.

An alternative to transporting plasmid DNA as the cargo is to replace it with a functional RNA, such as siRNA (small interfering RNA) or miRNA (micro RNA). RNA has the advantage of not needing to be imported into the nucleus.

Once the immunogene has escaped the endosome, the siRNA is able to enter the RISC (RNA-induced silencing complex) and cleave the complementary mutant RNA produced by the cell, effectively silencing further protein expression (Rogers & Rush, 2011). A downside to this approach is that applications of the therapy must repeatedly be given.

In summary, there is need for a treatment for MND. Non-viral gene therapy has the potential to be a robust, safe and effective therapeutic, which is not limited by disease subtype (i.e. sporadic or familial). The immunogene technology has the potential to fulfil this need as it is able to overcome the four barriers of successful gene delivery to prevent motor neuron death.

In a series of experiments described in this thesis, the hypothesis that p75NTR is a viable target for gene delivery to motor neurons will be explored. To answer this hypothesis, both neonatal mice and adult SOD1^{G93A} mice will have their spinal motor neurons analysed for p75NTR expression, before testing the transfection efficiency of the intraperitoneally injected MLR2-PEI-PEG12 immunogene (Figure 1.6).

Figure 1.5 Mechanism of the Immunogene

The mechanism of the immunogene is a multi-step process which relies on the 'proton sponge' theory.

- (1) After application of the immunogene (either *in vitro* or *in vivo*), the MLR2 antibody component of the immunogene binds to cell surface p75NTR
- (2) The MLR2 antibody causes the receptor and entire immunogene complex to be internalised into the cell
- (3) The default pathway for the MLR2-p75NTR interaction is to be degraded in the lysosome, and as such, H⁺ ions are pumped into the endosome to acidify the contents
- (4) The PEI component of the immunogene buffers the H⁺ ions, preventing degradation
- (5) Due to the high positive ionic concentration within the vesicle, Cl⁻ ions are pumped in
- (6) Osmosis drives water into the vesicle, due to the high ionic concentration
- (7) The influx of water into the vesicle causes it to rupture, spilling its contents into the cytoplasm
- (8) The plasmid DNA containing a DTS (DNA targeting sequence) interacts with cytoplasmic proteins containing NLS (Nuclear Localisation Sequences), which chaperones the pDNA into the nucleus via importins α and β

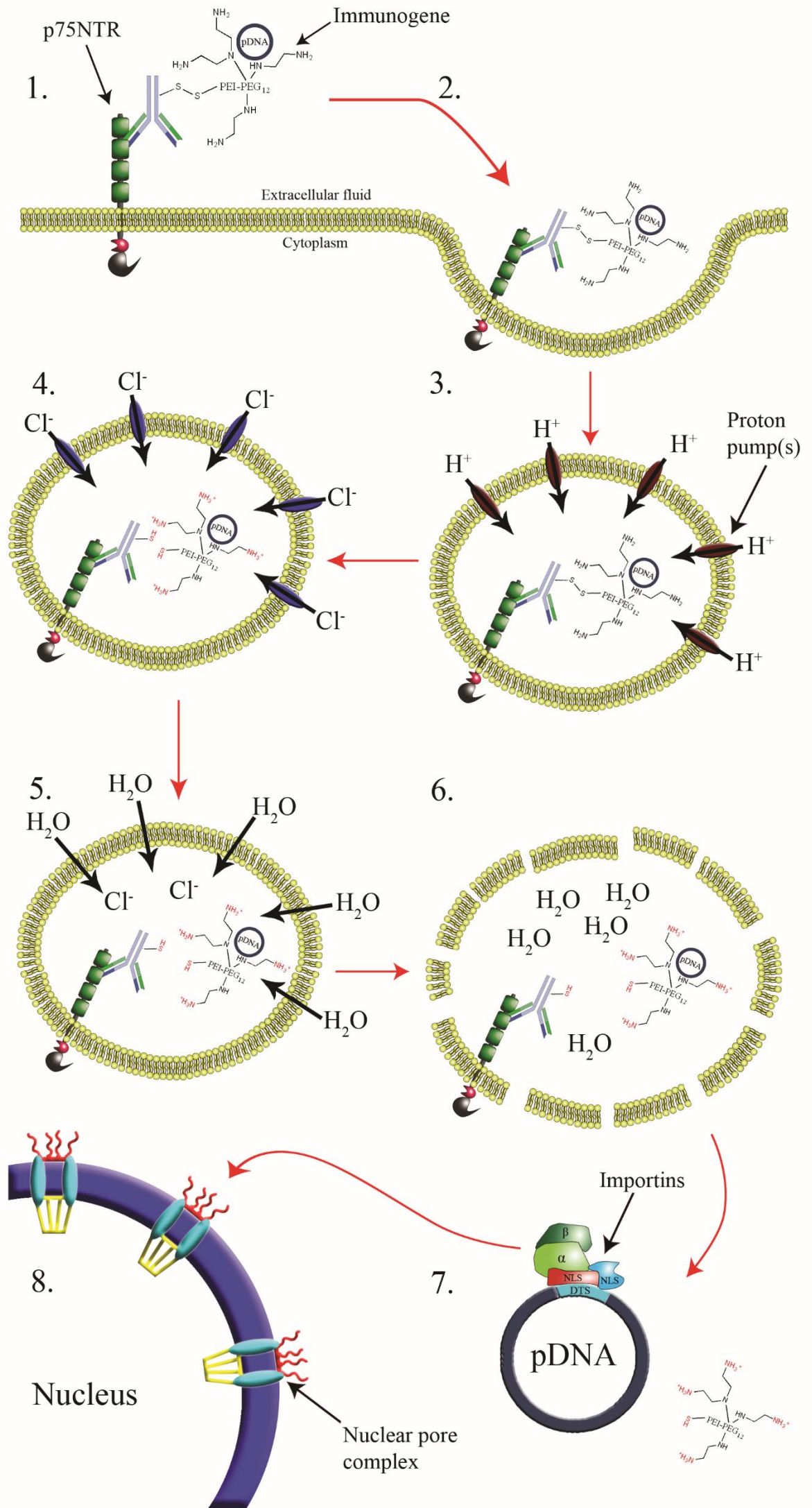
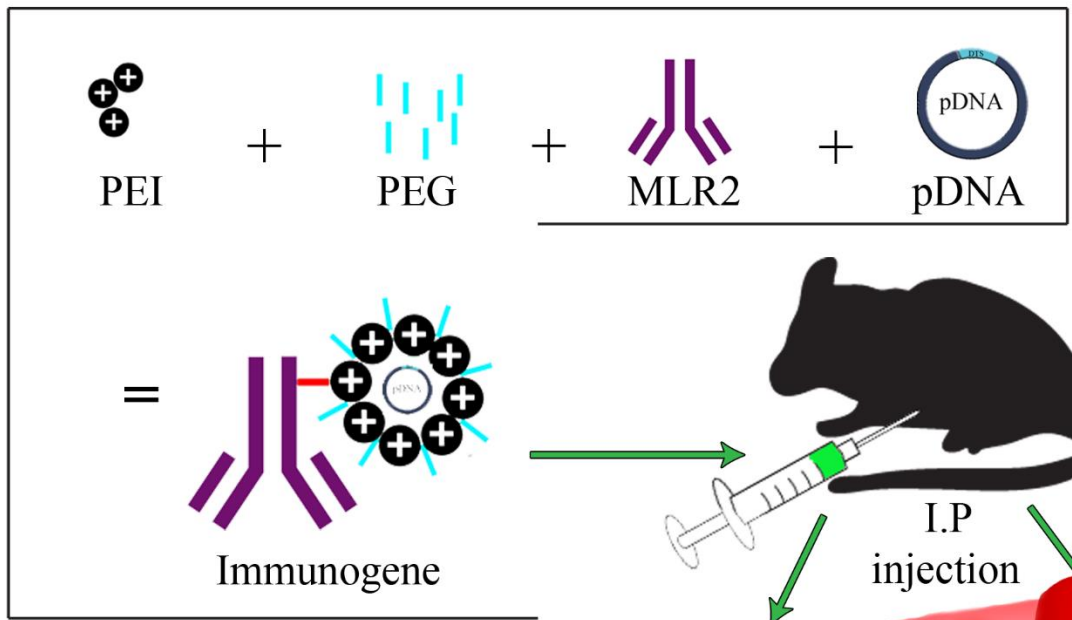


Figure 1.6 Overall plan of the Immunogene

The overall plan for the use of the immunogene is to first synthesize the entire construct, including the pDNA containing the DTS, inject it into both neonatal mice (with high motor neuron p75NTR expression) and adult SOD1^{G93A} mice (with motor neuron p75NTR re-expression), intraperitoneally. The immunogene will diffuse into the circulatory system, where it will bind to p75NTR at the neuromuscular junction, via the MLR2 antibody. The complex will be internalised into the motor neuron and be retrogradely transported back to the cell soma, where it will escape the endosome, delivering the pDNA to the cell nucleus expressing GFP (green fluorescent protein).



Blood vessel

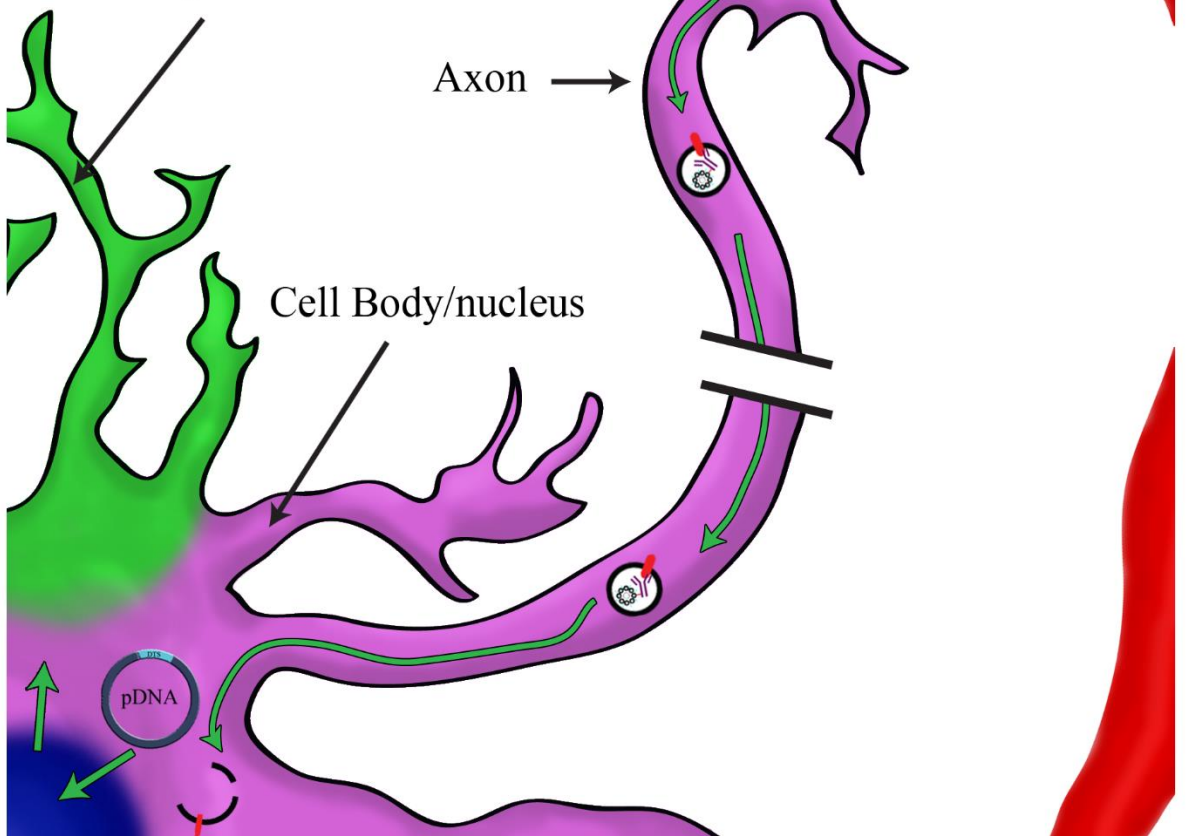
Muscle

Neuromuscular junction

GFP expression

Axon

Cell Body/nucleus



Chapter 2: Materials and Methods

2.1 Materials

2.1.1 Cell Culture

Dulbecco's Modified Eagle Medium (DMEM, #11965), Penicillin/Streptomycin/Glutamine (PSG, #15140-122), Glutamax I (GX; #35050-061), Hank's Buffered Salt Solution (HBSS, #14170), Natural Mouse Laminin (#23017-015), 0.05% Trypsin-EDTA 1X (#25300), 0.05% Trypsin-EDTA 10X (#15400), Neurobasal (NB, #2110), B27 (#17504-044), Horse serum (#26050-088), Minimum Essential Media (MEM, #10370), 4-(2-hydroxyethyl)piperazin-1-ethanesulfonic acid (HEPES, #15630-080), Roswell Park Memorial Institute 1640 media (RPMI, #61870-036), Hypoxanthine and Thymidine supplement (HT, #11067-030), were all from Invitrogen Life Technologies (Melbourne, Australia). Trypsin inhibitor (#T9253), 2-Mercaptoethanol (#M7154), Poly-L-Ornithine (PORN; #P4957), Donkey Serum (#D9663), were all from Sigma-Aldrich (Castle Hill, Australia). DNase (#104159), Hybridoma Fusion and Cloning Supplement (HFCS, #11363735001) was from Roche Diagnostics Australia. Recombinant human BDNF (#14-836-580) was from eBioscience (San Diego, California). Human GDNF (#EJJ GDNF1) was from Gro Pep (Adelaide, Australia). Recombinant Rat CNTF (#557-NT), was from R&D systems (Minneapolis, Minnesota). HyClone Fetal Bovine Serum (FBS, #15-010.02) was from Thermo Scientific (Victoria Australia). Lampire Cell Culture Bag (#7810601) was from Lampire Biological Laboratories (Pennsylvania, USA)

2.1.2 Antibodies

Rabbit anti-Choline Acetyltransferase (ChAT) P3YEB (a generous gift from Dr. M Schemann, Technische Universität München). Rabbit anti-ATF-3 (sc-188, Santa Cruz, USA). Goat anti-p75NTR (#N5788, Sigma-Aldrich, Castle Hill, Australia). Chicken anti-GFP (C-1322-100, Biosensis, Adelaide, Australia). Rabbit anti-Cleaved Caspase-3 (Asp175 #9661, Cell Signalling, Boston, USA). Donkey anti-rabbit (CY3), -sheep (ATTO-488), -sheep (CY5), -chicken (CY3), -mouse (ATTO-488) (Jackson ImmunoResearch Laboratories, USA). HiTrap desalting column (17-1408-01, GE Healthcare, Little Chalfont, UK). Sigma ATTO protein labelling kit (#38371, Sigma-Aldrich, Castle Hill, Australia)

2.1.3 Immunohistochemistry

Antibody diluents reagent solution (#003218), DAPI (#D1306) (Invitrogen Life Technologies, Melbourne, Australia). Paraformaldehyde (PF; #P6148), Fluoromount Mounting Media (#), Donkey Serum (D9663), were all from Sigma-Aldrich (Castle Hill, Australia). Isoflurane (V10316/1, Hospira Australia Pty Ltd, Mulgrave, Australia)

2.1.4 Immunoporters

PD-10 desalting column (17-0851-01), HiTrap SP HP column (17-1151-01, GE Healthcare, Little Chalfont, UK). DC- Protein Assay kit (#500-0114, BioRad

Laboratories, California, USA). Picrylsulfonic acid (TNBS, P2297, Sigma, Castle Hill, Australia). Branched Polyethylenamine polymer (PEI, 408727, C₂₄H₅₉N₁₁, MW 25 kDa Sigma-Aldrich, Castle Hill, Australia). Dimethylformamide, anhydrous (DMF, 227056, Sigma-Aldrich, Castle Hill, Australia). Branched (Methyl-PEO₁₂)₃-PEO₄-NHS ester (PEG, MW 2421 g/mol, ThermoScientific, Rockford, IL, USA)

2.1.5 Plasmid DNA

pVIVO2-GFP/LacZ plasmid DNA (pvivo2-gfplacz, Invivogen, San Diego, California). QIAGEN HiSpeed plasmid MAXI kit (12662, QIAGEN, Venlo, Netherlands). gWIZ GFP Mammalian Expression Vector (P040400, Genlantis, San Diego, California, USA). LB agar (L7025, Sigma-Aldrich, Castle Hill, Australia). Luria broth (L3522, Sigma-Aldrich, Castle Hill, Australia). Hygromycin B (H-1012-DI, A.G Scientific Inc., San Diego, USA).

Gel electrophoresis

10x TBE buffer pH 8.3 (27g Tris base, 13.75g boric acid, 2.33g EDTA). Agarose (V3121, Promega, Madison WI, USA). GelRed (41003, Biotium, Hayward CA, USA).

2.2 Methods

2.2.1 Animals

All procedures involving animals; pregnant C57BL/6J mice and embryos (approval #741/10), neonate C57BL/6J mice (approval #808/12) and adult C57BL/6J and SOD1^{G93A} mice (approval #800/11), were approved by the Animal Welfare Committee of Flinders University, which is in accordance with the Animal Welfare Act 1985 and the *Australian Code of Practice for the Care and Use of Animals for Scientific Purposes* 7th Edition.

Adult male transgenic mice expressing ~23 copies of the human mutant SOD1^{G93A} gene were bred with C57BL/6J mice, to reduce gender variation (Heiman-Patterson *et al.*, 2005), resulting in high copy (~23 copies) progeny (B6SJL-TgN(SOD1-G93A)1Gur, the SOD1^{G93A}G1H line (Gurney *et al.*, 1994, 1996), hereby known as simply ‘SOD1^{G93A}’ unless otherwise stated. Copy number was preserved in the colony by reverse transcriptase polymerase chain reaction (RT-PCR) analysis of all SOD1^{G93A} male breeders, and the colony was maintained as prescribed by earlier studies (Scott *et al.*, 2008; Perrin, 2014). Any progeny born with <23 copies of the mutant SOD1^{G93A} gene were removed from the colony. The colony used in our study (SOD1^{G93A}G1H strain) shows overt clinical symptoms, including decreased grip duration indicating motor deficits, by 100 days of age, with a further rapid decline to death at approximately 140 days (Shepherd *et al.*, 2014). ‘n’ represents number of animals used, unless otherwise stated.

2.2.2 Spinal cord, DRG, eye and mesentery extraction

C57BL/6J or SOD1^{G93A} mice (hereafter collectively called 'mice') were heavily anesthetised with isoflurane (for adults) or ice immersion (for neonates) and subsequently perfused transcardially with PBS containing 1% sodium nitrite, followed by Zamboni's fixative (4% paraformaldehyde (w/v), 7.5% saturated picric acid (v/v), 0.1M PBS, pH 7.4). Spinal cords, DRG's or eyes were removed and post fixed overnight in Zamboni's fixative at 4°C. The spinal cords/DRG's/eyes were then cryoprotected in PBS containing 30% sucrose (w/v) until they were white in colour. Once cryoprotected, spinal cords/DRGs were submerged in a mixture of OCT/PBS 1:1 for 5 minutes, then OCT for 5 minutes. The spinal cords were cut into cervical/thoracic/lumbar segments and embedded in OCT. The DRG's and eyes were mounted whole in the OCT. All were snap frozen on liquid nitrogen, then stored at -20°C until needed.

Mouse mesentery was acquired differently to the other tissue. Adult C57BL/6J mice were heavily anesthetised with isoflurane and then sacrificed by cervical dislocation. The abdomen was opened and the small intestine located and removed from the animal and placed in a dish containing PBS. The intestines were pinned down and spread out to easily remove the mesenteric tissue. The mesentery membrane was cut into smaller pieces and placed on a PEI coated microscope slide with PBS (as to not dry out) in a humidified chamber ready for immunohistochemistry.

2.2.3 Immunohistochemistry

Embedded spinal cord segments were cut at 30 μ m on a cryostat at -20 $^{\circ}$ C then collected in PBS. Sections were stored at 4 $^{\circ}$ C in 0.1% (v/v) Sodium Azide in PBS when not in use. DRG were cut at 12 μ m and eye sections were cut at 16 μ m, with both being immediately placed on PEI coated microscope slides. Mesentery sections were already on PEI coated slides. Sections were washed three times in PBS before being blocked in ADRS containing 10% donkey serum overnight at 4 $^{\circ}$ C. Sections were then incubated with primary antibodies in ADRS containing 1% donkey serum for 2-3 nights, 4 $^{\circ}$ C. Primary antibodies were diluted as follows; goat anti-p75NTR 1 μ g/ml, MLR2-ATTO-488 20 μ g/ml, rabbit anti-Choline Acetyltransferase P3YEB 1:5000, rabbit anti-ATF-3 1:200, chicken anti-GFP 1:500, rabbit anti-cleaved caspase-3 1:200. Sections were then washed three times in 1x PBS and incubated with secondary antibodies for 3 hours in ADRS containing 1% donkey serum, room temperature. All secondary antibodies were diluted to 1:800. After incubation, sections were washed three more times in 1x PBS, dried on glass microscope slides and mounted in Fluoromount with a glass coverslip for imaging. Imaging was carried out on an Olympus BX50 Fluorescence Microscope, with LED excitation sources (Olympus, Tokyo, Japan) with a 10x or 20x lens, and images were captured by using a Hamamatsu Orca cooled CCD camera (Hamamatsu Photonics, Hamamatsu City, Japan) connected to a PC running Micro-manager (version 1.4; Edelstein *et al.*, 2014).

2.2.4 Data Analysis

Quantitative data analysis and graphs were compiled with GraphPad PRISM 4 software and IBM SPSS Statistics 20. Image processing was performed with Adobe Photoshop CS5 and NIH ImageJ software.

2.2.5 Cell culturing

All cell lines, hybridomas and primary cells were maintained in a humidified incubator at 37°C and 5% CO₂. NSC-34 cells (kindly provided by Dr. Neil Cashman, Cashman et al. 1992), BSRc (kindly provided by Christine Tuffereau, (Tuffereau *et al.*, 1998)) and SH-SY5Y cell lines were all maintained in DMEM, supplemented with 10% FBS, 1x PSG and 1x GX.

MLR2 hybridomas (Rogers *et al.*, 2006) were maintained in RPMI- 1640 media supplemented with 10% FBS, 1x PSG and 1x HT. When hybridomas were revived in a 24 well cell culture plate, they were supplemented with a drop of HFCS until they produced antibody (media colour change), then they were transferred to T-75ml flasks with fresh media. The cells were moved again to 1L Lampire bags after antibody production, with 1L of media. After one week, media was harvested, centrifuged at 400g and supernatant stored at -20°C for antibody purification.

2.2.6 Isolation and purification of embryonic motor neurons

Before motor neuron purification and culture, identification of embryo age must be determined. Table 2.1 lists key physical features of embryonic mice which need to be satisfied in order to isolate healthy motor neuron cultures (adapted from mouse development atlas (Theiler, 1972)), and Figure 2.1 displays a E12.5 embryo.

Table 2.2 Important physical attributes of E12.5 murine embryos that must be examined to determine correct age.

	Age of mouse		
Physical feature	<E12.5 (too young)	E12.5-13	>E13 (too old)
Handplate	Round handplate. There is no indication of ridges, which signify the beginning of fingers/toes	Handplate has ridges, indicating fingers/toes are starting to form.	Fingers/toes are partially developed.
Size	<7mm. Along with the physical length, the embryo is very fragile and is easily damaged due to a large head to torso ratio. The torso looks 'serpent' like (long and thin)	7-11mm. Embryo is less likely to be damaged in the dissection procedure.	>11mm.
Neural tube/spinal cord properties	Very fragile. Membranous skin covering vertebrae tears easily. Difficult to dissociate neural tube from vertebrae without damaging spinal cord.	Embryo is more robust and skin covering spinal cord is easily peeled off. Meninges is easily cut and removed from spinal cord.	Skin covering embryo is less membranous and more rigid. Spinal cord has fused and meninges have thickened, resulting

	Meninges difficult to remove without damaging spinal cord.		in difficulty in separating the two.
Ears	No pinna.	Pinna barely visible.	Pinna start to take shape.
Gut	Very little gut, resulting in 'serpent' like appearance.	Gut increases in size dramatically, giving rise to a bulbous shape.	-
Snout	No whiskers and very round snout.	Beginnings of whiskers. Snout still largely undeveloped, but slightly protruding.	Whiskers noticeable with snout looking more developed (darker pigment), with lips and whisker pocks forming.



Figure 2.1 E12.5 murine embryo

A photo showing an E12.5 murine embryo that has just been removed from the mothers uterus. Key physiological features of to determine exact age include; total size, handplates, snout, pinna, gut and neural tube (scale = 2mm).

The acquisition and isolation of E12-13 mouse motor neurons requires a unique, multi-step method adapted and modified from a protocol developed in our laboratory and published in *Nature Protocols* (Wiese *et al.*, 2010).

Briefly, 24 well tissue culture plates were coated with 300 μ l/well PORN (Poly-L-Ornithine) at 4°C, overnight. Nunclon delta surface plates were coated with 1.5 μ l/mm² of immunopanning solution (1.5 μ g/ml MLR2, 10mM Tris-HCl, pH9.5) at 4°C, overnight (known as an ‘immunoplate’). The high pH buffer prevents the MLR2 antibody from becoming protonated, keeping the overall negative charge of the protein, allowing them to stick to the positively charged plate.

After overnight incubation, 24 well tissue culture plates were rinsed three times with sterile H₂O and left to air dry. Once dry, coverslips were coated in HBSS containing 2.5 μ g/ml natural mouse laminin for 2 hours at room temperature. The immunoplate was rinsed with HBSS three times, and stored in NB media containing 1x GX at room temperature until needed.

Confirmed time mated pregnant mice were sacrificed via cervical dislocation. The uterus was removed and placed in a 50ml tube containing room temperature HBSS, before embryo dissection.

The embryo was placed in a silicon based petri dish and submerged in RT HBSS. Decapitation was made near the developing midbrain. The embryo was secured and the spinal cord was removed. The meninges and DRGs were removed.

Removal of the meninges is important, as it protects the spinal cord from digestion, reducing the cell dissociation and can also proliferate and ‘contaminate’ the culture. The neurons within the DRGs express p75NTR and can contaminate the culture. As the only the lumbar sections of the spinal cords were needed, each

spinal cord was cut approximately in half. Dissected spinal cords were immediately transferred to an eppendorf tube containing 300µl/cord of HBSS and kept on ice. Spinal cords should not be kept on ice for longer than 45mins.

Spinal cords were transferred into a sterile laminar flow hood. Individual spinal cords had 1ml of 0.05% trypsin EDTA added to digest and dissociate cells. The tubes were mixed and digestion carried out at 37°C for 10 mins. Following trypsination, 1ml of trypsin inhibitor (MEM, 1M HEPES, 0.01mg/ml DNase, 0.14mg/ml trypsin inhibitor) was added to quench digestion. Spinal cords were triturated to make single cell suspensions. The trypsin was removed by spinning the cells at 100g for 10 mins with acceleration/deceleration set to 0. The pellet was then resuspended in NB (containing Glutamax).

The spinal cord cell suspension was transferred onto the immunoplate and incubated for 45mins in the dark, at room temperature. The incubation must be carried out in a place where there are no vibrations, as mechanical vibrations prevent antibody-cell binding. After incubation, the plate is washed three times with room temperature HBSS to remove unbound cells. Remaining attached cells were then detached by adding 1.5ul/mm² depolarising saline (30mM KCl, 0.8% NaCl, 2mM CaCl in tissue culture H₂O) for 30s max. The immunoplate was tapped to dislodge cells. The depolarising saline is very toxic to the cells, so 2.5ul/mm² pre-warmed complete motor neuron media (Neurobasal 1% B27, 1% Glutamax, 10% Horse Serum, 1ng/ml BDNF, 1ng/ml GDNF, 10ng/ml CNTF, 25um β-mercaptoethanol- seeding only) was added to the immunoplate and cells resuspended with three-five triturations/ washes before being transferred to a centrifuge tube. The addition of the media and trituration was then repeated a second time. Suspensions were centrifuged at 400g, 7mins, with 0 acceleration

and 1 deceleration. The pellets were then resuspended in complete motor neuron media.

Laminin is then removed from 24 well culture plate and replaced with 1ml of complete motor neuron media. All free laminin must be removed from wells, however care was taken to not allow plates to dry, as motor neurons will not grow on treated plates that have dried. Following isolation of motor neurons, a count of viable cells was carried out on a haemocytometer using 0.04% trypan blue. Cell seeding density was approximately 30,000 cells/well. After seeding, wells were filled to 90% of volume with complete motor neuron media. 50% of media was replaced after 24hrs with freshly made motor neuron media and then replaced every 48hrs thereafter. The β -mercaptoethanol is only added when seeding cells.

2.2.7 Immunocytochemistry

For primary motor neuron cultures that were counterstained, they first had their media removed and washed with 3x with cold PBS until all media was gone. The cells were fixed with cold 4% paraformaldehyde (pH 7.4) on ice for 15 mins. Cells were washed three times in PBS before being blocked in ADRS containing 10% donkey serum overnight at 4°C. Cells were then incubated with primary antibodies in ADRS containing 1% donkey serum overnight, 4°C. Primary antibodies were diluted as follows; chicken anti-GFP 1:500. Cells were then washed three times in 1x PBS and incubated with secondary antibodies for 3 hours in ADRS containing 1% donkey serum, room temperature. All secondary antibodies were diluted to 1:400. After incubation, sections were washed three

more times in 1x PBS, ready for imaging. Imaging was carried out on an Olympus IX71 inverted Fluorescence Microscope.

2.2.8 Purification of antibodies

Conditioned media from hybridomas stored at -20°C were thawed and filtered through a 0.2µm filter. Using a Pharmacia P-1 peristaltic pump, the filtered media was passed over a PBS equilibrated protein-G column for 3 nights at 4°C at a flow rate of ~2ml/min. After three nights, the protein-G column was washed for 30mins with PBS at a flow rate of ~2ml/min. The bound antibody was eluted with 0.1M glycine (pH 2.7) into 15 1-1.5ml fractions. Fractions containing antibodies were identified using a spectrophotometer (280nm) and pooled together. Antibody solutions were restored back to pH 7.0 using 2M Tris. Antibody was then desalted and concentrated to >2mg/ml using a 50kDa spin column (product and company) in PBS. Antibodies were stored at 4°C or -80°C for long term storage.

2.2.9 Conjugation of antibodies

Conjugation of fluorescent dyes to antibodies was achieved following manufacturer's instructions (Sigma ATTO protein labelling kit #38371). Briefly, ATTO dye was dissolved in sodium bicarbonate buffer before being added to antibody (>2mg/ml). The dye/antibody was incubated for 2 hours in the dark at room temperature. Conjugated antibody was separated from excess free dye was

achieved using two HiTrap desalting columns connected to each other.

Conjugated antibody was then measured for degree of labelling (DOL) using the following equation:

$$DOL = \frac{A_{498} \times \epsilon_{Protein}}{[A_{280} - (A_{498} \times 0.10)] \times 90,000}$$

A_{498} = absorbance at 498 nm measured in a cuvette with a path length of 1 cm

A_{280} = absorbance at 280 nm measured in a cuvette with a path length of 1 cm

$\epsilon_{Protein}$ = molar extinction coefficient of the protein at 280 nm. IgG usually have of 203,000.

90,000 = molar extinction coefficient (dye) of the ATTO 488 dye at 498 nm

0.10 = correction factor due to the fluorophore's absorbance at 280 nm

2.2.10 FACS

BSRc and SH-SY5Y cell lines stocks were cultured in complete DMEM (10% FBS, PSG, GX), were trypsinised, centrifuged at 400g for 5 minutes and resuspended in DMEM. 1.0×10^7 cells/ml were suspended in 50 μ l of PBS and incubated at 4°C for 30 minutes with antibodies at a concentration of 20 μ g/ml. The cells were then washed with cold PBS (pH 7.2)/1.0% normal bovine serum/0.1% azide (cell wash buffer) and then centrifuged for 3 minutes at 500g, twice. Unconjugated antibodies that required a secondary fluorescently labelled antibody were incubated with the secondary antibody for 20 mins, 4°C at a concentration of 1:100, and then washed in cell wash buffer/centrifuged twice

more. Cells were then read on an Accuri Cytometer C6 Flow Plus systems (BD Biosciences). At least 10,000 events were measured per treatment. Dead cells and debris were gated out of the analysis on the basis of forward and side scatter, and data analyzed by CFlow Plus Software (BD).

2.2.11 Immunoporter creation

The creation of the immunoporter is a multi-step process consisting of preparing the PEI, conjugating multiple PEGs to PEI, addition of SPDP to PEI-PEG and a monoclonal antibody (mAb;MLR2) antibody, conjugation of PEI-PEG-SPDP to MLR2-SPDP and finally purification of MLR2-PEI-PEG immunoporter (Figures 2.2 and 2.3 show this process schematically). Quantification and identification of PEI complexes were accomplished using a TNBS assay and DC-Assay.

2.2.11.1 BioRad DC-Assay

The BioRad DC-Assay for detecting and determining PEI containing samples during the immunogene creation process was as per assay instructions. Briefly, 5µl of PEI sample was added to one well of a 96-well microtiter plate with 25µl of Solution A and 200µl of Solution B. Wells which changed colour to a dark blue indicated the presence of PEI.

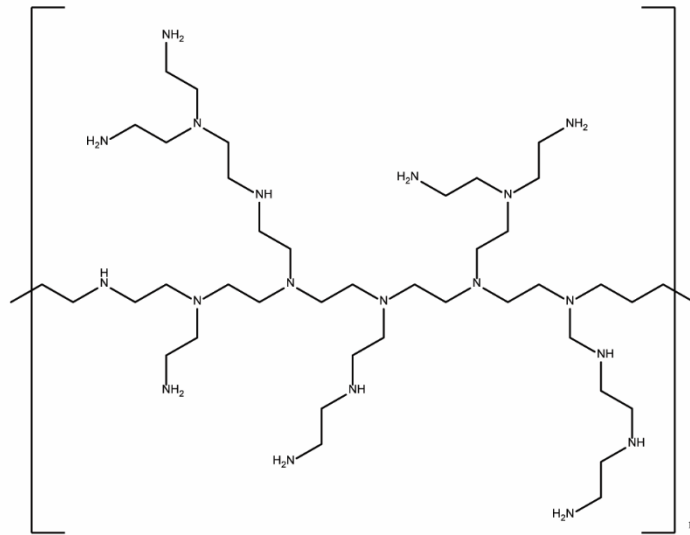
Figure 2.2- Schematic of polyethylenamine and polyethylene glycol

(1) shows one repeating unit of the ~25,000 Da branched polyethylenamine (PEI) molecule, with multiple primary and secondary amines

(2) shows the 2420.8 Da polyethylene glycol ((Methyl-PEG₁₂)-PEG₄-NHS) in both long and short hand forms.

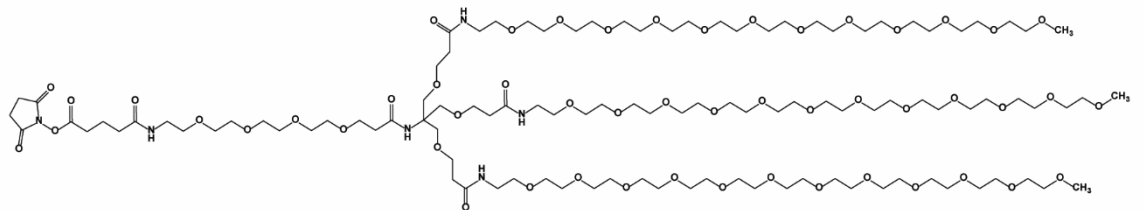
(3) shows one unit of a PEGylated PEI molecule, conjugated through a NHS-ester reaction. Approximately 12 PEG molecules are conjugated to one PEI molecule, which occupies ~6% of the total amines on the PEI.

1.

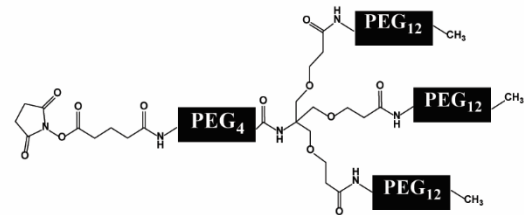


Polyethylenimine
branched (PEI)
 $M_w \sim 25,000$ Da

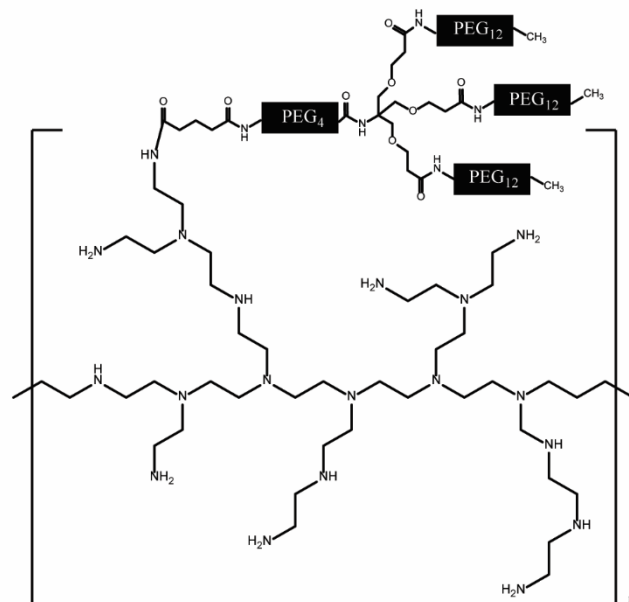
2.



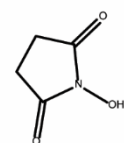
(Methyl-PEG₁₂)₃-PEG₄-NHS
MW = 2420.8



3.



PEGylated PEI
~12 PEG per PEI
(~6% of amines)



NHS leaving group

Figure 2.3- Schematic of Immunoporter synthesis

The following schematic displays the chemical synthesis of the immunoporter

(1) the antibody (MLR2) and PEGylated PEI are measured and prepared

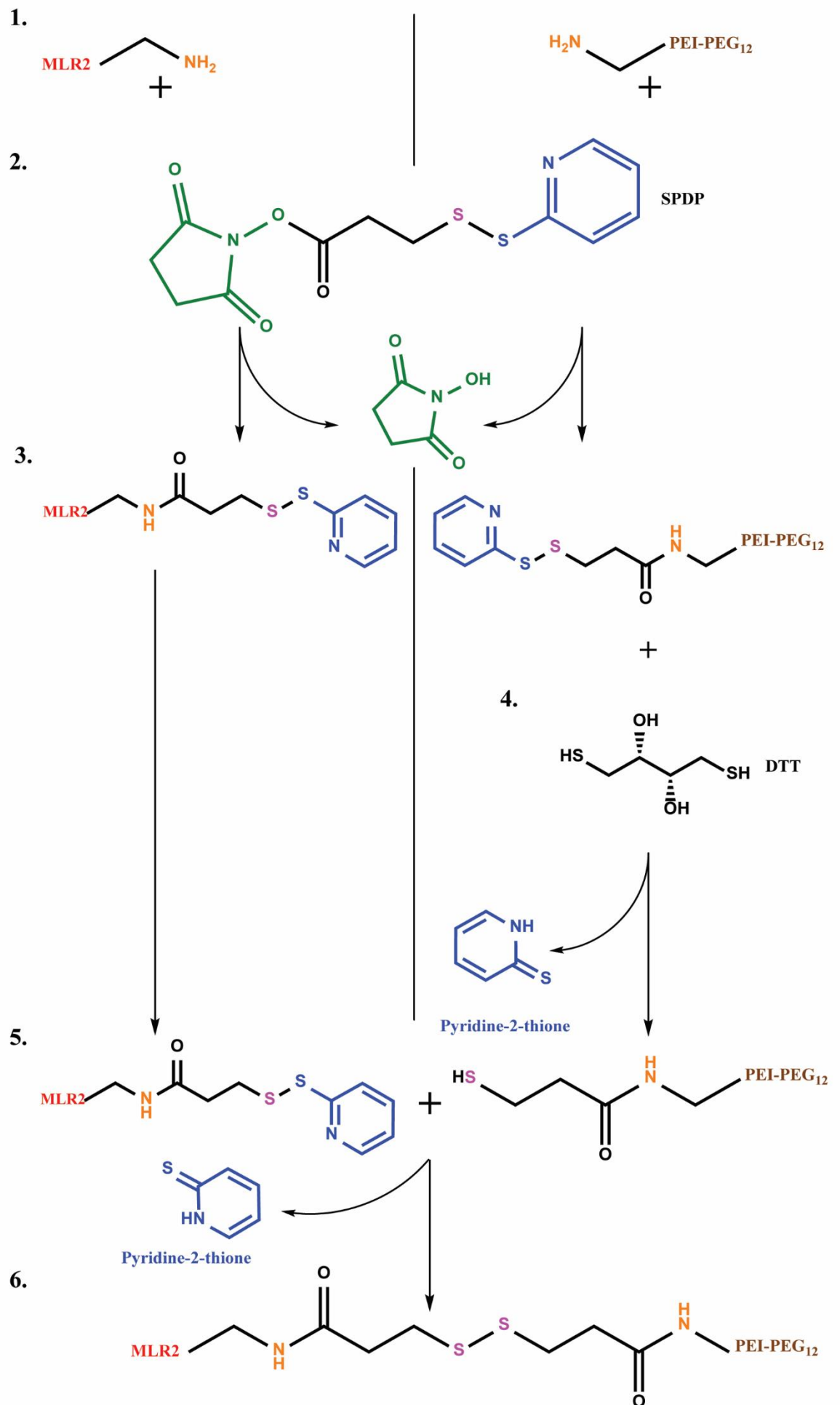
(2) seperately, the MLR2 antibody and PEGylated PEI are incubated with the SPDP linker, where the NH_2 of the MLR2 and PEI-PEG chain result in the cleavage of the ester

(3) this reaction conjugates the SPDP linker to both the MLR2 and PEGylated PEI, through the formation of an amide bond

(4) the PEGylated PEI is then reduced with DTT to remove the pyridine-2-thione component

(5) the MLR2 and PEGylated PEI are then able to be conjugated together through the removal of the pyridine-2-thione (which can be measured at 343nm for conjugation efficiency) from the MLR2, due to the naked thiol group on the PEGylated PEI

(6) the end result is an immunoporter of the MLR2 and PEGylated PEI, conjugated together through a di-sulphide bridge



2.2.11.2 TNBS assay

TNBS assay as per Snyder and Sobocinski (Snyder & Sobocinski, 1975). Briefly, PEI complexes and PEI standards were diluted in pre-warmed 0.1M sodium borate buffer (pH 9.3). Concentration range of PEI standard between 0.5-4ug/ml. TNBS labelling reagent diluted 1/500 in water. 150ul of PEI standard (sextuplicate) or PEI complex (triplicate) sample added to a well of a 96-well microtiter plate with 20ul of TNBS diluted reagent. The reaction was left to incubate at 37oC for 25mins and then read on an ELISA plate reader at 405nm. The concentration of PEI complexes were then determined using the PEI standard.

2.2.11.3 Preparation of PEI – dissolving and de-protonating PEI

A PD-10 desalting column was first washed and flushed with 20ml of HEPES solution (1M HEPES, 14.61g NaCl dissolved in H₂O, pH 7.9). Approximately 2g of PEI was dissolved in 20mL of water and was adjusted to pH 7.0 using HCl. 2.5ml (max loading volume of PD-10 column) of dissolved PEI was allowed to flow into the column. The PEI was eluted by off the column by a wash of ~10ml of HEPES solution and collected into 8 fractions. This process was repeated twice. PEI containing fractions were identified using a qualitative DC-Assay. PEI containing fractions were pooled and filtered through a 0.2µm filter. PEI concentration was then measured using a quantitative TNBS assay. Solution stored at 4°C.

2.2.11.4 Preparation of PEI-PEG – addition of 12 molecules of PEG to 1 molecule of PEI

Room temperature PEG was dissolved in DMF at a concentration of 125mM. 10x molar excess of PEG was added to 30mg of PEI (1.5ml at 20mg/ml in HEPES solution), using the following equation:

$$PEI(mg) \times \frac{1M\ PEI}{MW\ of\ PEI\ (25,000\ Da)} \times \frac{10mM\ PEG}{1mM\ PEI} = mM\ PEG$$
$$mM\ PEG \times \frac{1,000,000}{1L} \times \frac{1L}{125mM\ (PEG\ concentration)} = \mu l\ of\ PEG\ needed$$

PEI and PEG were incubated at room temperature for 1 hour in the dark under a nitrogen atmosphere. The PEI-PEG complex was loaded onto a HEPES solution equilibrated PD-10 column and eluted into 1ml fractions. PEI-PEG containing fractions were identified using a DC-Assay. PEI-PEG containing fractions were pooled and concentration quantified using a TNBS assay. NMR analysis shows that approximately 12 PEGs are added per 1 PEI molecule, when using this protocol (Rogers *et al.*, 2014).

2.2.11.5 Preparation of PEI-PEG-SPDP and mAb-SPDP conjugation

Two PD-10 desalting columns were washed and flushed with 20ml of HEPES solution, in preparation for the PEI-PEG-SPDP and mAb-SPDP. A 10mM solution of SPDP in sterile filtered absolute ethanol was prepared (1mg in 320µl is sufficient). 10mM SPDP was added to PEI-PEG at 6.5µl of SPDP per 1mg of PEI-PEG (8mg minimum) and incubated for 1 hour in the dark under nitrogen

atmosphere (1 hour incubation crucial for 1:1 SPDP:PEI-PEG). 45 minutes after starting the PEI-PEG-SPDP reaction, 10mM SPDP was added to mAb (MLR2) at 2.65ul of SPDP per 1mg of MLR2 for 2 hours in the dark under nitrogen atmosphere. The mAb must be at a concentration greater than 2mg/ml and over 7mg total.

During the MLR2-SPDP reaction after the incubation time, the PEI-PEG-SPDP was purified on the pre-equilibrated PD-10 column in 1ml fractions and checked qualitatively using a DC-assay. Fractions containing PEI-PEG-SPDP were pooled together and incubated with 150ul of 25mg/ml DTT in HEPES solution for 30 mins, room temperature in the dark under nitrogen atmosphere. The addition of DTT cleaves of pyridine 2-thione from the SPDP which was removed by desalting and eluting with HEPES on a PD-10 column. PEI-PEG-SPDP fractions were determined by a DC-assay, pooled and then concentration estimated with a TNBS assay.

After a 2 hour incubation, the MLR2-SPDP was desalted and eluted on a PD-10 column with HEPES. Fractions containing MLR2-SPDP were determined using a DC-assay and pooled. The concentration of the MLR2-SPDP was determined using a spectrophotometer at 240nm. The MLR2-SPDP was also measured at 343nm undiluted, which is necessary to determine conjugation efficiency by the release of pyridine 2-thione later on.

The PEI-PEG-SPDP and MLR2-SPDP were mixed together at a molar ratio of 2:1 (PEI:MLR2), with the entire MLR2-SPDP solution being used. 1ul of EDTA per total reaction volume was added to the mixture which was incubated overnight in the dark at room temperature.

2.2.11.6 Purification of MLR2-PEI-PEG immunoporter and desalting

After incubation overnight, the solution was desalted and eluted on an equilibrated PD-10 column using HEPES to remove pyridine 2-thione. Fractions were measured at 280nm with a spectrophotometer to determine antibody presence and pooled together (usually fractions 1-4). Up to 13 fractions were collected and measured at 343nm for pyridine 2-thione presence. Fractions that contained pyridine 2-thione were pooled and were measured again at 343nm, which was used to calculate the number of PEI-PEG molecules that actually bound to MLR2 antibody, using the following equation:

$$\frac{\Delta OD_{343}}{\text{pyridine 2 - thione extinction coefficient (8080)}} \times \frac{mAb MW (150,000)}{mAb mg}$$

(The ΔOD_{343} is the change in the optical density/absorbance of the pyridine 2-thione. This is acquired by calculating the difference between the OD_{343} of MLR2-PEI-PEG (multiplied by the volume) after conjugation and the OD_{343} of MLR2-SPDP (multiplied by the volume) before conjugation.)

Following conjugation, the MLR2-PEI-PEG immunogene was desalted on a HiTrap SP HP column to remove unbound antibody, PEI-PEG and unwanted salts using 20mM HEPES with increasing NaCl concentrations (0.5M, 1M, 2M and 3M). The HiTrap SP HP column was first washed with filtered water, equilibrated with 0.5M NaCl HEPES, charged with 3M NaCl HEPES (left for a minimum of 10 minutes) and then equilibrated again with 0.5M NaCl HEPES before desalting (5 column volumes used for equilibration/charging). The conjugated MLR2-PEI-PEG was recirculated over the HiTrap column 5 times. The final flow through

was measured to determine if any antibody did not bind to PEI-PEG (can be up to 0.5mg). Following binding of the MLR2-PEI-PEG to the HiTrap column, 4ml of 0.5M NaCl HEPES was passed over the column and 3x 1ml fractions collected. This was then repeated with 4ml of 1M, 2M and 3M NaCl HEPES, each with 3 fractions each. All fractions were then measured at 280nm to determine if what was eluted of the column contains the MLR2-PEI-PEG immunoporter. The immunoporter should elute in the 2M fractions. These fractions are then pooled and concentrated on a 100kDa spin column to >2mg/ml in a 0.15M NaCl HEPES buffer. The immunoporter can be stored at 4°C in the dark under nitrogen atmosphere for up to 2 months.

2.2.12 Bacterial growth and DNA purification

Frozen stocks of transformed *Escherichia coli* bacteria (pVIVO2-GFP/LacZ) were partially thawed out and were inoculated on sterilised LB agar (1 tablet in 50ml H₂O) containing 100µg/ml of hygromycin at 37°C, overnight. A single colony from the inoculated agar plate was selected and mixed into 10ml liquid TB media (55g/L) containing 100µg/ml hygromycin for 8 hours at 37°C while vigorously shaking. After 8 hours incubation, 125µl of the bacteria containing media was added to 125ml of fresh TB hygromycin media and incubated at 37°C for 12-16 hours while vigorously shaking. The media was then spun at 4500g, 25 mins and the pellet was stored at -80°C until needed.

Plasmid DNA was purified using QIAGEN Plasmid Maxi kits, as per manufacturer's instructions. Briefly, pellets were resuspended in 10ml of Buffer

P1 and then 10ml of Buffer P2 was added, inverted 4-6 times and incubated for 5 mins at room temperature. 10ml of pre-chilled Buffer P3 was added next and incubated for at room temperature for 10 mins in a QIAfilter cartridge. During this time, the HiSpeed Maxi Tip was equilibrated with 10ml of Buffer QBT. Following incubation, the cell lysate was filtered through the QIAfilter cartridge into the HiSpeed Maxi Tip, where the lysate will flow into the resin by gravity. The HiSpeed Maxi Tip resin was washed with 60ml of QC buffer, before being eluted with 15ml QF buffer. The DNA was precipitated with 10.5ml of iso-propanol. The iso-propanol/DNA mixture was then put through the QIAprecipitator, discarding the flowthrough. The QIAprecipitator was then washed with 2ml of 70% ethanol, dried by forcing air through the precipitator and finally eluted using 0.5-1ml water, and measured on a spectrophotometer at OD₂₆₀.

2.2.13 Immunogene N/P ratio

Addition of pDNA to the immunoportor (MLR2-PEI-PEG12) is determined by a nitrogen/phosphate (N/P) ratio. The nitrogens that are part of the amine groups on the PEI and the phosphates that are part of the pDNA backbone. The N/P ratio is used to find at what concentrations of immunoportor to pDNA is the immunogene able to fully bind pDNA and be charge neutralised, which can be found with the use of a gel retardation assay. The following calculation is used to determine immunoportor (N) to pDNA (P) ratio:

$$NP = \frac{(\text{ul of PEI stock solution}) \times 23.2\text{mM nitrogen residues}}{(\text{ug plasmid DNA}) \times 3\text{mmol phosphate}}$$

The equation assumes that the PEI stock is at 1mg/ml, so an additional step of conversion to the actual concentration must be done, which is achieved by dividing the PEI stock volume by the PEI concentration.

2.2.14 *Gel retardation Assay*

A gel retardation assay is used to determine which N/P ratio is sufficient to completely bind all pDNA and be charge neutralised. A 1% agarose in TBE (Tris base, boric acid, EDTA) buffer is boiled and left to cool until ~55°C. Once cool enough, 1:10,000 concentration of nucleic acid dye GelRed is added to the agarose solution before being poured into an electrophoresis unit and let solidify. Immunoporter/PEI complexes (MLR2-PEI-PEG12, PEI-PEG12 and/or PEI) and pDNA are diluted to 0.1mg/ml in 20mM HEPES 0.15M NaCl pH7.3 buffer. The complexes and pDNA (always 400ng) are mixed with N/P ratios from 2-20, made up to 10ul with HEPES buffer and left to incubate at room temperature for 10-15 mins, before the addition of 2ul loading dye. The electrophoresis unit is then filled with TBE buffer containing 1:10,000 concentration of GelRed. 12ul of each sample is loaded into the gel and run at 110V until dye has reached $\frac{3}{4}$ of the gel. The gel is then imaged on a fluorometer. A completely pDNA bound, charge neutralised sample will not show that it has run through the gel.

2.2.15 Neonate injections

Neonatal PND1 mice were injected intraperitoneally with 150ug (2x 75ug, 12 hours apart) of fluorescently labelled MLR2 antibody (MLR2-ATTO-488, (Rogers *et al.*, 2014)). 36 hours after initial injection, mice were anaesthetised on ice, transcardially perfused with 0.1% nitrite PBS solution and had their spinal cords removed. The spinal cords were post fixed overnight in Zamboni's fixative, before being cryoprotected in 30% sucrose solution and sectioned (30µm) at -20oC in OCT on a cryostat. The spinal cord sections were imaged under a fluorescent microscope for ATTO-488 signal.

An N/P ratio that has shown to be able to bind pDNA and be charge neutralised, determined by the gel retardation assay, is used for the immunogene injections. Due to the propensity for the immunogene to aggregate when mixed at high concentrations, pDNA was added to the immunoportor in 1/5 increments, and incubated for ~10 minutes between each addition. As above, neonatal PND1 mice were intraperitoneally injected with 150ug (2x75, 12 hours apart) MLR2-PEI-PEG12 carrying 116ug pDNA. The mice were perfused and spinal cords removed 72 hours after initial injection. The spinal cords were processed (Zamboni's and sucrose) before being sectioned and counterstained for GFP and ChAT.

2.2.16 Lipofectamine 2000 methods

Transfection of primary motor neuron cell cultures with Lipofectamine 2000 were as the manufacturer's instructions. Briefly per well, 0.8µg of pDNA was diluted in 50µl OptiMEM solution and separately, 2µl of Lipofectamine 2000 solution

was diluted in 50µl OptiMEM. After a 5 minute incubation, the Lipofectamine 2000 and pDNA were mixed and incubated for 20 mins, room temp. The mixture was then applied to cells for 4-6 hours, before fresh media change and imaging on an inverted IX 71 Olympus microscope, 24 hours after transfection.

Chapter 3: Expression levels
and targeting of p75NTR
positive motor neurons in
neonatal mice

3.1 Introduction

Gene therapy has great therapeutic potential for neurological diseases, such as Motor Neuron Disease (MND). Unfortunately, due to the anatomical spread of motor neurons throughout the central nervous system (CNS; spinal cord, brainstem and cortex), access to motor neurons for delivery of exogenous genetic material and specific targeting of motor neurons is difficult to achieve. Using a virus as a targeting vector (adeno associated virus; AAV6), it has been shown that intravenous tail vein injections in mice is able to deliver plasmid cargo to ~4% of motor neurons and express the gene of interest (Towne *et al.*, 2008). However, this study showed wide-spread transfection of non-motor neuron tissue, including heart, diaphragm and striated muscles. A continuation of this study was able to increase the total motor neuron transfection to a peak of ~12% using the AAV6 viral vector, but this required many painful injections directly into multiple muscles, and still had several off-target non-motor neuron transduced tissue (Towne *et al.*, 2010).

Non-viral gene delivery has several advantages over viral therapies for CNS-located neurons, with better specificity to target cells, lower immunogenic responses and non-integration into the host genome (Mintzer & Simanek, 2008; Rogers & Rush, 2012). However, most studies show less sustained gene expression than can be achieved with the use of viruses (Mintzer & Simanek, 2008; Rogers & Rush, 2012). The blood brain barrier (BBB) also contributes to the difficulty in neuronal transfection, as it is very effective at stopping infectious or unwanted material from entering the CNS, including many viral and non-viral gene delivery agents, including antibodies (Pardridge, 2006).

A method to bypass the BBB and access intracellular environments involves targeting internalizing cell surface receptors with antibodies. The antibody binds to its cognate receptor on the cell surface of motor neurons in the periphery, internalizes and retrogradely transports cargo to the cell soma in the CNS. p75NTR is an attractive target for receptor mediated non-viral delivery for MND, due to its re-expression in motor neurons in human MND (Kerkhoff *et al.*, 1991; Seeburger *et al.*, 1993; Lowry *et al.*, 2001) and SOD1^{G93A} mice (Copray *et al.*, 2003).

Previous work has revealed that p75NTR is able to be retrogradely trafficked in signalling endosomes in motor neurons when taken up at distal terminals (Lalli & Schiavo, 2002), making it an ideal *in vivo* receptor for targeting. Recent work has shown that a non-viral gene delivery complex (called an 'immunogene') which used p75NTR as a vector for pGDNF delivery, showed almost complete motor neuron recovery after total axonal transection in rats (Barati *et al.*, 2006). It is known that p75NTR is expressed in murine neonatal motor neurons during development, which has allowed motor neuron isolation (Wiese *et al.*, 2010). Rat motor neurons also express p75NTR in high levels during development up to PND10 neonatally, before being rapidly down-regulated so that in adults no receptor expression is seen (Yan & Johnson, 1987, 1988; Ernfors *et al.*, 1989b). Interestingly, the expression of p75NTR in neonatal murine motor neurons has not been quantified, which is important if it is to be used as a vector to mouse motor neurons in disease.

The objective of this study is to target motor neurons using p75NTR as a gateway into the cell using its ability to be retrogradely trafficked from the neuromuscular junction to motor neurons in all areas of the spinal cord after intraperitoneal

injection. As such, the only off-target effects expected are p75NTR expressing sensory fibres of the dorsal horn of the spinal cord and their respective DRG neurons (Yan & Johnson, 1988). Although cholinergic basal forebrain neurons also express p75NTR (Yan & Johnson, 1988; Sobreviela *et al.*, 1994; Yeo *et al.*, 1997), the antibody would have to be released from the cell soma of the lower motor neuron and transported to the basal forebrain to reach these neurons. The specificity of MLR2 was validated by flow cytometry on SHSY5Y p75NTR expressing cells as previously described (Rogers *et al.*, 2006; Secret *et al.*, 2013). Tissue specificity was tested by using p75NTR expressing mesentery neurons (Rogers *et al.*, 2006).

The following work investigates the expression levels of p75NTR in neonatal mouse motor neurons and validates the use of MLR2 as an antibody to target p75NTR receptors *in vivo*.

3.2 Results

3.2.1 *MLR2 and MLR2-ATTO-488 bind specifically to p75NTR expressing cells*

Flow cytometry was used to confirm specificity of the monoclonal p75NTR antibody MLR2 or MLR2 conjugated to a fluorescent dye. The antibodies were applied to cells that either express (neuroblastoma SHSY-5Y (Secret *et al.*, 2013)) or do not express (hamster fibroblasts –BSR (Tuffereau *et al.*, 1998; Rogers *et al.*, 2006) p75NTR on their cell surface. Fluorescently labelled donkey anti-mouse was used to detect un-labelled MLR2 on the cell surface of cells incubated at 4°C.

The stained cells were read on an Accuri Cytometer C6 Flow Plus. At least 30,000 cells were acquired by list mode and measurements were performed on a single cell basis, and were displayed as frequency distribution histograms. Dead cells and debris were gated out of the analysis on the basis of forward scatter

Figure 3.2.1 shows the frequency distribution histograms from a FACS analysis of MLR2 and the donkey anti-mouse 488 incubated with p75NTR expressing SHSY-5Y cells and BSR cells which lack the receptor. (A) shows that there is an increase in fluorescent intensity (purple), by a shift to the right, when MLR2 + donkey anti-mouse Alexa-Fluor 488 is applied to SHSY-5Y cells compared to cells only measurements (red). This increase in fluorescence is not seen when MLR2 + secondary antibody is applied to BSR cells, as both cells incubated with MLR2 (purple) and cells alone (red) overlap. The Alexa Fluor-488 secondary anti-mouse alone applied to either SHSY-5Y (C) or BSR (F), showed no increase in fluorescence (green and red lines overlap in both cell lines), indicating that the

secondary antibody was specific to primary mouse antibody bound to cell surface receptors.

Conjugating MLR2 to an ATTO-488 fluorescent dye does not inhibit its ability to bind to p75NTR expressing SHSY-5Y cells, as evident in (B) where there is an increase in fluorescence with cells incubated with MLR2-ATTO-488 (blue) compared to the cells alone (red). Importantly, the labelled antibody did not show signal when applied to cells lacking p75NTR, shown in (E) when the conjugated antibody is applied to BSR cells (blue and red lines overlap).

3.2.2 Labelled MLR2 is able to bind to p75NTR on neurons of fresh mouse mesentery

Having demonstrated that labelled MLR2 binds specifically to p75NTR, we next sought to show MLR2 binds p75NTR on mouse tissue before using it in *in-vivo* experiments in mice. Previous data has shown MLR2 is unable to stain tissue/cells that have been fixed (Rogers *et al.*, 2006). However, MLR2 can bind p75NTR on neurons located on non-fixed rat mesentery (Rogers *et al.*, 2006). In addition, using mouse monoclonal antibodies increases the risk of ‘mouse on mouse’ staining of secondary antibodies. Hence, labelling MLR2 with a fluorophore prevents the mouse on mouse reaction.

20µg/ml MLR2-ATTO-488 was applied to fresh mesentery tissue taken from adult C57BL/6J mice and compared to 5µg/ml polyclonal anti p75NTR goat antibody +2⁰ anti-sheep/goat ATTO-488. Figure 3.2.2 shows fluorescent images of mouse mesentery (A) positive for ATTO-488 fluorescence after MLR2-ATTO-488 incubation, which is comparable to (B), incubated with goat anti-p75NTR +

donkey anti-sheep ATTO-488. Both images show positive staining of p75NTR positive peripheral nerves surrounding blood vessels in mouse mesentery. Hence, MLR2 is able to bind to p75NTR expressing cells in non-fixed tissue.

3.2.3 *p75NTR expression in neonatal motor neurons decreases over 7 days and is absent by 14 days*

We wished to determine how long p75NTR expression persists in the motor neurons in neonatal mice. B6 mice lumbar spinal regions were analysed for p75NTR and choline acetyltransferase (ChAT, a marker for motor neurons) expression, with ages ranging from post-natal day (PND) 1-7 and also PND 14 (3 mice/age).

The p75NTR expression was analysed qualitatively and quantitatively.

Micrographs representing p75NTR/ChAT expression from PND 1-4 can be seen in figure 3.2.3a. Immunofluorescence of p75NTR appears to change slightly across these four days, with a decrease in brightness/expression level and decrease in the spread of expression throughout the ventral region. Figure 3.2.3b shows p75NTR/ChAT expression from PND 5-7 and PND 14. The loss of p75NTR expression is more apparent in ages PND 5-7, with a very low expression of p75NTR seen in PND 6 and 7, in both brightness and spread. PND 14 shows no p75NTR immunoreactivity in ventral motor neurons.

Lower resolution/magnification of lumbar spinal cord regions from PND 1-7 and PND 14 in figure 3.2.4 demonstrate that there is still a strong expression of p75NTR in the dorsal horn, regardless of the diminishing p75NTR expression in the ventral horn motor neurons.

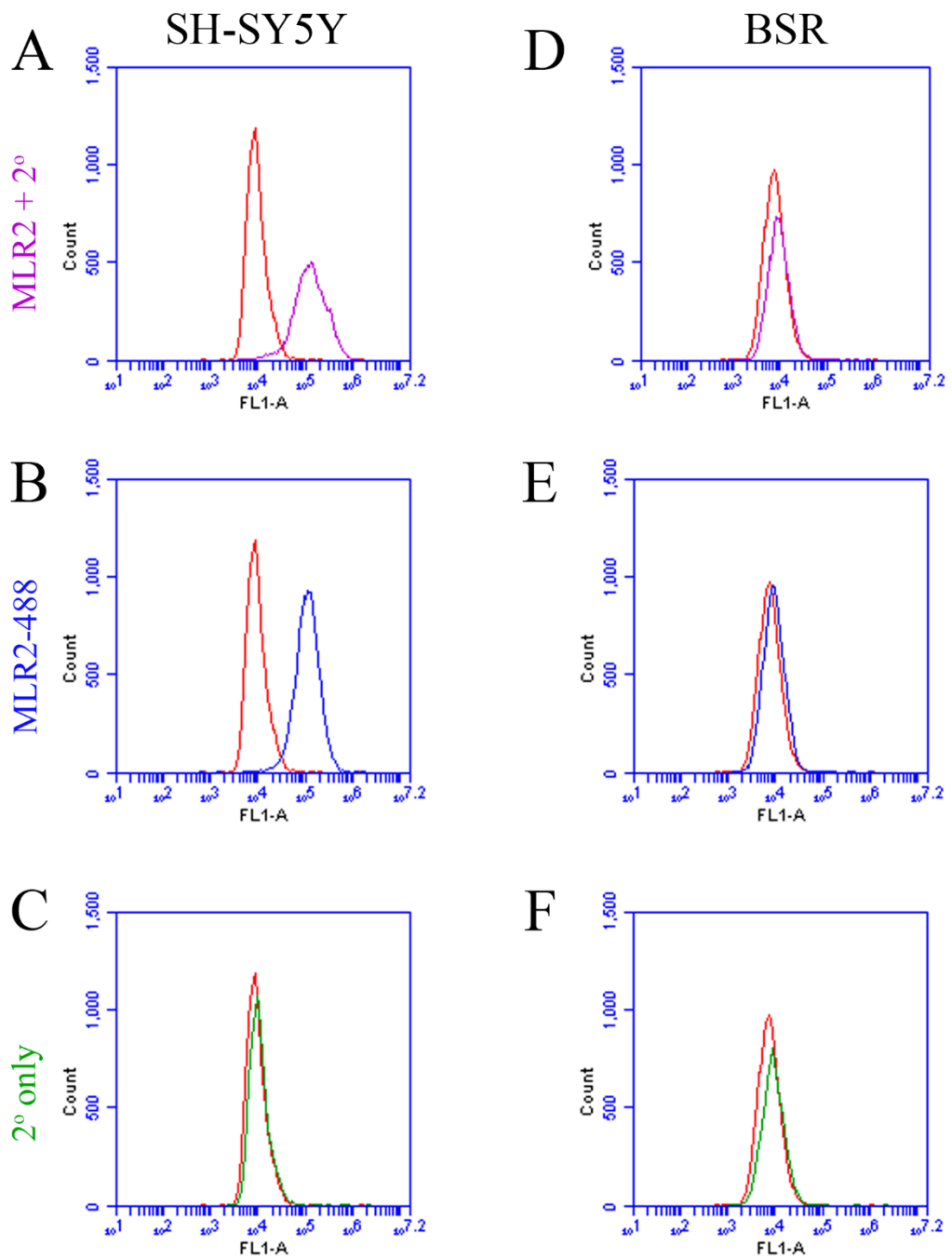


Figure 3.2.1 Conjugated and unconjugated MLR2 binds specifically to p75NTR expressing cells

Flow cytometry analysis shows that 20 μ g/ml MLR2 with 1:100 donkey anti-mouse ATTO-488 (A) and MLR2-ATTO-488 conjugated antibody (B) increases fluorescence intensity in p75NTR expressing SHSY-5Y neuroblastoma cells compared to baseline (untreated cells (red)). No increase from baseline is seen in p75NTR-ve BSR fibroblasts in both the unconjugated (D) and conjugated (E) MLR2. Secondary antibodies only (donkey anti-mouse ATTO-488) do not cause an increase in fluorescence intensity (C,F)

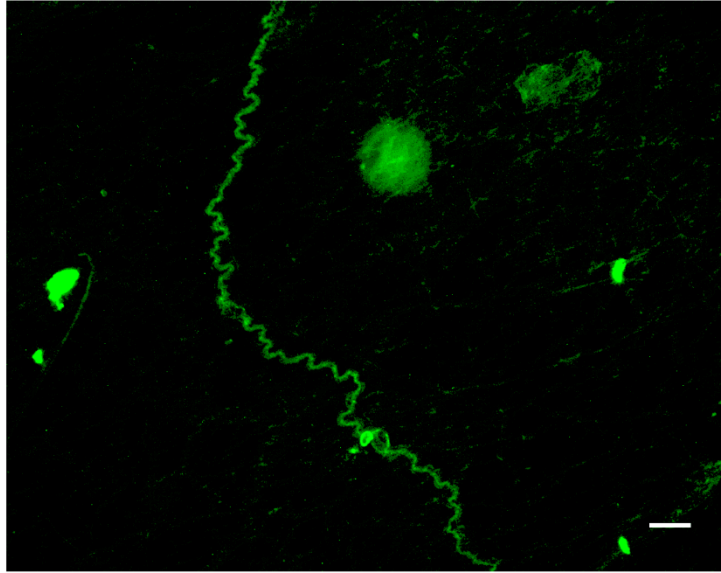
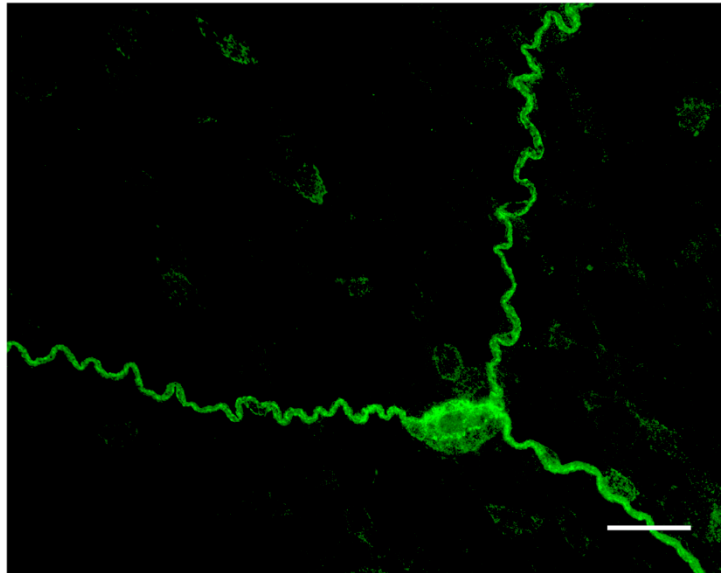
A**B**

Figure 3.2.2 MLR2-ATTO-488 binds to fresh mouse mesentery tissue

Mesentery taken from B6 mice show that (A) 20 μ g/ml MLR2-ATTO-488 is able to bind to peripheral neurons surrounding blood vessels, which is comparable to (B) polyclonal 3 μ g/ml goat anti-p75NTR antibody + 2^o anti-sheep ATTO-488 (1:800) antibody combination (scale =50 μ m).

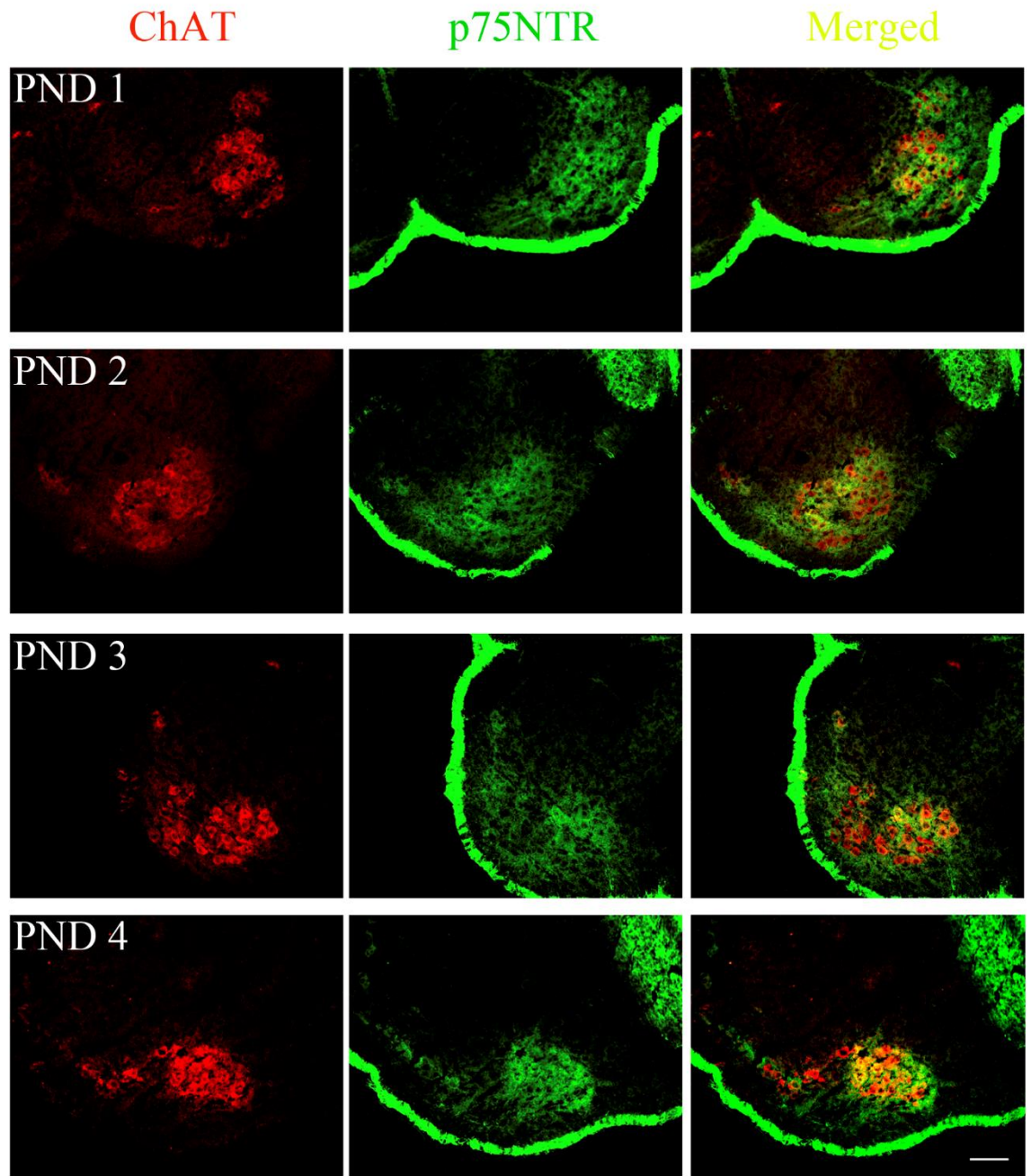


Figure 3.2.3a p75NTR expression in PND 1-4 neonatal spinal cords

Lumbar spinal cords from neonatal B6 mice were analysed for p75NTR expression in motor neurons from PND 1-4, using 1 μ g/ml goat anti-p75NTR + 2 $^{\circ}$ anti-sheep ATTO-488 (1:800) and 1:5000 rabbit anti-ChAT + 2 $^{\circ}$ anti-rabbit Cy3 (1:800). High expression of ChAT can be seen across the first 4 days after birth, with strong p75NTR expression at all 4 days, made apparent in the merged images. (scale = 50 μ m)

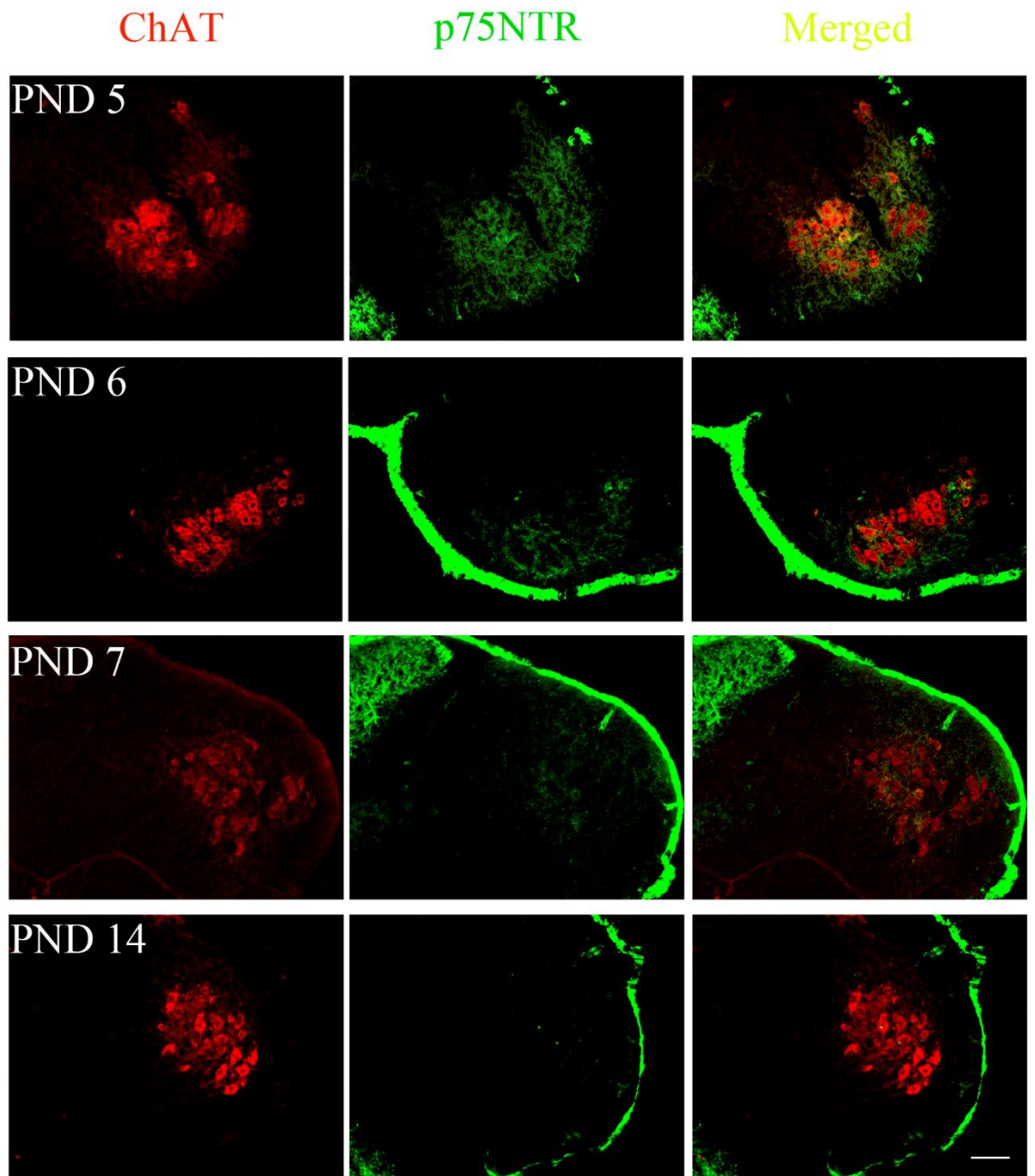


Figure 3.2.3b p75NTR expression in PND 5-7 and PND 14 neonatal spinal cords

Lumbar spinal cords from neonatal B6 mice were analysed for p75NTR expression in motor neurons, from PND 5-7 and PND 14, using 1 μ g/ml goat anti-p75NTR + 2 $^{\circ}$ anti-sheep ATTO-488 (1:800) and 1:5000 rabbit anti-ChAT + 2 $^{\circ}$ anti-rabbit Cy3 (1:800). High expression of ChAT can be seen across all ages, including PND 14. p75NTR expression is still high in PND 5, but drops rapidly in PND 6 and PND 7. p75NTR expression is completely absent by PND 14. (scale = 50 μ m)

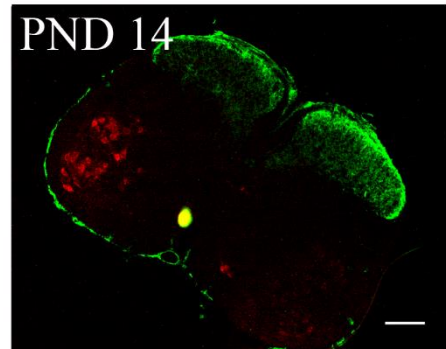
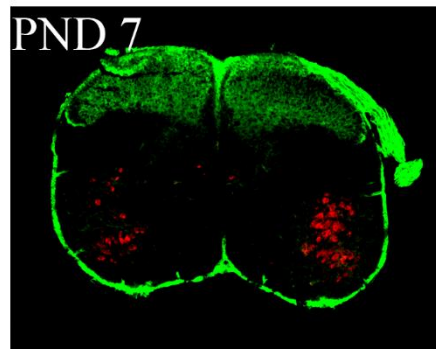
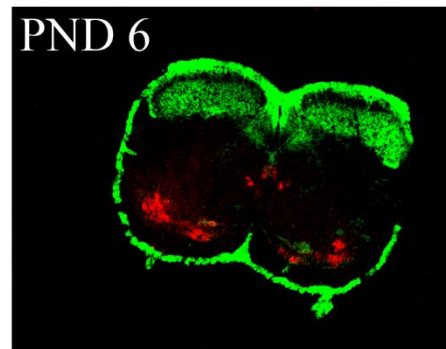
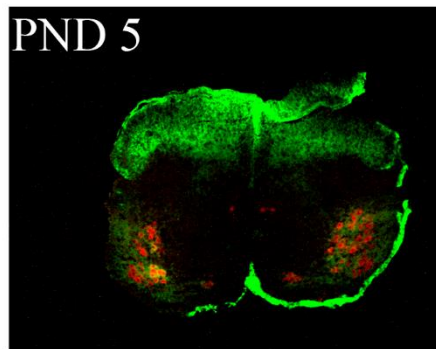
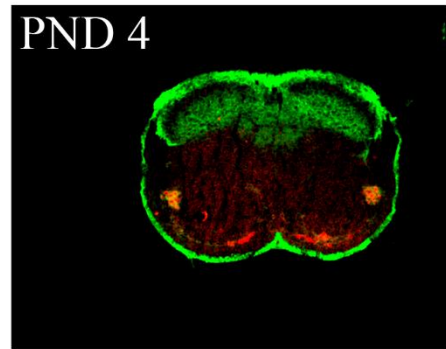
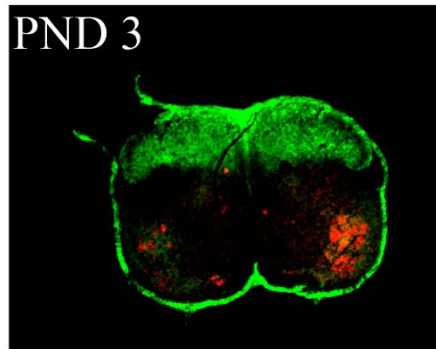
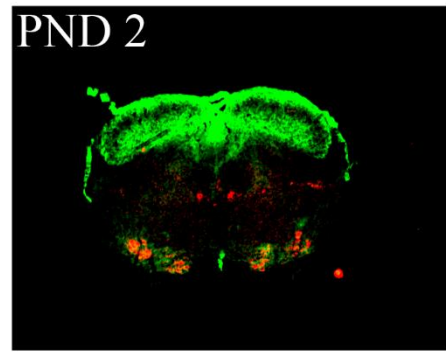
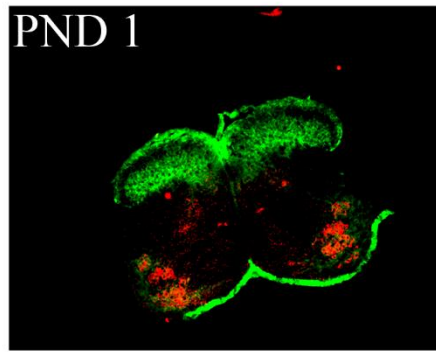


Figure 3.2.4 p75NTR expression does not change in the dorsal horn in PND 1-7 and 14 neonatal lumbar spinal cords

Lower magnification images of B6 spinal cords stained with 1 μ g/ml goat anti-p75NTR + 2 $^{\circ}$ anti-sheep ATTO-488 (1:800) and 1:5000 rabbit anti-ChAT + 2 $^{\circ}$ anti-rabbit Cy3 (1:800) show that p75NTR expression decreases in the ventral region of B6 neonatal mice from PND 1-7 and is completely gone by PND 14. However, the expression of p75NTR does not change in the dorsal horn, regardless of age. (scale = 200 μ m)

Figure 3.2.5 depicts the average number of p75NTR/ChAT+ve, ChAT+ve or p75NTR+ve neurons in PND 1-7 and 14 neonatal mice. 92.6% of all motor neurons express p75NTR at PND 1, which gradually declines to 44.5% by PND 7. Reciprocally, 7.4% of motor neurons do not express p75NTR at PND 1, which increases to 55.5% by PND 7. By PND 14, only 1.4% of motor neurons express p75NTR, while 98.2% of motor neurons do not express the receptor.

3.2.4 *MLR2-ATTO-488 is retrogradely transported to motor neurons in the spinal cord of neonatal mice*

Having determined that ~92.6% of motor neurons express p75NTR at PND1, we wanted to see if these motor neurons could be specifically targeted by our anti-p75NTR MLR2 antibody. Targeting spinal motor neurons expressing p75NTR in PND 1 B6 mice injected with 150µg MLR2-ATTO-488 (2x 75ug, 12 hours apart) shows MLR2 is able to be retrogradely transported to spinal motor neurons.

Motor neurons were identified by Choline Acetyltransferase (ChAT) antibody staining. Figure 3.2.6a shows fluorescent micrographs of lumbar spinal cord from neonatal mice 36 hours after injection of 150µg of MLR2-ATTO-488. (A) shows ATTO-488 fluorescence in ventral region neurons, (B) ChAT staining for motor neurons and (C) merged, where it can be seen that MLR2-ATTO-488 is only in ChAT expressing spinal motor neurons. Mice not injected show no ATTO-488 fluorescence (D), with ChAT immunofluorescence (E) and no overlap seen in the merged image (F).

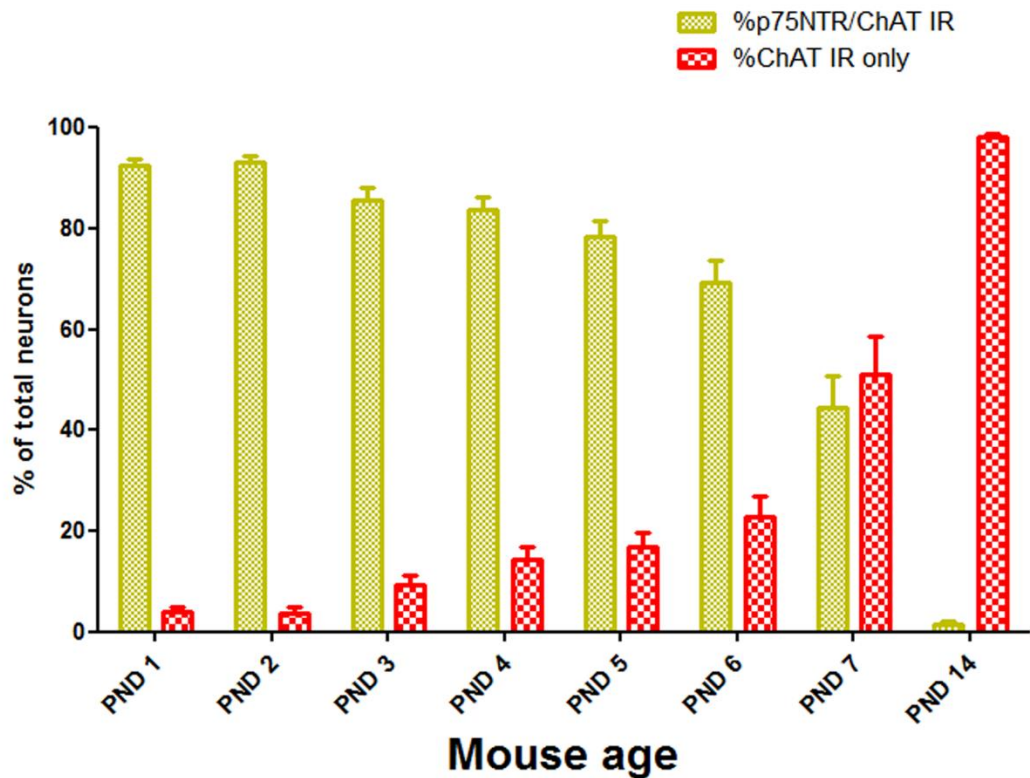


Figure 3.2.5 Expression of p75NTR in lumbar motor neurons of PND 1-7 and PND 14 neonatal mice

Lumbar spinal cords were taken from B6 neonatal mice aged 1-7 days and 14 days, and counterstained for ChAT and p75NTR. The percentage of motor neurons that co-expressed p75NTR and ChAT were quantified. 92.6% of all motor neurons expressed p75NTR at PND1, which declined to 44.5% by PND7. Only 1.4% of motor neurons expressed p75NTR at PND14. Reciprocally, 7.4% of motor neurons were p75NTR-ve at PND1, which increased to 55.5% by PND7 and 98.6% at PND14. (n=3, \pm SEM)

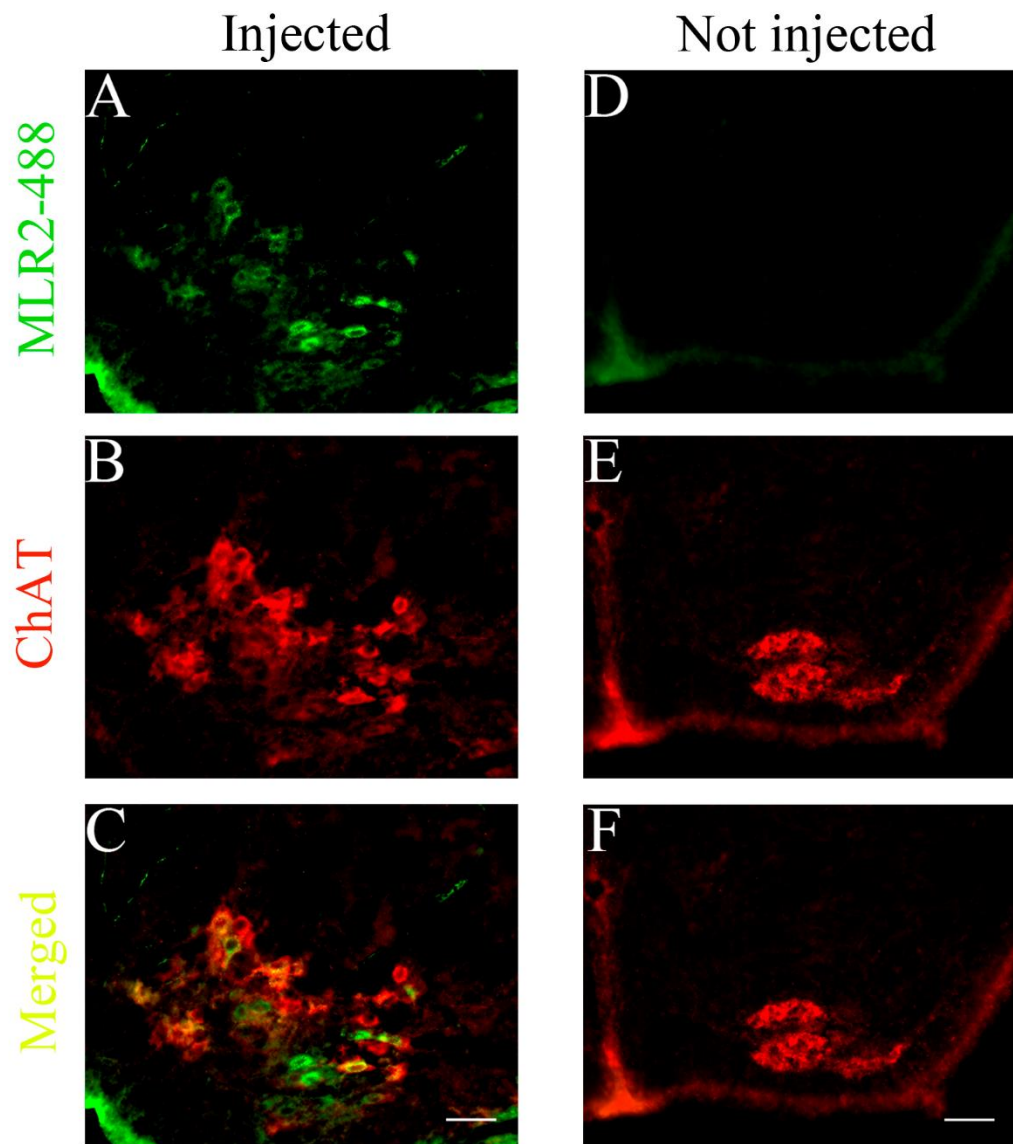


Figure 3.2.6a Retrograde transport of MLR2-ATTO-488 to the spinal cord of neonatal mice

PND1 B6 mice were intraperitoneally injected twice with 75ug (150ug total), twelve hours apart with MLR2-ATTO-488. Spinal cords were removed 36 hours after initial injection, processed, cut at 30 μ m and counterstained with 1:5000 rabbit anti-ChAT + 2 $^{\circ}$ anti-rabbit Cy3 (1:800). (A) MLR2-ATTO-488 was able to successfully retrogradely transported to the ventral motor neurons in the spinal cord, shown by ChAT immunoreactivity (B) and merging images together (C). (D) mice that were not injected showed no fluorescence in the channel for ATTO-488, yet showed staining of motor neurons (E), with no co-fluorescence (F). (scale bar = 50 μ m).

The retrograde transport of labelled MLR2 was quantified. MLR2 was found at all levels of the spinal cord (Figure 3.2.6b, 88.6±1.0% lumbar, 95.7±0.5% thoracic and 87.3±3.8% cervical) (Rogers *et al.*, 2014).

3.2.5 MLR2-ATTO-488 is transported to p75NTR expressing DRG neurons

The expression of p75NTR is not exclusive to spinal motor neurons. p75NTR is also expressed in sensory DRG neurons. Therefore, neonatal mice injected intraperitoneally with 150µg MLR2-ATTO-488 (75µg x2, 12 hours apart) had their DRGs removed and analysed for ATTO-488 fluorescence and p75NTR expression.

Figure 3.2.7 shows DRGs from mice injected with MLR2-ATTO-488 (A) with ATTO-488 fluorescence in many of the neurons, and (B) DRGs that from mice that have not been injected, showing no ATTO-488 fluorescence.

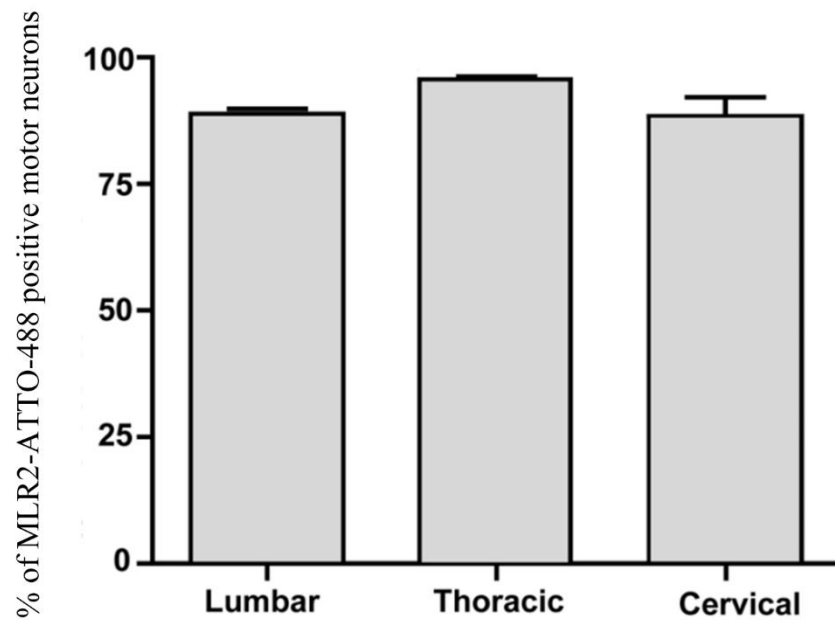
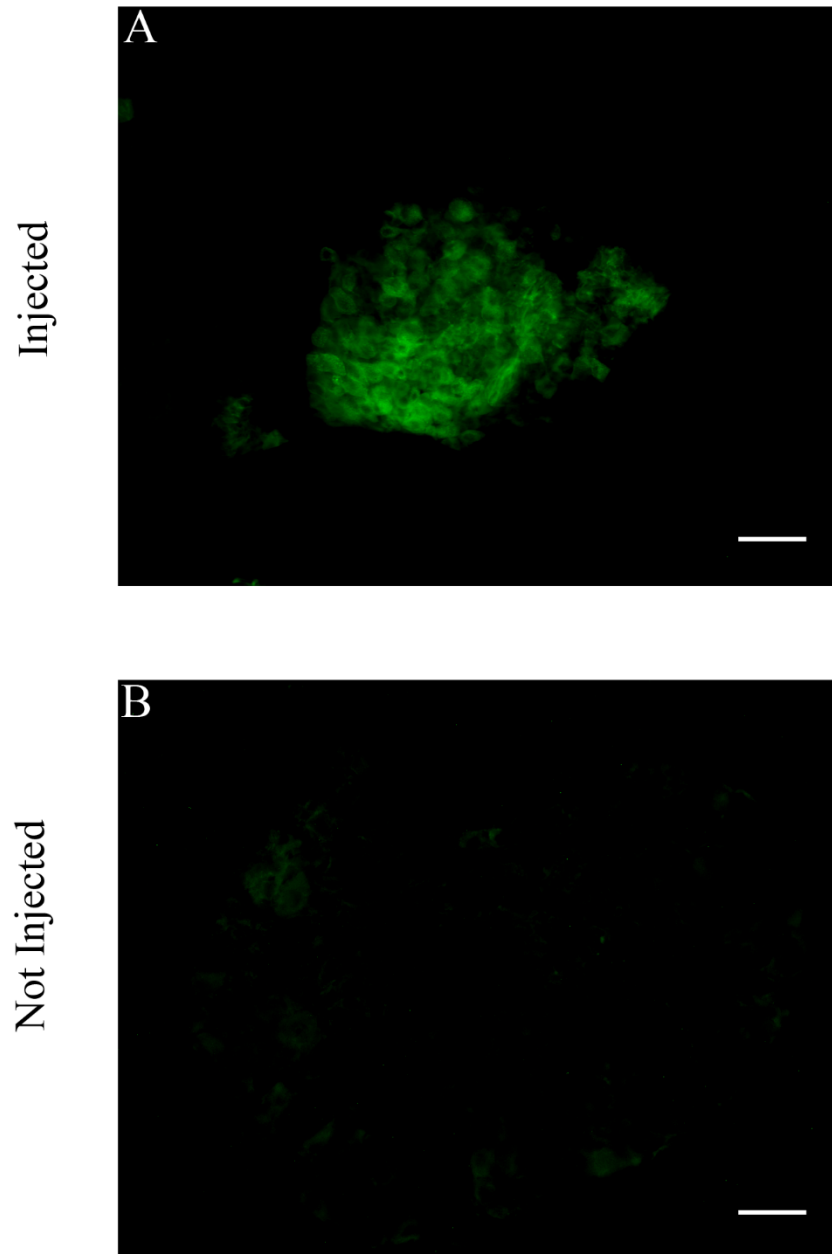


Figure 3.2.6b Quantification of retrogradely transported MLR2-ATTO-488 to neonatal spinal motor neurons

PND1 B6 mice were intraperitoneally injected twice with 75ug (150ug total), twelve hours apart with MLR2-ATTO-488. Spinal cords were removed 36 hours after initial injection, processed, cut at 30 μ m and counterstained. The percentage of motor neurons in each respective region of the spinal cord that showed ATTO-488 fluorescence were, 88.6 \pm 1.0% lumbar, 95.7 \pm 0.5% thoracic and 87.3 \pm 3.8% cervical (n=3, \pm SEM)

ATTO-488



3.2.7 MLR2-ATTO-488 is retrogradely transported to neonatal DRGs

Fluorescent micrographs taken from neonatal mice injected intraperitoneally with 150 μ g MLR2-ATTO-488 (75 μ g x2, 12 hours apart) show that in (A) fluorescent ATTO-488 can be seen in DRGs. Conversely, no ATTO-488 fluorescence can be seen in neonates that have not been injected with the labelled antibody (B). (scale = 50 μ m)

3.3 Discussion

p75NTR is an attractive vector for delivering genetic material to motor neurons in MND and MND model mice, due to motor neuron re-expression in disease (Seeburger *et al.*, 1993; Lowry *et al.*, 2001; Copray *et al.*, 2003). MLR2 is an internalising anti-p75NTR monoclonal antibody, with cross-species reactivity, including both mouse and human p75NTR. It is able to selectively bind to p75NTR expressing cells *in vitro* and *in vivo* and cause the receptor to be internalised (Rogers *et al.*, 2006; Matusica *et al.*, 2008).

MLR2 is able to be conjugated to a fluorophore without losing receptor affinity, as shown in both FACS analysis and mesentery immunohistochemistry. As the binding properties of MLR2 are stable when conjugated, it is possible to replace the fluorophore with a cargo carrying molecule, such as PEI (polyethylenamine) (Rogers & Rush, 2012).

The expression of p75NTR in the developing motor neurons has been shown to be high during development and neonatal age, down regulated in adulthood, and re-expressed after nerve trauma (Yan & Johnson, 1988; Ernfors *et al.*, 1989a; Wiese *et al.*, 1999; Je *et al.*, 2013). This work however, was performed in rats (E11-PND10, (Yan & Johnson, 1988)). p75NTR expression from PND1-7 drops from 92.6% to 44.5%, respectively, and is almost completely absent (1.4%) by 14 days. Therefore to use p75NTR as a vector for accessing motor neuron within the CNS of healthy B6 mice from the periphery, administration must be performed as soon as possible after birth to achieve the involvement of the maximum number of motor neurons. However, expression of p75NTR in sensory fibers in the dorsal horn from DRG sensory neurons does not diminish over time (Yan & Johnson,

1988), unless there has been a sciatic nerve injury near the DRG which causes a decrease in p75NTR expression (Sebert & Shooter, 1993). The ability to target these p75NTR sensory neurons may lead to understanding and/or treating pain, as p75NTR appears to be directly involved with mechanical hyperalgesia (Khodorova, Nicol & Strichartz, 2013).

Labeled MLR2 (MLR2-ATTO-488) injected intraperitoneally into neonatal mice (PND 1) was observed in the majority of spinal motor neurons 36 hours after administration. MLR2-ATTO-488 injected intraperitoneally revealed that over 90% of motor neurons were able to take up the labelled antibody (Rogers *et al.*, 2014). Previous work has shown the majority of motor neurons and sensory fibers in the spinal cord can be accessed in a similar manner by intravenous or intraperitoneally delivered agents that travel retrogradely in motor neurons and sensory fibers. This was shown where systemic delivery (both intraperitoneal and intravenous injections) of retrograde tracing agent cholera toxin subunit B (CTB) accessed all spinal motor neurons (Alisky, van de Wetering & Davidson, 2002) and produced similar profiles to those seen in the MLR2-ATTO-488 injected animals in this current study. Thus, the most likely travel route of MLR2 to the motor neuron somas is similar to that of the CTB, where it binds to cell surface receptors at the neuromuscular junctions, after intraperitoneal injections and it then is retrogradely transported back to the CNS.

As p75NTR levels are highest at PND1 and these motor neurons are able to be targeted after intraperitoneal injections, administration p75NTR targeting complexes to neonatal mice is the next step in the development of a non-viral gene therapy for MND.

Chapter 4: Construction of the
MLR2-immunogene and its
use for *in vitro* transfection

4.1 Introduction

Gene therapy has the potential to be developed for diseases, such as motor neuron disease (MND) that have both unknown spontaneous origins and identified genetic mutations. Our laboratory has been working on a method of utilizing antibodies to specific cell surface receptors (p75^{NTR}) that internalise with the receptor and deliver exogenous genes or RNA. These are termed ‘immunogenes’. They are composed of an antibody to a specific internalizing receptor that is conjugated to a PEGylated cationic molecule that is able to bind and condense DNA or RNA (Rogers & Rush, 2012). The antibody binds to its specific cognate cell surface receptor and internalizes into the cell, delivering the DNA/RNA cargo to achieve a functional transfection (see Figure 1.5 and 1.6 from introduction for delivery mechanism).

There are a number of effective DNA and RNA condensing agents that include cationic polymers, lipid based agents, modified peptides, dendrimers and nanoparticles, such as modified silica (Pérez-Martínez *et al.*, 2011). Cationic polymers such as poly-l-lysine (PLL) and polyethylenamine (PEI) have been extensively trialled as condensing agents. Polyethylenamine (PEI) possesses a high cationic charge density due to secondary amine groups that enables the endosomal/lysosomal release of complexes due to the “proton sponge effect” (Boussif *et al.*, 1995; Morille *et al.*, 2008). PEI, unlike PLL, also facilitates the entry of plasmid DNA into the nucleus (Godbey, Wu & Mikos, 1999). However, PEI can be also highly toxic (Boussif *et al.*, 1995; Ogris *et al.*, 1999; Morille *et al.*, 2008). The high number of amines on the PEI is integral for endosomal

escape and cargo delivery. However, it can be shielded by PEGylation (polyethylene glycol) and charge neutralised with the electrostatically bound negatively charged pDNA, which prevents the complex from interacting with blood components. Charge neutralising the complex is achieved by a ratio of PEI amine nitrogens (N) and DNA backbone phosphates (P, N/P ratio). The N/P ratio that neutralises charge can be found by using a gel retardation assay (Kircheis *et al.*, 1997).

Immunogenes targeting MND require an internalizing receptor predominantly expressed on motor neurons. The p75 neurotrophin receptor (p75NTR) is internalised into motor neurons after neurotrophin or specific antibody binding, as previously shown (Roux & Barker, 2002; Matusica *et al.*, 2008). p75NTR is the common neurotrophin receptor expressed on motor neurons during embryonic development, down-regulated during maturation but re-expressed after nerve trauma, such as axotomy (Yan & Johnson, 1988; Ernfors *et al.*, 1989a; Wiese *et al.*, 1999; Je *et al.*, 2013). p75NTR re-expression in motor neurons also occurs during MND in both humans (Kerckhoff *et al.*, 1991; Seeburger *et al.*, 1993; Lowry *et al.*, 2001) and SOD1^{G93A} mice (Copray *et al.*, 2003).

Initial research using immunogenes used an anti-rat p75NTR monoclonal antibody MC192 (Chandler *et al.*, 1984) to deliver pDNA expressing GDNF to motor neurons and showed almost complete motor neuron recovery after total axonal transection (Barati *et al.*, 2006). The MC192 antibody recognises rat, but not mouse or human p75NTR (Chandler *et al.*, 1984). However, an anti-human p75NTR monoclonal that recognises rat, human and mouse p75NTR called

MLR2 was subsequently made (Rogers *et al.*, 2006), and shown that it can be retrogradely transported to motor neurons in neonatal mice, after intraperitoneal injections (Fenech, Masters thesis, 2011). Hence, MLR2 can be used for p75NTR specific delivery to mouse motor neurons.

A major aim of this current study was to use immunogenes in SOD1^{G93A} mice. However, before the immunogene can be used *in vivo*, it must be validated *in vitro*, for both specificity and efficacy. The following work investigates the validity of MLR2 immunogenes in delivering pDNA to NSC-34 cells (motor neuron-like cell line) (Cashman *et al.*, 1992) and primary motor neurons purified and cultured from the spinal cords of E12.5 mice.

4.2 Results

4.2.1 *MLR2 immunogene gel retardation 1*

Before application of the immunogene, both *in vitro* and *in vivo*, the overall charge between the MLR2-PEI-PEG12 and pDNA (pVIVO2-GFP/LacZ) must be neutralised, due to toxicity caused by the high PEI positive charge (Boussif *et al.*, 1995; Ogris *et al.*, 1999), and therefore the correct ratio of immunoporters to pDNA must be found.

The complete immunoporters (MLR2-PEI-PEG12) and a polyplex lacking the antibody (PEI-PEG) were complexed with pDNA (400ng) at differing nitrogen/phosphate ratios (N/P), and run on a 1% agarose gel (Figure 4.2.1). Well 1 shows naked pDNA travels through the gel unhindered. Well 10 contained a 100 BP DNA ladder and well 11 was left blank, Wells 2-5 contained PEI-PEG12 mixed with pDNA at N/P ratios of 5, 7.5, 10 and 15, respectively. All PEI-PEG12 ratios successfully neutralised charge. Wells 6-9 contained MLR2-PEI-PEG12 mixed with pDNA at N/P ratios of 5, 7.5, 10, and 15, respectively. At an N/P ratio of 5 (well 6), the MLR2-PEI-PEG12 complex was unable to neutralise charge. At N/P 7.5, the charge was not completely neutralised, with a small amount of pDNA running through the gel. N/P ratios higher than 7.5 successfully neutralised charge, preventing pDNA movement.

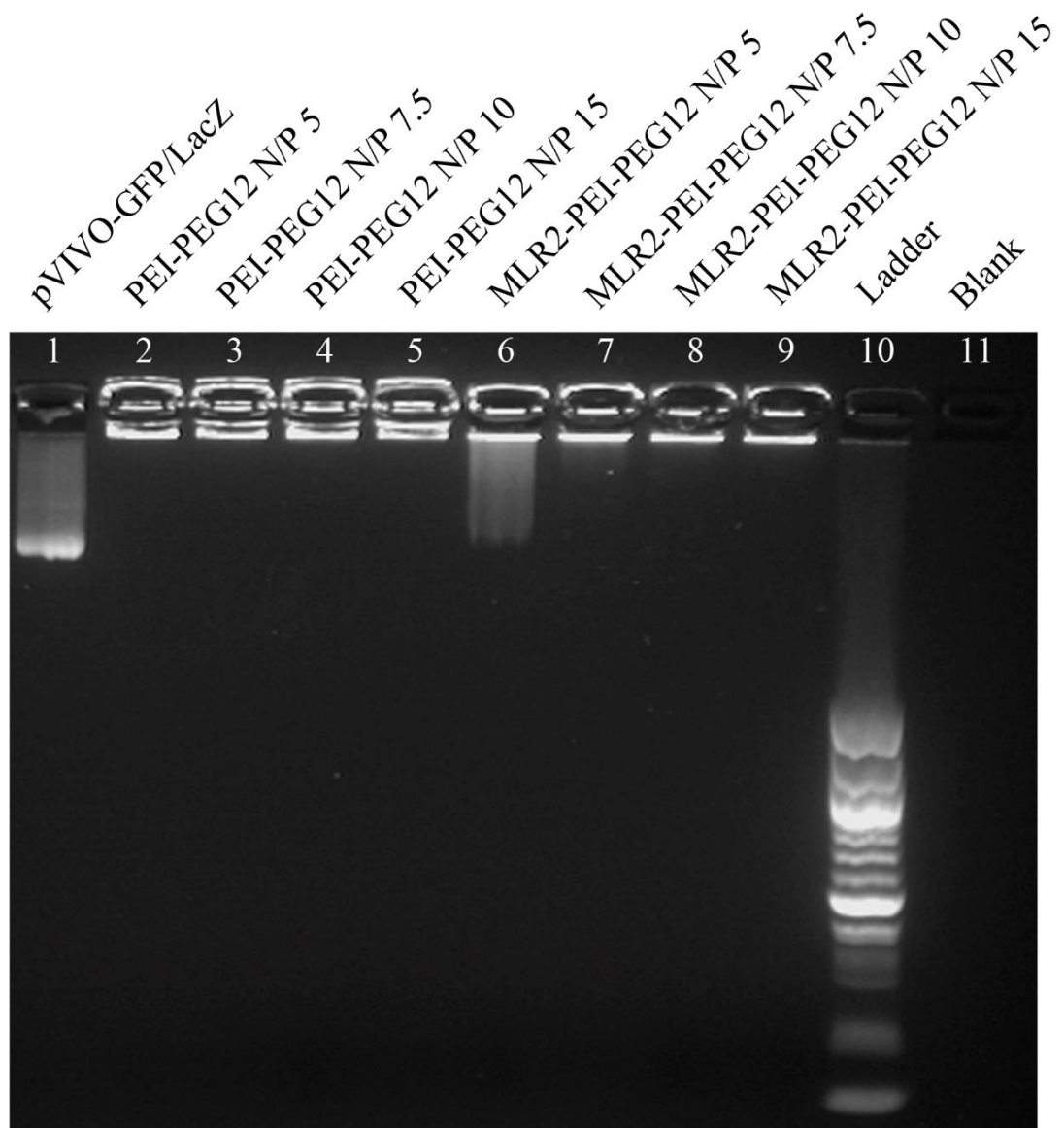


Figure 4.2.1 MLR2-PEI-PEG12 immunogene is able to bind pDNA and neutralise charge

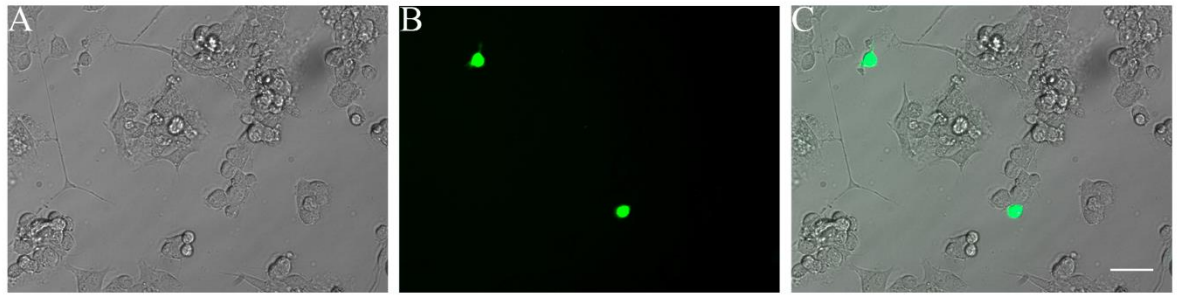
Gel retardation assay run to determine at which PEI-Nitrogen to pDNA-Phosphate ratio (N/P ratio) the immunogene complex carrying the pVIVO2-GFP/LacZ plasmid (4 μ g) is charge neutralised. Well (1) shows the naked plasmid travels through the gel. Wells (2-5) contain PEI-PEG12 mixed with pVIVO2-GFP/LacZ at N/P ratios of 5, 7.5, 10 and 15, respectively. All PEI-PEG12 ratios successfully bound pDNA and neutralised charge. Wells (6-9) contain MLR2-PEI-PEG12 mixed with pVIVO2-GFP/LacZ at N/P ratios of 5, 7.5, 10, and 15, respectively. At an N/P ratio of 5 (well 6), the MLR2-PEI-PEG12 complex was unable to neutralise charge. At N/P 7.5, the charge is not completely neutralised, with a small amount of pDNA running through the gel. N/P ratios higher than 7.5 successfully neutralised charge, preventing pDNA movement. Well (10) contained a 100 BP DNA ladder and well (11) was left blank.

4.2.2 Transfection of cell lines (NSC-34 and BSR) with the MLR2 immunogene and PEI polyplexes

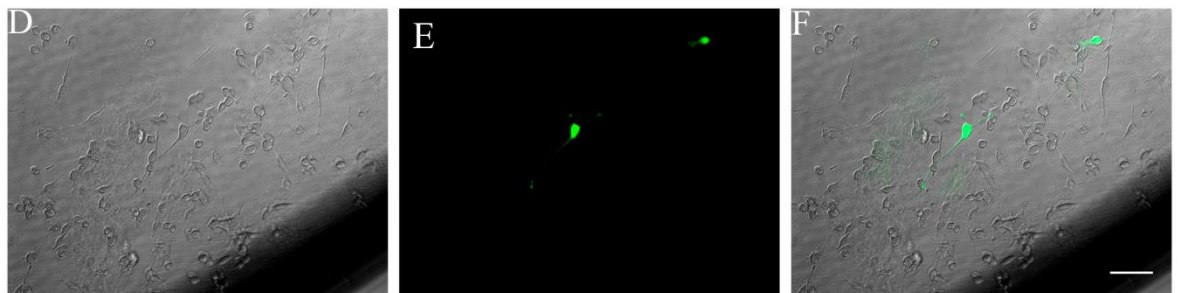
Motor neuron-like cell line NSC-34 express p75NTR on their cell surface (Turner *et al.*, 2004) and were used as an *in vitro* model for testing the transfection ability of the MLR2 immunoportor (MLR2-PEI-PEG12), PEI polyplex (PEI-PEG12) or PEI alone (PEI), with the pVIVO2-GFP/LacZ plasmid at N/P ratios where the charge was neutralised (described above). NSC-34 cells were grown in serum-free media for one hour, then incubated with 12.99 μ g MLR2-PEI-PEG12 (N/P 10), 6.50 μ g PEI-PEG12 (N/P 5) or 2.60 μ g PEI (N/P 2), each carrying 10 μ g pDNA for four to six hours before media was changed to complete media, including serum, and imaged 24 hours after complex application (Figure 4.2.2a). Brightfield (A) and fluorescent (B) images of NSC-34 cells that have been incubated with MLR2-PEI-PEG12 (N/P ratio 10) show healthy cells that express the GFP coded by the pVIVO2-GFP/LacZ plasmid. The transfection levels *in vitro* of the MLR2 immunogene is ~24% of the total cell population (Figure 4.2.2b).

Where PEI-PEG was used (N/P ratio 5) with pVIVO2, NSC-34 cells expressed GFP, while keeping the cells healthy. PEI without PEGylation is considered toxic due to its high positive charge. Image (G-I) show brightfield and fluorescent images of PEI (N/P ratio 2) treated cells, with a higher level of transfection compared to PEI-PEG12 and MLR2-PEI-PEG12. However, there is also a high degree of debris, indicating cell death.

MLR2-PEI-PEG12 N/P 10



PEI-PEG12 N/P 5



PEI N/P 2

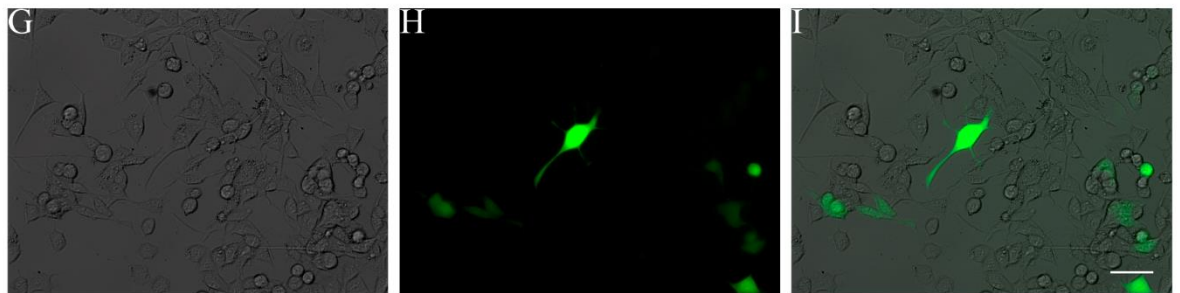
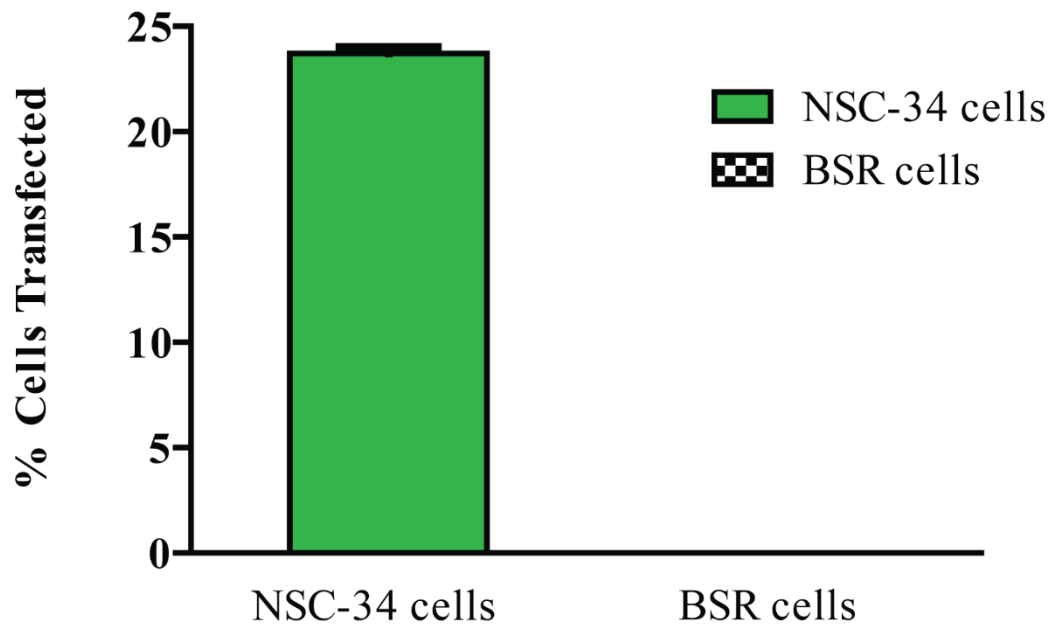


Figure 4.2.2a MLR2 Immunogene is able to transfect p75NTR expressing NSC34 cells

Brightfield and fluorescent images show NSC34 cells that have been treated with 12.99 μ g MLR2-PEI-PEG12 with pVIVO2-GFP/LacZ (10 μ g, N/P 10), 6.50 μ g PEI-PEG12 with pVIVO2-GFP/LacZ (10 μ g, N/P 5) or 2.60 μ g PEI with pVIVO2-GFP/LacZ (10 μ g, N/P 2), incubated for 4 hours before fresh media change. Image (A) shows NSC34 cells that were treated with MLR2-PEI-PEG12 N/P 10, with expression of GFP seen in (B-C). Image (D) contained PEI-PEG12 N/P 5 treated NSC34 cells again with GFP expression (E-F). The NSC34 cells in image (G) were treated with PEI N/P 2, which shows expression of GFP (H-I) in a higher number of cells compared to the immunogene and PEGylated PEI complex.

Expression of the pVIVO2-GFP/LacZ plasmid persisted for 7+ days in cell culture.
(scale = 50 μ m)



4.2.2b The average percentage of NSC34 and BSR cells transfected by the MLR2-PEI-PEG12 immunogene

NSC34 or BSR cells treated with 12.99 μ g MLR2-PEI-PEG12 carrying 10 μ g of pVIVO2-GFP/LacZ (N/P 10) were quantified for transfection percentage, measured by GFP expression. Approximately 23.7% of NSC34 cells were transfected with the MLR2 immunogene, while none of the of BSR cells showed transfection.

To show MLR2-p75NTR specificity, BSR cells (hamster fibroblast cells (Tuffereau *et al.*, 1998)) that do not express p75NTR were incubated with the same complexes, ratios, time and 10ug pDNA (Figure 4.2.3) as the NSC-34 cells. BSR cells incubated with PEI-PEG12-pVIVO2 (N/P ratio 5; D-F) shows transfection, indicating that PEI-PEG12 can transfect cells without the internalising p75NTR antibody MLR2. However, BSR cells incubated with MLR2-PEI-PEG12-pVIVO2 (N/P ratio 10, Image (A-C)) show no transfection (Figure 4.2.2b). Hence, MLR2-PEI-PEG12-pVIVO2 specifically transfect cells that contain p75NTR. Similar to the NSC-34 cells, there is also higher level of transfection seen with PEI alone (N/P ratio 2, G-I) and high cell death. When the BSR cells are incubated for 24 hours with PEI (N/P ratio 2), there is a very high level of transfection, as well as a very high level of cell death (J-L).

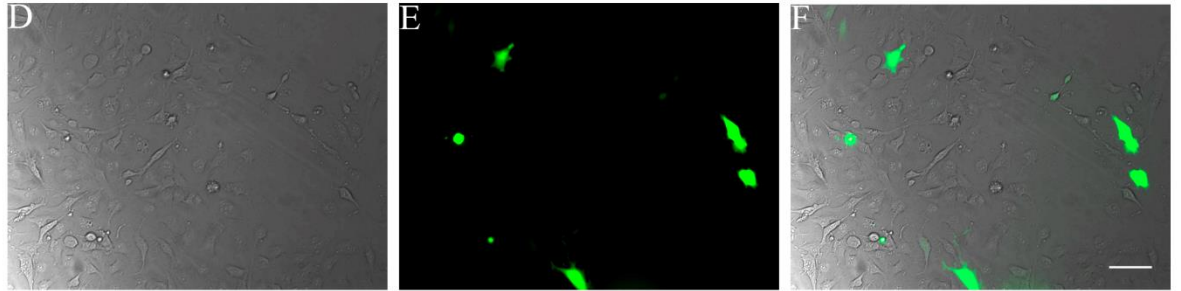
4.2.3 *MLR2 immunogene is able to transfect primary embryonic murine motor neurons*

Mixed cultures of embryonic motor neurons that express p75NTR and glial cells that do not (Wiese *et al.*, 2010) taken from E12.5 murine spinal cords were incubated with the MLR2 immunogene and PEI polyplexes to determine whether the pVIVO2-GFP/LacZ plasmid (20µg) can transfect primary neuronal cells (Figure 4.2.4). Primary cultures were treated identically to the NSC-34 and BSR cells, briefly; 1 hour in serum free media, and 4-6 hour incubation with complexes, full serum-media added and imaged 24 hours later. Image (A) shows an example of a motor neuron after application of MLR2-PEI-PEG12 (N/P ratio

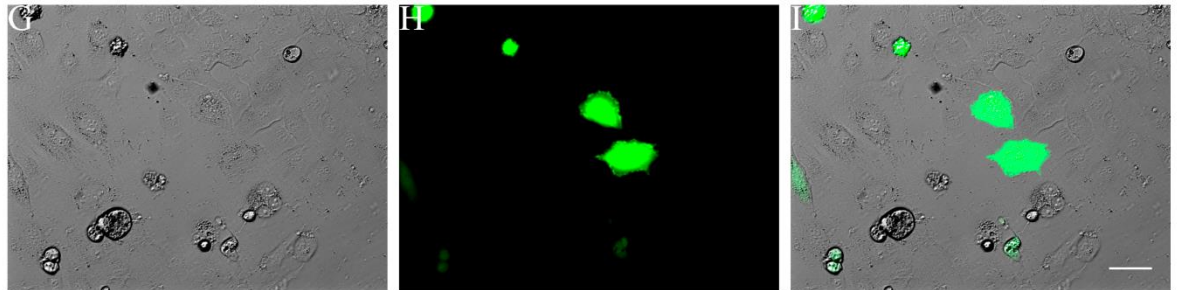
MLR2-PEI-PEG12 N/P 10



PEI-PEG12 N/P 5



PEI N/P 2



PEI N/P 2, 24 hour incubation

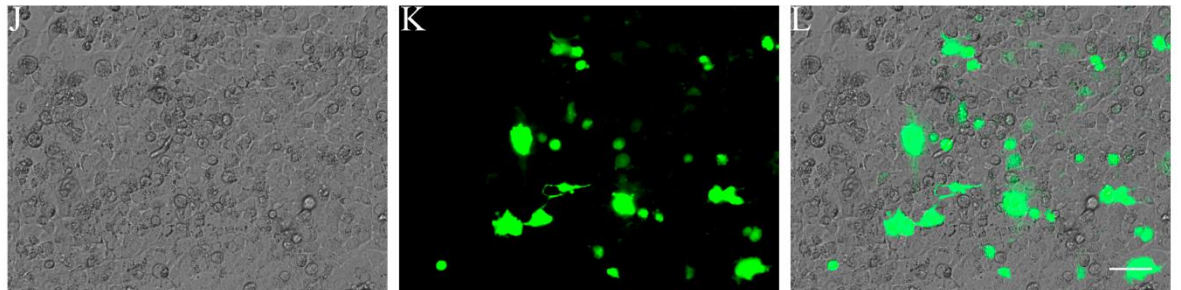


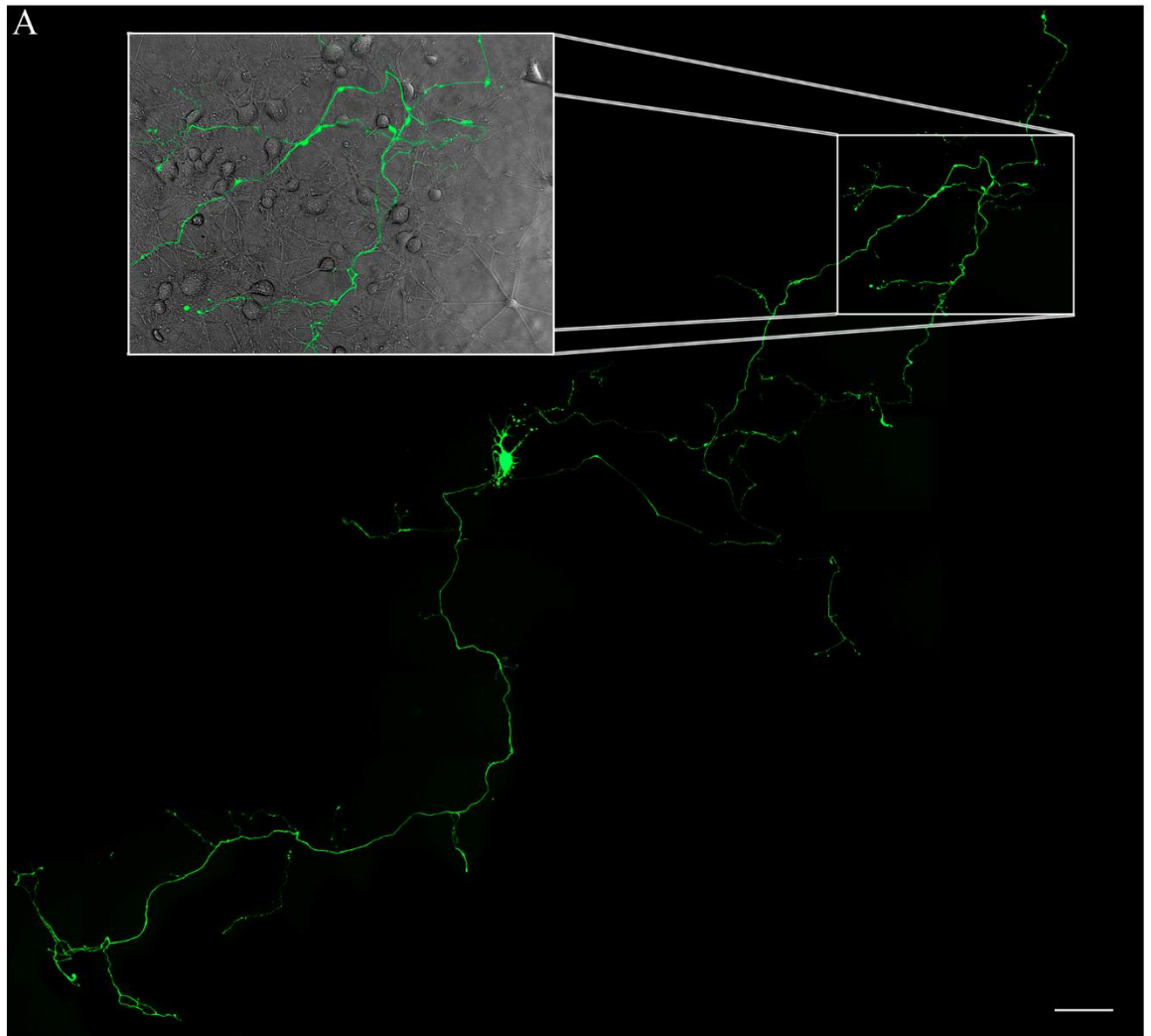
Figure 4.2.3 MLR2 Immunogene is unable to transfect p75NTR negative BSR cells

Fluorescent and brightfield images of BSR cells that have been treated with 12.99 μ g MLR2-PEI-PEG12 with pVIVO2-GFP/LacZ (10 μ g, N/P 10), 6.50 μ g PEI-PEG12 with pVIVO2-GFP/LacZ (10 μ g, N/P 5) or 2.60 μ g PEI with pVIVO2-GFP/LacZ (10 μ g, N/P 2), incubated for 4 hours (A-I) or 24 hours (J-L) before fresh media change. Image (A) shows BSR cells that were treated with MLR2-PEI-PEG12 N/P 10 (B) in a highly confluent and dense culture with no GFP expression. Image (D) contained PEI-PEG12 N/P 5 treated BSR cells with GFP expression (E-F). The BSR cells in image (G) were treated with PEI N/P 2, again with expression of GFP (H-I). Image (J) shows PEI N/P 2 treated BSR cells incubated for 24 hours, leading to high cell death, although high transfection (K-L). (scale = 50 μ m)

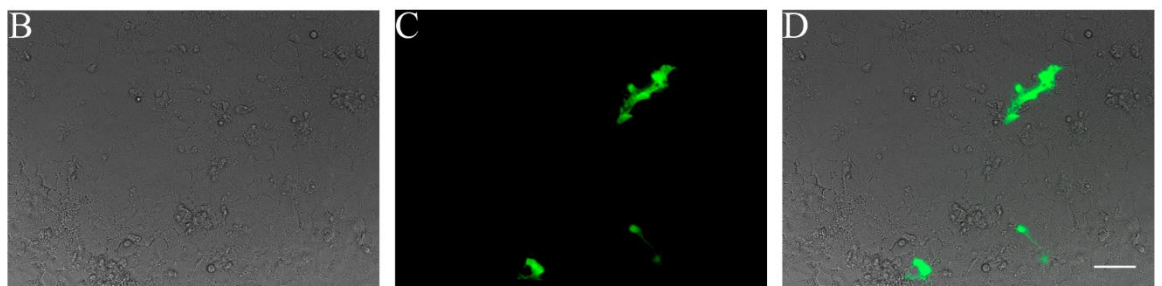
Figure 4.2.4 MLR2 immunogene and PEI polyplexes transfection of embryonic motor neuron mixed cultures

Motor neurons cultured from E12.5 embryonic murine spinal cords were incubated with MLR2-PEI-PEG12, PEI-PEG12 or PEI (20 μ g pDNA). Image (A) shows a motor neuron transfected by the MLR2-PEI-PEG12 N/P 10 expressing GFP throughout the soma and extensive processers, in a mixed culture (neurons/glia) shown in the white box insert. (B) shows a motor neuron mixed culture incubated with PEI-PEG12 N/P 5 displaying GFP expression (C-D) in non-neuronal glial cells, demonstrating the overall non-specificity of PEI in transfection. However, the PEI complex (PEGylated or alone) is still able to transfect motor neurons, as seen in (E-G) with PEI N/P 2 (scale = 50 μ m)

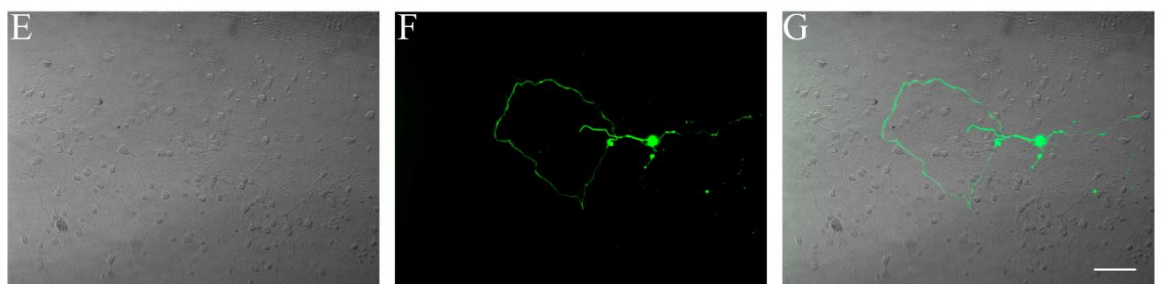
MLR2-PEI-PEG12 N/P 10



PEI-PEG12 N/P 5



PEI N/P 2



10) with extensive expression of GFP throughout the soma and processes. No expression of GFP was seen in glial cells, made more apparent by the insert, showing a mixed culture of neurons and glia. PEI complexes including PEI-PEG12 (N/P ratio 5, B-D) and PEI (N/P ratio 2, E-G) show indiscriminate expression of GFP in both motor neurons and glial cells.

Primary motor neuron cultures were also transfected with pVIVO2-GFP/LacZ using Lipofectamine as a control for anti-GFP counterstains (Figure 4.2.5).

Briefly, these cultures were fixed and counterstained with a chicken anti-GFP polyclonal antibody (1:500). Image (A) and (E) show primary cells expressing GFP. (B) and (F) show cultures counterstained for GFP. (C) and (G) are merged images of (A-B) and (E-F), respectively, showing GFP counterstaining on GFP expressing cells. (D) and (H) show merged images (C) and (G) overlaid on their respective brightfield images.

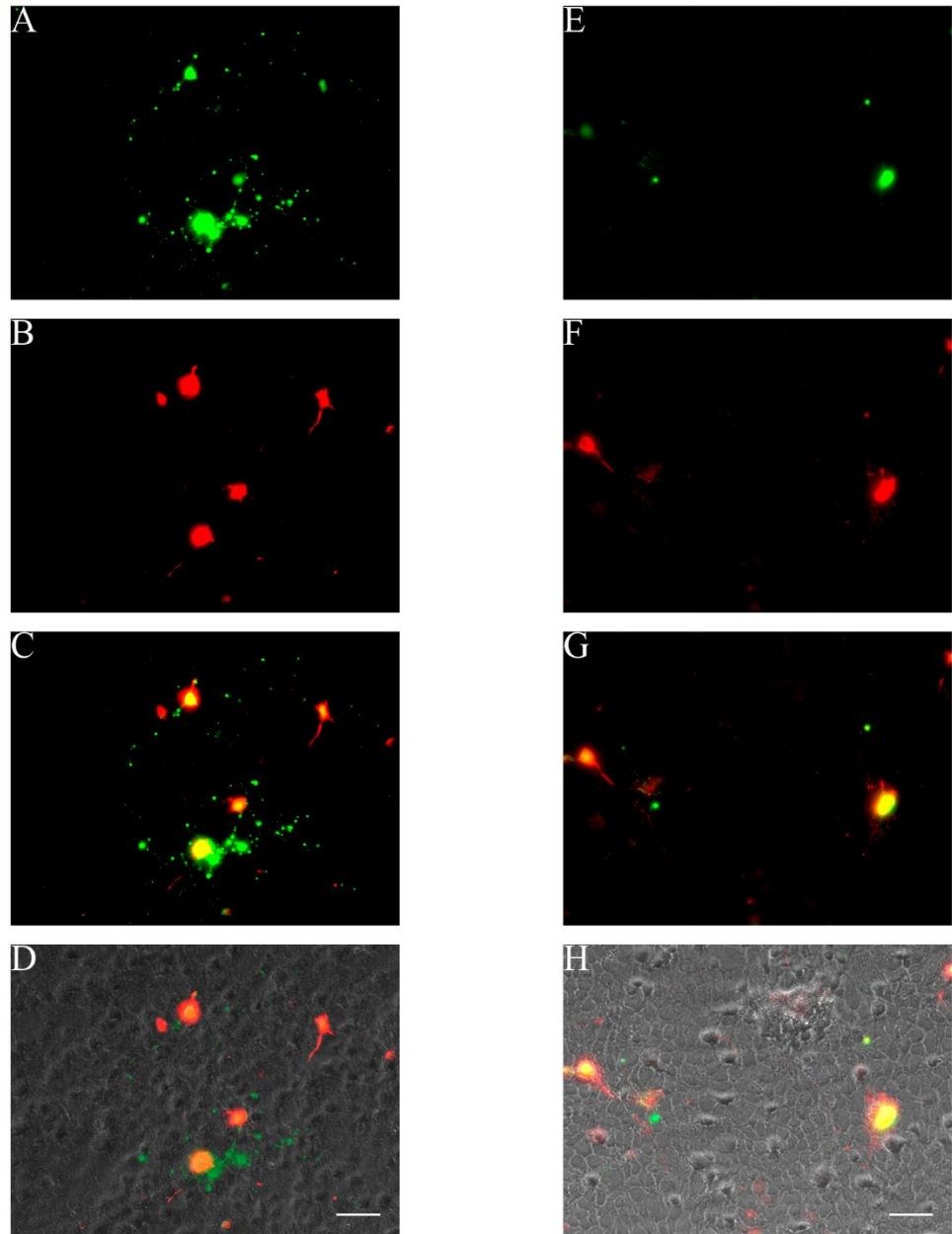


Figure 4.2.5 Anti-GFP antibody detects GFP expressing primary motor neuron cell cultures

Mixed primary cell cultures of motor neurons and astrocytes were transfected using lipofectamine with pVIVO2-GFP/LacZ and counterstained with chicken anti-GFP (1:500) + 2° donkey anti-chicken Cy3 (1:800), to determine if GFP can be immunofluorescently detected. Image (A) and (E) show primary cells expressing GFP. (B) and (F) show cultures counterstained for GFP. (C) and (G) are merged images of (A-B) and (E-F), respectively, showing GFP counterstaining on GFP expressing cells. (D) and (H) show merged images (C) and (G) overlaid on their respective brightfield images. (scale = 50 μ m)

4.3 Discussion

The MLR2 antibody is able to be conjugated to the polycation polyethylenamine (PEI) which has been PEGylated, creating a stable immunoportor, which does not affect the binding properties of MLR2 to p75NTR. The ability for PEI to bind, condense and retard pDNA in gel electrophoresis assays is not lost when conjugated to the MLR2 antibody. The attachment of the MLR2 antibody allows the PEI-PEG12 (immunoportor) to satisfy 3 of the 4 'barriers' of gene delivery: condensing pDNA (PEI), specific cell targeting (MLR2 to p75NTR) and, internalisation (MLR2) and subsequent endosomal escape (PEI) (Morris *et al.*, 2000). Correct PEGylation, antibody conjugation and PEI:DNA ratios also charge neutralises the complex, allowing avoidance of immune cell and blood components when applied *in vivo* (Allen & Hansen, 1991; Ogris *et al.*, 1999).

The MLR2 immunogene specifically transfects p75NTR expressing cells. GFP expression was seen when MLR2-PEI-PEG12-pVIVO2-GFP/LacZ was applied to p75NTR expressing NSC-34 cells. Complexes lacking the MLR2 antibody (PEI-PEG12 only) are also able to non-specifically deliver genetic cargo to cultured NSC-34 cells. However, when the MLR2 immunogene is applied to non-p75NTR expressing fibroblast cells (BSR), there is no GFP expression.

When PEI-PEG12 carrying pDNA is applied to BSR cells, transfection efficiency is high. Longer incubation of non-PEGylated PEI causes very high cell transfection, but also cell death. The ability for PEI complexes to transfect cells is

due to the interaction of cationic PEI and anionic cell surface receptors, such as proteoglycans (Mislick & Baldeschwieler, 1996; Hanzlikova *et al.*, 2011). The addition of PEG to the PEI reduces the cellular toxicity by reducing the overall positive charge, as un-PEGylated PEI shows toxicity, immune response and blood component aggregation (Ogris *et al.*, 1999; Moghimi *et al.*, 2005; Malek *et al.*, 2009).

The ability of the MLR2 immunogene to specifically transfect mouse p75NTR is demonstrated on embryonic primary mouse motor neurons. Adult motor neurons are difficult to extract, culture and transfect. A method of extracting, purifying and culturing motor neurons from embryonic mice by using immunopanning and selectively targeting p75NTR expressing neurons has made primary cultures more accessible (Wiese *et al.*, 2010). Transfecting non-dividing primary neurons is significantly more difficult to dividing cell lines. There is greater access for DNA translocation to the cell nucleus during mitosis in cell lines, while terminally differentiated post-mitotic neurons do not divide, hence nuclear entry is difficult (Akita *et al.*, 2008; Pérez-Martínez *et al.*, 2011; Van Gaal *et al.*, 2011).

Application of the MLR2 immunogene to primary cultures shows GFP expression specifically on motor neurons and not on other cells present, such as glial cells. The GFP expression is validated by the use of an anti-GFP antibody. The MLR2 immunogene shows that it is able to transfect non-proliferating primary motor neurons *in vitro*. However, the level of transfection in primary motor neurons was never more than 8%, as has been seen previously (Rogers *et al.*, 2014). Low transfection of primary cell cultures is not uncommon, as the conditions *in vitro* never truly represent *in vivo* environments (Van Gaal *et al.*, 2011).

These experiments have therefore provided a proof of concept that the MLR2 immunogene can transfect p75NTR expressing cells. This now allows experiments to determine whether the immunogene can be used for transfection of motor neurons *in vivo*. Neonatal mice will be used due to their high motor neuron p75NTR expression.

Chapter 5: Delivery of pDNA
to neonatal p75NTR
expressing motor neurons
via the MLR2 immunogene

5.1 Introduction

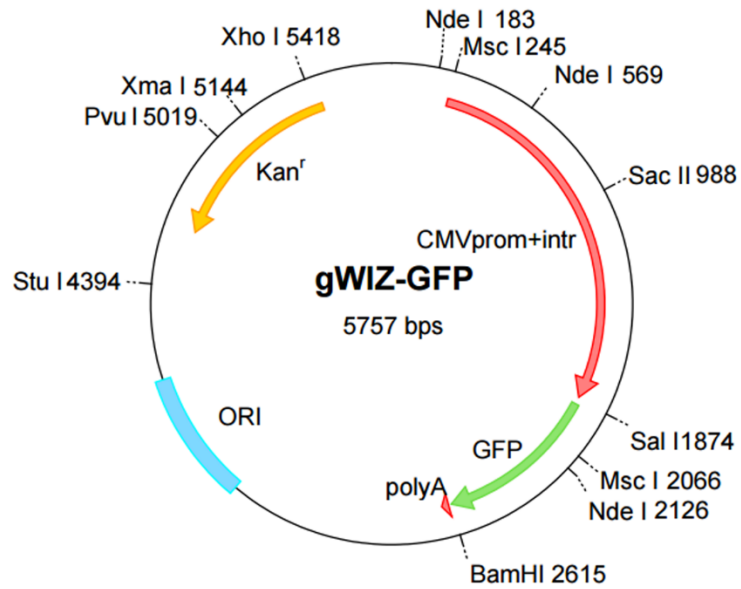
We have shown that it is possible to specifically target p75NTR expressing motor neurons using the monoclonal anti-p75NTR antibody MLR2 conjugated to a fluorescent tag, injected intraperitoneally in neonatal mice. This shows that the binding and retrograde activity to and within motor neurons *in vivo* of MLR2 is not blocked by conjugation. Replacing the fluorophore with a polycation carrying a pDNA cargo (immunogene), may allow the antibody to act as an *in vivo* non-viral delivery agent.

The technology of using an antibody as a non-viral gene delivery agent has previously been used in rats. The targeting antibody was MC192, a rat p75NTR-specific antibody (Chandler *et al.*, 1984), and the DNA binder/carrier was poly-L-lysine (PLL) (Barati *et al.*, 2006). We have now modified and optimised the immunogene for systemic use in mice.

The immunogene now targets p75NTR from many species (mouse, human, rat) with the MLR2 antibody (Rogers *et al.*, 2006) replacing the rat specific MC192 antibody used previously by Barati and colleagues (Barati *et al.*, 2006). The DNA binding and condensing component, poly-L-lysine (PLL), has been replaced with polyethylenamine (PEI), which facilitates better endosomal escape and is considered the gold standard for polycation gene delivery (Morille *et al.*, 2008). Furthermore, the PEI has been PEGylated (polyethylene glycol), to achieve a stealth that restricts attack from the immune system and a longer lasting half-life in the circulation (Allen & Hansen, 1991; Ogris *et al.*, 1999). The replacement of the antibody (MC 192 to MLR2) and polycation (PLL to PEI) has increased the ability for the immunogene to overcome three of the four barriers of successful *in*

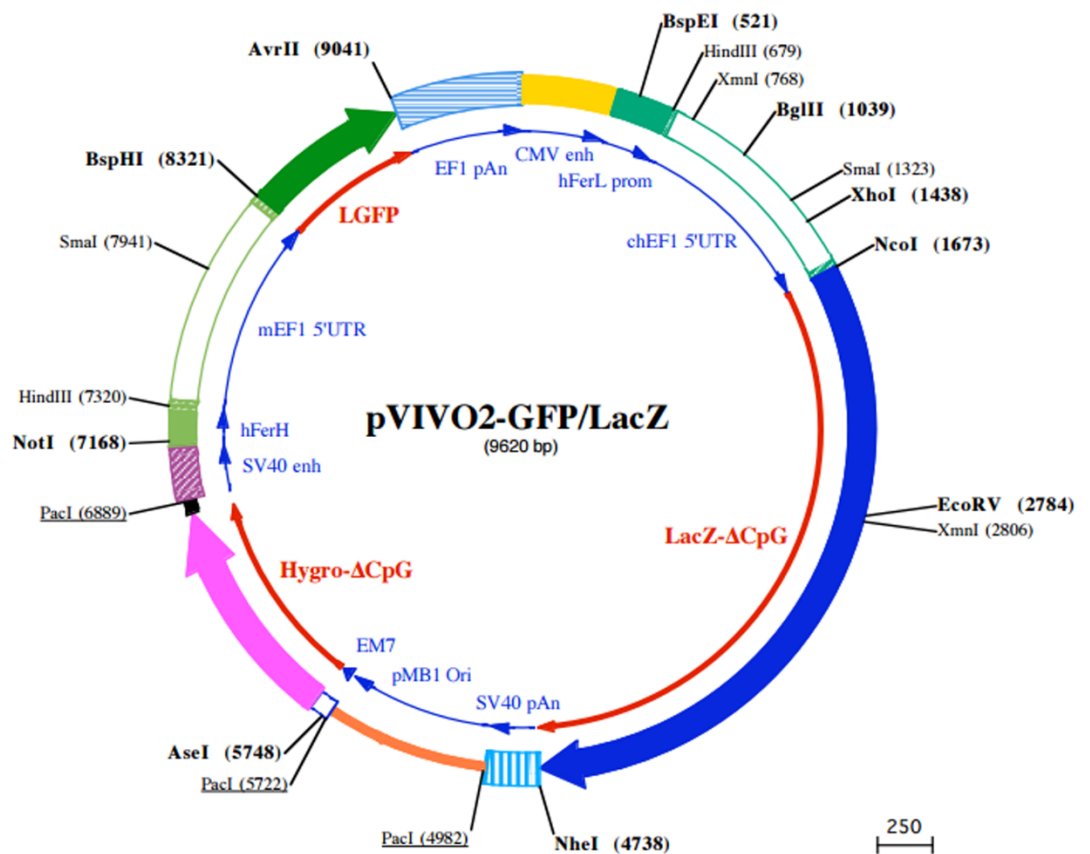
in vivo gene delivery (Morris *et al.*, 2000); DNA binding, condensing and shielding through the use of the PEGylated polyethylenamine (PEI-PEG12), cell specificity and retrograde transport with the use of the MLR2 anti-p75NTR antibody, and endosomal escape through the proton sponge effect facilitated by the PEI.

The final barrier, nuclear translocation of the pDNA, has been unachievable *in vivo*. Two plasmids have been used with the immunogene for transfection; the gWiz GFP-expressing plasmid (www.genlantis.com, Figure 5.1.1) and pVIVO2-GFP/LacZ (www.invivogen.com, Figure 5.1.2). The gWiz pDNA has been shown to charge neutralize immunogene complexes and *in vitro* use showed GFP expression in cells treated with the immunogene (Rogers *et al.*, 2014). However, high levels of bacterial CpG's in the plasmid backbone and CMV promoters have been shown to induce immune responses and lower *in vivo* transgene expression (Davies *et al.*, 2012). Conversely, the pVIVO2-GFP/LacZ has been specially designed for *in vivo* application, for enhanced and better transfection. The plasmid uses a mammalian Ferritin promoter, which is ubiquitously expressed, for longer lasting transfection efficiency compared to viral promoters (e.g. CMV). There are two reporter transgenes expressing LacZ and GFP, which can be replaced with a gene of interest. Bacterial CpG motifs, present highly in the gWiz pDNA, have been removed from pVIVO2-GFP/LacZ backbone, reducing immunogenicity. Most importantly, the plasmid contains the SV40 enhancer (simian virus 40), which acts as a DNA targeting sequence (DTS). The SV40 enhancer binds to cytoplasmic transcription factors containing NLS (nuclear localisation sequences), which interact with karyopherins (importin alpha and beta) and chaperone the whole DNA complex into the nucleus (Morris *et al.*, 2000).



5.1.1 gWiz GFP Mammalian Expression Vector

gWiz from www.genlantis.com is a high level GFP expressing plasmid. The plasmid contains a CMV promoter and GFP expressing transgene. Although the plasmid expresses high levels of the transgene in mammalian cells, the backbone of the plasmid contains many bacterial CpG's, which induce immune responses.



5.1.2 pVIVO2-GFP/LacZ plasmid

The pVIVO2-GFP/LacZ plasmid from www.invivogen.com is specifically designed for *in vivo* application. The plasmid contains a Ferritin promoter (hFerL prom) which is expressed ubiquitously in all cells, two replaceable reporter transgene sites (LacZ- Δ CpG and LGFP), a DNA targeting sequence for nuclear translocation (SV40 enh) and has bacterial CpG motifs removed from the plasmid backbone to reduce immunogenicity.

By using the pVIVO2-GFP/LacZ plasmid, instead of the gWiz pDNA, to overcome the nuclear localisation barrier, complete gene delivery through the use of the immunogene may be achievable. Taking advantage of the MLR2 anti-p75NTR internalising antibody (Rogers *et al.*, 2006; Matusica *et al.*, 2008), which can cause p75NTR to be retrogradely transported to the cell body (Lalli & Schiavo, 2002; Saxena *et al.*, 2004) may allow for specific targeting of p75NTR expressing motor neurons for gene delivery.

The following results demonstrate the ability of intraperitoneal injection of the MLR2 immunogene (MLR2-PEI-PEG12-pVIVO2-GFP/LacZ) into neonatal mice expressing high levels of p75NTR in motor neurons, to deliver pDNA expressing GFP.

5.2 Results

5.2.1 *MLR2-PEI-PEG12 immunogene is able to bind pgWiz DNA and tested in vivo*

The pgWiz plasmid was tested for its ability to charge neutralise the immunogene complex using a gel retardation assay and its ability to transfect motor neurons *in vivo* after intraperitoneal injections into neonatal mice.

The pgWiz (400ng) was conjugated at varying N/P ratios with the MLR2-immunoprotein and run on a gel retardation assay (1% agarose) to determine at which ratio the complex was charge neutralised (Figure 5.2.1). Well 1 contains pDNA only. Wells 2-5 contains PEI-PEG12 complexed with gWiz pDNA at N/P ratios of 5, 7.5, 10 and 15, respectively. Wells 6-9 contains MLR2-PEI-PEG12 complexed with gWiz pDNA at N/P ratios of 5, 7.5, 10 and 15, respectively. Well 10 contains a 100bp ladder.

At an N/P ratio of 15, 150ug (75ug x 2, 12 hours apart) of the MLR2-PEI-PEG12-pgWiz immunogene was injected into neonatal mice (PND 1) intraperitoneally. The mice were then left for 72 hours before being transcardially perfused with 1% sodium nitrite in 1x PBS, then having their spinal cords removed and post fixed in Zamboni's fixative overnight. The spinal cords were cryoprotected in 30% sucrose in 1x PBS, then cut at 30µm sections and counterstained for ChAT and GFP. While there was ChAT immunoreactivity in the motor neurons, no GFP expression could be found in any layer of the spinal cord.

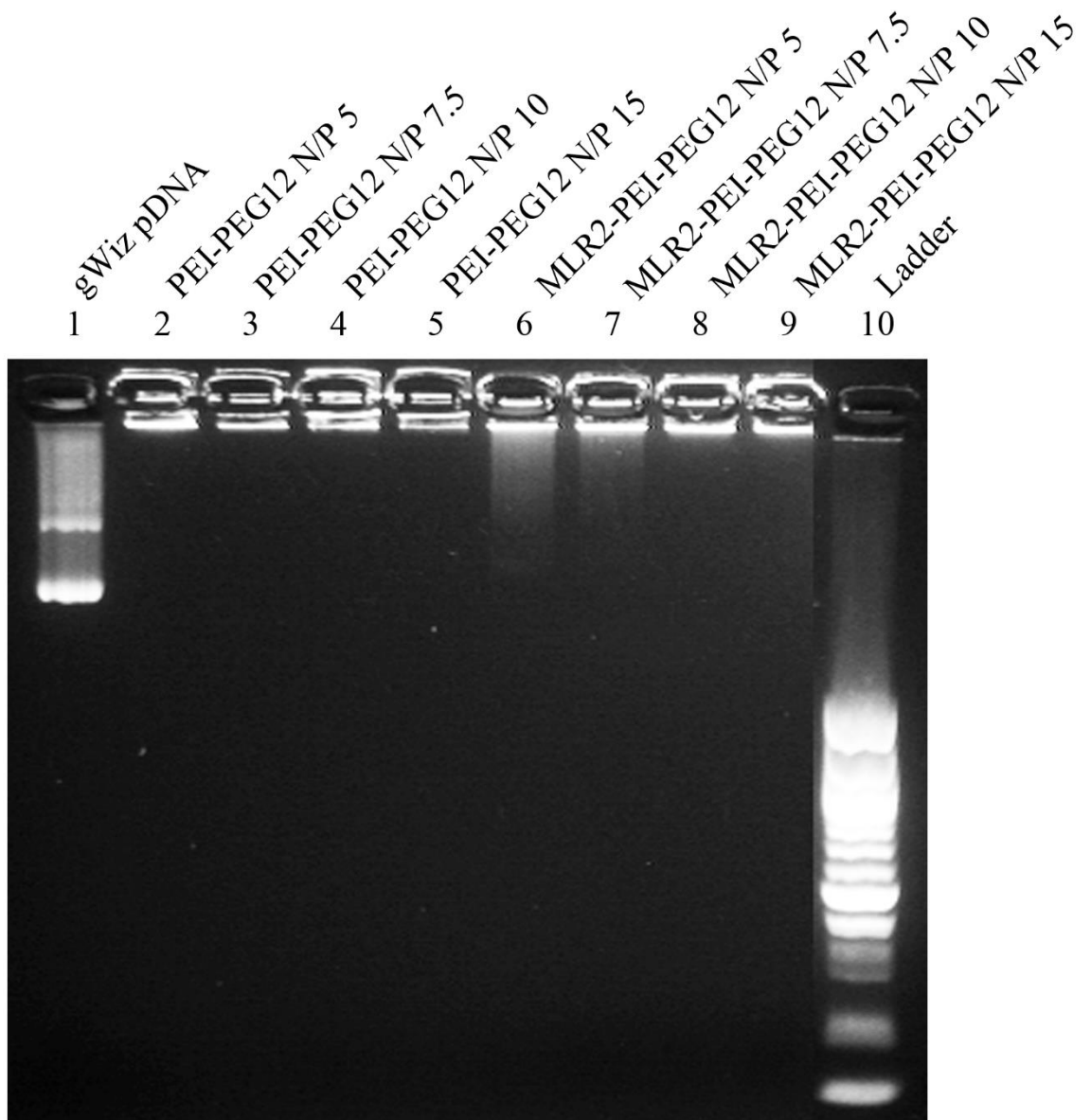


Figure 5.2.1 MLR2-PEI-PEG12 immunogene is able to bind pgWiz DNA

Gel retardation assay run to determine at which PEI-Nitrogen to pDNA-Phosphate ratio (N/P ratio) the immunogene complex carrying the pgWiz (4 μ g) is charge neutralised. Well (1) contains the naked pDNA. Wells (2-5) shows PEI-PEG12 at N/P ratios of 5, 7.5, 10 and 15, respectively, where the pDNA is completely retarded in the gel. Wells 6-9 contain MLR2-PEI-PEG12 complexed with pDNA at N/P ratios of 5, 7.5, 10 and 15, respectively. Wells (6-7) show pDNA that has travelled through the gel, while wells (8-9) shows the pDNA has been charge neutralised at N/P ratios 10 and 15. Well (10) contains the 100 bp ladder.

5.2.2 MLR2-PEI-PEG12-pVIVO2 immunogene gel retardation

For animal injections the N/P ratio was determined for charge neutralisation (Figure 5.2.2). Well 1 contains the 100bp ladder. Well 2 shows PEI-PEG at an N/P of 5, where the pDNA (pVIVO2-GFP/LacZ) is completely retarded in the gel. Wells 3-8 contain ML2-PEI-PEG complexed with pDNA at N/P ratios of 2, 5, 10, 12, 15 and 20, respectively. Wells 3-5 show pDNA that has travelled through the gel, while well 6 shows the pDNA has been charge neutralised at N/P 12. Well 9 contains the pDNA naked, where it has freely travelled through the gel. MLR2-PEI-PEG12 immunopporter needed N/P ratio of 12 for neutralisation.

5.2.3 MLR2-PEI-PEG12-pVIVO2 immunogene was able to transfect lumbar motor neurons of neonatal mice

Neonatal mice (PND 1) were injected with 150µg (75µg x 2, 12 hours apart) of MLR2-PEI-PEG12 carrying 58µg pVIVO2-GFP/LacZ intraperitoneally, with an N/P ratio of 12. The mice were then left for 72 hours before being transcardially perfused with 1% sodium nitrite in 1x PBS, then having their spinal cords removed and post fixed in Zamboni's fixative overnight. The spinal cords were cryoprotected in 30% sucrose in 1x PBS, then cut at 30µm sections and counterstained for Choline acetyltransferase (ChAT) for identification of motor neurons and GFP to identify expression of GFP from pVIVO2 (figure 5.2.3). Injected mice show ChAT expression in ventral motor neurons on both sides of the spinal cord can be seen in image (A), with strong GFP immunofluorescence in

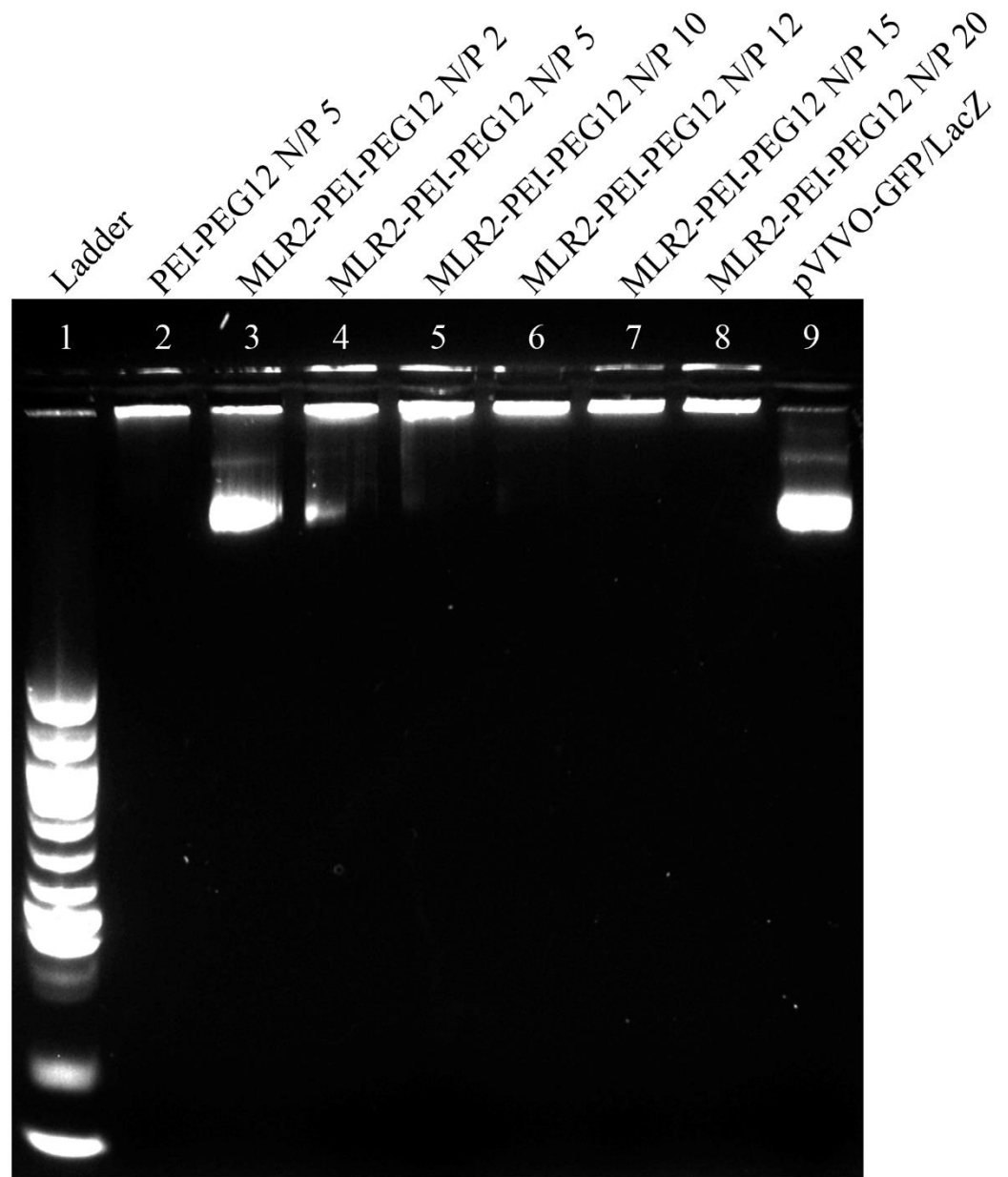


Figure 5.2.2 MLR2-PEI-PEG12 immunogene is able to bind pDNA pVIVO2-GFP/LacZ and be charge neutralised at N/P 12

Gel retardation assay run to determine at which PEI-Nitrogen to pDNA-Phosphate ratio (N/P ratio) the immunogene complex carrying the pVIVO2-GFP/LacZ plasmid (4 μ g) is charge neutralised. Well (1) contains the 100bp ladder. Well (2) shows PEI-PEG12 at an N/P of 5, where the pDNA is completely retarded in the gel. Wells (3-8) contain MLR2-PEI-PEG12 complexed with pDNA at N/P ratios of 2, 5, 10, 12, 15 and 20, respectively. Wells (3-5) show pDNA that has travelled through the gel, while well (6) shows the pDNA has been charge neutralised at N/P 12. Well (9) contains the pDNA naked, where it has freely travelled through the gel.

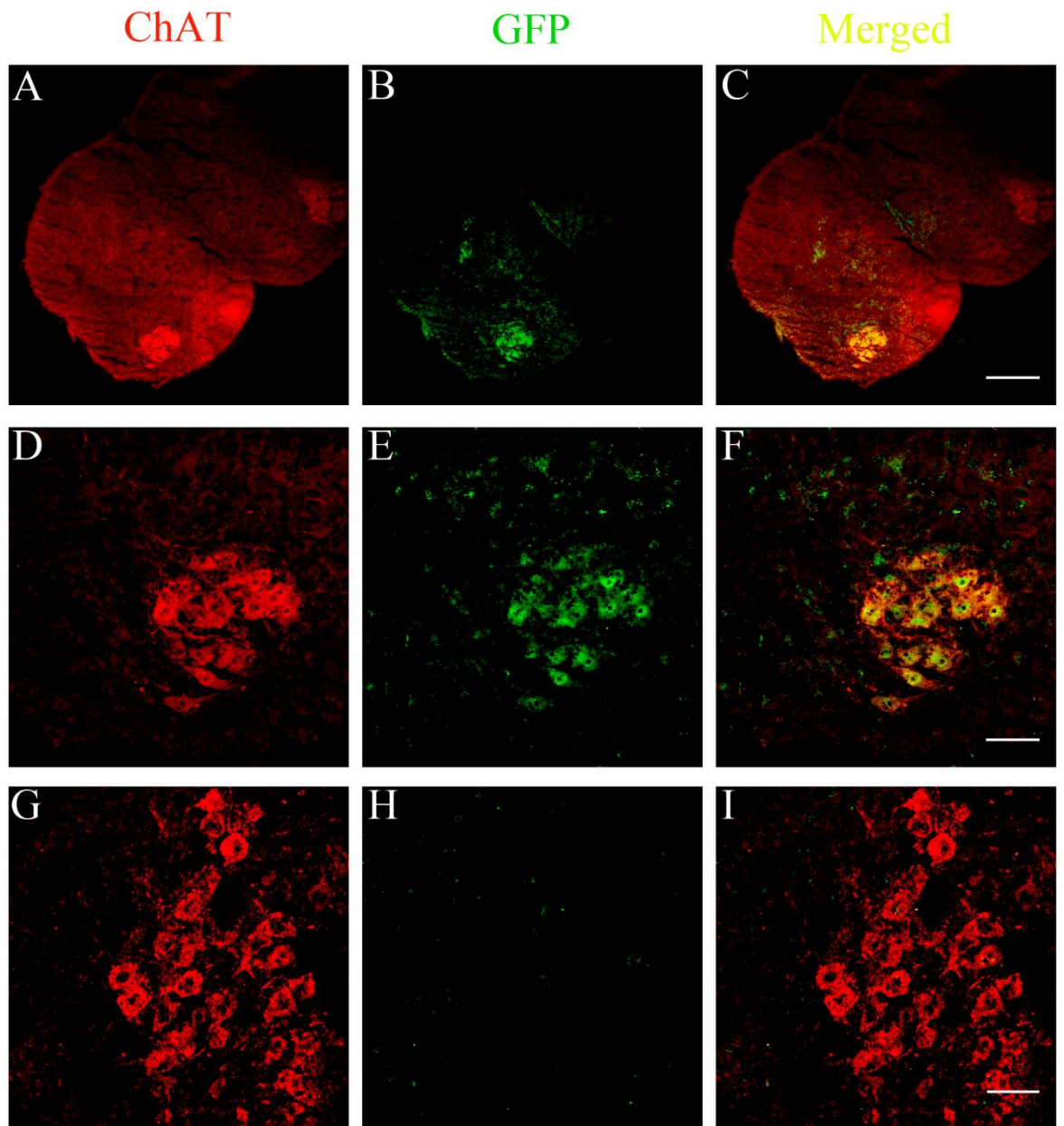


Figure 5.2.3 MLR2-PEI-PEG12 is able to deliver pDNA to motor neurons in the lumbar region of neonatal mice

Neonatal B6 mice (PND 1) were injected with 150 μ g (75 μ g x 2, 12 hours apart) of MLR2-PEI-PEG12, carrying 58 μ g pVIVO2-GFP/LacZ, intraperitoneally, at N/P 12. After 72 hours, spinal cords were removed and processed for immunohistochemistry. Spinal cords were sectioned at 30 μ m and counterstained for ChAT (rabbit anti-ChAT 1:5000 + 2 $^{\circ}$ donkey anti-rabbit Cy3 1:800) and GFP (chicken anti-GFP 1:500 + 2 $^{\circ}$ donkey anti-chicken 488 1:800). Low magnification image (A) shows high ChAT expression in ventral motor neurons on both side of the spinal cord, (B) shows strong GFP immunofluorescence in ventral neurons and (C) shows merged images of GFP expression in motor neurons. Higher magnification images of injected mice show (D) ChAT motor neurons, (E) high GFP immunoreactivity and (F) merged images displaying GFP in motor neurons. Mice not injected with the immunogene show ChAT positivity (G) but lack the strong GFP fluorescence (H) in the motor neurons (I). (scale (A-C) = 100 μ m, (D-I) = 50 μ m)

ventral neurons in image (B) and (C) shows merged images of GFP expression in motor neurons. Higher magnification images show (D) ChAT motor neurons, (E) high GFP immunoreactivity and (F) merged images displaying GFP in motor neurons. Mice not injected with the immunogene show ChAT positivity (G) but no GFP fluorescence in the motor neurons (H-I).

5.2.4 MLR2-PEI-PEG12-pVIVO2 injected intraperitoneally results in GFP expression at all levels of the spinal cord

In addition to the lumbar region, neonatal mice injected with the MLR2-PEI-PEG12-pVIVO2 had the thoracic and cervical areas of their spinal cords examined for GFP and ChAT (figure 5.2.4). (A) and (D) show expression of ChAT in two representative micrographs of a cervical and thoracic section, respectively. GFP immunofluorescence is seen in cervical (B) and (E) thoracic sections. The merged images show co-fluorescence of ChAT and GFP in cervical (C) and thoracic (F) sections.

The percentage of motor neurons from all regions of the spinal cord that showed GFP immunofluorescence is displayed in figure 5.2.5. From each region, the percentage of GFP expressing motor neurons was approximately 17.6% for cervical, ~18.3% for thoracic and ~24.8% for lumbar.

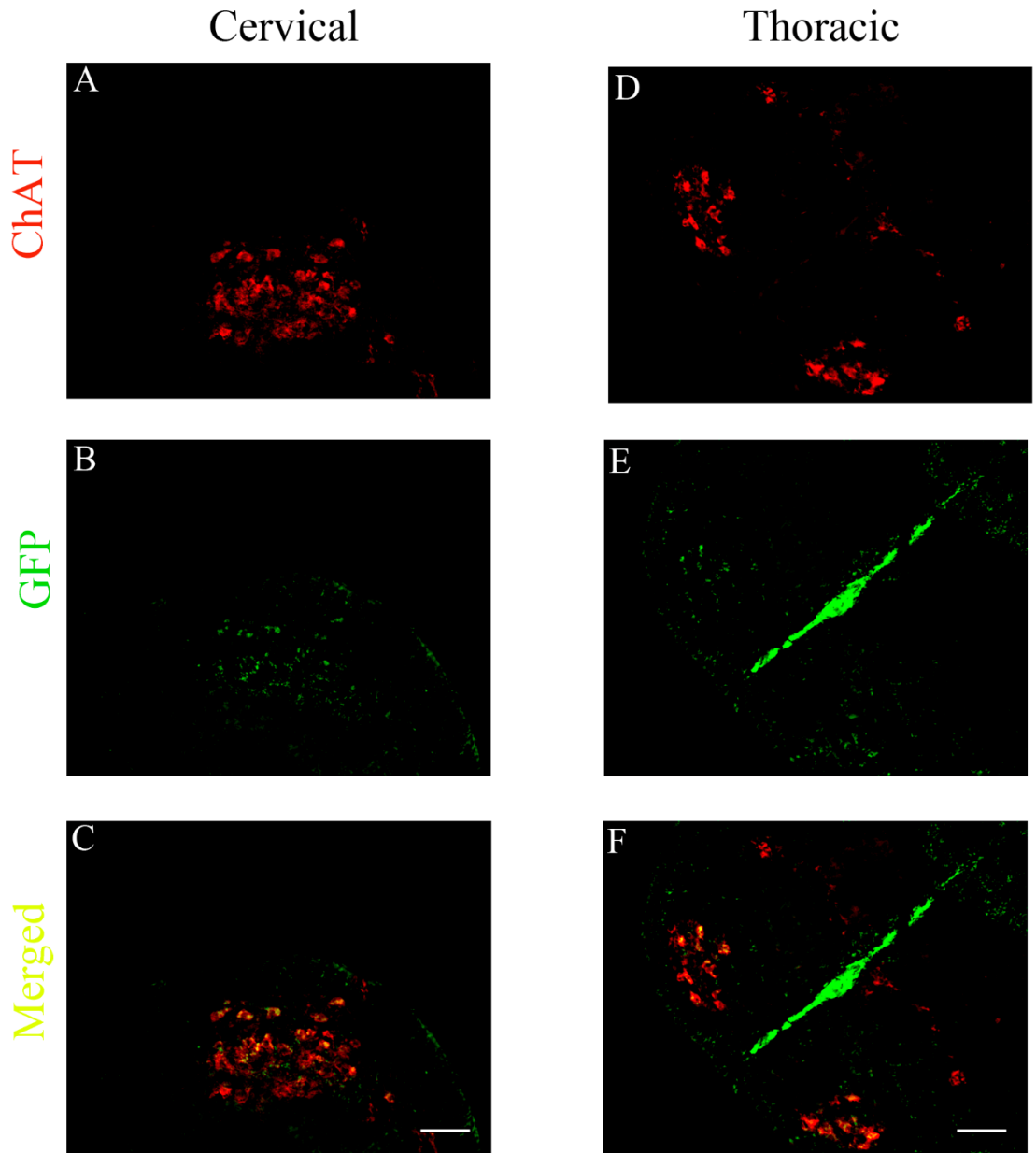


Figure 5.2.4 MLR2-PEI-PEG12 is able to deliver pDNA to motor neurons in the cervical and thoracic spinal regions

Spinal cords from injected B6 mice with 150 μ g MLR2-PEI-PEG12 carrying 58 μ g pVIVO2-GFP/LacZ at N/P 12 show GFP (chicken anti-GFP 1:500 + 2 $^{\circ}$ donkey anti-chicken 488 1:800) fluorescence in all regions of the spinal cord. ChAT (rabbit anti-ChAT 1:5000 + 2 $^{\circ}$ donkey anti-rabbit Cy3 1:800) positive motor neurons in (A) cervical and (D) throacic show GFP positive neurons (B,E), which show co-fluorescence in (C) and (F) (scale =50 μ m).

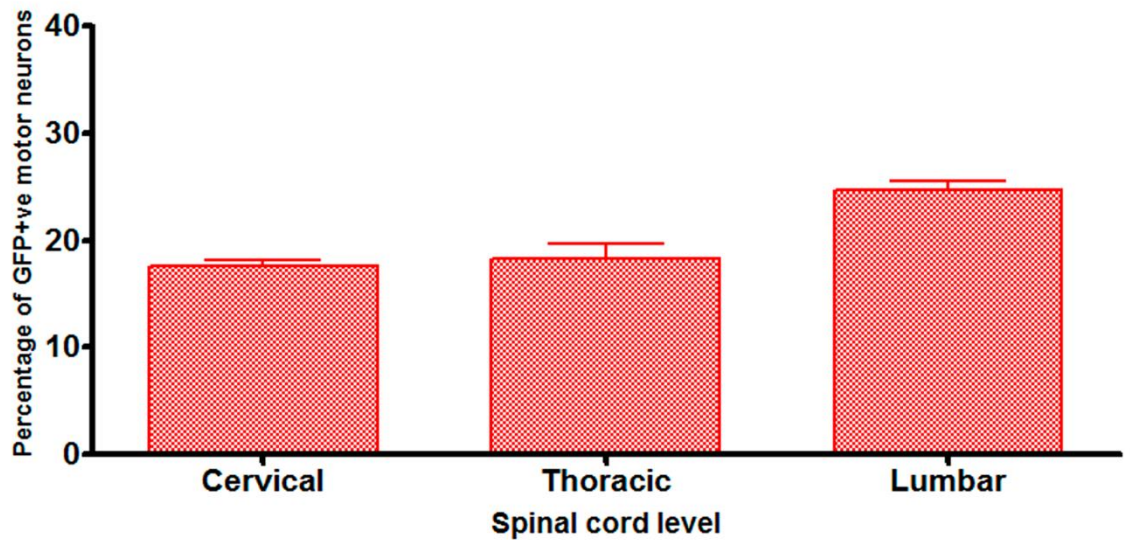


Figure 5.2.5 Approximately 20% of motor neurons express GFP after immunogene injections

The percentage of motor neurons that express GFP after intraperitoneal injections of 150ug MLR2-PEI-PEG12-pVIVO2-GFP/LacZ N/P 12, is shown to be similar across all regions of the spinal cord. Approximately 17.6% of cervical motor neurons express GFP, ~18.3% of thoracic express GFP and ~24.8% of lumbar express GFP (n=5, \pm SEM).

5.2.5 Motor neurons transfected with GFP delivered by MLR2-PEI-PEG12-pVIVO2 immunogene also express p75NTR

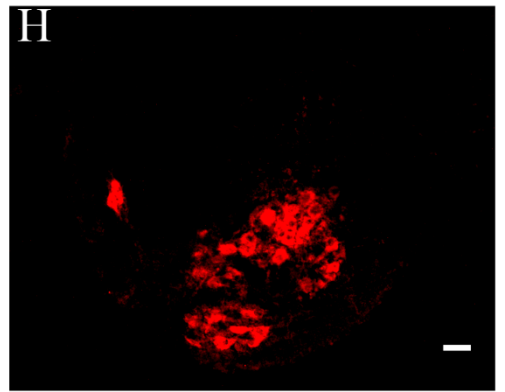
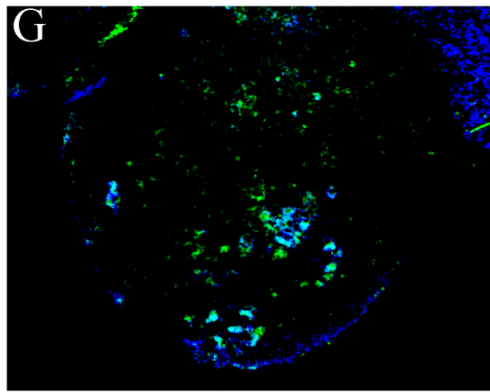
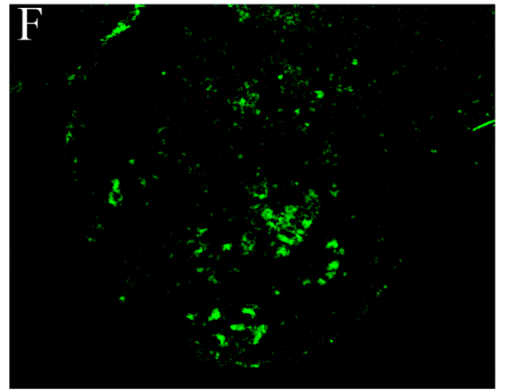
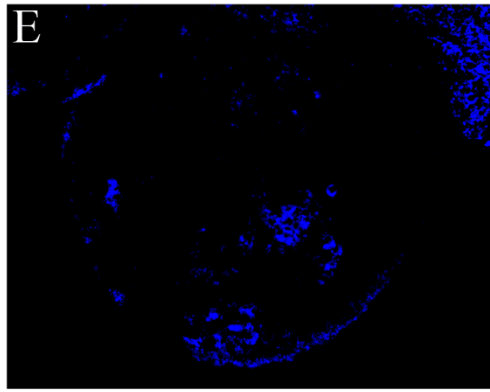
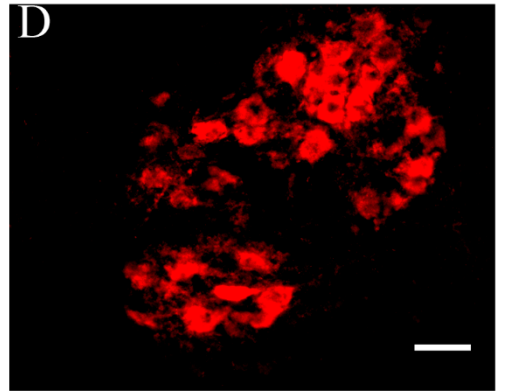
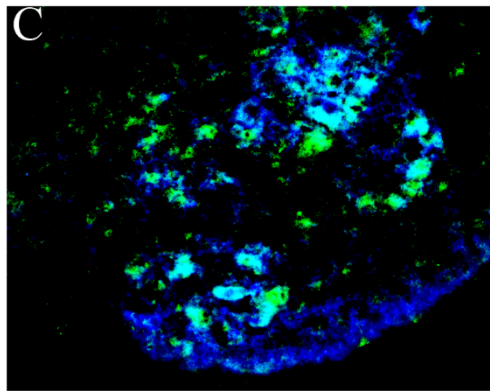
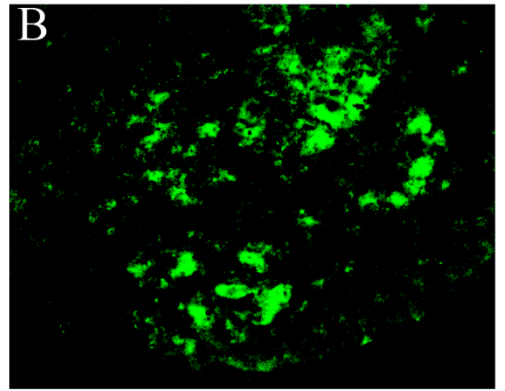
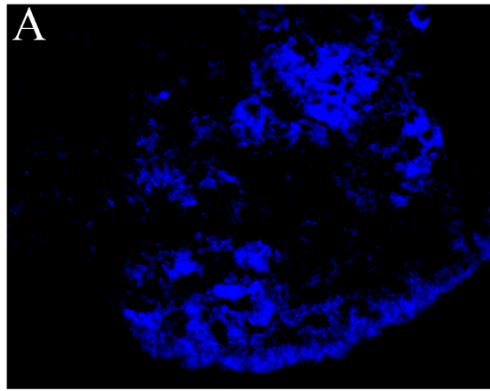
Neonatal mice (PND 1) that were injected with 150ug of MLR2-PEI-PEG-pVIVO2-GFP/LacZ intraperitoneally, were examined for p75NTR expression in motor neurons that expressed GFP (figure 5.2.6). The lumbar region of the spinal cord was examined and shows p75NTR immunofluorescence in neurons (A), strong GFP expression (B), both of which show co-fluorescence in and around the same neurons in the ventral region (C). These neurons were identified as motor neurons due to the presence of ChAT immunofluorescence (D). Lower magnification images show the same ventral p75NTR expression as well as expression in the dorsal horn (E, upper right corner), GFP expression (F) and merged images (G). Motor neuron confirmation by presence of ChAT immunoreactivity (H). This shows that the neurons that were transfected with MLR2-PEI-PEG12-pVIVO2 also express p75NTR.

5.2.6 GFP expression peaks at 144 hours after injection of MLR2-PEI-PEG12-pVIVO2

Neonatal mice (PND1) were injected with the MLR2-PEI-PEG12-pVIVO2 had spinal cords removed 72, 144, 240 or 336 hours after first injection (figure 5.2.7). Compared to the normal 72 hours (~17.6% cervical, ~24.8% lumbar), at 144 hours (6 days), the average percentage of motor neurons expressing GFP is ~26.6% in the cervical region and ~25.8% in the lumbar region. The expression of GFP drops to ~7.2% by 240 hours (10 days) in cervical and ~9.5% in cervical.

Figure 5.2.6 MLR2-PEI-PEG12 GFP positive motor neurons are p75NTR positive

Neonatal B6 mice (PND 1) that were injected with 150µg of MLR2-PEI-PEG12 carrying 58µg pVIVO2-GFP/LacZ intraperitoneally, were examined for p75NTR expression (goat anti-p75NTR 1µg/ml + 2° donkey anti-rabbit Cy5 1:800) in motor neurons that expressed GFP. Images of lumbar spinal cord show p75NTR immunofluorescence in neurons (A), strong GFP expression in neurons (B), both of which show co-fluorescence in the same neurons in the ventral region (C). (D) shows ChAT immunofluorescence for motor neuron clarification. Lower magnification images show ventral p75NTR expression as well as expression in the dorsal horn (E, upper right corner), GFP expression (F) and merged images (G), with the presence of ChAT (H). (scale = 50µm)



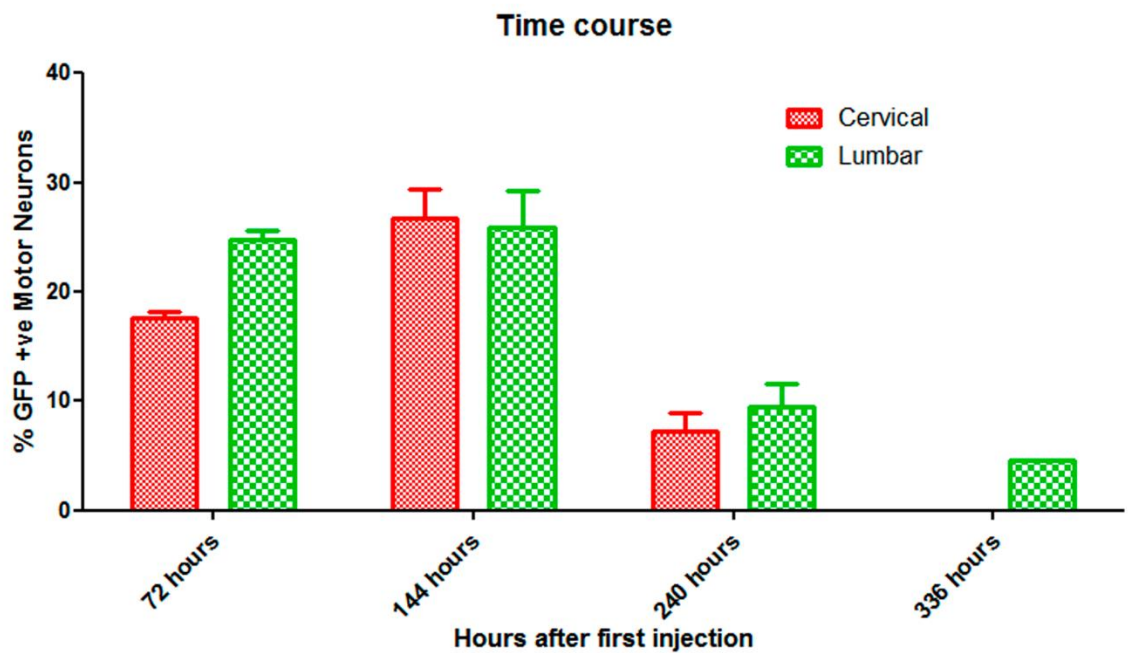


Figure 5.2.7 Motor neuron GFP expression after MLR2 immunogene injection time course

Neonatal mice (PND1) were injected with 150 μ g MLR2-PEI-PEG-pVIVO2-GFP/LacZ (75 μ g x 2, 12 hours apart) and then had spinal cords removed 72, 144, 240 or 336 hours after first injection. Compared to the normal 72 hours (17.6% cervical, 24.8% lumbar), at 144 hours (6 days), the average percentage of motor neurons expressing GFP is 26.6% in the cervical region and 25.8% in the lumbar region. The expression of GFP drops to 7.2% by 240 hours (10 days) in cervical and 9.5% in lumbar. 4.6% of lumbar motor neurons express GFP at 336 days (14 days) (mice n= 5 72 hours, n=2 144/240 hours, n=1 336 hours).

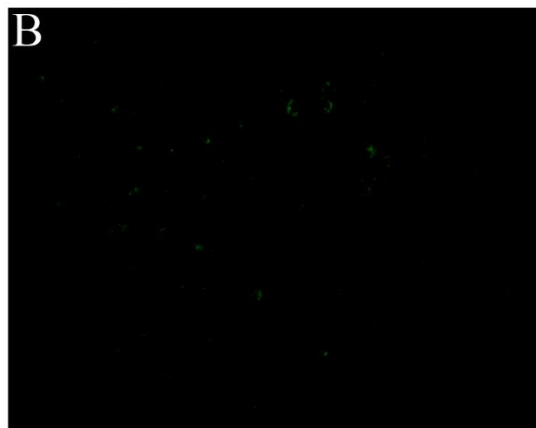
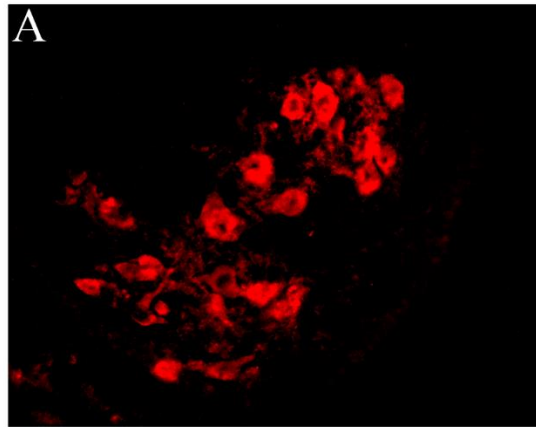
Approximately 4.6% of lumbar motor neurons express GFP at 336 days (14 days) (n= 5 72 hours, n=2 144/240 hours, n=1 336 hours).

5.2.7 PEI-PEG12 alone is unable to deliver pDNA to spinal motor neurons

PEI-PEG12 lacking the MLR2 antibody is able to transfect cell lines and primary motor neurons (Chapter 3), however it is unknown whether it can reach spinal motor neurons *in vivo*. 150ug of PEI-PEG-pVIVO-GFP/LacZ N/P ratio 7.5 (6x molar concentration compared to MLR2-immunogene injections) was injected I.P. into PND 1 mice, and treated/analysed the same as the MLR2-PEI-PEG12 injected mice. No immunofluorescence of GFP could be seen in spinal motor neurons taken from the PEI-PEG injected mice (figure 5.2.8).

5.2.8 Glucose (5%) buffer does not increase transfection efficiency

Formation of aggregates after addition of pDNA to immunocomplex is a common problem when creating the immunogene. Changing the buffer from 20mM HEPES 0.15M NaCl to 5% glucose in water reduces the visual appearance of aggregates during formation of the immunogene. Figure 5.2.9 displays the percentage of motor neurons positive for GFP immunofluorescence in the cervical, thoracic and lumbar regions of mice injected with the MLR2-PEI-PEG12 immunogene buffered in either 20mM HEPES 0.15M NaCl (HBS; HEPES buffered saline) or 5% glucose in water (Glu). The percentage for cervical



PEI-PEG12

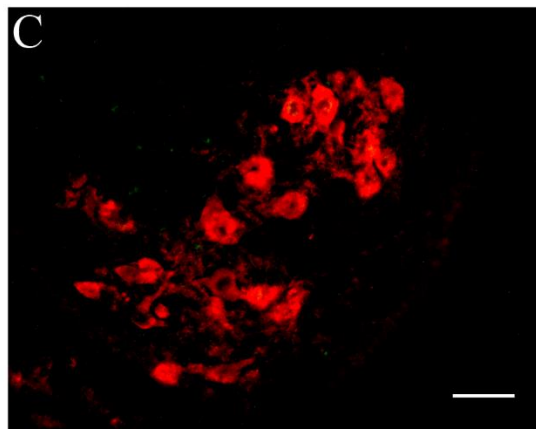


Figure 5.2.8 PEI-PEG alone is unable to transport pDNA to spinal motor neurons

Neonatal mice were injected with 150ug (2x 75ug, 12 hours apart) PEI-PEG12 carrying pVIVO2-GFP/LacZ (N/P ratio 7.5). 72 hours after injections, spinal cords were removed and analysed for GFP expression. Motor neurons in these mice lacked GFP expression (n=3).

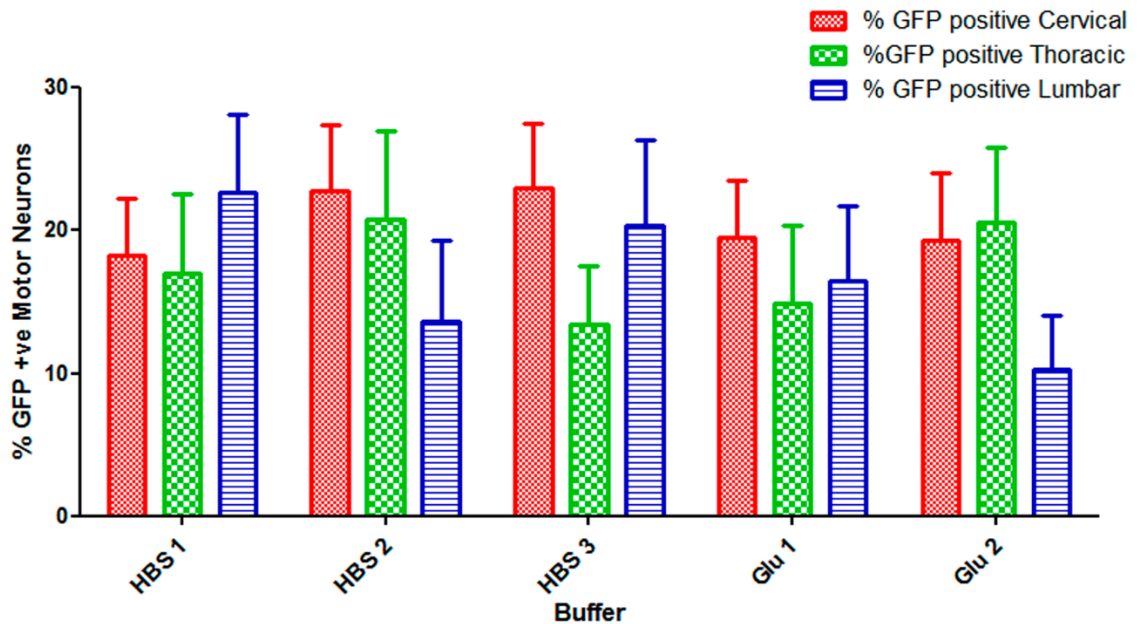


Figure 5.2.9 MLR2-PEI-PEG12 buffered with 5% glucose does not increase transfection efficiency

MLR2-PEI-PEG12-pVIVO2-GFP/LacZ were buffered in either the normal 20mM NaCl 0.15M HEPES buffered saline (HBS; n=3) or 5% glucose in water (Glu; n=2) and injected intraperitoneally. 5% glucose appeared to reduce aggregate formation during immunogene synthesis. 72 hours after initial injection, spinal cords were analyzed for GFP expression. Although 5% glucose reduced aggregate formation, this did not translate into higher transfection efficiency; cervical ~21.3% with HBS and ~19.4% with glucose, thoracic ~17% with HBS and ~17.8% with glucose, lumbar ~18.8% with HBS and ~13.4% with glucose. (\pm SEM).

ranged between 18.2-23% in HBS mice and 19.2-19.5% for Glu mice. Thoracic was between 13.4-20.7% in HBS mice and 14.9-20.6% for Glu mice. Finally, the lumbar GFP expression percentage was between 13.6-22.6% for HBS mice and 10.3-16.5% for Glu mice. On average, the glucose buffer did not increase transfection efficiency, but did reduce immunogene aggregate formation.

5.2.9 *GFP expression was found in Dorsal Root Ganglion Neurons after MLR2-PEI-PEG12-pVIVO2 in vivo injections*

Neonatal mice were injected with the MLR2 immunogene had their Dorsal Root Ganglions (DRG)'s removed, sectioned (10µm) and stained for p75NTR and GFP expression (figure 5.2.10). Images (A-D) are from an MLR2 immunogene injected mouse, showing GFP expression, p75NTR expression, DAPI and merged images, respectively. Image (D) shows p75NTR positive DRG neurons (red) expressing GFP (green). Images (E-H) show a DRG taken from a mouse not injected, with GFP expression, p75NTR expression, DAPI and merged images, respectively. Merged image (H) shows a small amount of positive GFP cells, but with far fewer compared to the injected mouse (background levels). Images (I-L) show a DRG from a mouse injected with PEI-PEG carrying the pVIVO2-GFP/LacZ plasmid, showing GFP expression, p75NTR expression, DAPI and merged images, respectively. The merged image (L) shows some positive GFP/p75NTR neurons, but much lower than the MLR2 immunogene injected mouse.

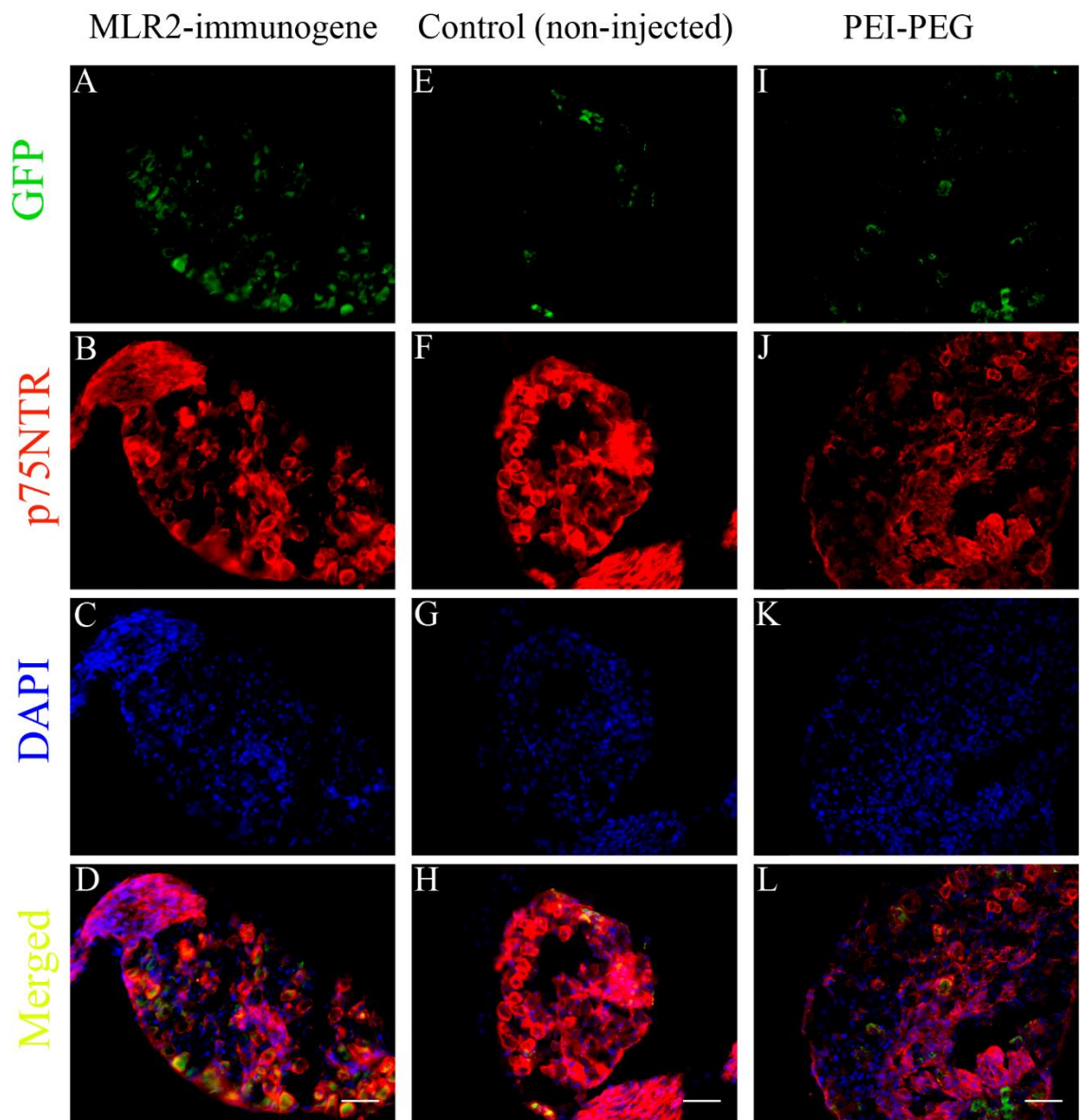


Fig 5.2.10 GFP expression in MLR2 immunogene injected neonatal mice DRG's

Neonatal B6 mice were injected 150 μ g (2x 75 μ g, 12 hours apart) of MLR2-PEI-PEG12 carrying 58 μ g pVIVO2-GFP/LacZ had their DRG's removed, sectioned (10 μ m) and stained for p75NTR (goat anti-p75NTR 1 μ g/ml + 2 $^{\circ}$ donkey anti-sheep Cy3 1:800) and GFP (chicken anti-GFP 1:500 + 2 $^{\circ}$ donkey anti-chicken 488 1:800) expression. Images (A-D) are from an MLR2 immunogene injected mouse, showing GFP expression, p75NTR expression, DAPI and merged images, respectively. Image (D) shows p75NTR positive DRG neurons (red) expressing GFP (green). Images (E-H) show a DRG taken from a mouse not injected, with GFP expression, p75NTR expression, DAPI and merged images, respectively. Merged image (H) shows a small amount of positive GFP cells, but with far fewer compared to the injected mouse. Images (I-L) show a DRG from a mouse injected with 150 μ g (2x 75 μ g, 12 hours apart) of PEI-PEG12-pVIVO2-GFP/LacZ, showing GFP expression, p75NTR expression, DAPI and merged images, respectively. The merged image (L) shows some positive GFP/p75NTR neurons, but much lower than the MLR2 immunogene injected mouse (scale = 50 μ m)

5.3 Discussion

Delivery of compounds or drugs to the CNS is difficult due to the highly protective and selective nature of the blood brain barrier, particularly when administered into the periphery. Previously, we have shown that intraperitoneally injected antibodies (MLR2) are able to be retrogradely transported to p75NTR expressing motor neurons, in the spinal cord of neonatal mice. Here we have replaced the MLR2 antibody with the full MLR2 immunogene (MLR2-PEI-PEG12-pVIVO2-GFP/LacZ) and demonstrated the delivery pDNA (expressing GFP) to spinal motor neurons in the CNS, via the same intraperitoneal injection method in neonatal mice.

Both the gWiz and pVIVO2-GFP/LacZ plasmids can successfully bind to, and charge neutralise, the MLR2-PEI-PEG immunoportor, as seen on gel retardation assays. Similarly, the pVIVO2-GFP/LacZ (Chapter 4) and gWiz plasmids (Rogers *et al.*, 2014) are able to transfect p75NTR expressing cells when delivered by the MLR2-PEI-PEG12 immunogene. As such, both plasmids were tested *in vivo*.

Previously, it was found that a dosage of 150µg (2x 75µg, 12 hours apart) MLR2 injected intraperitoneally was able to reach ~90% of all spinal motor neurons (Chapter 4). Hence, the same dosage was used in intraperitoneal injections of the MLR2 immunogene into neonatal mice, at fully charge-neutralised respective N/P ratios for both the gWiz and pVIVO2-GFP/LacZ.

Both plasmids (gWiz and pVIVO2-GFP/LacZ) were injected into neonatal mice, however, the gWiz plasmid failed to successfully transfect cells, while the

pVIVO2-GFP/LacZ was able to achieve positive results. Henceforth, the gWiz plasmid was not used for *in vivo* immunogene experiments.

Seventy-two hours post injection of the MLR-PEI-PEG12 immunoportor carrying the pVIVO2-GFP/LacZ plasmid, there was GFP expression in p75NTR expressing motor neurons. This was observed at all levels of the spinal cord, specifically 17.0% of cervical, 18.3% thoracic and 25.4% of lumbar motor neurons identified by ChAT were expressing GFP after transfection with the pVIVO2-GFP/LacZ plasmid. In *in vitro* transfection of primary motor neurons with pVIVO2, the GFP expression persisted for 7+ days after MLR2 immunogene application. A similar result was found *in vivo*, where the GFP expression persisted for up to 336 hours (14 days) after injection (4.6% lumbar motor neurons), with peak GFP expression seen at 144 hours (6 days) with 26.6% of cervical and 25.8% lumbar motor neurons showing GFP expression. Removal of the MLR2 antibody from the immunogene complex (PEI-PEG12) showed no motor neuron transfection in neonatal mice after intraperitoneal injection, signifying the importance of the MLR2 antibody for motor neuron selectivity and retrograde transport to the spinal cord.

Compared to viral gene delivery, the immunogene and other non-viral gene delivery agents in general have a much lower transfection efficiency, due to the barriers non-viral vectors must overcome that viral vectors have evolved naturally to bypass (Mintzer & Simanek, 2008; Rogers & Rush, 2012). However viral transfection of motor neurons *in vivo* is still poor. This is not due to the level of transfection that is possible with viral transfection agents, rather the inability to

reach the motor neurons through the blood brain barrier. Viral delivery to mice *in vivo* even with serotyping for improved retrograde delivery is only able to deliver to around 28% of cervical motor neurons after numerous intramuscular injections (Towne *et al.*, 2010). It was concluded by Towne *et al.*, 2010 that specific delivery to motor neurons is important. This is what has been achieved using immunogenes, even though the efficiency is low, the specificity is 100%.

A factor that may influence the low motor neuron transfection level of immunogenes, particularly compared to the high level of targeting by the MLR2 antibody alone (~90%), is that polycation complexes have a tendency to aggregate out of solution when complexed with DNA after charge neutralisation (Ward, Read & Seymour, 2001; Suzie & Davis, 2002; Sharma, Thomas & Klibanov, 2005; Lynch, Behan & Birkinshaw, 2007). In fact, PEI can be used to precipitate DNA via charge neutralisation (Burgess, 1991). We used PEG to reduce aggregate formation as this has been demonstrated previously to be efficacious (Ogris *et al.*, 1999; Mishra *et al.*, 2004), however some aggregates still form. Many studies using a polycation for non-viral gene delivery substitute their buffers with 5% glucose, which increases viscosity of the buffer, reducing potential aggregation. While it was found that adding 5% glucose to the HEPES buffer for the MLR2 immunogene reduced the appearance of aggregates, this did not translate into higher transfection efficiency.

No obvious off-target effects or off-target transfection were seen within the spinal cord after injection of the MLR2 immunogene. However, p75NTR expression is

not limited to motor neurons. p75NTR positive sensory neurons in DRGs showed GFP expression, as p75NTR is expressed in these neurons (Yan & Johnson, 1988). This highlights the specificity for p75NTR targeting by the immunogene and its ability to be retrogradely transported from the circulation to cell bodies, and may even lead to applications of the immunogene for DRG related ailments. Earlier studies using pre-immunogene technology, showed delivery of pDNA through p75NTR in neuronal injury models, again expanding the application of the immunogene through p75NTR (Barati *et al.*, 2006).

Plasmid design is an integral part of successful gene delivery, which is most likely the reason why the gWiZ failed *in vivo*, yet the pVIVO2-GFP/LacZ plasmid did not. While *in vitro* applications of the immunogene carrying gWiZ showed transfection, *in vivo* experiments showed no result. This may be due to the high levels of bacterial CpGs in the plasmid backbone and viral promoters (CMV) that gWiZ contains, which is known to induce immune response (Davies *et al.*, 2012). Conversely, the pVIVO2-GFP/LacZ plasmid which is tailored for *in vivo* use, have had all bacterial CpGs removed, uses a Ferritin promoter, and most importantly, has a DTS (DNA targeting sequence) for nuclear translocation.

As p75NTR is only re-expressed in MND and MND model mice motor neurons (Seeburger *et al.*, 1993; Lowry *et al.*, 2001; Copray *et al.*, 2003), they can be specifically targeted by the MLR2 immunogene. However, it is unknown at what level p75NTR is expressed over the disease course both in human MND and the SOD1^{G93A} mice. While tracking p75NTR expression in humans is beyond the scope of this work, investigating p75NTR motor neuron re-expression in the high

copy SOD1^{G93A} mice is achievable and will pinpoint the age at which the highest level of p75NTR is expressed for immunogene delivery.

Chapter 6: Characterisation of
p75NTR positive motor
neurons in SOD1^{G93A} mice

6.1 Introduction

Data from Chapter 5 showed how it is possible to deliver exogenous genetic material to motor neurons in neonatal mice through the p75NTR receptor. This potentially can be translated into a therapeutic for MND, as spinal motor neurons re-express p75NTR during the disease. p75NTR is naturally expressed during embryonic development in motor neurons, down-regulated during maturation but re-expressed after nerve trauma, such as axotomy (Ernfors *et al.*, 1989a; Je *et al.*, 2013). p75NTR re-expression in motor neurons occurs in both human MND (Kerckhoff *et al.*, 1991; Lowry *et al.*, 2001; Seeburger *et al.*, 1993) and SOD1^{G93A} mice (Copray *et al.*, 2003). Despite the possible therapeutic potential of targeting p75NTR, the re-expression of the receptor has previously been thought to influence motor neuron cell death in MND, due to the receptors apoptotic signalling (Copray *et al.*, 2003; Frey *et al.*, 2000; Kust *et al.*, 2003; Lowry *et al.*, 2001; Turner *et al.*, 2003; Turner *et al.*, 2004). Intriguingly, significant amounts of the extracellular domain of p75NTR has been found in SOD1^{G93A} mouse urine, and increases as the disease progresses (Shepherd *et al.*, 2014).

By targeting the p75NTR expressing motor neurons with the MLR2 immunogene (in both SOD1^{G93A} mice and humans), it may be possible to prevent cell death by directly delivering therapeutic pDNA to affected motor neurons. However, before administering the immunogene to adult SOD1^{G93A} mice, the peak p75NTR re-expression must be determined. The only study quantifying p75NTR re-expression in SOD1 mice was undertaken in the low copy number strain (SOD1^{G93A} G1L) (Copray *et al.*, 2003), and not the more commonly used strain (SOD1^{G93A} G1H high copy strain, used in this study). In the low copy strain, only

about 10% of motor neurons were found to re-express p75NTR. Copray et al. (2003) interpreted the low p75NTR positive (+ve) motor neuron number to be the result of the short time p75NTR is re-expressed due to fast apoptotic events. As p75NTR is commonly known as a 'death receptor', Copray et al. (2003) investigated co-expression of p75NTR with the stress, pre-apoptotic marker activating transcription factor 3 (ATF-3) (Hai *et al.*, 1999; Tsujino *et al.*, 2000) which has been shown to influence motor neuron number and survival in SOD1^{G93A} mice (Seijffers *et al.*, 2014), and the classic apoptotic marker, cleaved caspase 3 (Martin & Green, 1995; Alnemri *et al.*, 1996; Hengartner, 2000). They observed that all motor neurons re-expressing p75NTR expressed ATF-3 but only about 30% expressed cleaved caspase 3 (Coprax *et al.*, 2003).

Adult motor neurons do not normally express high levels of nuclear ATF3. However, after motor neuron trauma or disease (e.g. MND or sciatic nerve injury), it has been shown that lumbar motor neurons upregulate ATF3 expression, which is translocated to the nucleus (Tsujino *et al.*, 2000; Vlug *et al.*, 2005). Previous work in low copy number SOD1^{G93A} G1L mice revealed ATF3 expression levels are directly proportional to the degree of ubiquitinated protein aggregation inside motor neurons and non-existent in background (FV/FB) control mice (Vlug *et al.*, 2005). Interestingly, ATF3 expression was not co-localised with caspase-3 expression. This was thought to be either that caspase-3 is activated in a different sub-population of cells than ATF3, or most likely, ATF3 expression and subsequent down-regulation occurs before the expression of cleaved caspase-3 (Vlug *et al.*, 2005). Copray et al. (2003) reported the majority of motor neurons re-expressing p75NTR in SOD1^{G93A} G1L mice also contained ATF3. However, they did not limit their count by nuclear ATF3 expression, but

total cellular immunofluorescence, which may not reflect actual ATF3 upregulation. Recent work by Nardo et al. (2013) showed that the background mouse strain used for breeding SOD1^{G93A} mice has dramatic effects on mouse pathologies and protein expression. ATF3 expression was shown to be significantly different between SOD1^{G93A} mouse backgrounds, which may affect ATF3 interpretation (Nardo *et al.*, 2013). It is not known if p75NTR re-expression in motor neurons coincides with nuclear expression of ATF3 in SOD1^{G93A} mice or cleaved caspase-3. It is of importance to examine more than one marker of cell death or stress over the entire lifespan of mice to determine their ultimate fate and to better understand p75NTR's role in this disease.

Alpha motor neurons are preferentially affected in MND and in the SOD1^{G93A} mice (Swash *et al.*, 1986; Mohajeri, Figlewicz & Bohn, 1998), and are characterised by a larger cell body than smaller gamma motor neurons (McHanwell & Biscoe, 1981; Friese *et al.*, 2009; Shneider *et al.*, 2009). There is sparse research investigating the relationship between p75NTR and motor neuron cell size. What information exists in the literature contains conflicting data on size measurements of SOD1^{G93A} mice motor neurons re-expressing p75NTR. Both small size somas with retracted dendrites (G1L strain) (Copray *et al.*, 2003) and large somas (G1H strain) (Pehar *et al.*, 2004) have been described for motor neurons expressing p75NTR. As motor neuron size is directly correlated to the number of target motor fibres innervated (Henneman, Somjen & Carpenter, 1964; McPhedran, Wuerker & Henneman, 1965; Mcphedran, Wuerker & Henneman, 1965; Tyc & Vrbová, 2007; Kanning *et al.*, 2010), and size determines motor neuron type, proper longitudinal documentation of p75NTR positive and p75NTR

negative motor neuron size may reveal morphological changes in SOD1^{G93A} mice, which relate to functional decline in disease progression.

The following results define p75NTR re-expression in motor neurons of the lumbar spinal cord of high copy number SOD1^{G93A} mice over the course of the disease (60 days to end stage at approximately 140 days), as well total motor neuron number and the ability to target p75NTR expressing motor neurons with the same anti-p75NTR MLR2 antibody used in the neonatal/immunogene experiments. Important characteristics of motor neurons are also defined, including both biochemical and morphological changes, of p75NTR expressing motor neurons in SOD1^{G93A} mice over the course of the disease.

6.2 Results

6.2.1 *SOD1^{G93A} mice express p75NTR in lumbar motor neurons*

To determine if p75NTR is able to be detected in the spinal cord of SOD1^{G93A} mice, spinal cord from a 120 day old SOD1^{G93A} mouse and aged matched B6 control were removed, fixed in Zamboni's fixative, sectioned (30µm) and analysed for p75NTR expression. Figure 6.2.1 shows (A) low magnification image of p75NTR-positive neuron in the ventral horn and nerve fibres in the dorsal horn, (B) ChAT-positive motor neurons in the ventral horn, and (C) merged images. Higher magnification images of areas marked show (D) p75NTR positive staining on the cell body and along processes and (B) staining of ChAT in motor neurons. Merged images (F) display that the p75NTR positive neuron is also positive for ChAT. In wild type B6 controls, the dorsal horn shows natural p75NTR expression (G) and there are many positively stained ChAT positive motor neurons (H), however there are no p75NTR positive motor neurons, made clearer by the lack of co-immunofluorescence in the merged image (I).

6.2.2 *Intraperitoneally injected MLR2-ATTO-488 is retrogradely transported to p75NTR positive motor neurons in SOD1^{G93A} mice*

As MLR2 is the targeting component of the immunogene, it needs to be able to reach p75NTR positive motor neurons in the spinal cord of SOD1^{G93A} mice. Based on previous immunoprecipitation and western blot data (Shepherd *et al.*, 2014) as well as extrapolation of data from the low copy SOD1^{G93A} mouse to the high copy (Coprav *et al.*, 2003), ~100 days of age is where p75NTR expression is highest before overt clinical symptoms are present. Therefore, three 110 day old

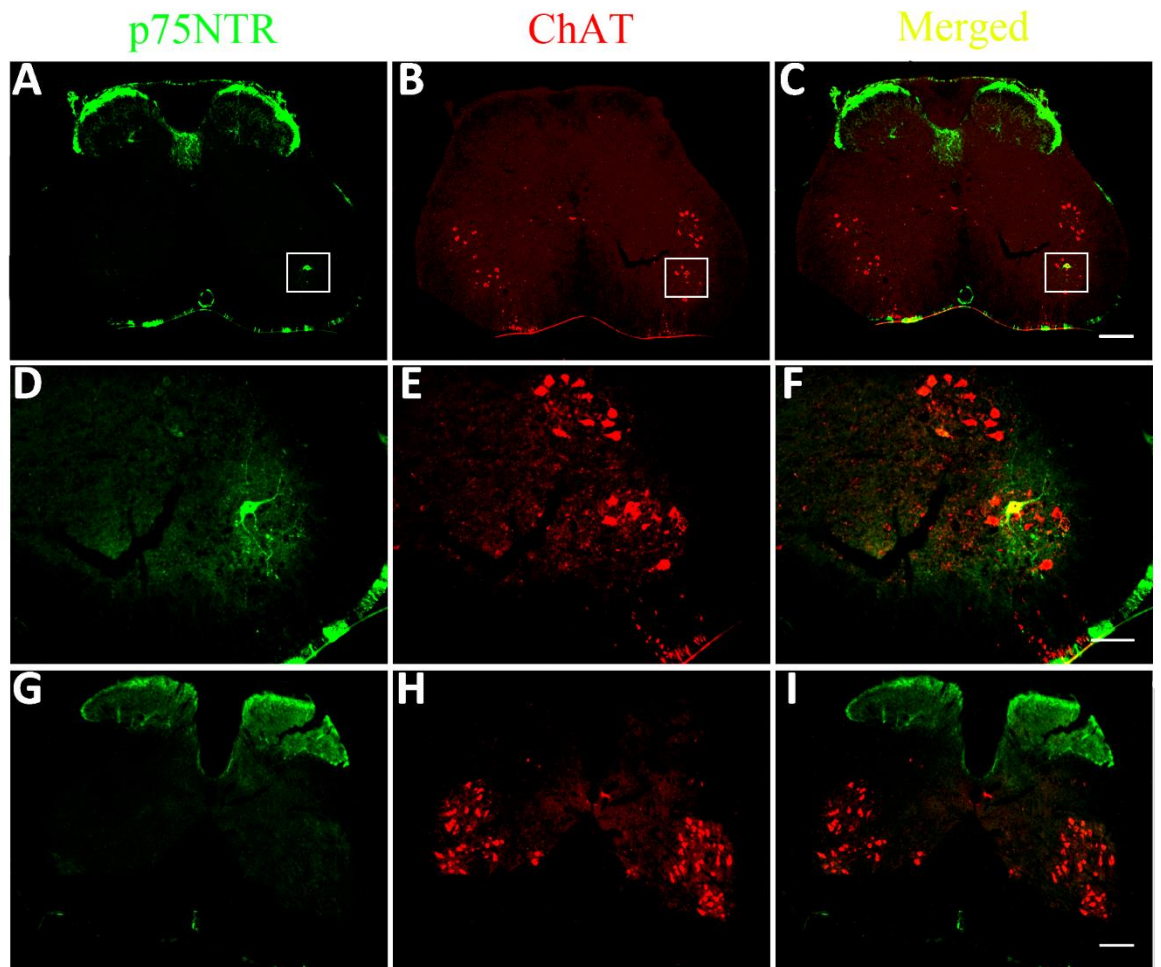


Figure 6.2.1 p75NTR is expressed in SOD1^{G93A} mouse motor neurons, but not B6 controls

Spinal cord sections (30 μ m) were stained for p75NTR (goat anti-p75NTR 1 μ g/ml + 2 $^{\circ}$ donkey anti-sheep 488 1:800) and ChAT (rabbit anti-ChAT 1:5000 + 2 $^{\circ}$ donkey anti-rabbit Cy3 1:800). (A) shows p75NTR-positive neuron in the ventral horn and nerve fibres in the dorsal horn, (B) ChAT-positive motor neurons in the ventral horn, and (C) merged images, from a SOD1^{G93A} mouse.

Higher magnification images of areas marked show (D) p75NTR positive staining on cell body and along processes and (E) staining of ChAT in motor neurons. Merged images (F) display that the p75NTR positive neuron is also positive for ChAT.

In aged matched B6 controls, the dorsal horn shows natural p75NTR expression (G) and there are many positively stained ChAT motor neurons (H), however there are no p75NTR positive motor neurons, made clearer by the lack of co-immunofluorescence in the merged image (I). (scale bar; (A-C, G-I) 200 μ m, (D-F) 100 μ m)

SOD1^{G93A} mice were injected with 1300µg MLR2-ATTO-488 (2x 650ug, 12 hours apart) and every tenth section of their lumbar spinal regions examined for ATTO-488 fluorescence at either 24, 48 or 72 hours after the first injection. Figure 6.2.2 shows fluorescent micrographs of (A) a neuron positive for MLR2-ATTO-488, (B) a neuron positive for p75NTR, (C) ChAT staining showing motor neurons, and (D) overlaid image displaying the ATTO-488+ve neuron is also positive for p75NTR and is a motor neuron. Table 6.1 shows that at 24 hours, only 2 motor neurons in the lumbar region were found to express p75NTR and have retrogradely transported MLR2-ATTO-488 in their soma. There is no difference in the number of p75NTR+ve motor neurons also positive for ATTO-488 between 48 and 72 hours, with 9 found in both mice. There is some variability in the number of p75NTR+ve motor neurons lacking ATTO-488 fluorescence across the three time points. The number of ATTO488+ve motor neurons, but p75NTR-ve is lower in the 24 hour injected mouse (8), but similar between 48 and 72 hours (19 and 17 respectively).

Interestingly, not all p75NTR+ve motor neurons are ATTO-488+ve and not all ATTO-488+ve motor neurons are p75NTR+ve. Figure 6.2.3 shows two more sections from injected mice. (A) displays ATTO-488+ve neurons, (B) lacks any p75NTR positive neurons, (C) ChAT immunoreactivity and (D) overlaid images, where it is seen that the MLR2-ATTO-488+ve motor neuron is not expressing p75NTR. (E) shows an absence of ATTO-488 fluorescence, (F) p75NTR expression, (G) ChAT immunoreactivity and (H) overlaid images. The merged image here shows that not all p75NTR+ve motor neurons uptake the MLR2-ATTO-488.

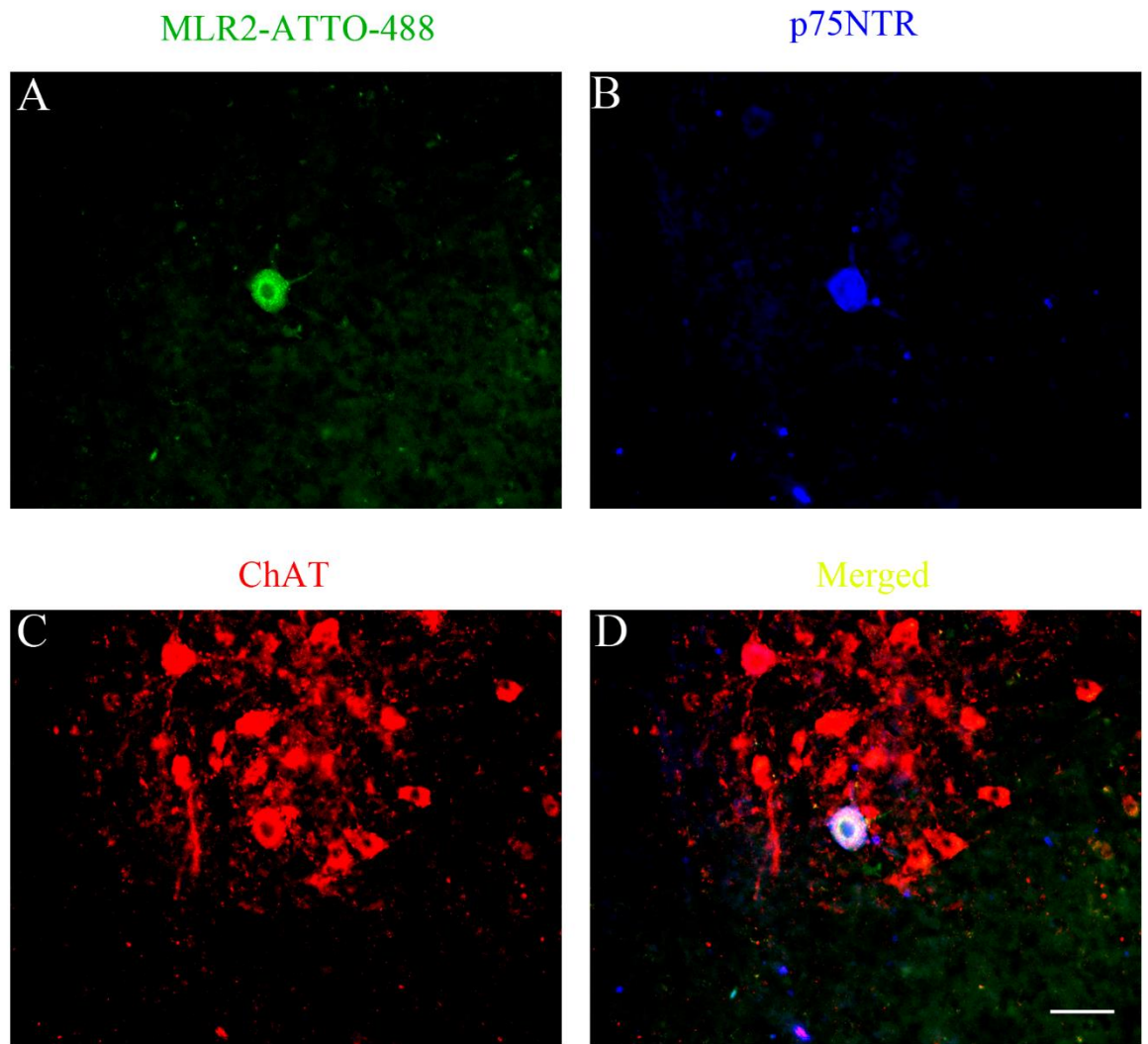


Figure 6.2.2 Fluorescently tagged antibodies are retrogradely transported to spinal motor neurons in SOD1^{G93A} mice after I.P injection

110 day old SOD1^{G93A} mice were injected twice (12 hours apart) with 650 μ g (1300 μ g total) of MLR2-ATTO-488 intraperitoneally. Once the spinal cord was removed, it was sectioned at 30 μ m and counterstained for p75NTR (goat anti-p75NTR 1 μ g/ml + 2 $^{\circ}$ donkey anti-sheep Cy5 1:800) and ChAT (rabbit anti-ChAT 1:5000 + 2 $^{\circ}$ donkey anti-rabbit Cy3 1:800). Image (A) shows that the fluorescently labelled anti-p75NTR MLR2 antibody was able to be retrogradely transported to neurons in the lumbar spinal cord from the circulation in the transgenic mouse. To clarify that these neurons are p75NTR positive motor neurons, sections were counter stained for p75NTR and ChAT. As can be seen in image (B) the MLR2-ATTO-488 positive neuron is p75NTR positive and in image (C) expresses ChAT, confirming it is a motor neuron, which is confirmed in the overlaid image (D) (scale = 50 μ m).

Table 6.1 Number of motor neurons that are positive for ATTO-488 fluorescence, or p75NTR positive, or both, after intraperitoneal injection of MLR2-ATTO-488 in 110 day old SOD1^{G93A} mice, at three time points after injection (n=1 mouse/injection time point)

Hours after injection	MLR2-ATTO-488 +ve MN's	p75NTR+ve MN's	MLR2-ATTO-488 /p75NTR+ve MN's
24	8	5	2
48	19	3	9
72	17	13	9

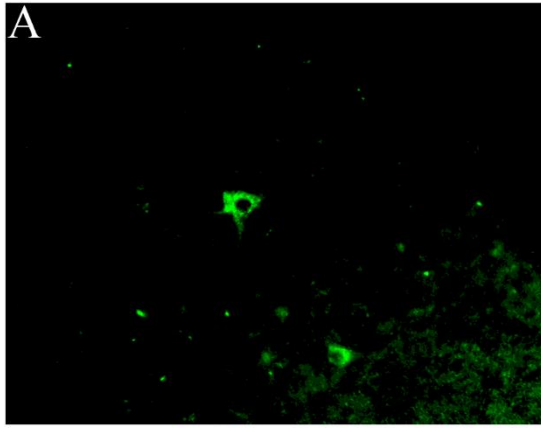
Figure 6.2.3 Not all MLR2-ATTO-488 positive motor neurons are p75NTR positive and not all p75NTR positive motor neurons show ATTO-488 fluorescence

Mice injected with 1300 μ g MLR2-ATTO-488 show some ChAT positive lumbar motor neurons (rabbit anti-ChAT 1:5000 + 2 $^{\circ}$ donkey anti-rabbit Cy3 1:800) lacking p75NTR expression (goat anti-p75NTR 1 μ g/ml + 2 $^{\circ}$ donkey anti-sheep Cy5 1:800) and others expressing p75NTR but show no retrograde transport of the tagged antibody.

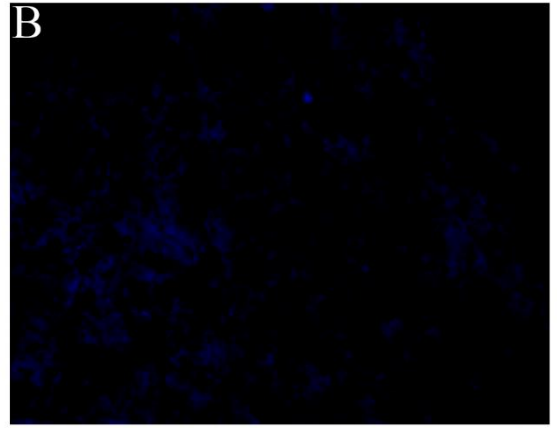
Image (A) shows ATTO-488 fluorescence in a neuron, (B) no p75NTR expressing cells, (C) ChAT positive motor neurons and (D) merged images. The merge image shows a motor neuron with ATTO-488 fluorescence, but is p75NTR negative.

Image (E) shows a section of lumbar spinal cord with no ATTO-488 fluorescence, (F) a neuron positive for p75NTR expression, (G) ChAT positive motor neurons and (H) merged images. It is clear there is a positive p75NTR motor neuron that has not taken up the MLR2-ATTO-488 antibody (scale = 50 μ m).

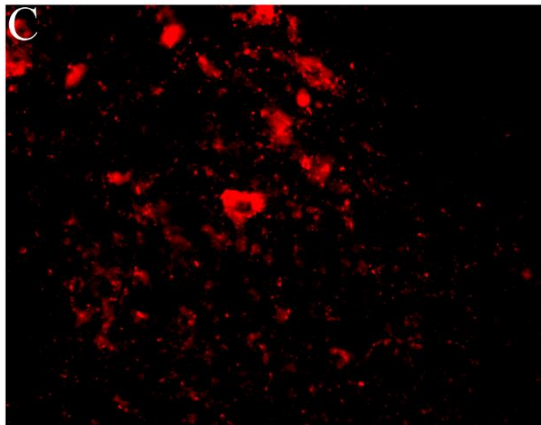
MLR2-ATTO-488



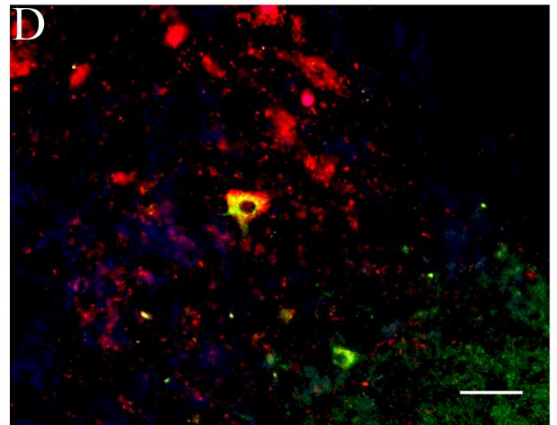
p75NTR



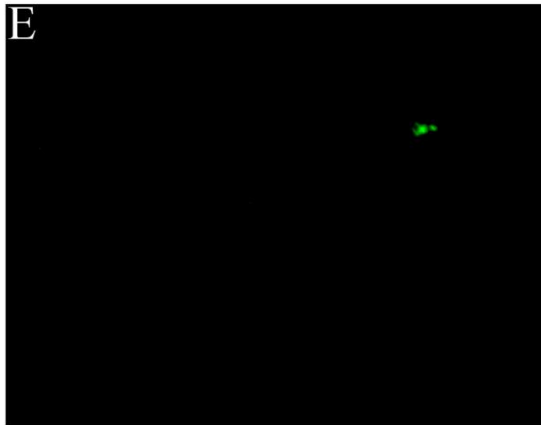
ChAT



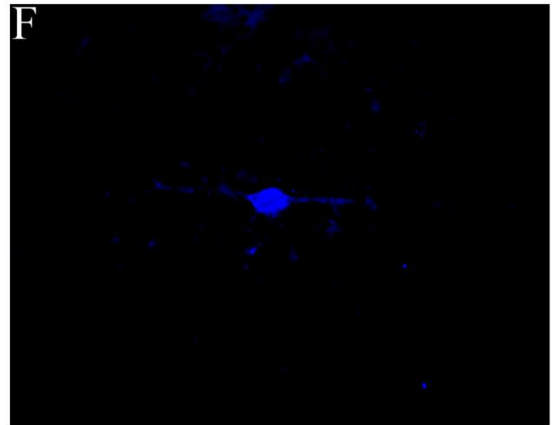
Merged



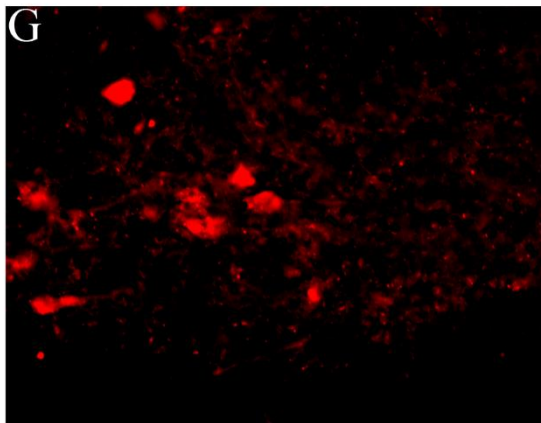
MLR2-ATTO-488



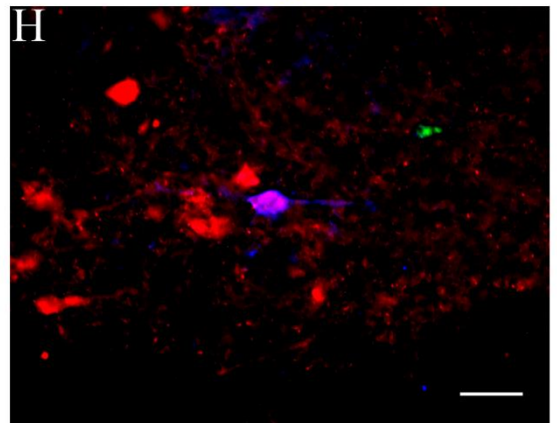
p75NTR



ChAT



Merged



6.2.3 *MLR2-ATTO-488 is transported to p75NTR positive DRG neuronal cell bodies*

Motor neurons are not the only cell type that express p75NTR, cells within the dorsal root ganglia (DRG) also express the receptor. Because of this, DRG's from SOD1^{G93A} mice injected with MLR2-ATTO-488 were examined for fluorescence. A substantial number, but not all, neurons within the DRG's were found to be positive for ATTO-488 (figure 6.2.4a). These DRG's were counterstained with 1ug/ml goat anti-p75NTR and a donkey anti-sheep CY3 secondary (1:800). Figure 6.2.4b (A) shows ATTO-488 fluorescence in DRG neurons, (B) shows neurons positive for p75NTR and (C) overlaid images. Of the total number of p75NTR/MLR2-ATTO-488+ve, p75NTR+ve and MLR2-488+ve DRG neurons, approximately 90.36% were p75NTR/MLR2-ATTO488+ve, 6.02% were p75NTR+ve only and 3.61% were MLR2-ATTO48+ve only. As well as cell bodies, nerve fibres exiting the DRG were examined. (D) shows ATTO-488 fluorescence along nerve fibres, (E) shows p75NTR immunoreactive fibres and (F) overlaid images. It can be seen in the overlaid image that many of the fibres show both p75NTR and ATTO-488 co-fluorescence.

6.2.4 *Loss of ChAT positive motor neurons in the lumbar region of SOD1^{G93A} mice*

Lumbar spinal cord sections from SOD1^{G93A} and B6 (n=4 mice per strain, per age 60-140 days) mice were stained for ChAT and counted (Figure 6.2.5). At 60 days, while not statistically significant, a trend of total motor neuron decline is apparent, indicating that motor neuron loss begins before 60 days. The loss of

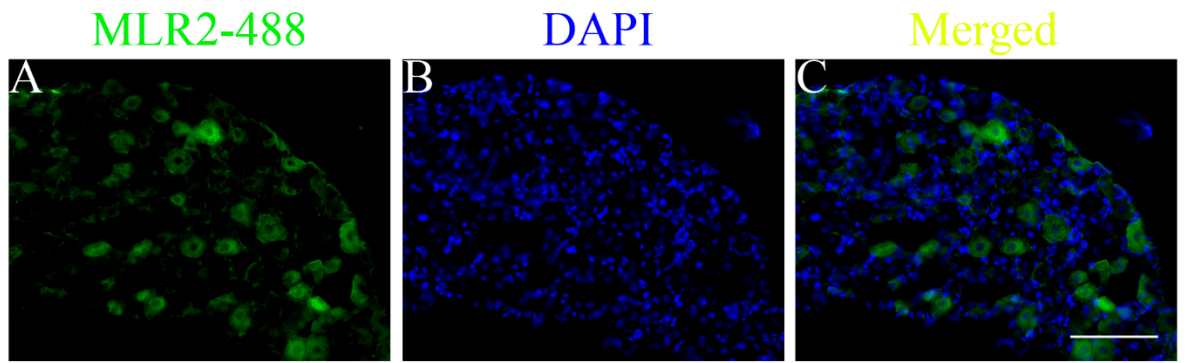


Figure 6.2.4a MLR2-488 is transported to DRG neurons

110 day old SOD1^{G93A} mice injected with MLR2-ATTO-488 (from figure 6.2.2) show that the conjugated antibody is able to be retrogradely transported to specific neuronal cell bodies (A) within DRGs, but not all neurons, as evident by the lack of 488 fluorescence in majority of DAPI positive cells (B, C). (scale = 50µm)

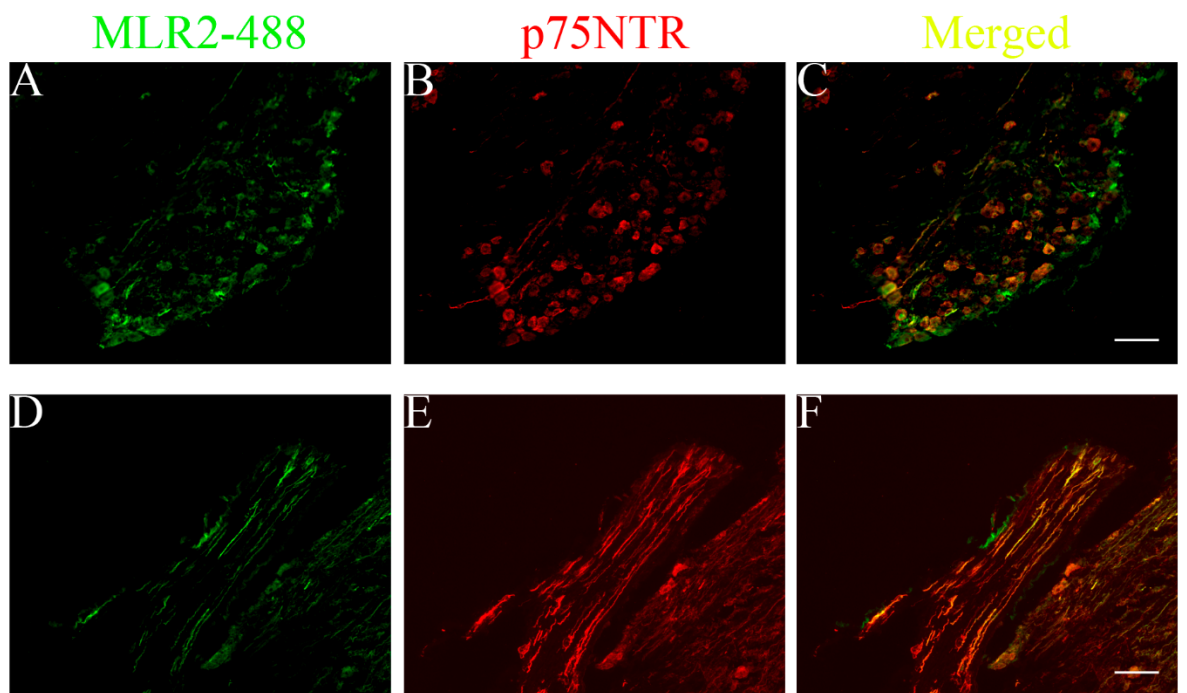


Figure 6.2.4b MLR2-488 is transported to p75NTR+ve DRG neurons

DRGs taken from 110 day old SOD1^{G93A} mice injected with MLR2-ATTO-488 (A) were counterstained for p75NTR (goat anti-p75NTR 1µg/ml + 2° donkey anti-sheep Cy3 1:800) (B). In the merged image (C), all MLR2-488+ve neurons are positive for p75NTR. Interestingly, MLR2-ATTO-488 showed positive labelling on fibres connected to DRGs (D) and these fibres were p75NTR positive (E), which showed complete overlap when merged (F). (scale = 50µm).

motor neurons becomes significant ($p < 0.01$) by age 80 days in $SOD1^{G93A}$ mice (Figure 6.2.5a), as seen by 2way ANOVA. There is a natural decline in motor neurons in the B6 controls as they age, seen for example in Figure 6.2.5.

6.2.5 *Motor neuron number declines to 50% by end stage in $SOD1^{G93A}$ mice*

The percentage decline of ChAT positive motor neurons with age was quantified (Figure 6.2.5b). As early as 60 days, there was a 20% loss in the number of motor neurons in the $SOD1^{G93A}$ mouse. The number of motor neurons continues to decrease, such that by 100 days, approximately 35% of all lumbar motor neurons have been lost. This loss of motor neurons continues throughout the life of the animal, until end stage when approximately 50% loss of motor neurons has occurred.

6.2.6 *The percentage of motor neurons that express p75NTR increases with age in $SOD1^{G93A}$ mice*

To establish the percentage of motor neurons that re-express p75NTR, lumbar spinal cord sections from $SOD1^{G93A}$ and B6 mice were stained for p75NTR concurrently with ChAT (n=4 per strain, per age 60–140 day). The numbers of neurons containing p75NTR were calculated as a percentage of ChAT-containing motor neurons in the lumbar region of $SOD1^{G93A}$ mice at each respective age (Figure 6.2.6). At 60 days, no ChAT-containing motor neurons expressed p75NTR. By 80 days, 1.1% of motor neurons expressed p75NTR, but this

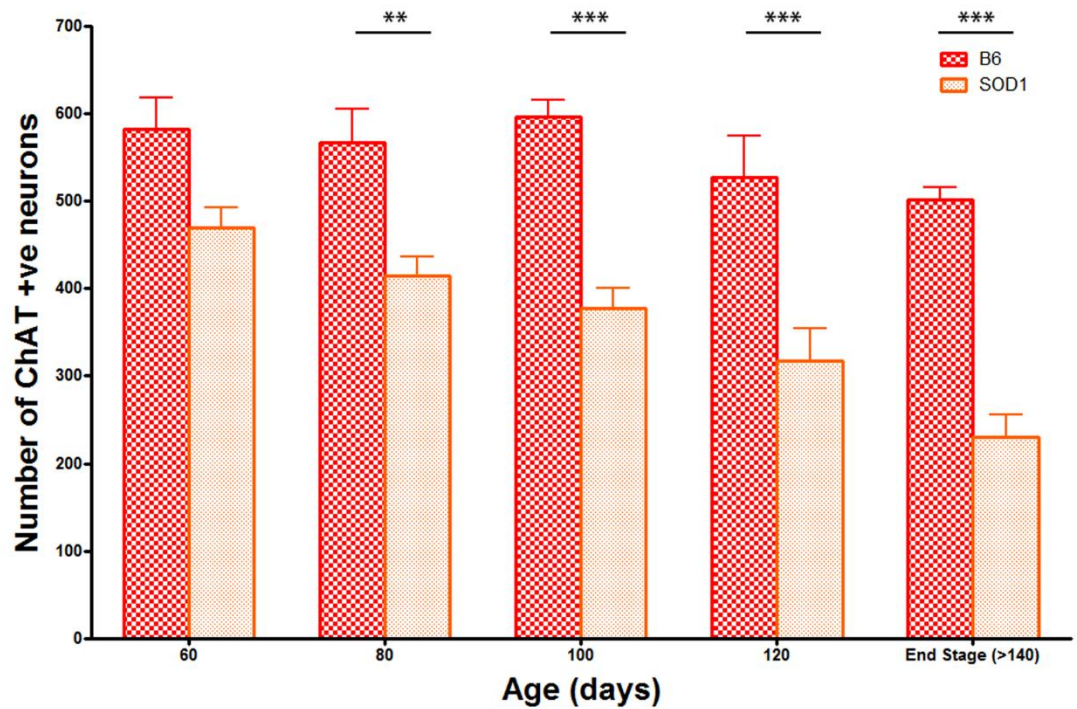


Figure 6.2.5a The number of motor neurons in the lumbar region of SOD1^{G93A} mice declines compared to B6 aged matched controls
 SOD1^{G93A} ChAT+ve lumbar motor neurons show a decline in number over time, compared to B6 age matched controls from 60-140+ days. There is a significant difference in ChAT+ve neurons from 80 days onward between SOD1^{G93A} mice and B6 controls (**=p<0.01, ***=p<0.001). ChAT+ve ventral horn neurons from every tenth section were counted throughout the entire lumbar region. (n=4 per strain, per age)

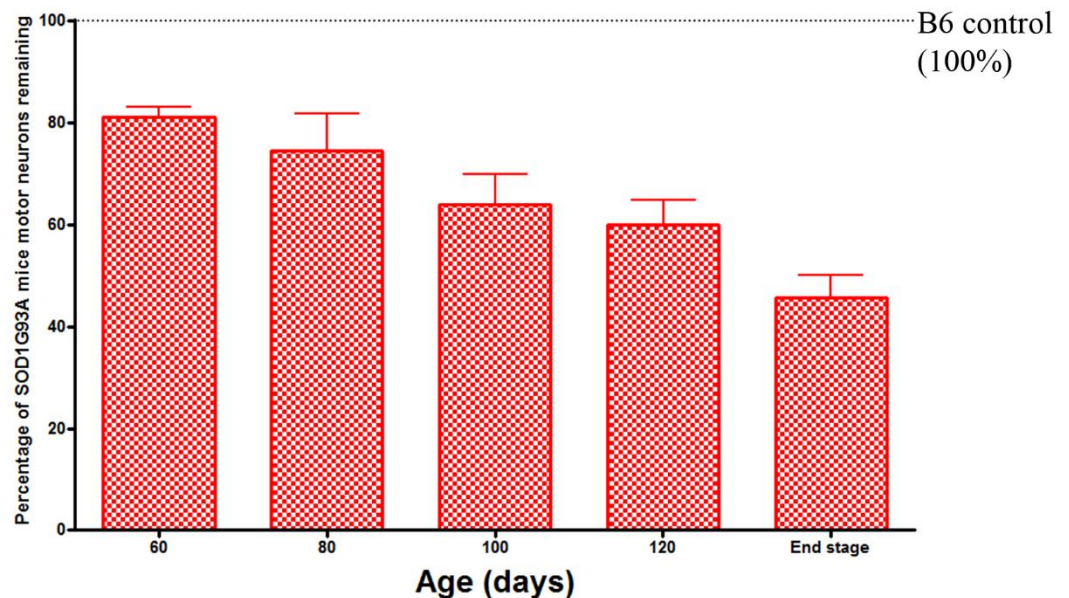


Figure 6.2.5b SOD1^{G93A} motor neurons as a percentage of aged matched B6 controls
 Histogram representing the total number of ChAT +ve neurons in the ventral horn of the lumbar region remaining as a percentage at each stage of disease in SOD1^{G93A} mice. There is already a 20% loss of motor neurons by 60 days of age, which continues to ~50% by end stage (n=4 per strain, per age)

occurred in only two of the four mice. By 100 days, the percentage of motor neurons with p75NTR increased to 3.40%. There was a slight percentage increase from 100 days to 120 days, to 3.85%. By end stage (140 days), the percentage increased to 4.36%. B6 control mice at 140 days of age also showed minimal p75NTR expression in some motor neurons, but at a much lower percentage (0.35%).

6.2.7 The number of p75NTR positive motor neurons is influenced by total motor neuron number

Figure 6.2.6 shows p75NTR neurons as a percentage of motor neurons identified by ChAT from 80 to 140 days, but does not take into consideration neuron loss. The total numbers of p75NTR re-expressing motor neurons in the entire lumbar section of four SOD1^{G93A} and B6 control mice were counted (Figure 6.2.7). Motor neurons re-expressing p75NTR first appeared at 80 days of age, but at a very low number of 47/mouse in the lumbar region and in only two of four mice. At 100 days, motor neurons increased to 123.4/mouse. The difference between 100 days and 120 was minimal, with 131.7/mouse in the older animals. However, there was some variation between SOD1^{G93A} mice, as shown by the spread of the data at 100- and 120-day- old animals.

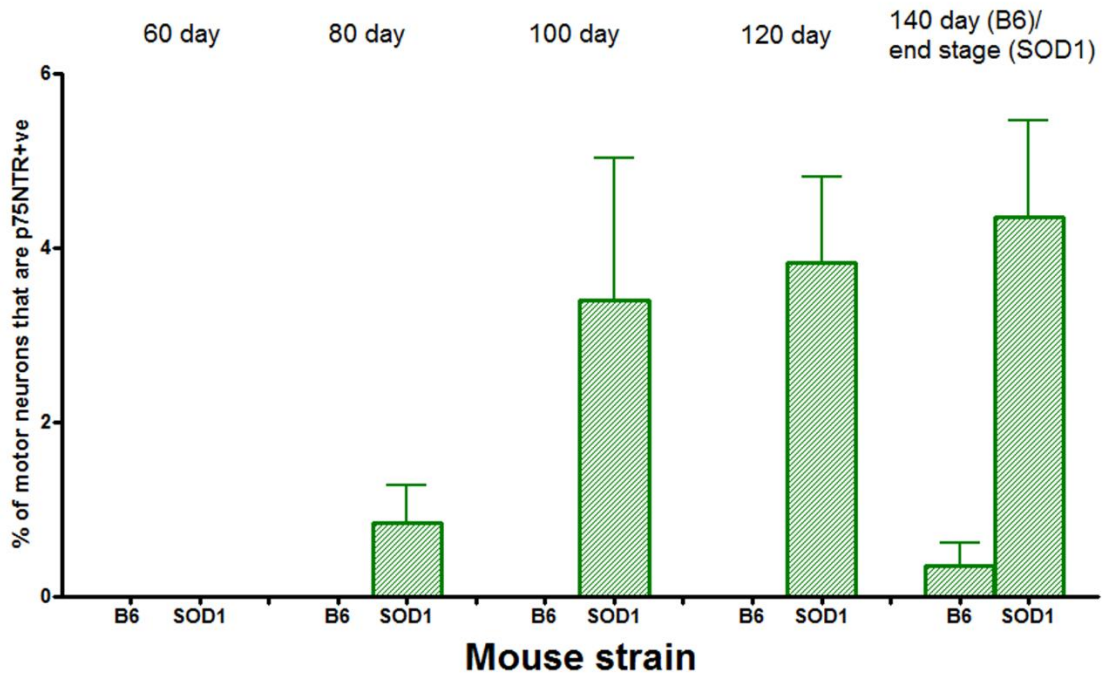


Figure 6.2.6 The percentage of motor neurons that express p75NTR increases with age in SOD1^{G93A} mice, but is under 5%

SOD1^{G93A} and B6 age matched control lumbar spinal cords were analysed for p75NTR expression in motor neurons from 60-140+ days. ChAT/p75NTR positive ventral horn neurons from every tenth section were counted throughout the entire lumbar region. The expression of p75NTR can be seen immunohistochemically around the 80 day mark, which accounts for 0.84% of all motor neurons. At 100 days, the number of motor neurons expressing p75NTR increases to 3.4%, then slightly increases to 3.85% at 120 days and 4.36% at end stage. There is also some low level, naturally occurring p75NTR expression in the 140 day control mice (0.35%). (n=4 per strain, per age).

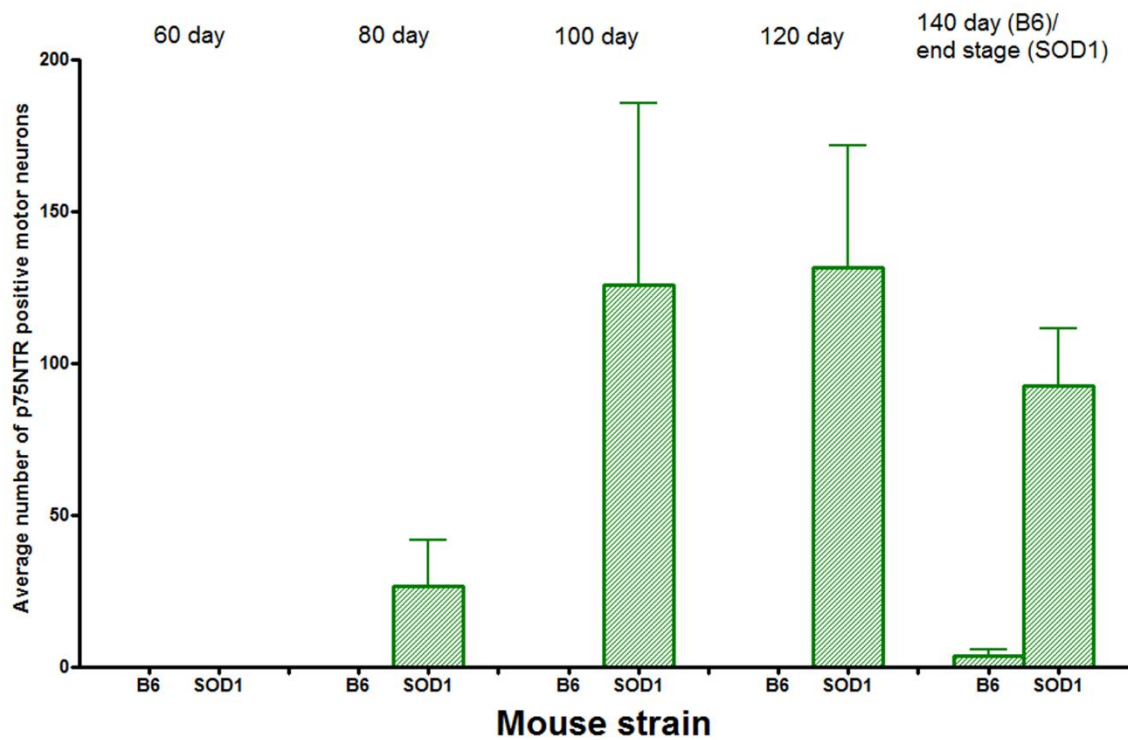


Figure 6.2.7 The average number of p75NTR positive motor neurons in SOD1^{G93A} mice peaks between 100-120 days

The average number of p75NTR positive motor neurons in the lumbar region of SOD1^{G93A} mice and B6 age matched controls were counted from 60-140+ days. Positive ventral horn neurons from every tenth section were counted throughout the entire lumbar region and multiplied to represent the entire lumbar region. The expression of p75NTR can be seen immunohistochemically at 80 days with 35.3 neurons/mouse, and peaks around 100-120 days, with 125.9 neurons/mouse and 131.9 neurons/mouse respectively. The average drops at the end stage (140 days) of the disease, with 92.7 neurons/mouse. The naturally occurring p75NTR expression in the 140 day control mice is 7.2 neurons/mouse. (n=4 per strain, per age).

6.2.8 Motor neurons expressing p75NTR are larger than motor neurons that are p75NTR negative

Intriguingly in SOD1^{G93A} mice, particularly at older ages, p75NTR+ve lumbar motor neurons were on average larger than p75NTR-ve motor neurons. An example of this observation can be seen in Figure 6.2.8 which shows p75NTR+ve neurons that are larger than their surrounding p75NTR-ve neuron neighbours, in 120 day old SOD1^{G93A} mice. These p75NTR+ve motor neurons also show multiple dendrites connected to the soma. All p75NTR+ve motor neuron soma areas from all ages in SOD1^{G93A} mice were quantified and compared to p75NTR-ve motor neurons from both SOD1^{G93A} and B6 mice, which is displayed in Figure 6.2.9 (n= 4 mice/age/strain). The average area of p75NTR-ve neurons in SOD1^{G93A} mice decreases with age (from 718.4 μm^2 at 60 days, to 418.8 μm^2 at end stage); conversely p75NTR+ve motor neurons are approximately the same size as B6 motor neurons (~600-800 μm^2). At 80 days, p75NTR+ve neurons appear larger than the p75NTR-ve neurons in SOD1^{G93A} mice, however the variability is high in part due to low numbers of motor neurons. At 100 days of age, the difference in soma area between p75NTR+ve motor neurons (739.7 μm^2) and p75NTR-ve neurons (495.2 μm^2) is significant (p<0.05) as seen by 2way ANOVA, which continues to be significant at 120 days (763.4 μm^2 p75NTR+ve motor neurons and ~431.2 μm^2 p75NTR-ve motor neurons, p<0.05) in SOD1^{G93A} mice. End stage has the greatest difference in size (p<0.01), with p75NTR+ve (778.1 μm^2) neurons being 54% larger than p75NTR-ve neurons (~418.8 μm^2). The average size of p75NTR+ve motor neurons does not differ at any age of SOD1^{G93A} mice (~739-800 μm^2).

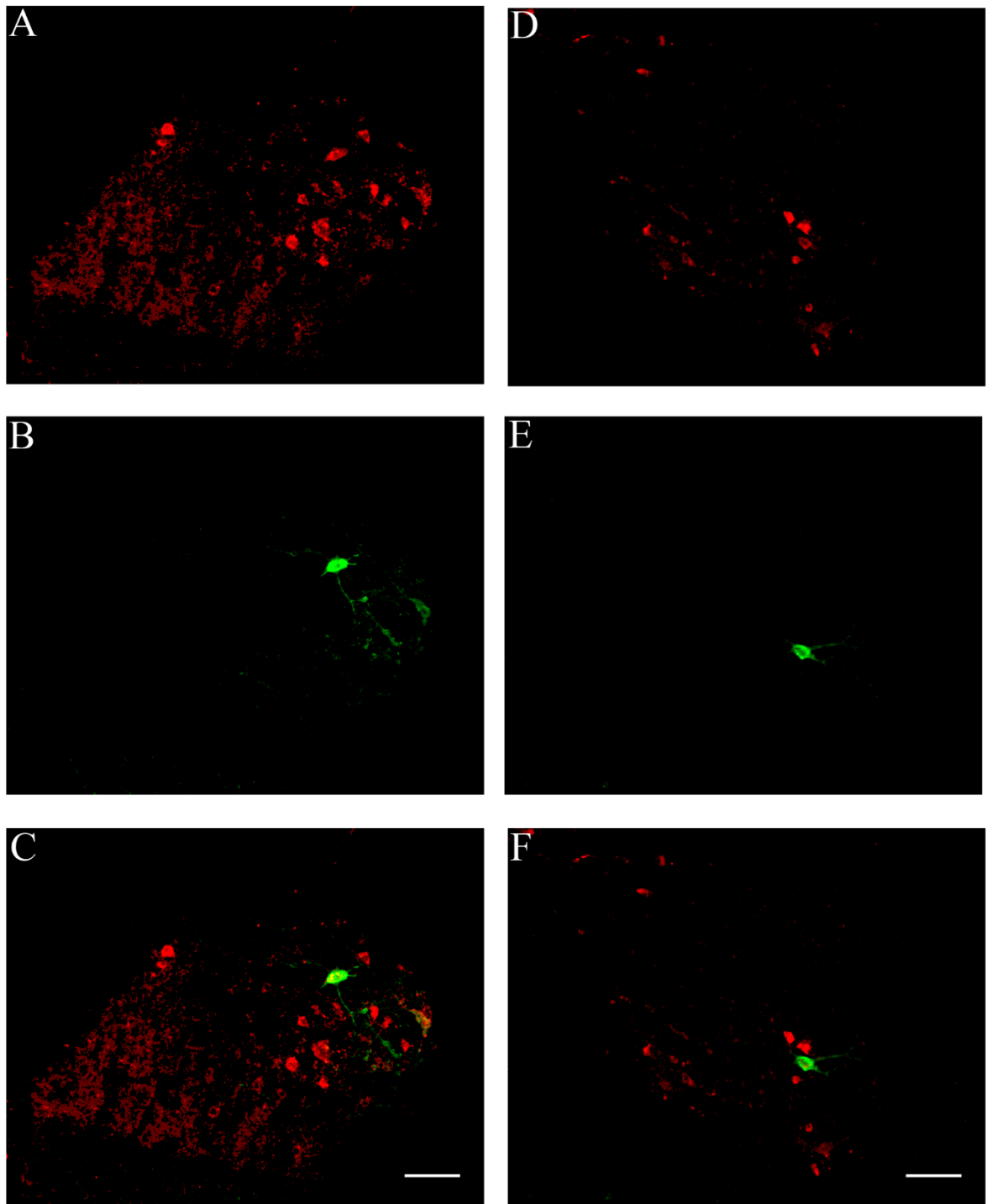


Figure 6.2.8 p75NTR positive motor neurons appear larger than p75NTR negative motor neurons

The above images show p75NTR +ve neurons in the lumbar region of 120 day old SOD1^{G93A} mice. (A, D) shows positive staining for ChAT. (B, E) shows p75NTR+ve neurons. (C, F) are overlays of (A,B) and (C,D), respectively. The merged images accentuate the size differences between p75NTR+ve and p75NTR-ve neurons, with positive neurons appearing larger than majority of the surrounding motor neurons (scale bar 50µm).

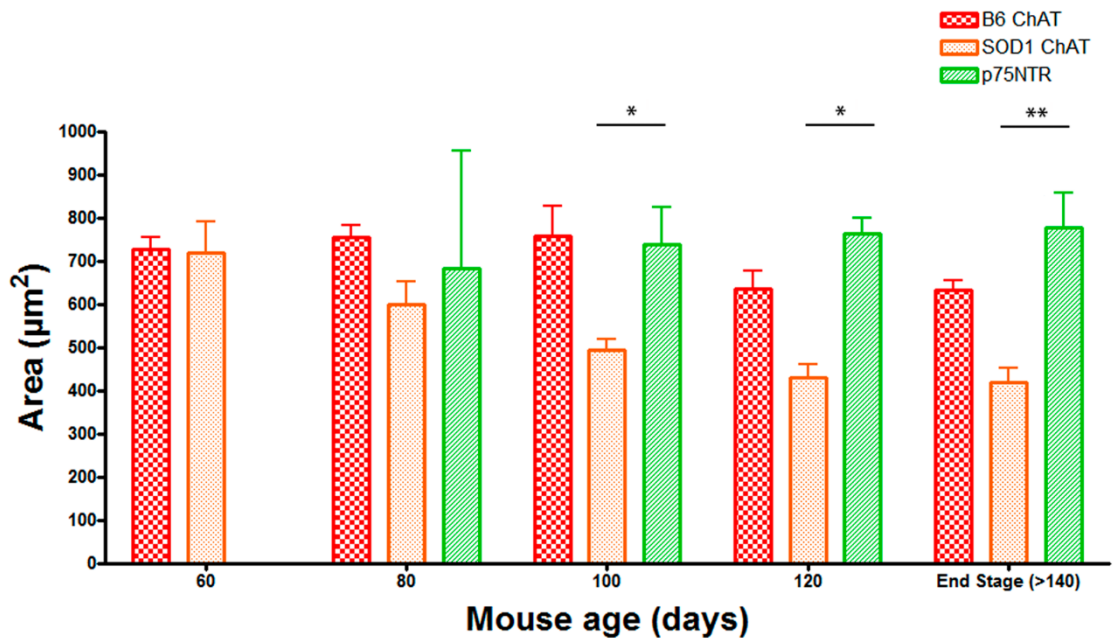


Figure 6.2.9 p75NTR positive motor neurons are larger than p75NTR negative motor neurons in SOD1^{G93A} mice

The area (µm²) of p75NTR +ve lumbar motor neurons in SOD1^{G93A} mice was measured and compared to B6 age matched control motor neurons and p75NTR-ve SOD1^{G93A} motor neurons, from 60-140+ days. The area of the p75NTR+ve neurons from SOD1^{G93A} mice are comparable to that of the B6 motor neurons up until 120 days, while the difference to the SOD1^{G93A} motor neurons increases, at all ages. At 100, 120 days and end stage, the difference between the SOD1^{G93A} p75NTR+ve and p75NTR-ve motor neurons is significant (*=p<0.05, **=p<0.01, respectively). There is no statistical significance between p75NTR+ve motor neurons and B6 p75NTR-ve motor neurons at any age (±SEM, n=4 per age, per strain).

6.2.9 *p75NTR expressing motor neuron size verified by dual fluorescent channel measurements and retrograde transport in-vivo*

To clarify that the size changes seen were not an artefact of immunohistochemical procedures or staining profile, every motor neuron that was p75NTR+ve was measured for area and diameter in both fluorescent channels for p75NTR and ChAT. There was no difference in staining profile between p75NTR and ChAT when measured on the same cell (Figure 6.2.10), as tested by 2way ANOVA. Following this, adult 110 day old SOD1^{G93A} mice (n=3) were injected intraperitoneally with 1300µg (650µg x2, 12 hours apart) of p75NTR antibody conjugated to a fluorescent tag (MLR2-ATTO-488). 72 hours after first injection, spinal cords were removed, processed and analysed for ATTO-488 fluorescence, as well as counterstaining for ChAT and p75NTR (from Figure 6.2.2). When comparing the average size of p75NTR expressing motor neurons post-stained in SOD1^{G93A} mice (718.8µm²) and injected SOD1^{G93A} mice (640.7µm²), there is no statistical difference in area (Figure 6.2.11), as tested by 2way ANOVA. Hence, all p75NTR expressing motor neuron sizes are comparable to ChAT stained motor neurons.

6.2.10 *p75NTR and ATF-3 are rarely co-expressed in SOD1^{G93A} motor neurons*

To better understand the time frame at which p75NTR is expressed, lumbar spinal cord sections from SOD1^{G93A} and B6 mice were stained for both p75NTR and ATF-3, which is considered a cell stress, pre-apoptotic marker when upregulated and translocated to the nucleus (Hai et al. 1999). Figure 6.2.12 shows spinal cord

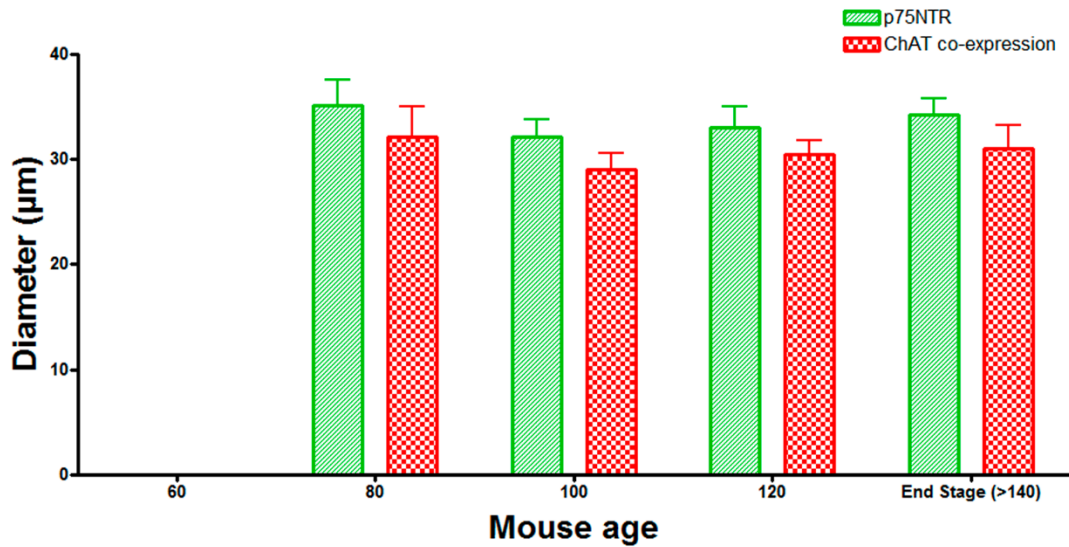


Figure 6.2.10a Diameter measurements are not affected by staining profiles of p75NTR and ChAT

Histogram representing the average diameter of p75NTR +ve neurons in the lumbar region of the spinal cord of SOD1^{G93A} mice compared to the diameter of the same cell, but in the ChAT expressing fluorescent channel, from 60-140+ days. Every p75NTR +ve neuron found was measured. There is no significant difference in the soma diameter of the cells when measuring in different channels (n=4 per strain, per age)

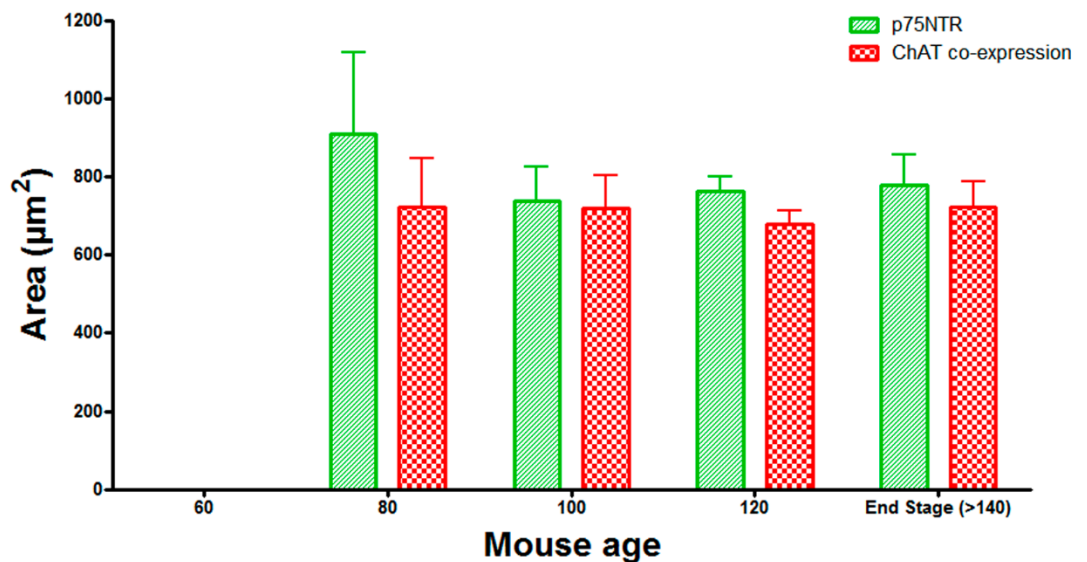


Figure 6.2.10b Area measurements are not affected by staining profiles of p75NTR and ChAT

Histograms representing the average area of p75NTR +ve neurons of SOD1^{G93A} mice compared to the area of the same cell, but in the fluorescent channel for ChAT, from 60-140 days. Every p75NTR positive neuron found was measured. There is no significant difference in the area of the cells when measuring in different channels (±SEM, n=4 per strain, per age)

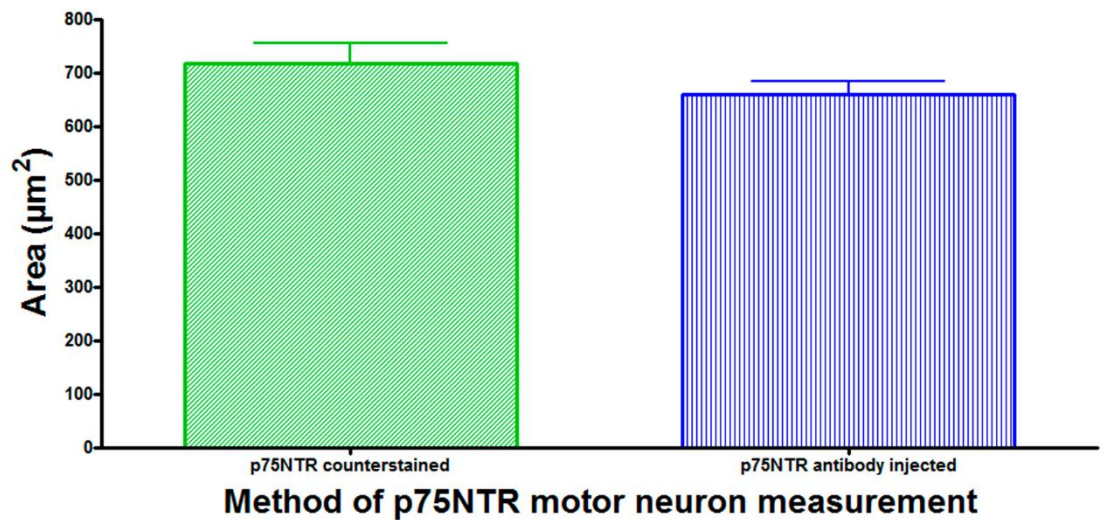


Figure 6.2.11 p75NTR motor neurons tagged by I.P. injected MLR2-ATTO-488 are the same size as counterstained p75NTR motor neurons

The area of motor neurons from 110 day old SOD1^{G93A} mice that were injected intraperitoneally with 1300µg of MLR2-ATTO-488 were analysed and compared to p75NTR counterstained motor neurons. The average size of p75NTR expressing motor neurons post-stained in SOD1^{G93A} mice (718.8µm²) and injected SOD1^{G93A} G1H mice (640.7µm²) were not statistically different in area (±SEM, n=3).

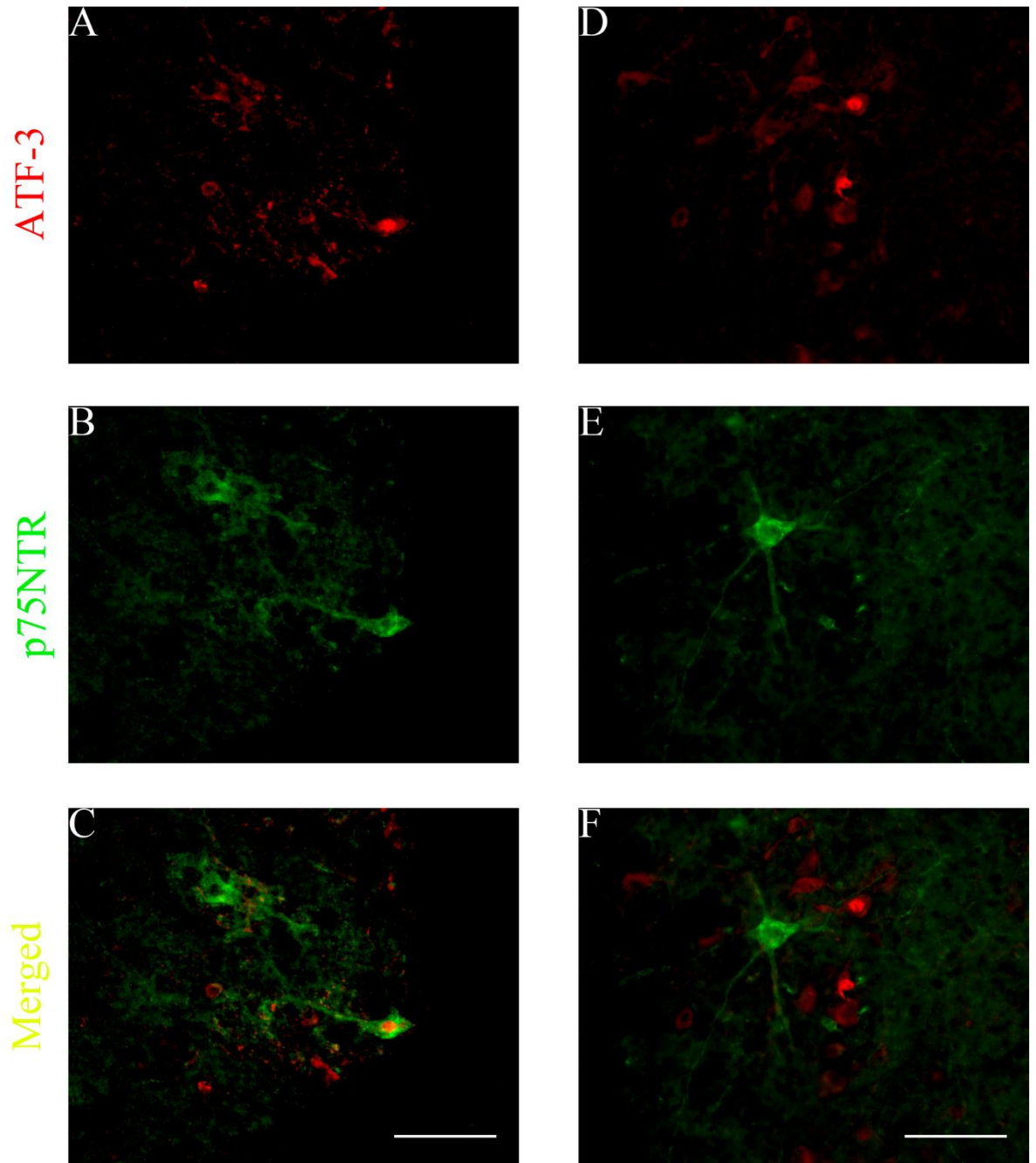


Figure 6.2.12 Expression of ATF-3 and p75NTR in the ventral horn of the lumbar spinal cord of 100 day old SOD1^{G93A} mice.

Spinal cord sections showing (A, D) positive ATF-3 stained motor neuron nuclei (rabbit anti-ATF-3 1:200+ 2° donkey anti-rabbit Cy3 1:800), which is indicative of cell stress, (B, E) p75NTR positive motor neurons (goat anti-p75NTR 1µg/ml + 2° donkey anti-sheep 488 1:800) and (C, F) merged images. In image (C), the co-expression of p75NTR on the cell membrane and ATF-3 in the nucleus can be easily seen. However, in image (F) the p75NTR positive motor neuron is not positive for ATF-3, while two cells in the vicinity are. On average, ~6% of motor neurons co-express p75NTR and nuclear ATF-3 concurrently (scale = 50µm)

sections positive for nuclear ATF3 (A, D), which is indicative of cell stress, (B, E) p75NTR positive motor neurons and (C, F) merged images. In image (C), the co-expression of p75NTR on the cell membrane and ATF-3 in the nucleus can be easily seen. However, in image (F) the p75NTR positive motor neuron is not positive for ATF-3, while two cells in the vicinity are stained. Table 6.2 shows that there is an increasing number of ATF-3 +ve motor neurons from 80 days in parallel with an increase in the number of p75NTR+ve motor neurons. However, the average number of motor neurons that express both p75NTR and ATF-3 is very low. On average, ~6% of motor neurons co-express p75NTR and nuclear ATF-3 concurrently. No B6 control mouse motor neurons were positive for nuclear translocated ATF-3.

6.2.11 *Cleaved caspase-3 is expressed in a majority of p75NTR positive motor neurons*

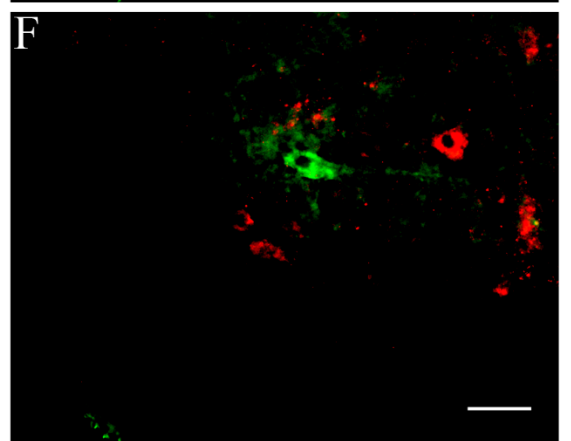
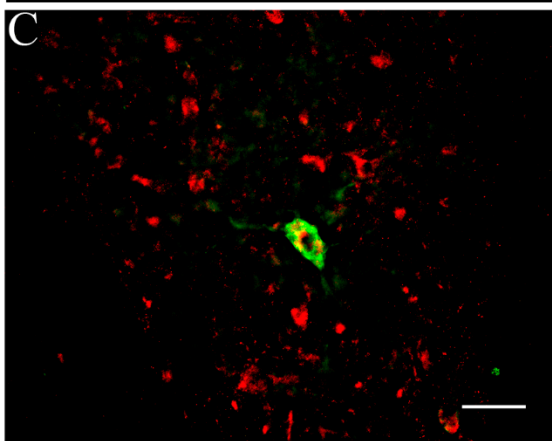
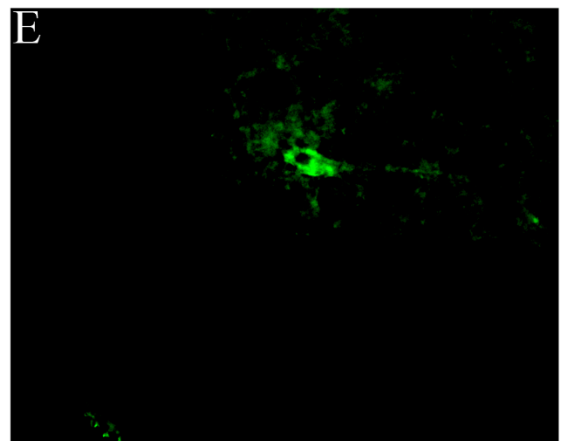
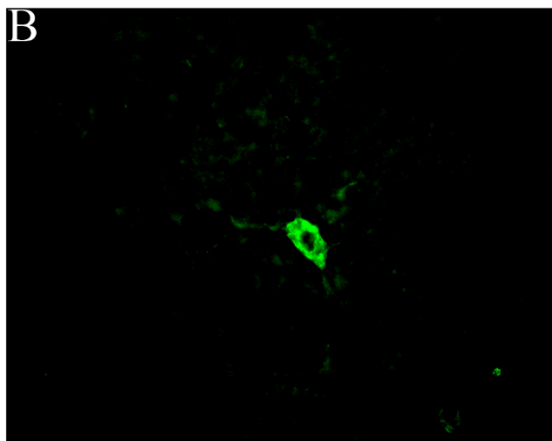
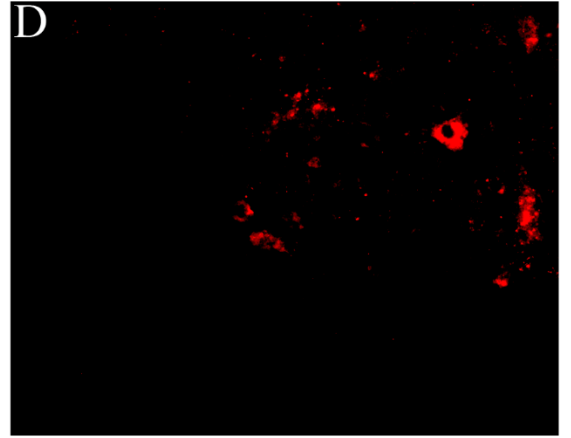
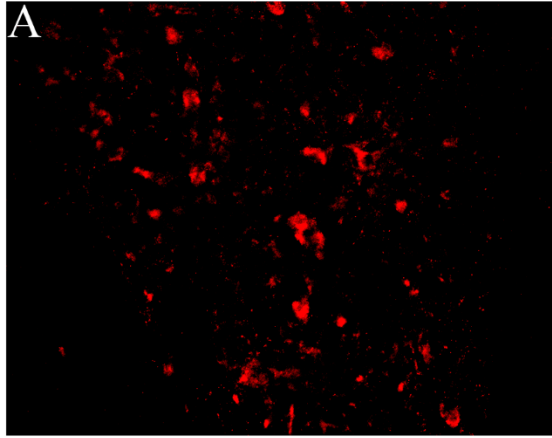
Cleaved caspase-3 is a standard marker for cells undergoing apoptosis. Lumbar regions from SOD1^{G93A} mice aged between 100-140 days (n=5) were stained for p75NTR and the common apoptotic marker cleaved caspase-3 (Figure 6.2.13). Images (A, E) show cleaved caspase-3 immunofluorescence in several cells, from a 120 and 100 day old mouse, respectively. p75NTR expression is seen in images (B, F), with a large p75NTR positive neuron in each image. Images (D, H) are merged images (A-C) and (E-G), respectively. (D) shows a motor neuron positive for both p75NTR and cleaved caspase-3, while (H) shows a p75NTR positive motor neuron that is not expressing cleaved caspase-3, with surrounding neurons expressing the apoptotic marker. The percentage of

Table 6.2 The following table shows the average number of cells expressing ATF-3, motor neurons expressing p75NTR, or both ATF-3 and p75NTR, from SOD1^{G93A} mice lumbar spinal cords. Very rarely are p75NTR and ATF-3 expressed in the same cell concurrently. Not a single ATF-3 motor neuron was found in B6 control mouse motor neurons. (n=4 mice/age, ±SEM)

Mouse age	ATF-3 only	p75NTR only	ATF-3/p75NTR co-expression
80	3.6 (±3.2)	3.2 (±3.2)	0.0
100	28.5 (±3.9)	11.4 (±1.7)	1.8 (±1.2)
120	32.1 (±6.5)	13.2 (±0.88)	0.0
End Stage	43.8 (±8.4)	8.6 (±0.58)	0.4 (±0.33)

Figure 6.2.13 p75NTR and cleaved caspase-3 co-express in majority of motor neurons in SOD1^{G93A} mice

Lumbar regions from SOD1^{G93A} G1H mice aged between 100-140 days were stained for p75NTR (goat anti-p75NTR 1µg/ml + 2° donkey anti-sheep 488 1:800) and cleaved caspase-3 (rabbit anti-cleaved caspase-3 1:200+ 2° donkey anti-rabbit Cy3 1:800). Images (A, D) show cleaved caspase-3 immunofluorescence in several cells, from a 120 day old and 100 day old mouse, respectively. p75NTR expression is seen in images (B, E), with a large p75NTR positive neuron in each image. Images (C, F) are merged images (A-C) and (E-G), respectively. (D) shows a motor neuron positive for both p75NTR and cleaved caspase-3, while (H) shows a p75NTR positive motor neuron that is not expressing cleaved caspase-3, with surrounding neurons expressing the apoptotic marker. On average, 71.1% of all p75NTR positive motor neurons express cleaved caspase-3, concurrently in the SOD1^{G93A} mouse (scale = 50µm).



p75NTR motor neurons that express cleaved caspase-3 is 84.4% in the lumbar region of SOD1^{G93A} mice (Table 6.3).

6.2.12 *Motor neuron diameter decreases during disease in the SOD1^{G93A} mouse*

There is a substantial amount of information in the literature concerning changes within motor neurons of the various strains of SOD1 mice, such as morphological and biochemical alterations (see Kanning, Kaplan, & Henderson, 2010 for review). Although many features of SOD1^{G93A} mouse motor neurons have been identified, the soma diameter has not been explored. In figure 6.2.14a, the average motor neuron soma diameter declines with age in SOD1^{G93A} mice (33.7µm at 60 days to 21.9µm at end stage). There is a gradual decline in soma diameter in SOD1^{G93A} motor neurons, which becomes significant at 120 days (23.5µm in SOD1^{G93A} mice, to 30.9µm in B6 controls) and end stage (21.9µm in SOD1^{G93A} mice, to 33.9µm in B6 controls, *=p<0.05, **=p<0.01, respectively, as tested by 2way ANOVA). The longest diameter across the soma of every ChAT+ve ventral motor neuron was measured from two lumbar sections per mouse, in every B6 and SOD1^{G93A} mouse (see figure 6.2.14b for measuring method). By the end stage of the disease, the remaining ChAT +ve motor neurons are approximately 35% smaller in soma diameter than that of the healthy B6 motor neurons.

Table 6.3 The following table shows the number of motor neurons expressing; p75NTR only, p75NTR and cleaved caspase 3 concurrently, total p75NTR positive neurons and percentage of p75NTR motor neurons expressing cleaved caspase 3, from 4 SOD1^{G93A} mice lumbar spinal cords between the ages of 100-140 days.

SOD1 ^{G93A} mouse age	p75NTR only	p75NTR + cleaved caspase 3	Total p75NTR+ve motor neurons	% of p75NTR with cleaved caspase 3
100	0	120	120	100
110	0	118	118	100
120	50	80	130	61.5
End stage	23	65	86	75.6
Total	73	383	454	84.4

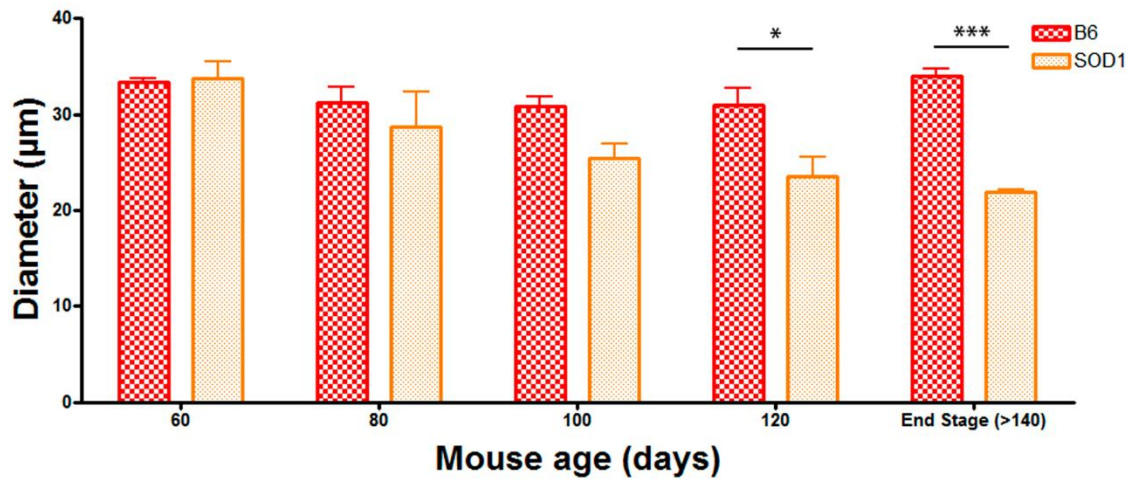


Figure 6.2.14a SOD1^{G93A} mouse motor neurons decrease in diameter over time compared to B6 age matched controls

The average soma diameter (µm) of ChAT+ve neurons in the lumbar region of SOD1^{G93A} mice and B6 age matched controls between 60-140+ days were measured and compared. There is a gradual decline in soma diameter in SOD1^{G93A} motor neurons, which becomes significant at 120 days and end stage (*=p<0.05, **=p<0.01, respectively). Two sections from each animal were taken and every ChAT +ve cell in the ventral horn had its soma width measured using imageJ (see figure below)(n=4 per strain, per age).

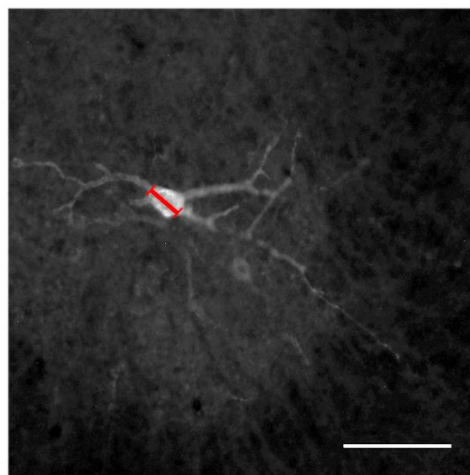


Figure 6.2.14b Example of measuring the soma width of a motor neuron

The longest diameter of each neuron (red line) was measured using imageJ (scale bar 100µm)

6.2.13 *Motor neuron area decreases during disease in the SOD1^{G93A} mouse*

An analysis of soma area was also undertaken in order to determine if motor neuron soma area changed in SOD1^{G93A} mice as they aged. Figure 6.2.15a shows that there is an overall reduction in motor neuron soma area in SOD1^{G93A} mice (718.4 μm^2 at 60 days to 418.8 μm^2 at end stage). By 80 days of age, the soma area of the ChAT +ve motor neurons in the lumbar region of SOD1^{G93A} mice shows minimal reduction. By 100 days, the reduction in area is significant (495.2 μm^2 in SOD1^{G93A} mice compared to 757.5 μm^2 in B6 controls, $p < 0.001$, as tested by 2way ANOVA). By 120 days (431.2 μm^2 SOD1^{G93A}, 636.9 μm^2 B6 control) and at end stage of the disease (418.8 μm^2 SOD1^{G93A}, 632.3 μm^2 B6 control), the area between the two strains are still significantly different. The B6 control mice had a small decrease in soma area as they aged, however the reduction in size was not as severe as in the SOD1^{G93A} mice. Figure 6.2.15b shows the procedure used to measure motor neuron soma area.

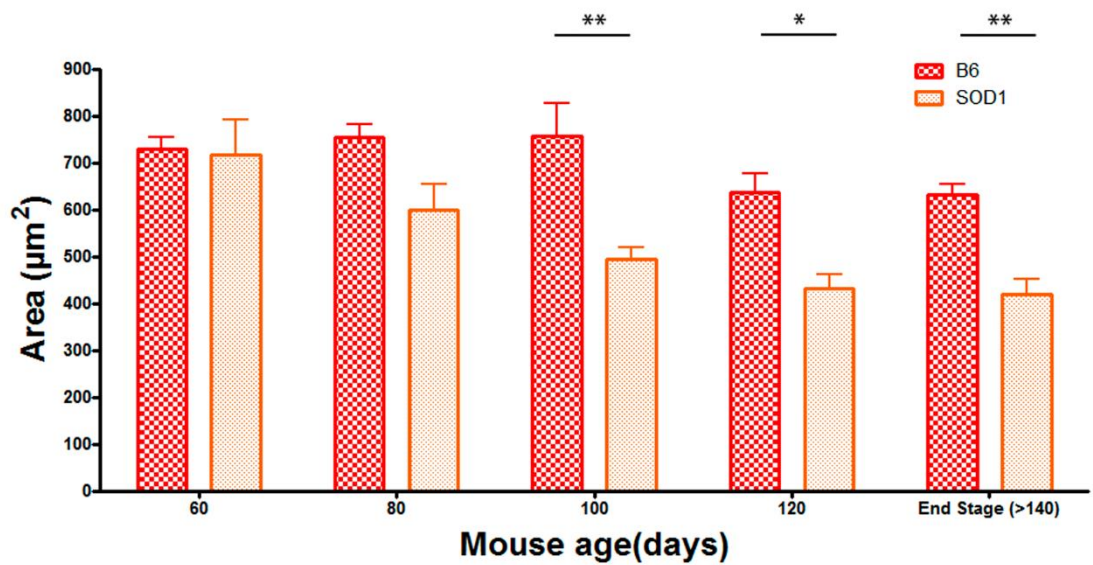


Figure 6.2.15a SOD1^{G93A} mouse motor neurons decrease in area over time compared to B6 age matched controls

The average soma area (µm²) of ChAT+ve neurons in the lumbar region of SOD1^{G93A} mice and B6 age matched controls between 60-140+ days were measured and compared. There is a small decrease in soma size at 80 days, which becomes significant by 100 days and continues through 120 days and end stage (*=p<0.05, **=p<0.01) Two sections from each animal were taken and every ChAT +ve cell in the ventral horn had its area measured using imageJ (see below). (n=4 per strain, per age)

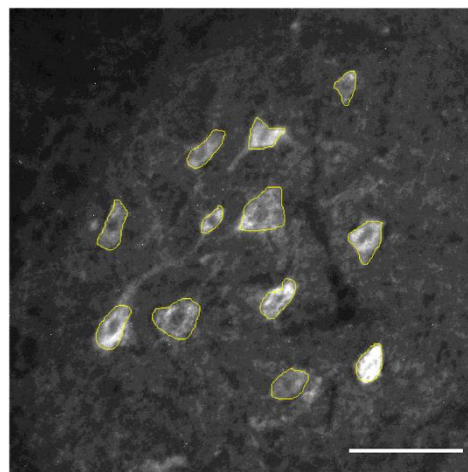


Figure 6.2.15b Example of measuring the area of a motor neuron

The total soma area of each neuron (yellow lines) were measured using imageJ (scale bar 100µm).

6.2.14 *Motor neuron diameter and area decline are correlated in SOD1^{G93A} mice*

As previously shown, both the overall diameter and area of motor neurons in the lumbar region of the SOD1^{G93A} mice decrease in size over the disease course. To determine whether there is a correlation between the area and diameter, the results from these two parameters were plotted against each other and analysed. Figure 6.2.16 shows that diameter and area are strongly correlated ($R^2 = 0.828$), with a Pearson's $r = 0.91$ and a significance $p < 0.001$. As there is a strong relationship between the diameter and the area, only the motor neuron area is investigated in the subsequent results.

6.2.15 *Frequency distribution of soma area in SOD1^{G93A} mice indicates motor neuron shrinkage over time*

It was previously shown that p75NTR positive motor neurons are larger than p75NTR negative neurons in SOD1^{G93A} mice, however it is unclear if the motor neurons are shrinking with disease progression, or if the larger alpha motor neurons are dying leaving smaller gamma neurons, or both. The size data of p75NTR negative motor neurons from Figure 6.2.15 were plotted as a percentage frequency distribution histogram (Figure 6.2.17) to determine if motor neuron area is changing dynamically over time. Motor neurons from SOD1^{G93A} mice and B6 controls were allocated into size groupings from 200-1100+ μm^2 , at 100 μm^2 increments (200-300 μm^2 , 300-400 μm^2 , 400-500 μm^2 , etc.), with each size bin representing a percentage of the total number of motor neurons for each

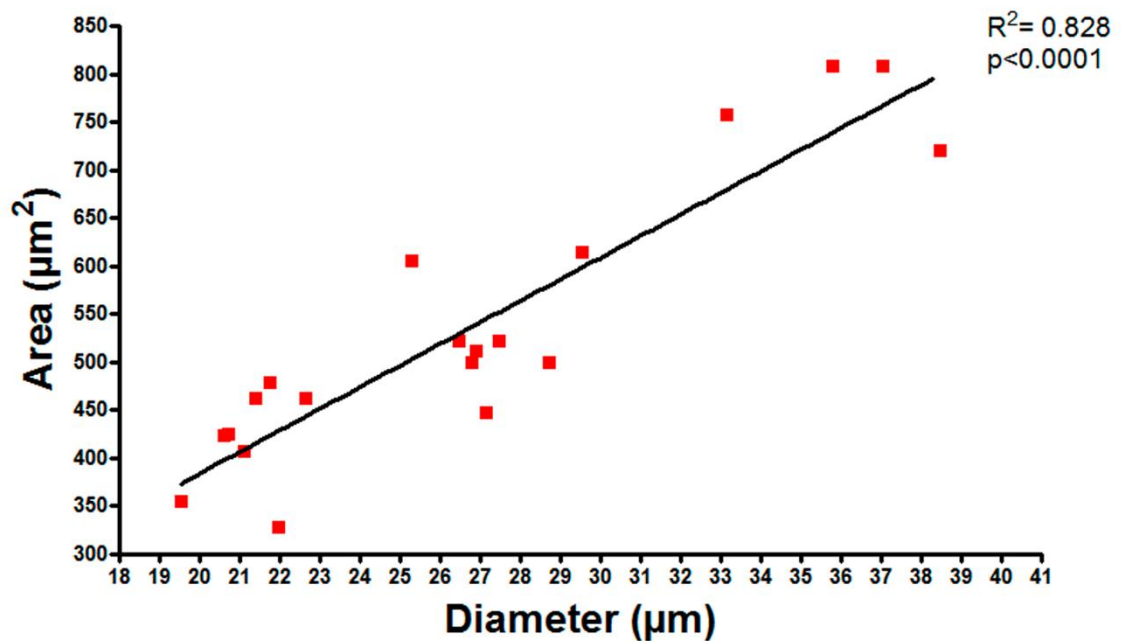


Figure 6.2.16 Soma area decline is highly correlated with diameter decline in lumbar motor neurons of SOD1^{G93A} mice

Graph showing the correlation between soma area and diameter from ventral motor neurons in the lumbar region of the SOD1 mouse. Each point represents the average diameter/area of motor neurons from one mouse. As can be seen, the two parameters for measuring cell size are strongly correlated ($R^2 = 0.828$), with a Pearson's $r = 0.91$ and a significance $p < 0.0001$.

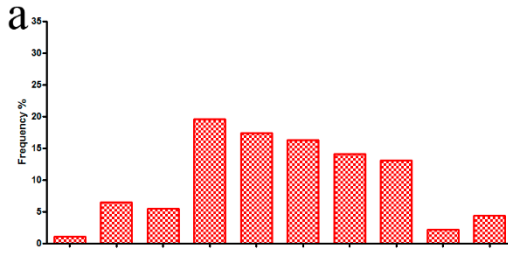
Figure 6.2.17 Frequency distribution as a percentage of soma area in SOD1^{G93A} mice and B6 age matched controls.

Histograms representing the frequency distribution as a percentage of motor neuron area in SOD1^{G93A} and B6 mice. a-e show soma area distribution from 60-140days in the B6 mice. f-j show soma area distribution from 60days-end stage in the SOD1^{G93A} mouse. At 60 days of age, the difference in distribution between SOD1^{G93A} (f) and B6 (a) is not significant ($p=0.255$). By 80 days, the distribution of motor neurons in the SOD1^{G93A} mice changes to favour motor neurons $<800\mu\text{m}^2$, which is significantly different to the B6 motor neuron distribution (b) ($***p<0.0001$). The increase in smaller sized neuron area and decrease in larger sized neuron area continues in the 100 day (h) and 120 (i) day old mice, with significant differences in the distribution to their respective B6 controls (c, d. $***p<0.0001$). At the end stage of the disease, there is still a significant difference in soma area between SOD1^{G93A} (j) and B6 (e) mice motor neuron are distribution ($***p<0.0001$), with a heavy weighting of motor neurons in the smaller sizes ($<400\mu\text{m}^2$) in SOD1^{G93A} mice (j).

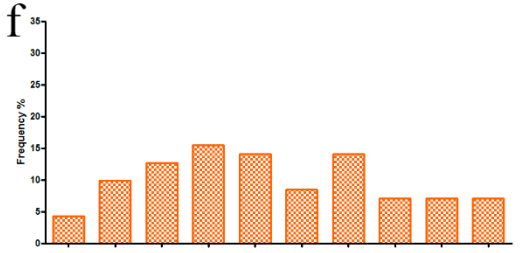
B6

SOD1^{G93A}

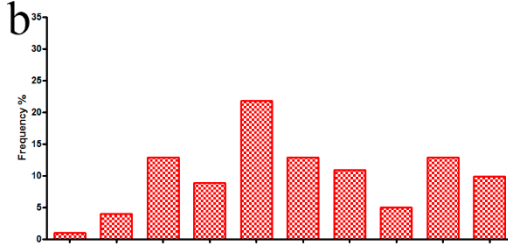
60 days



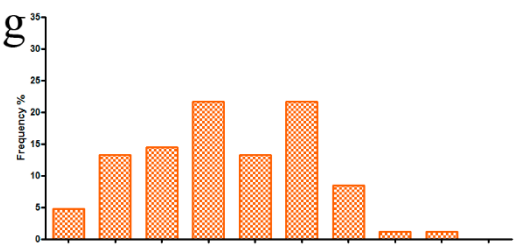
f



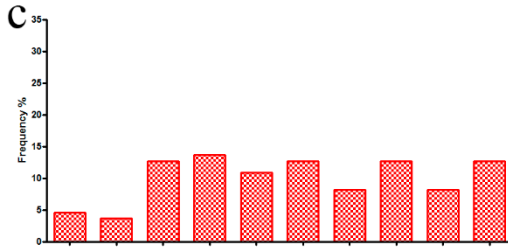
80 days



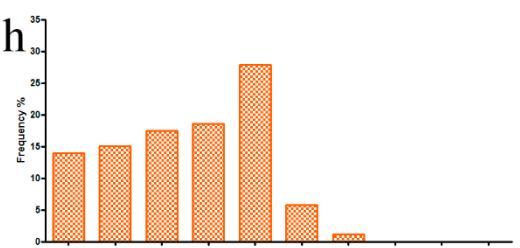
g



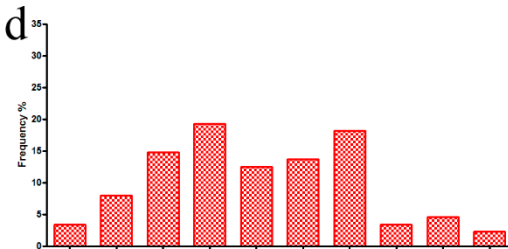
100 days



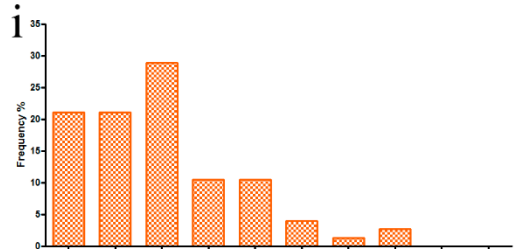
h



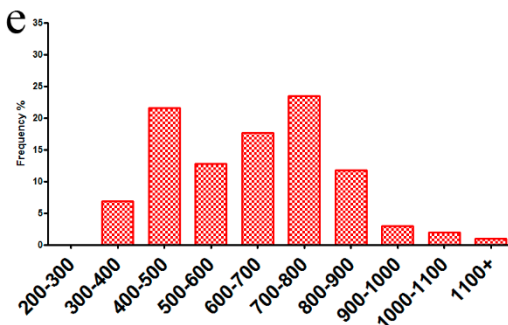
120 days



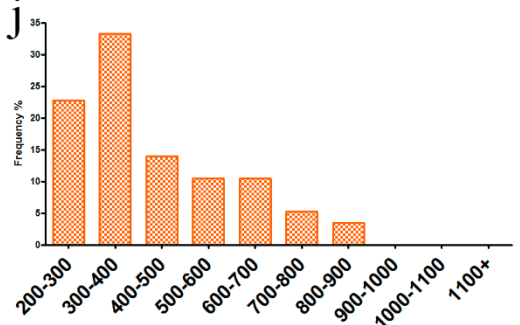
i



End stage/
(>140 days)



j



Area (μm²)

age/strain. B6 mice show an even distribution of motor neuron soma area from 60 to 100 days, with no apparent variation in size. At 120 days there is a decrease in the number of large area neurons ($>900\mu\text{m}^2$). This loss of large area sized neurons is also present in 140+ day old control mice.

SOD1^{G93A} mice has a similar distribution to B6 control, with no statistical difference determined by a chi-squared analysis at 60 days. By 80 days, there is a loss of motor neurons $>800\mu\text{m}^2$ (from 35.2% at 60 days, to 10.8% at 80 days) and an increase in neurons $<800\mu\text{m}^2$. From 100 days to 120 days to end stage (140+ days), there is a continued loss of larger sized motor neurons ($>700\mu\text{m}^2$), however there is also an increase in the percentage of motor neurons $<600\mu\text{m}^2$. A chi-squared analysis shows from 80 days to end stage, there is a difference in the distribution of motor neuron soma area of SOD1^{G93A} mice compared to B6 ($p<0.0001$). The percentage of motor neurons that are between 200 and $300\mu\text{m}^2$ in SOD1^{G93A} mice increases from 4.2% at 60 days to 22.8% at end stage, while the percentage of neurons in the B6 that are between 200 and $300\mu\text{m}^2$ remains less than 5% between 60-140 days.

6.2.16 *Primary processes on p75NTR positive motor neurons are not affected by age*

Every motor neuron that was p75NTR positive in SOD1^{G93A} mouse was analysed for 'primary processes' number, at each age (60-140 days). A 'primary processes' was determined as a process that was attached directly to motor neuron cell soma (Figure 6.2.18b). The average number of processes ranged from 2.35-3.1 processes per p75NTR positive motor neuron, with no significant difference seen

between ages (Figure 6.2.18a), as tested by 2way ANOVA. This analysis showed that the average number of primary processes on a p75NTR+ve neuron is independent of the age of the animal. Due to the ChAT antibody not staining the processes, the average number of primary processes for p75NTR-ve neurons was unable to be collected.

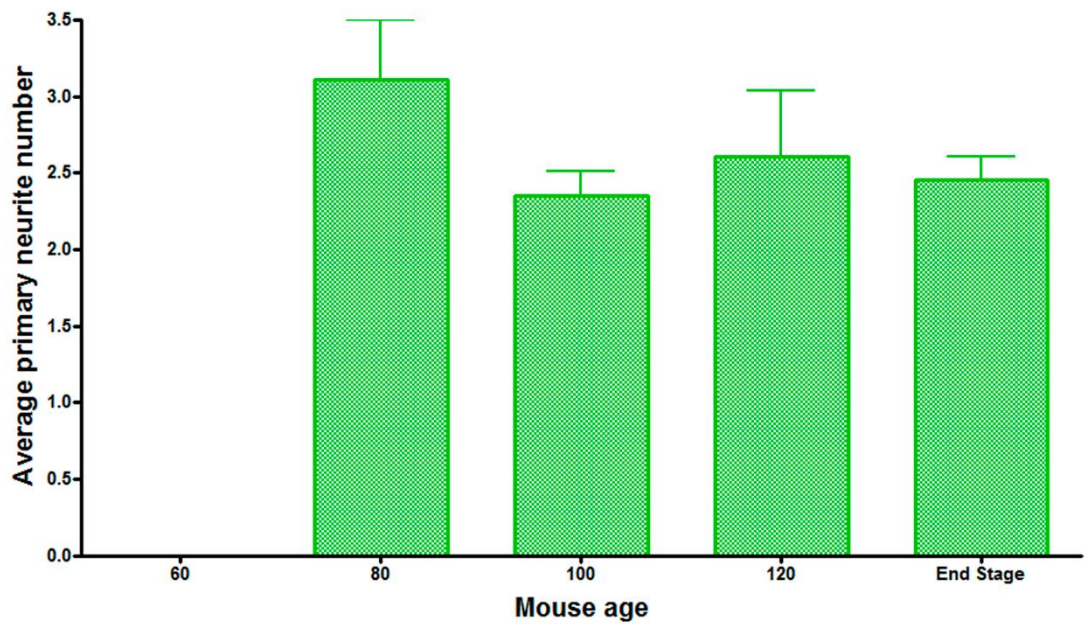


Figure 6.2.18a Number of primary processers on p75NTR positive neurons in SOD1^{G93A} mice do not change with age

The average number of primary processers connected directly to the soma of all p75NTR +ve motor neurons were counted in SOD1^{G93A} mice, from 60-140+ days. There is no significant difference between the number of primary processers at any age, which range from 2.35-3.1 neurites/motr neuron soma (n=4 per strain, per age).

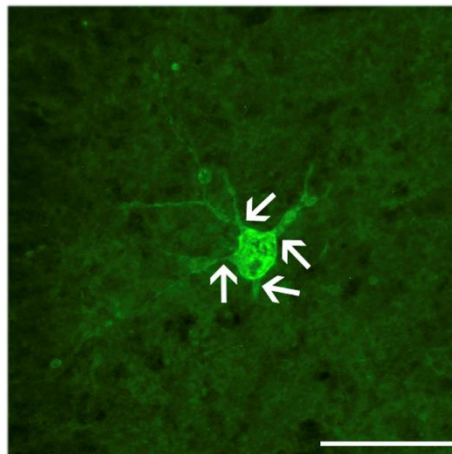


Figure 6.2.18b Example of primary processers on a p75NTR positive motor neuron

The arrows point to 'primary' processer; processers that connect directly to the soma. Note, the top arrow points to a processer that splits in two, however this is counted as one, as they spilt off the same primary trunk. (scale bar 100um)

6.3 Discussion

This study aimed to establish an expression profile of p75NTR, by measuring the number of ventral motor neurons within the lumbar spinal cord of the high copy number SOD1^{G93A} mouse which express p75NTR, and if they are able to be targeted by antibody injections into the periphery. This has a potential for therapeutic targeting (Barati et al., 2006; Rogers et al., 2014; Rogers and Rush, 2012), by using the immunogene described in the last chapter. Morphological and biochemical attributes of these p75NTR motor neurons were also investigated. The purpose of tracking the morphological changes in the SOD1^{G93A} mouse is to add to the database of pathological changes seen as ventral motor neurons become affected by the disease. The disease dynamics within the G1H high copy number SOD1^{G93A} mouse are significantly different to the G1L low copy number strain. The influence of SOD1^{G93A} expression levels produced by the number of mutant SOD1^{G93A} genes creates a more severe phenotype at an earlier age in the GIH compared to G1L mice, even though they have similar end stage pathologies. For example, end-stage disease in the G1H is ~140 days, whereas in the G1L mice is ~300 days (Turner & Talbot, 2008). The expression levels may also extend to other differences, including p75NTR expression, apoptotic marker expression and motor neuron morphology. Documentation of this process is essential for understanding underlying disease mechanisms.

6.3.1 Targeting of p75NTR positive motor neurons after peripheral injections

In chapter 4, neonatal mice were injected with the anti-p75NTR MLR2 antibody, conjugated to a fluorescent tag (ATTO-488). Those results showed the MLR2-ATTO-488 was able to bind to and be retrogradely transported to most motor neurons in the spinal cord. As the immunogene technology has a goal as a therapeutic for MND, it is important to determine if the conjugated antibody is able to reach p75NTR expressing motor neurons in the adult SOD1^{G93A} mouse. This is vital, as the hypothesis for the immunogene is binding of the complex to the p75NTR receptor on the cell surface, and subsequent retrograde transport of the cargo. If the immunogene is leaking into the central nervous system through a ‘not fully developed’, or most likely, fragile blood brain barrier being disrupted by high volumes of injectant (Saunders, Joakim Ek & Dziegielewska, 2009), then it would not be applicable to adult, fully developed animals. While intraperitoneal injections of anti-p75NTR MLR2-ATTO-488 was able to reach spinal motor neurons in SOD1^{G93A} mice, interestingly, not all p75NTR motor neurons were targeted by the MLR2-ATTO-488, and conversely, not all MLR2-ATTO-488 positive motor neurons expressed p75NTR. This mismatch in expression/targeting may be because of a short expression time of p75NTR based on the mechanisms of cell, mentioned by Copray et al., which is addressed in the next chapter or down-regulation of p75NTR to levels too low to be seen immunohistochemically. p75NTR is retrogradely transported to the soma after binding of neurotrophins, such as BDNF (Curtis et al., 1995; Deinhardt et al., 2007; Johnson et al., 1987; Lalli and Schiavo, 2002), which can be mimicked with the use of functional

antibodies, including the MLR2 antibody (Rogers et al., 2014). As such, injection of the anti p75NTR MLR2-ATTO-488 was able to be retrogradely transported to motor neuron somas after intraperitoneal injection and revealed two important features of these p75NTR expressing motor neurons. Firstly, the antibody binds to p75NTR at the neuromuscular junction, and these motor neurons are still connected to their target muscle fibres to some degree. Secondly, it has been found that there is axonal trafficking problems in SOD1^{G93A} motor neurons, including retrograde transport in SOD1^{G93A} mice (Kanning et al., 2010; Ligon et al., 2005; Perlson et al., 2009) and cultured motor neurons carrying the mutant SOD1 gene (De Vos et al., 2007; Kieran et al., 2005), yet motor neurons in these 110 day old mice still have the ability to retrogradely transport cargo to the soma. Intriguingly, p75NTR cleavage fragments (~25kD fragments, most likely the signalling intracellular domain) have been shown to have increased transport in these mice (Perlson et al., 2009), showing an active p75NTR metabolism is still present.

6.3.2 *Anti-p75NTR MLR2 is transported to p75NTR positive DRG neurons*

Many sensory neurons within DRG express p75NTR (Carroll, Silos-Santiago & Frese, 1992; Wright & Snider, 1995), and in chapter 5, the immunogene was able to deliver GFP expressing cargo to p75NTR positive DRG neurons. In adult mice, the MLR2-ATTO-488 antibody was also able to target and be transported to p75NTR positive DRG neurons and fibres. As this is an off-target cell type, caution must be undertaken when delivering genetic material, in case of

disruption of normal cell behaviour. However, it may also be useful in targeting these particular cell types for other applications.

6.3.3 Neuronal loss and p75NTR expression

The primary region of disease onset within the spinal cord of SOD1^{G93A} mice is within the lumbar alpha motor neurons (Gurney *et al.*, 1994; Mohajeri *et al.*, 1998), where this research has been focused. The disease dynamics within the GIH high copy number SOD1^{G93A} mouse are considerably different to the G1L low copy number strain. The influence of SOD1^{G93A} expression levels produced by the number of mutant SOD1^{G93A} genes produces a more severe phenotype at an earlier age in the GIH compared to G1L mice, even though they have similar end stage pathologies. For example end-stage disease in the GIH mice is ~140 days, whereas in the G1L mice is ~300 days (Turner & Talbot, 2008). p75NTR expression levels may be influenced by the difference in strains. Also, the difference between this study and Copray and colleagues (Coprpy *et al.*, 2003) may be because of the different backgrounds used. This study used the female C57BL/6J, while Copray and colleagues used the female FVB background and it has shown that background for the SOD1^{G93A} mouse can heavily influence pathophysiology (Heiman-Patterson *et al.*, 2005).

A significant loss of motor neurons begins by age 80 days in SOD1^{G93A} mice. It was previously reported that significant motor neuron loss occurs at 98 days, but not 70 days (Martin *et al.*, 2007). At around this age, these transgenic mice have been reported to develop an abnormal gait (Wooley *et al.*, 2005).

The loss of motor neurons, while not statistically significant, appears to start before day 60. Vinsant et al (2013) found that motor neuron pathologies occur much earlier than actual motor neuron loss. They showed that between 44-60 days is when the initiation of motor neuron degeneration occurs in SOD1^{G93A} mice, which agrees with the data presented here (Vinsant *et al.*, 2013). By disease end stage, 50% of the total motor neuron pool is lost, confirming previous findings with this transgenic mouse (Chiu et al., 1995; Kanning et al., 2010).

Seeburger et al. (1993) were first to report the re-expression of p75NTR in the spinal motor neurons of patients with MND using *in situ* hybridization (Seeburger *et al.*, 1993). p75NTR was later found immunohistochemically in the motor neurons of the lumbar region of SOD1^{G93A} mice and also in MND patient spinal cord tissue (Lowry et al., 2001).

As p75NTR is commonly referred to as a cell death receptor, it has been investigated in potentially influencing motor neuron cell death in MND. Previous work has shown that antisense DNA inhibition of p75NTR expression can cause a slight delay in symptoms and increase in lifespan for SOD1^{G93A} mice (Turner et al., 2003). Interestingly, SOD1^{G93A} mice crossed with p75NTR^{exonIII} knockout mice (exon III of the p75NTR gene is responsible for the extracellular neurotrophin binding domains (Lee et al., 1992; von Schack et al., 2001)) slightly decreased symptom onset and increased lifespan in female mice only (Kust et al., 2003). However, p75NTR antagonists that block neurotrophin binding do not have any effect on symptoms or life span when administered to SOD1^{G93A} mice (Turner et al., 2004). This coupled with the fact that motor neuron loss and pathology occurs before the expression of p75NTR implies that p75NTR is not

directly involved with/initiates the cell death pathway in the SOD1^{G93A} mouse, but is instead expressed as a by-product of motor neuron health.

In the study undertaken by Copray et al. (2003), where they investigated p75NTR expression over time in SOD1^{G93A} G1L mice using *in situ* hybridization and immunohistochemistry, they found a low (~10%) number of motor neurons that expressed p75NTR. Their mouse model was the less-used SOD1^{G93A} G1L mouse and FVB background. The G1L strain has a low copy of the mutant human SOD1^{G93A} gene (8 ± 1.5 copies), whereas the more commonly used SOD1^{G93A} G1H line has a higher copy number of the mutant gene (25 ± 1.5 copies) (Gurney et al., 1996), and is the accepted model to use for pre-clinical trials. Copray et al. (2003) examined p75NTR expression at three ages in the 4th lumbar segment of the spinal cord in SOD1^{G93A} G1L mouse. The three ages used (early pre-symptomatic 10 weeks, late pre-symptomatic 20 weeks, and symptomatic 30 weeks) does not cover the entire lifespan (missing end stage).

According to the data found here in the G1H strain, the highest percentage of p75NTR expressing motor neurons is at end stage. However, this is a ratio of p75NTR+ve neurons to total motor neurons, meaning that while the highest percentage of p75NTR+ve motor neurons are at end stage, there are a much lower number of these neurons overall. This indicates that p75NTR is expressed more rapidly at end stage, as overall there are less motor neurons present (~50% compared to healthy controls).

Although there was motor neuron loss before 80 days, p75NTR was not detectable immunohistochemically before that time, indicating that the loss of motor neurons is not dependent on the expression of p75NTR, rather the

expression is a consequence of the disease. In contrast, the contribution that p75NTR makes to neuronal death is much higher in injury or axotomy models where reduction of p75NTR expression has a significant positive effect on motor neuron survival (Ferri et al., 1998).

6.3.4 *Motor neurons are larger when they re-express p75NTR*

An interesting characteristic seen in SOD1^{G93A} mouse motor neurons is that p75NTR expression coincided with an increased soma area. Intriguingly, p75NTR positive neurons were comparable in soma area to that of the healthy B6 motor neurons. p75NTR+ve motor neurons in the SOD1^{G93A} mouse were on average 1.1-1.9x larger than their p75NTR-ve SOD1^{G93A} mouse counterparts. In fact, p75NTR-ve motor neurons became significantly smaller as SOD1^{G93A} mice aged. p75NTR expressing motor neurons being larger than neighbouring non-p75NTR motor neurons has been briefly mentioned before (Pehar et al., 2004). The average size of p75NTR expressing motor neurons identified by immunohistochemistry (718.8µm²) or retrograde tracing (640.7µm²) suggests they are alpha motor neurons. Interestingly, Kust et al., (2003) showed SOD1^{G93A} mice crossed with p75NTR^{exonIII} knockout mice (Lee *et al.*, 1992; von Schack *et al.*, 2001) had fewer large motor neurons, agreeing with our observation that large motor neurons contain p75NTR. In contrast to this, Copray et al. (2003) described p75NTR containing motor neurons in the spinal cord of SOD1^{G93A} G1L mice as shrunken, rounded off with most of their dendrites retracted. However, the actual size of the neurons was not mentioned. Interestingly we did not find the number

of processors in p75NTR expressing motor neurons change with age in SOD1^{G93A} mice.

It is a possibility that there is a pool of larger alpha motor neurons that re-express p75NTR, or that these neurons swell in size. This increase in size is not due to an artefact of the staining procedure, as the p75NTR cellular expression profile is the same whether the neurons are counterstained after spinal cord extraction, or labelled in vivo after intraperitoneal injection (i.e. MLR2-ATTO-488).

6.3.5 *p75NTR* expressing motor neurons rarely co-express ATF-3, but co-express cleaved caspase-3

Currently, it is not known at what phase of the cell death cycle p75NTR is re-expressed in the motor neurons of SOD1^{G93A} mice, and as such, spinal cord sections were stained for p75NTR concurrently with either ATF-3 or cleaved caspase-3. ATF-3 is considered to be a stress induced transcription factor and therefore can be considered pre- or early apoptotic. It is upregulated and translocated to the nuclei during cell stress, and has been used extensively as a marker for cell stress in neurons, including motor neurons in MND (Copray et al., 2003; Hai et al., 1999; Saxena et al., 2009; Tsujino et al., 2000; Vlug et al., 2005). However, research shows conflicting results with quantifying and identifying ATF3 expression. Firstly, ATF3 gene expression appears to be related to the SOD1^{G93A} mouse background used. In studies by Vlug et al. (2005) and Nardo et al. (2013), female breeders other than C57BL/6J were used and ATF3 up-regulation was observed in symptomatic but not control mice (Vlug *et al.*, 2005; Nardo *et al.*, 2013). When C57BL/6J were used as background (Nardo *et al.*,

2013) there was little difference between SOD1^{G93A} mice and their litter mates in terms of ATF-3 gene or protein expression. More notably, ATF-3 immunohistochemistry is difficult to interpret as cytoplasmic ATF-3 is much more visible in the C57BL/6J background, making translocation of ATF-3 difficult to detect. When interpreting ATF3 expression, we scored only clear nuclear ATF-3 as a 'hit' to prevent false positives. Nevertheless, ATF-3 was not observed in C57BL/6J background mice. Interestingly, Copray et al. (2003) did not indicate if they counted ATF-3 in the nucleus or cytoplasmic ATF-3.

Cleaved caspase-3 is a classic marker for cell apoptosis (Alnemri et al., 1996; Hengartner, 2000; Martin and Green, 1995) and is commonly used for identifying dying cells, including motor neurons in MND (Coprpy et al., 2003; Li et al., 2000; Martin et al., 2007; Meyerowitz et al., 2011; Pasinelli et al., 2000; Soo et al., 2012; Vlug et al., 2005).

The results showed that the average number of ATF-3/p75NTR positive motor neurons was very low (~6%). However, this was not the case with cleaved caspase-3, where the majority (~85%) of motor neurons expressing p75NTR also expressed the apoptotic marker. This indicates that apoptosis has already been initiated in motor neurons expressing p75NTR, and that these cells are destined to die.

These findings are in contrast with Copray et al (2003) however, where they found every p75NTR expressing motor neuron to co-express ATF-3 and very little to co-express cleaved caspase-3. The variation in results seen between this study and Copray et al (2003) again appears to extend to the difference in pathologies of the G1H and G1L strains, and/or mouse backgrounds used.

6.3.6 Motor neurons that are p75NTR negative shrink in size over time in *SOD1^{G93A}* mice

It was shown that non-p75NTR expressing motor neurons decreased in size as *SOD1^{G93A}* mice aged. The data presented here shows that not only do motor neurons in *SOD1^{G93A}* mice appear smaller than B6 motor neurons, but the motor neurons are shrinking, demonstrated by a decreased percentage of larger motor neurons ($>700\mu\text{m}^2$) and an increase in percentage of smaller motor neurons ($<700\mu\text{m}^2$). The most common way of differentiating between alpha and gamma motor neurons is by using size exclusion criteria, as alpha motor neurons are larger than gamma motor neurons (Kawamura et al., 1977a; Kawamura et al., 1977b). Alpha motor neurons are on average between $600\text{-}800\mu\text{m}^2$ and gamma motor neurons are between $200\text{-}400\mu\text{m}^2$ (Friese et al., 2009; McHanwell and Biscoe, 1981; Shneider et al., 2009). As all ChAT positive neurons were counted as motor neurons in this study, both alpha and gamma motor neurons were analysed. The data shows that motor neurons $>700\mu\text{m}^2$ are lost, it is clear that these large alpha motor neurons are preferentially and heavily affected in the *SOD1^{G93A}* mouse. The 'increase' in percentage of smaller sized motor neurons is due to larger alpha motor neurons dying off and increasing the percentage of smaller sized neurons, seen in the frequency histogram. In addition to large alpha motor neurons dying, motor neuron shrinkage has been identified before, where one study showed approximately 60% less motor neurons with a diameter $>15\mu\text{m}$ in *SOD1^{G93A}* mice compared to WT controls (Kust et al., 2003) and another specifically showing significantly smaller transversus abdominus and soleus innervating motor neurons as early as P34 (Vinsant et al., 2013b).

It can be speculated that the shrinkage of the neurons is due to the denervation of target muscle fibres, which proceeds significant motor neuron loss (40-50 days) (Fischer et al., 2004; Frey et al., 2000; Kennel et al., 1996; Pun et al., 2006; Vinsant et al., 2013a). Studies have shown that partial axotomy of individual motor neurons in rats leads to an overall decrease in motor neuron size (Tyc and Vrbova, 2007) and that motor neuron size is proportional to the number of muscle fibres innervated by each motor neuron. Therefore it is possible that when the motor neurons disconnect from target muscle fibers, the cell soma reduces in size.

Although the expression of p75NTR in motor neurons is linked with disease (Copray et al., 2003; Kust et al., 2003; Lowry et al., 2001; Seeburger et al., 1993; Shephard et al., 2014; Turner et al., 2003; Turner et al., 2004) and injury (Ernfors et al., 1989; Koliatsos et al., 1991; Saika et al., 1991), the maximum number of p75NTR+ve motor neurons found was very low (less than 5%). On average in SOD1^{G93A} mice, approximately 30-35 neurons are lost per day (based on numbers of motor neuron loss over the disease course). Apoptosis happens between 4-24 hours for most cells (Saraste and Pulkki, 2000) and about 30 hours for motor neurons (facial) in mice (de Bilbao and Dubois-Dauphin, 1996). As p75NTR is only expressed in adult motor neurons that are injured or diseased, with the majority co-expressing with the apoptotic cleaved caspase-3, it can be argued that the expression time of p75NTR is short, as the apoptotic process itself happens within 24-30 hours. Therefore seeing a motor neuron expressing p75NTR can be considered rare. This idea of a short time frame of p75NTR expression has been proposed before, where it was suggested that seeing a p75NTR expressing motor neuron is a 'chance-hit' (Copray et al., 2003). These

p75NTR expressing motor neurons are most likely to be alpha motor neurons, as no small gamma-sized neurons showed p75NTR expression, and all motor neurons expressing p75NTR were in the range of healthy alpha motor neuron size (600-800 μm^2) (Friese et al., 2009; McHanwell and Biscoe, 1981).

While the expression of p75NTR appeared low in SOD1^{G93A} mice, interestingly the neurons that expressed p75NTR displayed altered morphological and biochemical markers. The expression of p75NTR in motor neurons of adult SOD1^{G93A} mice appears to coincide with extreme changes in morphology and cell death. Intervening or targeting p75NTR motor neurons in SOD1^{G93A} mice for a therapeutic may not lead to positive results, as these neurons are already undergoing apoptosis and the time at which p75NR expression is highest, many alpha motor neurons have already been lost or have potentially denervated significantly, as shown by their shrunken appearance.

While investigating ChAT expressing ventral motor neurons in SOD1^{G93A} mice and age matched controls, differences were seen in V0_C interneurons – the second and only other ChAT expressing spinal cord neuron.

Chapter 7: Quantification of
the V0_C interneurons
in SOD1^{G93A} mice

7.1 Introduction

Ventral motor neurons within the spinal cord express the enzyme choline acetyltransferase (ChAT). There is however, a second distinct population of ChAT expressing interneurons. These neurons surround the central canal (Laminar X) and are named the V_{0C} interneurons (also known as central canal cluster cells). V_{0C} interneurons were first described in 1984 by Barber and colleagues while mapping out the distribution and morphology of ChAT expressing cells in the rat spinal cord (Barber et al., 1984). Since their discovery in 1984, V_{0C} interneurons have been described as multi- or bi-polar, have processes that extend toward both dorsal and ventral horns, are positive for nitric oxide and are thought to be a relay between the sensory and motor areas of the spinal cord (Borges & Iversen 1986; N. Dun et al. 1992; Zagoraiou et al. 2009). In the B6 mice, ventral motor neurons average ~35µm in diameter, and have an area of ~700µm² (See chapter 7), while V_{0C} interneurons are smaller, with a diameter averaging ~16µm and an area of ~200µm². These neurons usually exist in small clusters, with some clusters consisting of 15 or more cells. There are fewer of these neurons in total compared with the total number of ventral motor neurons, with the best estimate being about 10% in comparison (Zagoraiou *et al.*, 2009).

The function and role of V_{0C} interneurons are sporadically investigated, but more consistent information is gradually emerging. Importantly, V_{0C} interneurons are known to be the exclusive origin of C boutons, with approximately 80 – 100 endings per neuron, making them the largest and most prominent terminating nerve endings found on ventral motor neuron (Miles *et al.*, 2007; Zagoraiou *et al.*, 2009). The boutons are only found to terminate on the soma and proximal

dendrites of the ventral motor neurons and contain very high levels of ChAT in the presynaptic terminal, making them very easy to identify by immunohistochemistry (Nagy, Yamamoto & Jordan, 1993; Li *et al.*, 1995). Based on previous studies, V0_C interneurons have been classed as pre-motor interneurons, playing a role in locomotion by modulating motor neuron firing and influencing overall motor programs. During locomotion, these neurons have been shown to be activated and fire at a rhythmic pace. The targets (muscle fibres) of the motor neurons innervated by these rhythmically firing V0_C interneurons show the same periodic activation (contractions). That is, the V0_C interneurons, their innervated motor neuron, and the motor neuron skeletal muscle target are all ‘tightly phase locked’ in activity (Huang *et al.*, 2000; Zagoraïou *et al.*, 2009).

C boutons, until recently discovered to be exclusive to V0_C interneurons, have been shown to be affected in MND, particularly in regards to the decrease in VAcHT production (Nagao *et al.*, 1998). Changes in C boutons also extend to SOD1^{G93A} mice, with an increase in size as the disease progresses (Pullen & Athanasiou, 2009) and by end stage, are significantly reduced in number (Chang & Martin, 2009). Intriguingly, a recent study showed that C boutons only increase in size in the male SOD1^{G93A} mouse, with no difference being detected in the female (Herron & Miles, 2012). Recently, another mouse model of MND has arisen based on a mutation in a membrane-vesicle protein (P56S VAPB), causing a translocation of this protein in C boutons, which is thought to affect vesicle release in these cells (Aliaga *et al.*, 2013).

Examination of V0_C interneurons in SOD1^{G93A} mice is absent from the literature, which is surprising considering these neurons are the sole source of C boutons, which are known to be affected in MND and SOD1^{G93A} mice. In this final

chapter, changes in $V0_C$ interneuron number were studied over the course of the disease.

7.2 Results

7.2.1 *V0_C interneuron number are decreased in SOD1^{G93A} mice*

V0_C interneurons are ChAT+ve cells located around the central canal throughout the spinal cord (Figure 7.2.1). These cells can be easily distinguished from the ventral motor neurons by their size and position. In parallel with counting the ventral motor neurons, V0_C interneurons were also quantified in the SOD1^{G93A} mouse and compared to B6 controls (Figure 7.2.2a). There was an overall loss of V0_C interneurons in SOD1^{G93A} mice compared to the B6 controls, although the loss of cells is not statistically significant at any specific age, shown by two way ANOVA ($p>0.05$). However, when the strains were compared regardless of age (total cell number comparison), the SOD1 mutation was shown to have a significant effect on the V0_C cell number ($p=0.003$). This reduction does not correlate with disease progression as age does not have an effect on cell number ($p>0.05$), as seen in figure 8.2.2b. The average percentage loss (16.3%) is very similar across the age of the mice, with no trend either positive or negative, towards end stage for each strain (SOD1^{G93A} or B6) remaining approximately the same.

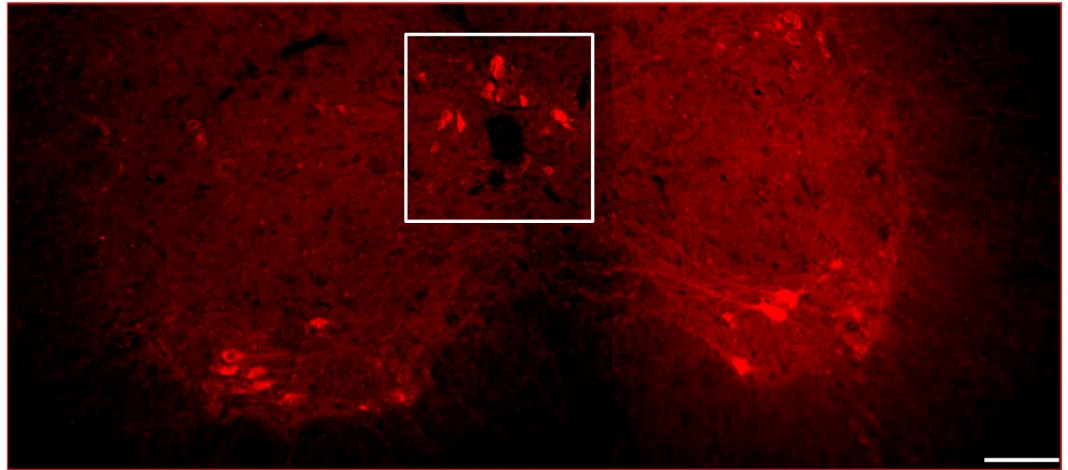


Figure 7.2.1 $V0_c$ interneurons strongly express ChAT

$V0_c$ interneurons are small diameter, ChAT +ve neurons that are not located in the ventral horn (laminar VIII, IX), but are seen around the central canal (laminar X). The highlighted area shows a group of $V0_c$ interneurons surrounding the central canal. They are rarely seen in isolation and usually found in clusters, which can reach more than 15 (scale bar 100 μ m).

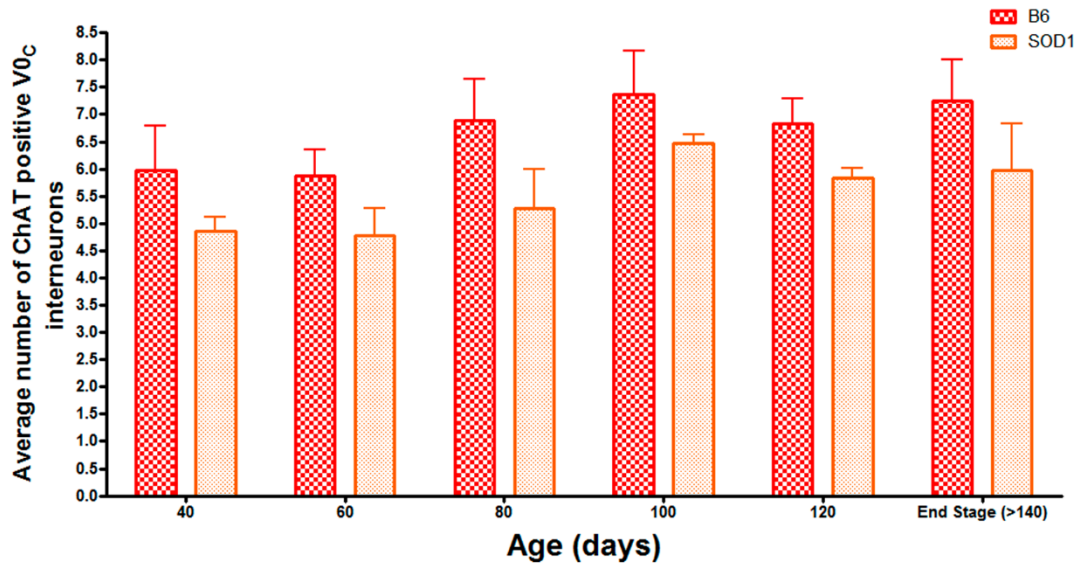


Figure 7.2.2a Comparison of V0_c interneuron counts between SOD1^{G93A} and B6 age matched controls

V0_c interneurons located by ChAT expression were counted in SOD1^{G93A} mice and B6 age matched controls, from 40-140+ days. There is a lower number of V0_c interneurons in the SOD1^{G93A} mouse compared to B6 controls at all ages, however this difference is not statistically significant (n=4 per strain, per age)

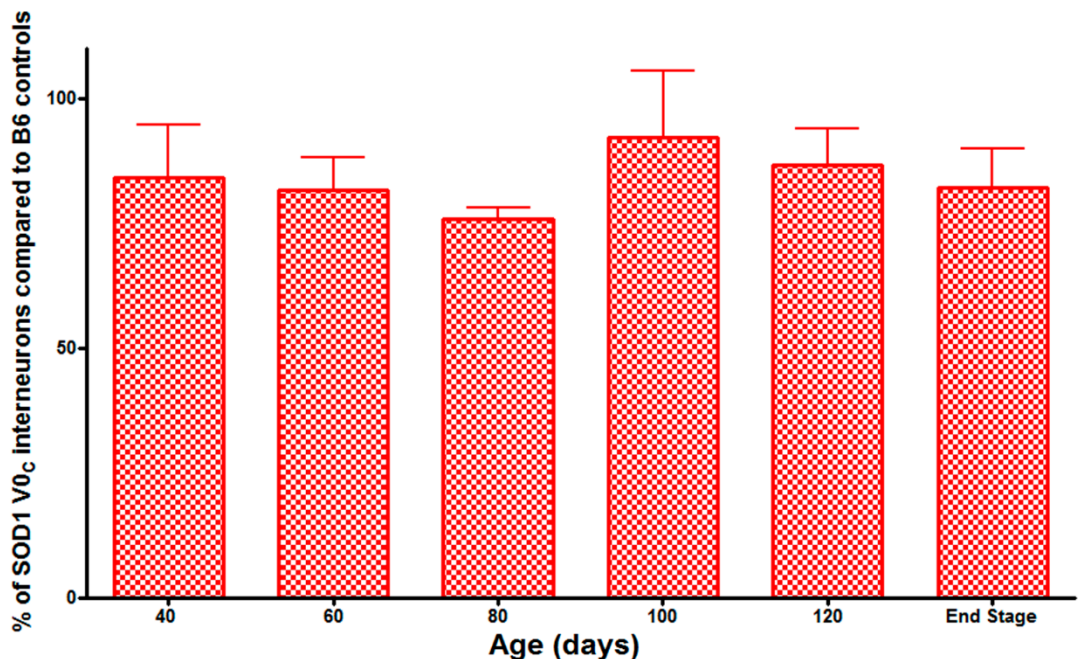


Figure 7.2.2b V0_c interneurons from SOD1^{G93A} mice as a percentage of B6 age matched controls

V0_c of SOD1^{G93A} mice as a percentage of B6 age matched controls, from 40-140+ days. As the SOD1^{G93A} mouse ages, the average number of V0_c interneurons does not increase/decrease. However across all ages, there is an average of 16.3% less V0_c interneurons in the SOD1^{G93A} mouse compared to B6 controls (n=4 per strain, per age)

7.3 Discussion

The second population of ChAT positive cells in the spinal cord, the V0_C interneurons, have not been thoroughly investigated, even though they were first documented over 30 years ago (Barber *et al.*, 1984). Compared to ventral motor neurons, they are about half to a third smaller and about 10x less in number (Zagoraiou *et al.*, 2009). Even though there is a lack of information on V0_C interneurons, what is known is they are pre-motor interneurons that play roles in locomotion, modulate motor neuron firing and influence overall motor programs (Huang *et al.*, 2000; Zagoraiou *et al.*, 2009). As these cells are involved with the motor system, surprisingly they are rarely investigated in regards to motor neuron ailments, such as MND, even though a loss or impairment of these cells causes a reduction in muscle recruitment during swimming and to a lesser extent walking (Zagoraiou *et al.*, 2009). Their terminations on motor neurons, C boutons, have been looked at in detail in MND (Nagao *et al.*, 1998; Pullen & Athanasiou, 2009; Herron & Miles, 2012; Aliaga *et al.*, 2013; Witts, Zagoraiou & Miles, 2014).

This study, although small, has shown that in SOD1^{G93A} mice there is slight loss of these important V0_C interneurons. However, the loss is not affected by time. This shows that the loss of these cells occurs before 40 days of age or even at birth, which may account for the early problems seen in these mice before the massive loss of motor neurons during the disease state. Other studies have shown that interneurons in general are lost in both human MND spinal cords (Oyanagi, Ikuta & Horikawa, 1989; Terao *et al.*, 1994; Stephens *et al.*, 2006) and the SOD1^{G93A} mouse spinal cords (Martin *et al.*, 2007) and cortex (Minciacchi *et al.*, 2009), which would include V0_C interneurons. In the SOD1^{G93A} mouse, large

interneuron loss occurs around 40 days of age, with a rapid decline to about 60 days, where the loss plateaus (Martin *et al.*, 2007). Of the V0_C interneuron terminals, the C boutons, loss (Chang & Martin, 2009) and then subsequent enlargement (Pullen & Athanasiou, 2009; Herron & Miles, 2012) suggests a compensatory mechanism exhibited by these cells when damaged. This loss of the C boutons is most likely due to the overall reduced number of V0_C interneurons in the SOD1^{G93A} mice. The C boutons are also larger in size long before symptoms (Herron & Miles, 2012) and the loss of the V0_C interneurons (before day 40) is evident even before significant neuron loss (day 80). As these interneurons are affected in MND, perhaps the V0_C interneurons play a much larger role in the disease overall than previously thought, considering they are the biggest relay to ventral spinal motor neurons and may receive synaptic input from descending tracts from upper motor neurons (Zagoraiou *et al.*, 2009; Witts *et al.*, 2014). Further investigation into the timing of V0_C interneuron loss may elucidate whether these neurons have a crucial role to play in the disease of this animal and/or human MND.

Chapter 8: Conclusions and Future Directions

Chapter 8

Accessing neurons in the CNS, including motor neurons in MND, is a problematic process for any potential therapeutic due to the highly protective nature of the blood brain barrier. The difficulty is increased when the potential therapeutic is a non-viral gene delivery agent that must overcome the four barriers of successful gene delivery; DNA condensation and avoidance of immune system surveillance, cell specificity and retrograde transport, endosomal escape, and nuclear translocation. Experiments utilising the MLR2 immunogene (MLR2-PEI-PEG12-pVIVO2-GFP/LacZ) have shown that it has the capability to access spinal motor neurons and overcome these four barriers.

This is the first study to show that a large complex (the immunogene) injected into the periphery is able to be retrogradely transported within spinal motor neurons in the CNS, bypassing the blood brain barrier and delivering pDNA. The MLR2 immunogene has shown that in neonatal mice expressing p75NTR in over 90% of their spinal motor neurons, approximately 20% can be successfully transfected and visualised by GFP expression, with just two single injections.

However, the use of the MLR2 immunogene as a treatment for adult MND patients appears to be of limited value due to the low number of p75NTR expressing motor neurons seen in adult SOD1^{G93A} mice. In addition, these p75NTR-expressing neurons only express p75NTR for a short period of time, and appear destined to die. Although the MLR2 immunogene seems unsuitable for use in treating MND in its current form, this does not diminish the ability for the immunogene concept to be suitable in other applications and potentially be altered/optimised for MND.

8.1 Increasing transfection efficiency of the immunogene

From the experiments undertaken in this study, approximately 20% of all spinal motor neurons in neonatal mice were transfected after intraperitoneal injection of the MLR2 immunogene. It is generally considered that non-viral gene vectors have much lower transfection ability compared to viral vectors, due to the barriers non-viral vectors must overcome (Mintzer & Simanek, 2008; Pérez-Martínez *et al.*, 2011; Rogers & Rush, 2012). However, spinal motor neuron viral gene delivery was used for a study which used serotyping for improved retrograde delivery and was only able to deliver to around 28% of cervical motor neurons after numerous intramuscular injections (Towne *et al.*, 2010), approximately 8% better than the results in this study, with a single injection.

To improve the transfection efficiency of the immunogene, there are several options available. Increasing the dosage injected (specifically in neonates targeting p75NTR), giving multiple injections or application with a long term infusion pump, which may increase transfection. Investigating the interaction of the immunogene at the NMJ with p75NTR may also shed light on the kinetics of the complex and its retrograde transport. Another option is to modify components of the immunogene for increased transfection efficiency.

8.2.1 Changing the cargo carrier

Currently, the component of the immunogene that binds and carries the cargo is PEI (polyethylenamine). This molecule is considered the gold standard for polycation-related gene delivery (Morille *et al.*, 2008), however there are other options available.

One option is to replace the PEI with liposomes. Liposomes are artificial vesicles that are able to bind and store cargo in their lumen, and subsequently deliver the cargo to cells. The positively charged head interacts spontaneously with negatively charged pDNA, then the phospholipid bilayer forms around the cargo, encapsulating it in this vesicle shape. (Felgner *et al.*, 1987; Pérez-Martínez *et al.*, 2011). Use of liposomes as a therapeutic has recently taken off, particularly with the conjugation of liposomes to antibodies (immunoliposomes). Immunoliposome technology has been shown to have promise in many areas, including; anti-cancer treatment (Shi *et al.*, 2015), fibrosis in wound healing (Schuster *et al.*, 2015), malaria (Moles *et al.*, 2015) and recently has shown to be an effective delivery method of GDNF to treat Parkinson's Disease (Zhang & Pardridge, 2009), as they are able to penetrate the brain *in vivo* (Loureiro *et al.*, 2015). In conjunction with the MLR2 antibody, the creation of an immunoliposome may show promise in treating MND.

Another alternate cargo carrier are silicon nanoparticles. In some collaborative work, the MLR2 antibody was conjugated to a porous silicon nanoparticles

(MLR2-pSi), which are able to be loaded with drugs or toxins (Secret *et al.*, 2013). The study showed that the MLR2-pSi loaded with the highly cytotoxic camptothecin caused cell death of p75NTR expressing cells, but not p75NTR negative cells. The MLR2-pSi was also fluorescently tagged and applied to a mixed culture of p75NTR expressing motor neurons and p75NTR negative glia. The tagged MLR2-pSi complex showed specific staining of p75NTR motor neurons and not glia. The wafers have been since replaced with ‘nanopills’ (silica nanotubes) and nanodiscs, which have shown to be more easily controlled in terms of the pharmacokinetics of the drugs or toxins loaded into the particles (Alba *et al.*, 2015; Alhmod *et al.*, 2015). Further modification of these nanoparticles is needed before application *in vivo*, however they have great potential.

8.2.2 Altering the MLR2 antibody

The immunogene uses a full, intact MLR2 antibody for p75NTR specificity. However, replacing that full IgG for Fab (antibody-binding fragments) or scFv (single chain variable fragments), may increase transfection efficiency.

Within the therapeutic world there are pros and cons to using Fab and scFv antibody fragments. The major advantages, particularly with scFv fragments, is the ability to penetrate tissue easier than full IgG (Yokota *et al.*, 1992) and more related to therapeutic development is ease of mass production (Nelson, 2010; Manjappa *et al.*, 2011), making it a more cost-effective molecule compared to IgGs. The major disadvantage with these fragments is their decreased half-life *in vivo*. These fragments lack the Fc domain of a full IgG, leaving them less stable

and more easily cleared by the body (Cumber *et al.*, 1992; Nelson, 2010).

However, if these fragments were conjugated to a PEGylated-PEI complex, the lack of Fc domain would be irrelevant, making a potentially cheaper and better penetrating immunogene.

8.2.3 *Changing the antibody for different receptor targets*

The MLR2 immunogene has shown success in transfecting motor neurons through p75NTR in neonatal mice. However, as discovered in this study, there is a low and short level of p75NTR expression in adult SOD1^{G93A} mouse motor neurons. Another neurotrophin receptor, TrkC, is expressed on motor neurons throughout life (Henderson *et al.*, 1993), making it an attractive target. Targeting TrkC would remove the limitation of the re-expression of p75NTR in motor neurons.

Activation of TrkC has been shown to have potent pro-survival effects on motor neurons (Henderson *et al.*, 1993). Activation of this receptor has been successfully mimicked with the use of an anti-TrkC antibody, 2B7 (Chen *et al.*, 2009; Guillemard *et al.*, 2010). Replacing the MLR2 with 2B7 could potentially work as a ‘double-hit’ therapeutic, by delivering pDNA expressing pro-survival molecules and by activating TrkC, increasing endogenous pro-survival signalling.

Essentially, the immunogene can be modified to accommodate any antibody-receptor combination, on the premise that the antibody causes receptor internalisation.

8.3 Potential for Spinal Muscular Atrophy treatment

In this study, pDNA coding for GFP was delivered to motor neurons, with the hypothesis that this could be replaced with a therapeutic gene (such as GDNF) to prevent motor neuron death in MND and SOD1^{G93A} mice. However, the pDNA cargo carried by the immunogene can be changed to target other diseases, such as Spinal Muscular Atrophy (SMA).

In its current form targeting p75NTR, the immunogene was able to transfect ~20% of all motor neurons when injected intraperitoneally into neonatal mice. This may allow the MLR2 immunogene to be used in childhood diseases, such as SMA. SMA is a motor neuron disorder which is similar to MND, as it causes motor neuron death. However, SMA is caused by deletion or inactivating mutations in SMN1 and retention of SMN2, resulting in insufficient levels of SMN protein (Survival Motor Neuron), leading to motor neuron cell death (Lefebvre *et al.*, 1995). By delivering pDNA which expresses the complete SMN protein to children or SMA model mice at a very young age, where p75NTR is still naturally expressed, the disease could potentially be alleviated.

8.4 p75NTR short time frame expression

As mentioned in Chapter 7, the low levels of p75NTR expressing motor neurons seen in SOD1^{G93A} mice may be due to the short expression time of the receptor. There are several lines of evidence that support this idea.

Firstly, the SOD1^{G93A} G1H mouse strain has a very aggressive disease phenotype (due to the high number of transgenes), leading to a rapid loss of motor neurons (Gurney *et al.*, 1994). The G1H strain loses approximately 1-2 motor neurons per hour, which translates to ~30-35 motor neurons a day. Considering that ~85% of p75NTR motor neurons in SOD1^{G93A} mice are co-expressing cleaved caspase-3 (apoptotic marker), it is safe to assume that these cells are undergoing apoptosis. Cellular apoptosis occurs between 4-24 hours for most cells (Saraste and Pulkki, 2000) and about 30 hours for motor neurons (facial) in mice (de Bilbao and Dubois-Dauphin, 1996). Therefore, a motor neuron undergoing apoptosis may only express p75NTR within that ~30 hour event.

Secondly, during the apoptosis of these motor neurons, which were shown to be shrinking, only motor neurons between 600-800 μm^2 expressed p75NTR. This indicates that in the timeline of complete cell death (~30 hours), from large motor neuron to shrunken motor neuron, there is only a small window of 600-800 μm^2 where p75NTR is expressed.

Finally, injection experiments in Chapter 6, where MLR2-ATTO-488 was injected into adult 110 day old SOD1^{G93A} mice, not all p75NTR expressing motor neurons showed ATTO-488 fluorescence, and not all ATTO-488 motor neurons showed p75NTR expression. Considering that these mice were euthanased and had their spinal cords examined 72 hours after initial injection, it is possible that between injection and examination, motor neurons re-expressed p75NTR after antibody had been cleared, or stopped p75NTR expression before examination, or perhaps the levels of p75NTR expressed were below the level that immunohistochemistry could detect.

Figure 8.1 depicts the theorised timeline of events motor neurons undergo, in relation to p75NTR.

8.3 Targeting other cell types that express p75NTR

In its current form, the MLR2 immunogene specifically targets p75NTR. Both the MLR2 antibody alone and MLR2 immunogene showed targeting of non-motor neuron p75NTR cells, in both the DRG and retina.

The MLR2 immunogene may be used to target p75NTR expressing DRG sensory neurons that may lead to treatments, for example in injury induced apoptosis of p75NTR expressing sensory neurons (Arnett, Ryals & Wright, 2007), and/or mediate pain induced by p75NTR expressing sensory neurons (Fukui *et al.*, 2010).

Interestingly, p75NTR is also expressed in retinal cells (Müller cells) which are glia that span the entire retina and tightly surround and wrap around retinal ganglion cells (Hu, Yip & So, 1998; Lebrun-Julien *et al.*, 2009). Activation of p75NTR in Müller cells promotes p75NTR retinal ganglion cell death, and prevents TrkA neuroprotective signals, while reciprocally, activation of TrkA promotes retinal cell ganglion survival and prevents p75NTR neurotoxicity (Lebrun-Julien *et al.*, 2009; Bai *et al.*, 2010). Neonatal mice injected with fluorescently tagged MLR2 showed that the antibody was able to reach these p75NTR expressing retinal glia (see Appendix I). Targeting these other cells with the MLR2 immunogene may lead to new treatment options that affect those particular cell types, such as glaucoma in the retina (Nakazawa *et al.*, 2006;

Lebrun-Julien *et al.*, 2010) or hyperalgesia caused by downstream p75NTR signaling (Khodorova *et al.*, 2013).

8.4 Concluding remarks

This study has shown that it is possible to deliver GFP expressing pDNA to primary motor neurons, both *in vitro* and *in vivo*, through p75NTR via the immunogene technology. While its application as a therapeutic for treating MND or SOD1^{G93A} mice may seem difficult in its current form, it does not diminish that the results for a non-viral gene delivery agent obtained (~20% neonatal motor neuron transfection) are edging closer to that of viral gene delivery. This study also characterised particular biochemical and morphological attributes of motor neurons in SOD1^{G93A} mice, indicating that these neurons are undergoing many dynamic changes as they degenerate.

While the MLR2 immunogene may not be the ‘golden bullet’ therapeutic for MND right now, the technology has potential. Gene therapy in general has the potential to be a treatment for many diseases, including both genetic diseases, where the faulty/mutated gene/protein can be rectified and sporadic diseases such as MND, where the treatment can be adapted to prevent cell death regardless of the overarching cause.

Figure 8.1 p75NTR expressing motor neuron hypothesis

(1) A motor neuron innervating its muscle target in a SOD1^{G93A} mouse is affected by the disease

(2) The motor neuron begins to degenerate and disconnects from its target muscle

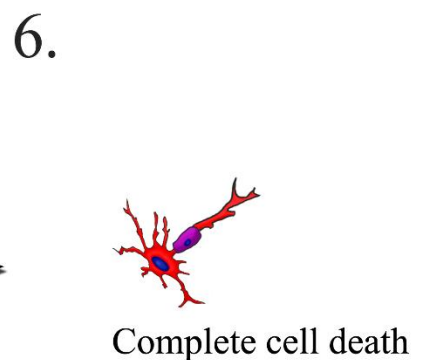
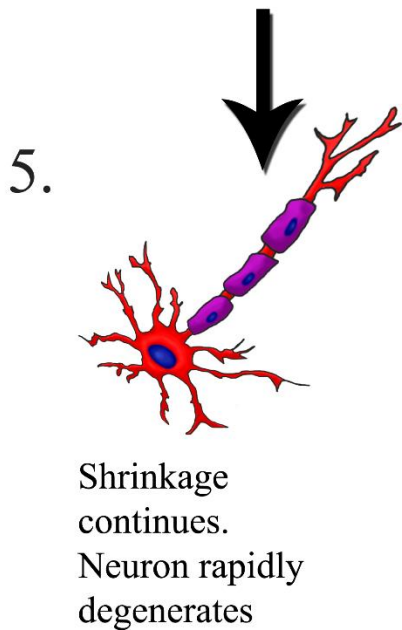
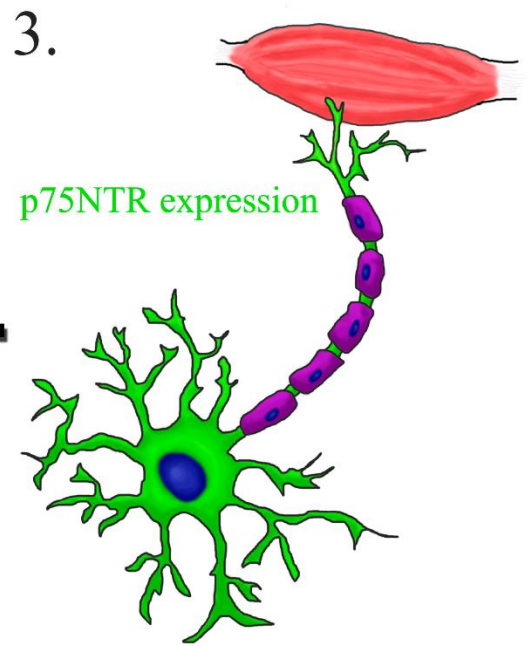
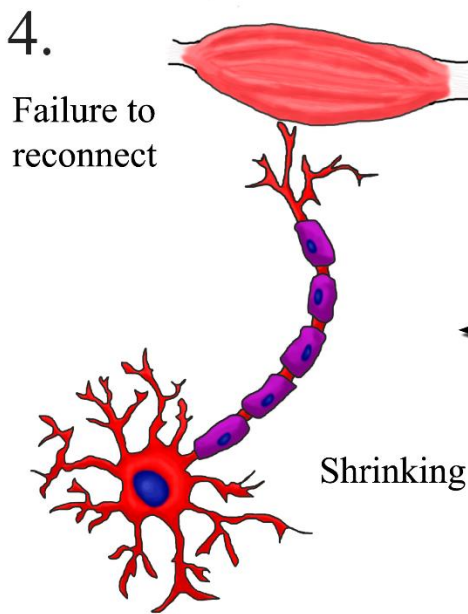
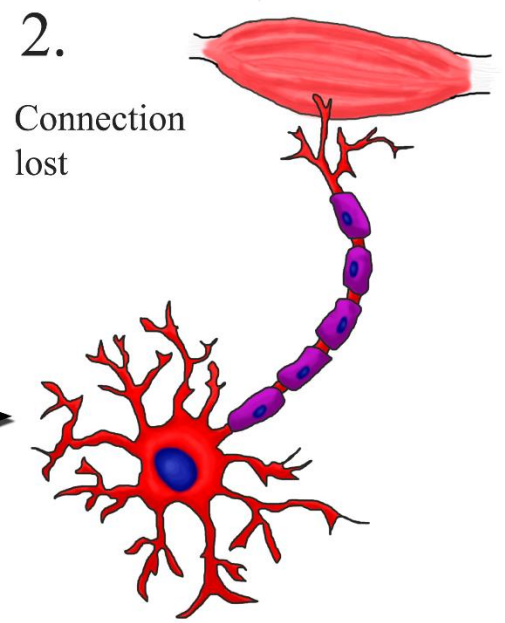
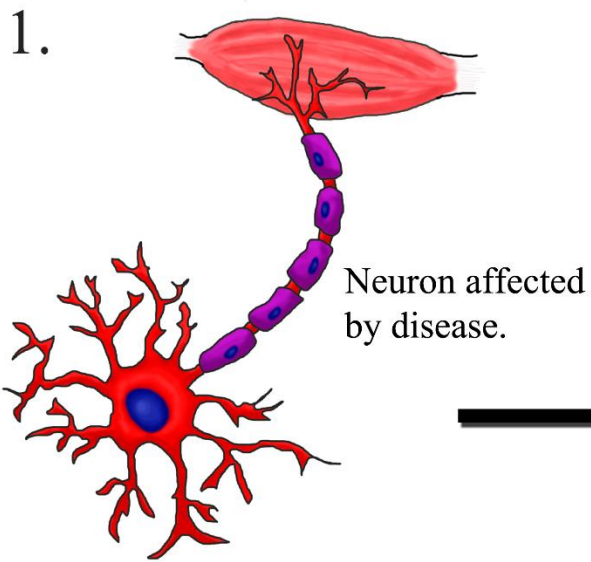
(3) Degeneration continues until it crosses a degenerative threshold where p75NTR is re-expressed

(4) The motor neuron is unable to reconnect to the muscle target and continues to be affected by the disease, shrink in size, and p75NTR expression is turned off

(5) Shrinkage of the motor neuron continues and rapidly declines

(6) Finally, the motor neuron completely retracts and dies

This entire process takes place between 1-2 days.



Appendix

Appendix I

Injection of neonatal mice with MLR2-ATTO-488 resulted in p75NTR expressing retinal glia to be targeted and stained.

Figure A1 show that (A) retinal cells are positive for ATTO-488 fluorescence that are also (B) positive for p75NTR, seen clearly in merged images (C). There is also high ATTO-488 fluorescence seen near the optic nerve (D) which is highly positive for p75NTR (E, F). Neonates not injected show no ATTO-488 fluorescence in the retina (G) where there is still p75NTR expression (H, I) and no ATTO-488 fluorescence in the optic nerve (J), also positive for p75NTR (K, L). Higher resolution images (Figure A2) taken from injected mice show MLR2-ATTO-488 is able to penetrate all layers of the retina (A) where there is p75NTR expression (B). Intriguingly, when the retina is counterstained with DAPI (C) the ATTO-488 fluorescence and p75NTR expression is highest in the areas lacking positive DAPI staining (D, inner plexiform layer) in the developing eye.

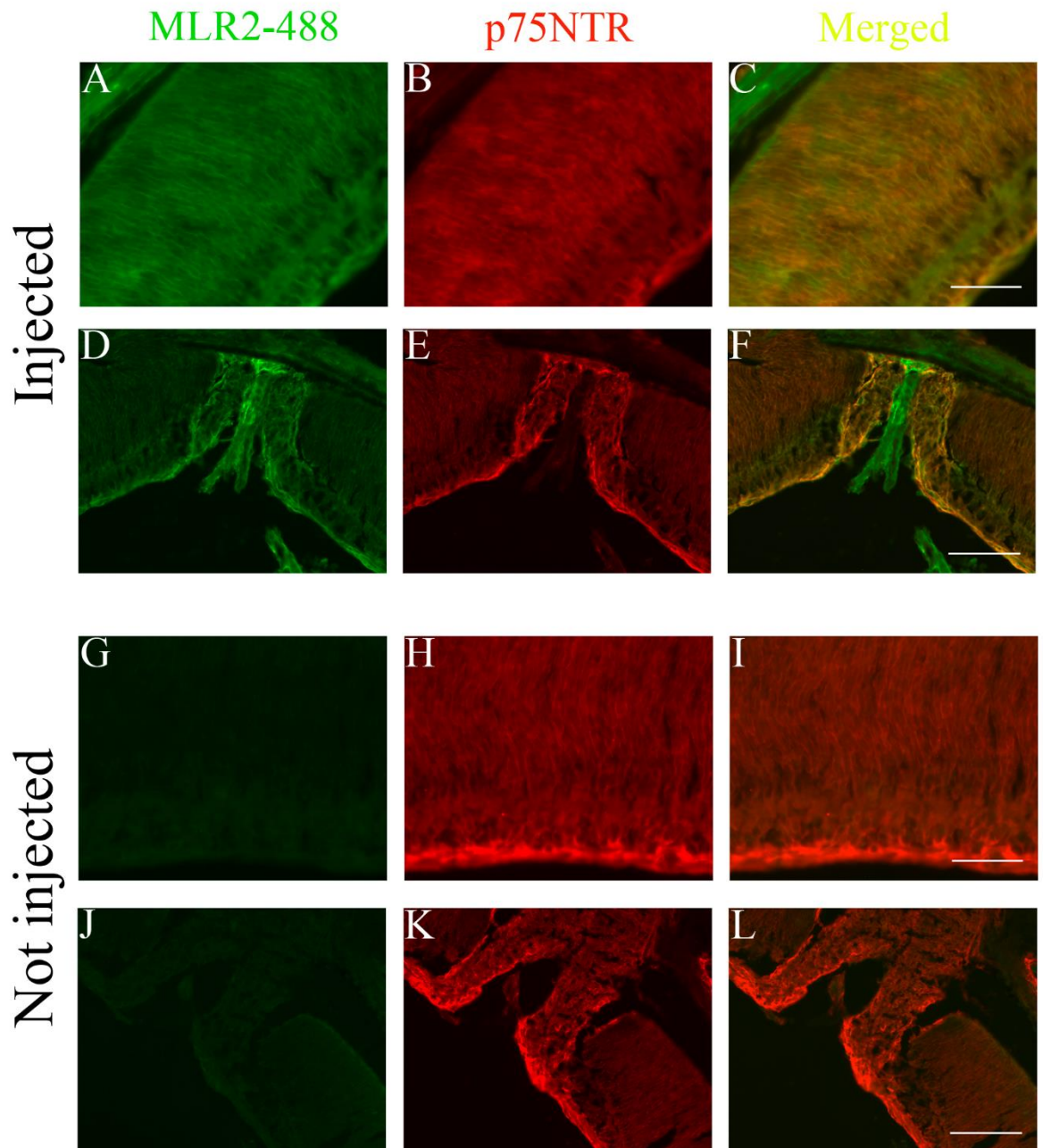
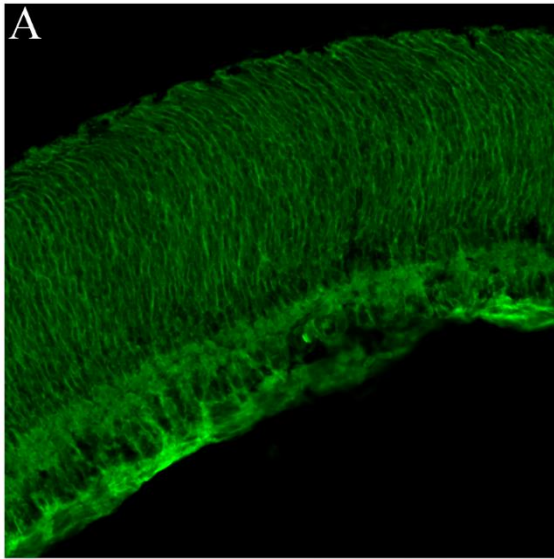


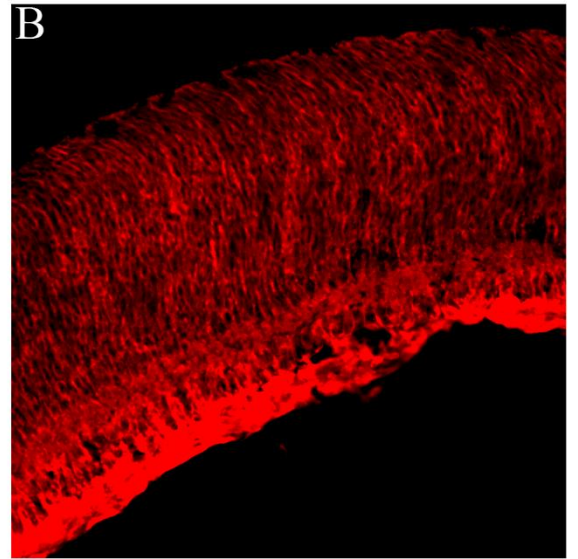
Figure A1 Injected MLR2-ATTO-488 is transported to p75NTR positive retinal neurons

Fluorescent micrographs taken from neonatal mice injected intraperitoneally with 150 μ g MLR2-ATTO-488 (75 μ g x2, 12 hours apart) show that in (A) retinal cells are positive for ATTO-488 fluorescence that are also (B) positive for p75NTR counterstaining seen clearly in (C). There is also high ATTO-488 fluorescence seen near the optic nerve (D) which is also highly positive for p75NTR (E, F). Neonates not injected show no ATTO-488 fluorescence in the retina (G) where there is p75NTR expression (H, I) and no ATTO-488 fluorescence in the optic nerve (J) positive for p75NTR (K, L). (scale = 50 μ m A-C, G-I, 100 μ m D-F, J-L)

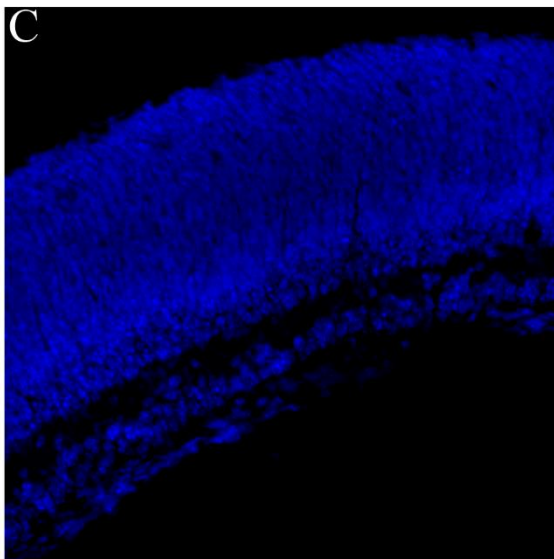
MLR2-488



p75NTR



DAPI



Merged

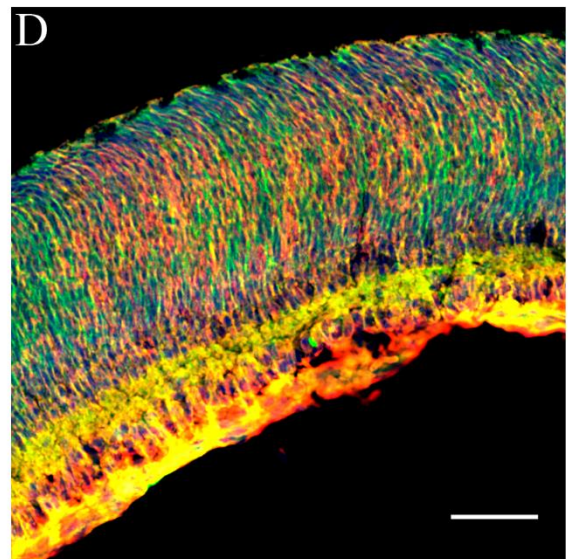


Figure A2 p75NTR is expressed across all layers of the mouse retina
High resolution images of MLR2-ATTO-488 (A) injected neonate retina show that p75NTR is expressed across all retinal layers (B), as evident by DAPI counterstaining (C), which has similar morphology to that of the embryonic eye seen during development. Merged images (D) show a high concentration of MLR2-ATTO-488/p75NTR co-fluorescence in the region lacking nuclei. (scale = 50 μ m)

References

- Acsadi, G., Anguelov, R.A., Yang, H., Toth, G., Thomas, R., Jani, A., Wang, Y., Ianakova, E., Mohammad, S., Lewis, R.A. & Shy, M.E. (2002). Increased survival and function of SOD1 mice after glial cell-derived neurotrophic factor gene therapy. *Human gene therapy* **13**, 1047–59.
- Airaksinen, M.S. & Saarma, M. (2002). The GDNF family: signalling, biological functions and therapeutic value. *Nature Reviews Neuroscience* **3**, 383–394.
- Airaksinen, M.S., Titievsky, a & Saarma, M. (1999). GDNF family neurotrophic factor signaling: four masters, one servant? *Molecular and cellular neurosciences* **13**, 313–325.
- Ajrourd-driss, S. & Siddique, T. (2014). Sporadic and hereditary amyotrophic lateral sclerosis (ALS). *Biochimica et biophysica acta* 6–11.
- Akita, H., Ito, R., Kamiya, H., Kogure, K. & Harashima, H. (2008). Cell cycle dependent transcription, a determinant factor of heterogeneity in cationic lipid-mediated transgene expression. *Gene therapy* **9**, 197–207.
- Akizuki, M., Yamashita, H., Uemura, K., Maruyama, H., Kawakami, H., Ito, H. & Takahashi, R. (2013). Optineurin suppression causes neuronal cell death via NF-κB pathway. *Journal of neurochemistry* **126**, 699–704.
- Alba, M., Delalat, B., Formentín, P., Rogers, M.-L., Marsal, L.F. & Voelcker, N.H. (2015). Silica Nanopills for Targeted Anticancer Drug Delivery. *Small*.
- Alexianu, M.E., Ho, B.K., Mohamed, A.H., La Bella, V., Smith, R.G. & Appel, S.H. (1994). The role of calcium-binding proteins in selective motoneuron vulnerability in amyotrophic lateral sclerosis. *Annals of Neurology* **36**, 846–858.
- Alhmoud, H., Delalat, B., Elnathan, R., Cifuentes-Rius, A., Chaix, A., Rogers, M.-L., Durand, J.-O. & Voelcker, N.H. (2015). Porous Silicon Nanodiscs for Targeted Drug Delivery. *Advanced Functional Materials* **25**, 1137–1145.
- Aliaga, L., Lai, C., Yu, J., Chub, N., Shim, H., Lixin, S., Chengsong, X., Wan-Jou, Y., Lin, X., O'Donovan, M.J. & Cai, H. (2013). Amyotrophic Lateral Sclerosis-related VAPB P56S Mutation Differentially Affects the Function and Survival of Corticospinal and Spinal Motor Neurons. *Human molecular genetics* **22**, 4293–4305.
- Alisky, J.M., van de Wetering, C.I. & Davidson, B.L. (2002). Widespread dispersal of cholera toxin subunit b to brain and spinal cord neurons following systemic delivery. *Experimental neurology* **178**, 139–146.
- Allen, T.M. & Hansen, C. (1991). Pharmacokinetics of stealth versus conventional liposomes: effect of dose. *Biochimica et biophysica acta* **1068**, 133–41.

- Alnemri, E.S., Livingston, D.J., Nicholson, D.W., Salvesen, G., Thornberry, N.A., Wong, W.W. & Yuan, J. (1996). Human ICE/CED-3 Protease Nomenclature. *Cell* **87**, 171.
- Al-Sakere, B., André, F., Bernat, C., Connault, E., Opolon, P., Davalos, R. V, Rubinsky, B. & Mir, L.M. (2007). Tumor ablation with irreversible electroporation. *PLoS ONE* **2**, e1135.
- Andersen, P.M. (2006). Amyotrophic lateral sclerosis associated with mutations in the CuZn superoxide dismutase gene. *Current neurology and neuroscience reports* **6**, 37–46.
- Arai, T., Hasegawa, M., Akiyama, H., Ikeda, K., Nonaka, T., Mori, H., Mann, D., Tsuchiya, K., Yoshida, M., Hashizume, Y. & Oda, T. (2006). TDP-43 is a component of ubiquitin-positive tau-negative inclusions in frontotemporal lobar degeneration and amyotrophic lateral sclerosis. *Biochemical and biophysical research communications* **351**, 602–11.
- Arnett, M.G., Ryals, J.M. & Wright, D.E. (2007). pro-NGF, sortilin, and p75NTR: Potential mediators of injury-induced apoptosis in the mouse dorsal root ganglion. *Brain Research* **1183**, 32–42.
- Atkin, J.D., Farg, M.A., Turner, B.J., Tomas, D., Lysaght, J.A., Nunan, J., Rembach, A., Nagley, P., Beart, P.M., Cheema, S.S. & Horne, M.K. (2006). Induction of the unfolded protein response in familial amyotrophic lateral sclerosis and association of protein-disulfide isomerase with superoxide dismutase 1. *The Journal of biological chemistry* **281**, 30152–65.
- Atkin, J.D., Farg, M.A., Walker, A.K., McLean, C., Tomas, D. & Horne, M.K. (2008). Endoplasmic reticulum stress and induction of the unfolded protein response in human sporadic amyotrophic lateral sclerosis. *Neurobiology of disease* **30**, 400–7.
- Ayala, Y.M., Pantano, S., D'Ambrogio, A., Buratti, E., Brindisi, A., Marchetti, C., Romano, M. & Baralle, F.E. (2005). Human, Drosophila, and C.elegans TDP43: nucleic acid binding properties and splicing regulatory function. *Journal of molecular biology* **348**, 575–88.
- Ayala, Y.M., Zago, P., D'Ambrogio, A., Xu, Y.-F., Petrucelli, L., Buratti, E. & Baralle, F.E. (2008). Structural determinants of the cellular localization and shuttling of TDP-43. *Journal of cell science* **121**, 3778–85.
- Azzouz, M., Ralph, G.S., Storkebaum, E., Walmsley, L.E., Mitrophanous, K.A., Kingsman, S.M., Carmeliet, P. & Mazarakis, N.D. (2004). VEGF delivery with retrogradely transported lentivector prolongs survival in a mouse ALS model. *Nature* **429**, 413–417.
- Bai, O., Wei, Z., Lu, W., Bowen, R., Keegan, D. & Li, X.-M. (2002). Protective effects of atypical antipsychotic drugs on PC12 cells after serum withdrawal. *Journal of neuroscience research* **69**, 278–83.
- Bai, Y., Dergham, P., Nedev, H., Xu, J., Galan, A., Rivera, J.C., ZhiHua, S., Mehta, H.M., Woo, S.B., Sarunic, M. V, Neet, K.E. & Saragovi, H.U. (2010). Chronic and acute

- models of retinal neurodegeneration TrkA activity are neuroprotective whereas p75NTR activity is neurotoxic through a paracrine mechanism. *The Journal of biological chemistry* **285**, 39392–400.
- Baldwin, A. & Shooter, E. (1995). Zone mapping of the binding domain of the rat low affinity nerve growth factor receptor by the introduction of novel N-glycosylation sites. *Journal of Biological Chemistry*.
- Bamji, S.X., Majdan, M., Pozniak, C.D., Belliveau, D.J., Aloyz, R., Kohn, J., Causing, C.G. & Miller, F.D. (1998). The p75 neurotrophin receptor mediates neuronal apoptosis and is essential for naturally occurring sympathetic neuron death. *The Journal of cell biology* **140**, 911–23.
- Barati, S., Hurtado, P.R., Zhang, S.H., Tinsley, R., Ferguson, I.A. & Rush, R.A. (2006). GDNF gene delivery via the p75(NTR) receptor rescues injured motor neurons. *Experimental neurology* **202**, 179–88.
- Barber, R.P., Phelps, P.E., Houser, C.R., Crawford, G.D., Salvaterra, P.M. & Vaughn, J.E. (1984). The morphology and distribution of neurons containing choline acetyltransferase in the adult rat spinal cord: an immunocytochemical study. *The Journal of comparative neurology* **229**, 329–46.
- Barker, P. (1998). p75NTR: A study in contrasts. *Cell death and differentiation* **5**, 346–56.
- Barker, P.A., Barbee, G., Misko, T.P. & Shooter, E.M. (1994). The low affinity neurotrophin receptor, p75LNTR, is palmitoylated by thioester formation through cysteine 279. *The Journal of biological chemistry* **269**, 30645–50.
- Barker, P.A. & Shooter, E.M. (1994). Disruption of NGF binding to the low affinity neurotrophin receptor p75LNTR reduces NGF binding to TrkA on PC12 cells. *Neuron* **13**, 203–15.
- Barrett, G.L. & Bartlett, P.F. (1994). The p75 nerve growth factor receptor mediates survival or death depending on the stage of sensory neuron development. *Proceedings of the National Academy of Sciences of the United States of America* **91**, 6501–5.
- Bartlett, J.S., Samulski, R.J. & McCown, T.J. (1998). Selective and rapid uptake of adeno-associated virus type 2 in brain. *Human gene therapy* **9**, 1181–6.
- Basso, M., Massignan, T., Samengo, G., Cheroni, C., De Biasi, S., Salmona, M., Bendotti, C. & Bonetto, V. (2006). Insoluble mutant SOD1 is partly oligoubiquitinated in amyotrophic lateral sclerosis mice. *The Journal of biological chemistry* **281**, 33325–35.
- Baumgartner, B.J. & Shine, H.D. (1998). Neuroprotection of spinal motoneurons following targeted transduction with an adenoviral vector carrying the gene for glial cell line-derived neurotrophic factor. *Experimental neurology* **153**, 102–12.
- Bell, P., Wang, L., Lebherz, C., Flieder, D.B., Bove, M.S., Wu, D., Gao, G.P., Wilson, J.M. & Wivel, N.A. (2005). No evidence for tumorigenesis of AAV vectors in a large-scale

- study in mice. *Molecular Therapy* **12**, 299–306.
- Bellingham, M.C. (2011). A review of the neural mechanisms of action and clinical efficiency of riluzole in treating amyotrophic lateral sclerosis: what have we learned in the last decade? *CNS neuroscience & therapeutics* **17**, 4–31.
- Belzil, V. V., Valdmanis, P.N., Dion, P.A., Daoud, H., Kabashi, E., Noreau, A., Gauthier, J., Hince, P., Desjarlais, A., Bouchard, J.-P., Lacomblez, L., Salachas, F., Pradat, P.-F., Camu, W., Meininger, V., Dupré, N. & Rouleau, G.A. (2009). Mutations in FUS cause FALS and SALS in French and French Canadian populations. *Neurology* **73**, 1176–9.
- Bendotti, C., Calvaresi, N., Chiveri, L., Prella, A., Moggio, M., Braga, M., Silani, V. & De Biasi, S. (2001). Early vacuolization and mitochondrial damage in motor neurons of FALS mice are not associated with apoptosis or with changes in cytochrome oxidase histochemical reactivity. *Journal of the Neurological Sciences* **191**, 25–33.
- Bendotti, C., Marino, M., Cheroni, C., Fontana, E., Crippa, V., Poletti, A. & De Biasi, S. (2012). Dysfunction of constitutive and inducible ubiquitin-proteasome system in amyotrophic lateral sclerosis: implication for protein aggregation and immune response. *Progress in neurobiology* **97**, 101–26.
- Bennett, M., Gibson, W. & Lemon, G. (2002). Neuronal cell death, nerve growth factor and neurotrophic models: 50 years on. *Autonomic Neuroscience* **95**, 1–23.
- Bensimon, G., Lacomblez, L. & Meininger, V. (1994). A controlled trial of riluzole in amyotrophic lateral sclerosis. *ALS/Riluzole Study Group. The New England journal of medicine*.
- Van Den Berg, J.P., Kalmijn, S., Lindeman, E., Veldink, J.H., De Visser, M., Van Der Graaff, M.M., Wokke, J.H.J. & Van Den Berg, L.H. (2005). Multidisciplinary ALS care improves quality of life in patients with ALS. *Neurology* **65**, 1264–1267.
- Berkemeier, L.R., Winslow, J.W., Kaplan, D.R., Nikolics, K., Coeddel, D. V & Rosenthal, A. (1991). Neurotrophin-5 : A Novel Neurotrophic That Activates trk and trkB **7**, 857–866.
- Bertram, L., Hiltunen, M., Parkinson, M., Ingelsson, M., Lange, C., Ramasamy, K., Mullin, K., Menon, R., Sampson, A.J., Hsiao, M.Y., Elliott, K.J., Velicelebi, G., Moscarillo, T., Hyman, B.T., Wagner, S.L., Becker, K.D., Blacker, D. & Tanzi, R.E. (2005). Family-based association between Alzheimer's disease and variants in UBQLN1. *The New England journal of medicine* **352**, 884–894.
- Bessis, N., GarciaCozar, F.J. & Boissier, M.-C. (2004). Immune responses to gene therapy vectors: influence on vector function and effector mechanisms. *Gene therapy* **11 Suppl 1**, S10–S17.
- Bhakar, A.L., Howell, J.L., Paul, C.E., Salehi, A.H., Becker, E.B.E., Said, F., Bonni, A. & Barker, P.A. (2003). Apoptosis induced by p75NTR overexpression requires Jun kinase-dependent phosphorylation of Bad. *The Journal of neuroscience : the official journal of*

the Society for Neuroscience **23**, 11373–81.

- Bibel, M., Hoppe, E. & Barde, Y.A. (1999). Biochemical and functional interactions between the neurotrophin receptors trk and p75NTR. *The EMBO journal* **18**, 616–22.
- Bilsland, L.G., Sahai, E., Kelly, G., Golding, M., Greensmith, L. & Schiavo, G. (2010). Deficits in axonal transport precede ALS symptoms in vivo. *Proceedings of the National Academy of Sciences of the United States of America* **107**, 1–6.
- Borges, L.F. & Iversen, S.D. (1986). Topography of choline acetyltransferase immunoreactive neurons and fibers in the rat spinal cord. *Brain research* **362**, 140–8.
- Van Den Bosch, L., Van Damme, P., Bogaert, E. & Robberecht, W. (2006). The role of excitotoxicity in the pathogenesis of amyotrophic lateral sclerosis. *Biochimica et biophysica acta* **1762**, 1068–82.
- Bottaro, D.P., Rubin, J.S., Faletto, D.L., Chan, A.M., Kmiecik, T.E., Vande Woude, G.F. & Aaronson, S. a. (1991). Identification of the hepatocyte growth factor receptor as the c-met proto-oncogene product. *Science (New York, N.Y.)* **251**, 802–4.
- Boussif, O., Lezoualc'h, F., Zanta, M.A., Mergny, M.D., Scherman, D., Demeneix, B. & Behr, J.P. (1995). A versatile vector for gene and oligonucleotide transfer into cells in culture and in vivo: polyethylenimine. *Proceedings of the National Academy of Sciences of the United States of America* **92**, 7297–301.
- Bruijn, L.I., Becher, M.W., Lee, M.K., Anderson, K.L., Jenkins, N.A., Copeland, N.G., Sisodia, S.S., Rothstein, J.D., Borchelt, D.R., Price, D.L. & Cleveland, D.W. (1997). ALS-linked SOD1 mutant G85R mediates damage to astrocytes and promotes rapidly progressive disease with SOD1-containing inclusions. *Neuron* **18**, 327–38.
- Bucchia, M., Ramirez, A., Parente, V., Simone, C., Nizzardo, M., Magri, F., Dametti, S. & Corti, S. (2015). Therapeutic Development in Amyotrophic Lateral Sclerosis. *Clinical Therapeutics* **37**, 668–680.
- Buchan, J.R. & Parker, R. (2009). Eukaryotic stress granules: the ins and outs of translation. *Molecular cell* **36**, 932–41.
- Buratti, E. & Baralle, F.E. (2010). The multiple roles of TDP-43 in pre-mRNA processing and gene expression regulation. *RNA biology* **7**, 420–9.
- Burgess, R.R. (1991). Use of polyethyleneimine in purification of DNA-binding proteins. *Methods in enzymology* **208**, 3–10.
- Burke, R., Levine, D., Tsairis, P. & Zajac, F. (1973). Physiological types and histochemical profiles in motor units of the cat gastrocnemius. *The Journal of Physiology* **234**, 723–748.
- Byrne, S., Walsh, C., Lynch, C., Bede, P., Elamin, M., Kenna, K., McLaughlin, R. & Hardiman, O. (2011). Rate of familial amyotrophic lateral sclerosis: a systematic review

- and meta-analysis. *Journal of neurology, neurosurgery, and psychiatry* **82**, 623–7.
- Carriedo, S.G., Sensi, S.L., Yin, H.Z. & Weiss, J.H. (2000). AMPA exposures induce mitochondrial Ca(2+) overload and ROS generation in spinal motor neurons in vitro. *The Journal of neuroscience : the official journal of the Society for Neuroscience* **20**, 240–250.
- Carroll, S., Silos-Santiago, I. & Frese, S. (1992). Dorsal root ganglion neurons expressing trk are selectively sensitive to NGF deprivation in utero. *Neuron* **9**, 779–788.
- Casaccia-Bonnel, P., Carter, B., TR, D. & Chao, M. (1996). Death of oligodendrocytes mediated by the interaction of nerve growth factor with its receptor p75. *Nature* **383**, 716–9.
- Casademunt, E., Carter, B.D., Benzel, I., Frade, J.M., Dechant, G. & Barde, Y.A. (1999). The zinc finger protein NRIF interacts with the neurotrophin receptor p75(NTR) and participates in programmed cell death. *The EMBO journal* **18**, 6050–61.
- Cashman, N.R., Durham, H.D., Blusztajn, J.K., Oda, K., Tabira, T., Shaw, I.T., Dahrouge, S. & Antel, J.P. (1992). Neuroblastoma x spinal cord (NSC) hybrid cell lines resemble developing motor neurons. *Developmental dynamics : an official publication of the American Association of Anatomists* **194**, 209–21.
- Cassel, J.A. & Reitz, A.B. (2013). Ubiquitin-2 (UBQLN2) binds with high affinity to the C-terminal region of TDP-43 and modulates TDP-43 levels in H4 cells: Characterization of inhibition by nucleic acids and 4-aminoquinolines. *Biochimica et Biophysica Acta - Proteins and Proteomics* **1834**, 964–971.
- Chandler, C.E., Parsons, L.M., Hosang, M. & Shooter, E.M. (1984). A monoclonal antibody modulates the interaction of nerve growth factor with PC12 cells. *Journal of Biological Chemistry* **259**, 6882–6889.
- Chang, Q. & Martin, L.J. (2009). Glycinergic innervation of motoneurons is deficient in amyotrophic lateral sclerosis mice: a quantitative confocal analysis. *The American journal of pathology* **174**, 574–85.
- Charcot, J. (1869). Deux cas d'atrophie musculaire progressive avec lesions de la substance grise et des faisceaux antero-lateraux de la moelle epiniere. *Arch Physiol Norm Pathol (Paris)* **869**, 744–760.
- Chen, D., Brahimi, F., Angell, Y., Li, Y.C., Moscovicz, J., Saragovi, H.U. & Burgess, K. (2009). Bivalent peptidomimetic ligands of TrkC are biased agonists and selectively induce neurite outgrowth or potentiate neurotrophin-3 trophic signals. *ACS chemical biology* **4**, 769–781.
- Chen, Y., Bennett, C.L., Huynh, H.M., Blair, I.P., Puls, I., Irobi, J., Dierick, I., Abel, A., Kennerson, M.L., Rabin, B.A., Nicholson, G.A., Auer-Grumbach, M., Wagner, K., De Jonghe, P., Griffin, J.W., Fischbeck, K.H., Timmerman, V., Cornblath, D.R. & Chance,

- P.F. (2004). DNA/RNA helicase gene mutations in a form of juvenile amyotrophic lateral sclerosis (ALS4). *American journal of human genetics* **74**, 1128–1135.
- Cheroni, C., Marino, M., Tortarolo, M., Veglianesi, P., De Biasi, S., Fontana, E., Zuccarello, L.V., Maynard, C.J., Dantuma, N.P. & Bendotti, C. (2009). Functional alterations of the ubiquitin-proteasome system in motor neurons of a mouse model of familial amyotrophic lateral sclerosis. *Human molecular genetics* **18**, 82–96.
- Cheroni, C., Peviani, M., Cascio, P., De Biasi, S., Monti, C. & Bendotti, C. (2005). Accumulation of human SOD1 and ubiquitinated deposits in the spinal cord of SOD1G93A mice during motor neuron disease progression correlates with a decrease of proteasome. *Neurobiology of disease* **18**, 509–22.
- Chonn, A., Semple, S.C. & Cullis, P.R. (1992). Association of blood proteins with large unilamellar liposomes in vivo. Relation to circulation lifetimes. *The Journal of biological chemistry* **267**, 18759–65.
- Chow, C.Y., Landers, J.E., Bergren, S.K., Sapp, P.C., Grant, A.E., Jones, J.M., Everett, L., Lenk, G.M., McKenna-Yasek, D.M., Weisman, L.S., Figlewicz, D., Brown, R.H. & Meisler, M.H. (2009). Deleterious variants of FIG4, a phosphoinositide phosphatase, in patients with ALS. *American journal of human genetics* **84**, 85–8.
- Chung, Y.-C., Chang, F.-H., Wei, M.-F. & Young, T.-H. (2010). A variable gene delivery carrier--biotinylated chitosan/polyethyleneimine. *Biomedical materials (Bristol, England)* **5**, 065012.
- Ciolina, C., Byk, G., Blanche, F., Thuillier, V., Scherman, D. & Wils, P. (1999). Coupling of nuclear localization signals to plasmid DNA and specific interaction of the conjugates with importin alpha. *Bioconjugate chemistry* **10**, 49–55.
- Colombrita, C., Zennaro, E., Fallini, C., Weber, M., Sommacal, A., Buratti, E., Silani, V. & Ratti, A. (2009). TDP-43 is recruited to stress granules in conditions of oxidative insult. *Journal of neurochemistry* **111**, 1051–61.
- Copray, J., Jaarsma, D., Kust, B., Bruggeman, R., Mantingh, I., Brouwer, N. & Boddeke, H. (2003). Expression of the low affinity neurotrophin receptor p75 in spinal motoneurons in a transgenic mouse model for amyotrophic lateral sclerosis. *Neuroscience* **116**, 685–694.
- Cordon-Cardo, C., Tapley, P., Jing, S., Nanduri, V., O'Rourke, E., Lamballe, F., Kovary, K., Klein, R., Jones, K.R., Reichardt, L.F. & Barbacid, M. (1991). The trk tyrosine protein kinase mediates the mitogenic properties of nerve growth factor and neurotrophin-3. *Cell* **66**, 173–183.
- Corrado, L., Del Bo, R., Castellotti, B., Ratti, A., Cereda, C., Penco, S., Sorarù, G., Carlomagno, Y., Ghezzi, S., Pensato, V., Colombrita, C., Gagliardi, S., Cozzi, L., Orsetti, V., Mancuso, M., Siciliano, G., Mazzini, L., Comi, G. Pietro, Gellera, C., Ceroni, M., D'Alfonso, S. & Silani, V. (2010). Mutations of FUS gene in sporadic

- amyotrophic lateral sclerosis. *Journal of medical genetics* **47**, 190–4.
- Coulson, E.J. (1999). p75 Neurotrophin Receptor-mediated Neuronal Death Is Promoted by Bcl-2 and Prevented by Bcl-xL. *Journal of Biological Chemistry* **274**, 16387–16391.
- Coulson, E.J., Reid, K., Baca, M., Shipham, K.A., Hulett, S.M., Kilpatrick, T.J. & Bartlett, P.F. (2000). Chopper, a new death domain of the p75 neurotrophin receptor that mediates rapid neuronal cell death. *The Journal of biological chemistry* **275**, 30537–45.
- Couthouis, J., Hart, M.P., Erion, R., King, O.D., Diaz, Z., Nakaya, T., Ibrahim, F., Kim, H.-J., Mojsilovic-Petrovic, J., Panossian, S., Kim, C.E., Frackelton, E.C., Solski, J.A., Williams, K.L., Clay-Falcone, D., Elman, L., McCluskey, L., Greene, R., Hakonarson, H., Kalb, R.G., Lee, V.M.Y., Trojanowski, J.Q., Nicholson, G.A., Blair, I.P., Bonini, N.M., Van Deerlin, V.M., Mourelatos, Z., Shorter, J. & Gitler, A.D. (2012). Evaluating the role of the FUS/TLS-related gene EWSR1 in amyotrophic lateral sclerosis. *Human molecular genetics* **21**, 2899–911.
- Couthouis, J., Hart, M.P., Shorter, J., DeJesus-Hernandez, M., Erion, R., Oristano, R., Liu, A.X., Ramos, D., Jethava, N., Hosangadi, D., Epstein, J., Chiang, A., Diaz, Z., Nakaya, T., Ibrahim, F., Kim, H.-J., Solski, J.A., Williams, K.L., Mojsilovic-Petrovic, J., Ingre, C., Boylan, K., Graff-Radford, N.R., Dickson, D.W., Clay-Falcone, D., Elman, L., McCluskey, L., Greene, R., Kalb, R.G., Lee, V.M.-Y., Trojanowski, J.Q., Ludolph, A., Robberecht, W., Andersen, P.M., Nicholson, G.A., Blair, I.P., King, O.D., Bonini, N.M., Van Deerlin, V., Rademakers, R., Mourelatos, Z. & Gitler, A.D. (2011). A yeast functional screen predicts new candidate ALS disease genes. *Proceedings of the National Academy of Sciences of the United States of America* **108**, 20881–90.
- Cox, P.A. & Sacks, O.W. (2002). Cycad neurotoxins, consumption of flying foxes, and ALS-PDC disease in Guam. *Neurology* **58**, 956–959.
- Cudkowicz, M.E., McKenna-Yasek, D., Sapp, P.E., Chin, W., Geller, B., Hayden, D.L., Schoenfeld, D.A., Hosler, B.A., Horvitz, H.R. & Brown, R.H. (1997). Epidemiology of mutations in superoxide dismutase in amyotrophic lateral sclerosis. *Annals of neurology* **41**, 210–21.
- Cumber, A.J., Ward, E.S., Winter, G., Parnell, G.D. & Wawrzynczak, E.J. (1992). Comparative stabilities in vitro and in vivo of a recombinant mouse antibody FvCys fragment and a bisFvCys conjugate. *Journal of immunology* **149**, 120–126.
- Dadon-Nachum, M., Melamed, E. & Offen, D. (2011). The “dying-back” phenomenon of motor neurons in ALS. *Journal of Molecular Neuroscience*.
- Davey, F. & Davies, A.M. (1998). TrkB signalling inhibits p75-mediated apoptosis induced by nerve growth factor in embryonic proprioceptive neurons. *Current biology* **8**, 915–918.
- Davies, L.A., Hyde, S.C., Nunez-Alonso, G., Bazzani, R.P., Harding-Smith, R., Pringle, I.A., Lawton, A.E., Abdullah, S., Roberts, T.C., McCormick, D., Sumner-Jones, S.G. & Gill,

- D.R. (2012). The use of CpG-free plasmids to mediate persistent gene expression following repeated aerosol delivery of pDNA/PEI complexes. *Biomaterials* **33**, 5618–5627.
- Deinhardt, K. & Chao, M. V. (2014). Neurotrophic Factors. In , Handbook of Experimental Pharmacology: 103–119. Lewin, G.R. & Carter, B.D. (Eds). . Berlin, Heidelberg: Springer Berlin Heidelberg.
- DeJesus-Hernandez, M., Mackenzie, I.R.R., Boeve, B.F.F., Boxer, A.L.L., Baker, M., Rutherford, N.J.J., Nicholson, A.M.M., Finch, N.A.A., Flynn, H., Adamson, J., Kouri, N., Wojtas, A., Sengdy, P., Hsiung, G.-Y.R.R., Karydas, A., Seeley, W.W.W., Josephs, K.A.A., Coppola, G., Geschwind, D.H.H., Wszolek, Z.K.K., Feldman, H., Knopman, D.S.S., Petersen, R.C.C., Miller, B.L.L., Dickson, D.W.W., Boylan, K.B.B., Graff-Radford, N.R.R. & Rademakers, R. (2011). Expanded GGGGCC Hexanucleotide Repeat in Noncoding Region of C9ORF72 Causes Chromosome 9p-Linked FTD and ALS. *Neuron* **72**, 245–256.
- Deng, H., Chen, W., Hong, S. & Boycott, K. (2011a). Mutations in UBQLN2 cause dominant X-linked juvenile and adult-onset ALS and ALS/dementia. *Nature* **477**, 211–215.
- Deng, H.-X., Chen, W., Hong, S.-T., Boycott, K.M., Gorrie, G.H., Siddique, N., Yang, Y., Fecto, F., Shi, Y., Zhai, H., Jiang, H., Hirano, M., Rampersaud, E., Jansen, G.H., Donkervoort, S., Bigio, E.H., Brooks, B.R., Ajroud, K., Sufit, R.L., Haines, J.L., Mugnaini, E., Pericak-Vance, M.A. & Siddique, T. (2011b). Mutations in UBQLN2 cause dominant X-linked juvenile and adult-onset ALS and ALS/dementia. *Nature* **477**, 211–5.
- Deng, H.-X., Shi, Y., Furukawa, Y., Zhai, H., Fu, R., Liu, E., Gorrie, G.H., Khan, M.S., Hung, W.-Y., Bigio, E.H., Lukas, T., Dal Canto, M.C., O’Halloran, T. V & Siddique, T. (2006). Conversion to the amyotrophic lateral sclerosis phenotype is associated with intermolecular linked insoluble aggregates of SOD1 in mitochondria. *Proceedings of the National Academy of Sciences of the United States of America* **103**, 7142–7.
- Deng, H.-X., Zhai, H., Bigio, E.H., Yan, J., Fecto, F., Ajroud, K., Mishra, M., Ajroud-Driss, S., Heller, S., Sufit, R., Siddique, N., Mugnaini, E. & Siddique, T. (2010). FUS-immunoreactive inclusions are a common feature in sporadic and non-SOD1 familial amyotrophic lateral sclerosis. *Annals of neurology* **67**, 739–48.
- Ding, H., Schwarz, D.S., Keene, A., Affar, E.B., Fenton, L., Xia, X., Shi, Y., Zamore, P.D. & Xu, Z. (2003). Selective silencing by RNAi of a dominant allele that causes amyotrophic lateral sclerosis. *Aging cell* **2**, 209–17.
- Dodge, J.C., Haidet, A.M., Yang, W., Passini, M.A., Hester, M., Clarke, J., Roskelley, E.M., Treleaven, C.M., Rizo, L., Martin, H., Kim, S.H., Kaspar, R., Taksir, T. V, Griffiths, D.A., Cheng, S.H., Shihabuddin, L.S. & Kaspar, B.K. (2008). Delivery of AAV-IGF-1 to the CNS extends survival in ALS mice through modification of aberrant glial cell

- activity. *Molecular therapy : the journal of the American Society of Gene Therapy* **16**, 1056–64.
- Dodge, J.C., Treleaven, C.M., Fidler, J.A., Hester, M., Haidet, A., Handy, C., Rao, M., Eagle, A., Matthews, J.C., Taksir, T. V, Cheng, S.H., Shihabuddin, L.S. & Kaspar, B.K. (2010). AAV4-mediated expression of IGF-1 and VEGF within cellular components of the ventricular system improves survival outcome in familial ALS mice. *Molecular therapy : the journal of the American Society of Gene Therapy* **18**, 2075–84.
- Dormann, D., Rodde, R., Edbauer, D., Bentmann, E., Fischer, I., Hruscha, A., Than, M.E., Mackenzie, I.R.A., Capell, A., Schmid, B., Neumann, M. & Haass, C. (2010). ALS-associated fused in sarcoma (FUS) mutations disrupt Transportin-mediated nuclear import. *The EMBO journal* **29**, 2841–57.
- Drepper, C., Herrmann, T., Wessig, C., Beck, M. & Sendtner, M. (2011). C-terminal FUS/TLS mutations in familial and sporadic ALS in Germany. *Neurobiology of Aging* **32**, 548.e1–4.
- Dun, N.J., Dun, S.L., Forstermann, U. & Tseng, L.F. (1992). Nitric oxide synthase immunoreactivity in rat spinal cord. *Neuroscience letters* **147**, 217–20.
- Duvshani-Eshet, M., Keren, H., Oz, S., Radzishevsky, I.S., Mor, A. & Machluf, M. (2008). Effect of peptides bearing nuclear localization signals on therapeutic ultrasound mediated gene delivery. *Journal of Gene Medicine* **10**, 1150–1159.
- Dykens, J.A. (1994). Isolated cerebral and cerebellar mitochondria produce free radicals when exposed to elevated CA²⁺ and Na⁺: implications for neurodegeneration. *Journal of neurochemistry* **63**, 584–591.
- Eastman, S.J., Baskin, K.M., Hodges, B.L., Chu, Q., Gates, A., Dreusicke, R., Anderson, S. & Scheule, R.K. (2002). Development of catheter-based procedures for transducing the isolated rabbit liver with plasmid DNA. *Human gene therapy* **13**, 2065–77.
- Ebens, A., Brose, K., Leonardo, E.D., Hanson, M.G., Bladt, F., Birchmeier, C., Barres, B.A. & Tessier-Lavigne, M. (1996). Hepatocyte growth factor/scatter factor is an axonal chemoattractant and a neurotrophic factor for spinal motor neurons. *Neuron* **17**, 1157–72.
- Edelstein, A.D., Tsuchida, M.A., Amodaj, N., Pinkard, H., Vale, R.D. & Stuurman, N. (2014). Advanced methods of microscope control using µManager software. *Journal of Biological Methods* **1**, 10.
- Elden, A.C., Kim, H.-J., Hart, M.P., Chen-Plotkin, A.S., Johnson, B.S., Fang, X., Armakola, M., Geser, F., Greene, R., Lu, M.M., Padmanabhan, A., Clay-Falcone, D., McCluskey, L., Elman, L., Jühr, D., Gruber, P.J., Rüb, U., Auburger, G., Trojanowski, J.Q., Lee, V.M.-Y., Van Deerlin, V.M., Bonini, N.M. & Gitler, A.D. (2010). Ataxin-2 intermediate-length polyglutamine expansions are associated with increased risk for ALS. *Nature* **466**, 1069–75.

- Ernfors, P., Andreas, H., Olson, L. & Persson, H. (1989a). Expression of nerve growth factor receptor mRNA is developmentally regulated and increased after axotomy in rat spinal cord motoneurons. *Cell* **2**, 1605–1613.
- Ernfors, P., Henschen, A., Olson, L. & Persson, H. (1989b). Expression of nerve growth factor receptor mRNA is developmentally regulated and increased after axotomy in rat spinal cord motoneurons. *Neuron* **2**, 1605–1613.
- Esposito, D., Patel, P., Stephens, R.M., Perez, P., Chao, M. V, Kaplan, D.R. & Hempstead, B.L. (2001). The cytoplasmic and transmembrane domains of the p75 and Trk A receptors regulate high affinity binding to nerve growth factor. *The Journal of biological chemistry* **276**, 32687–95.
- Farg, M.A., Soo, K.Y., Walker, A.K., Pham, H., Orian, J., Horne, M.K., Warraich, S.T., Williams, K.L., Blair, I.P. & Atkin, J.D. (2012). Mutant FUS induces endoplasmic reticulum stress in amyotrophic lateral sclerosis and interacts with protein disulfide-isomerase. *Neurobiology of aging* **43**.
- Fecto, F., Yan, J., Vemula, S.P., Liu, E., Yang, Y., Chen, W., Zheng, J.G., Shi, Y., Siddique, N., Arrat, H., Donkervoort, S., Ajroud-Driss, S., Sufit, R.L., Heller, S.L., Deng, H.-X. & Siddique, T. (2011). SQSTM1 Mutations in Familial and Sporadic Amyotrophic Lateral Sclerosis. *Archives of Neurology*.
- Feinstein, E., Kimchi, A., Wallach, D., Boldin, M. & Varfolomeev, E. (1995). The death domain: a module shared by proteins with diverse cellular functions. *Trends in biochemical sciences*.
- Felgner, P.L., Gadek, T.R., Holm, M., Roman, R., Chan, H.W., Wenz, M., Northrop, J.P., Ringold, G.M. & Danielsen, M. (1987). Lipofection: a highly efficient, lipid-mediated DNA-transfection procedure. *Proceedings of the National Academy of Sciences of the United States of America* **84**, 7413–7.
- Figlewicz, D.A., Krizus, A., Martinoli, M.G., Meininger, V., Dib, M., Rouleau, G.A. & Julien, J.P. (1994). Variants of the heavy neurofilament subunit are associated with the development of amyotrophic lateral sclerosis. *Human molecular genetics*.
- Frey, D., Schneider, C., Xu, L., Borg, J., Spooren, W. & Caroni, P. (2000). Early and selective loss of neuromuscular synapse subtypes with low sprouting competence in motoneuron diseases. *The Journal of neuroscience* **20**, 2534–42.
- Friese, A., Kaltschmidt, J.A., Ladle, D.R., Sigrist, M., Jessell, T.M. & Arber, S. (2009). Gamma and alpha motor neurons distinguished by expression of transcription factor Err3. *Proceedings of the National Academy of Sciences of the United States of America* **106**, 13588–93.
- Fukui, Y., Ohtori, S., Yamashita, M., Yamauchi, K., Inoue, G., Suzuki, M., Orita, S., Eguchi, Y., Ochiai, N., Kishida, S., Takaso, M., Wakai, K., Hayashi, Y., Aoki, Y. & Takahashi, K. (2010). Low affinity NGF receptor (p75 neurotrophin receptor) inhibitory antibody

- reduces pain behavior and CGRP expression in DRG in the mouse sciatic nerve crush model. *Journal of Orthopaedic Research* **28**, 279–283.
- Furukawa, Y., Fu, R., Deng, H.-X., Siddique, T. & O’Halloran, T. V. (2006). Disulfide cross-linked protein represents a significant fraction of ALS-associated Cu, Zn-superoxide dismutase aggregates in spinal cords of model mice. *Proceedings of the National Academy of Sciences of the United States of America* **103**, 7148–53.
- Van Gaal, E.V.B., Van Eijk, R., Oosting, R.S., Kok, R.J., Hennink, W.E., Crommelin, D.J.A. & Mastrobattista, E. (2011). How to screen non-viral gene delivery systems in vitro? *Journal of Controlled Release* **154**, 218–232.
- Gage, F.H., Batchelor, P., Chen, K.S., Chin, D., Higgins, G.A., Koh, S., Deputy, S., Rosenberg, M.B., Fischer, W. & Bjorklund, A. (1989). NGF receptor reexpression and NGF-mediated cholinergic neuronal hypertrophy in the damaged adult neostriatum. *Neuron* **2**, 1177–84.
- Gibson, S.B. & Bromberg, M.B. (2012). Amyotrophic Lateral Sclerosis: Drug Therapy from Bench to Bedside. *Seminars in Neurology* **32**, 173–178.
- Gil, J., Funalot, B., Verschuere, A., Danel-Brunaud, V., Camu, W., Vandenberghe, N., Desnuelle, C., Guy, N., Camdessanche, J.P., Cintas, P., Carlier, L., Pittion, S., Nicolas, G., Corcia, P., Fleury, M.-C., Maugras, C., Besson, G., Le Masson, G. & Couratier, P. (2008). Causes of death amongst French patients with amyotrophic lateral sclerosis: a prospective study. *European journal of neurology : the official journal of the European Federation of Neurological Societies* **15**, 1245–51.
- Godbey, W.T., Wu, K.K. & Mikos, A.G. (1999). Tracking the intracellular path of poly(ethylenimine)/DNA complexes for gene delivery. *Proceedings of the National Academy of Sciences of the United States of America* **96**, 5177–5181.
- Greenway, M.J., Andersen, P.M., Russ, C., Ennis, S., Cashman, S., Donaghy, C., Patterson, V., Swingler, R., Kieran, D., Prehn, J., Morrison, K.E., Green, A., Acharya, K.R., Brown, R.H. & Hardiman, O. (2006). ANG mutations segregate with familial and “sporadic” amyotrophic lateral sclerosis. *Nature genetics* **38**, 411–3.
- Grob, P.M., Ross, A.H., Koprowski, H. & Bothwell, M. (1985). Characterization of the human melanoma nerve growth factor receptor. *The Journal of biological chemistry* **260**, 8044–9.
- Groen, E.J.N., van Es, M.A., van Vught, P.W.J., Spliet, W.G.M., van Engelen-Lee, J., de Visser, M., Wokke, J.H.J., Schelhaas, H.J., Ophoff, R.A., Fumoto, K., Pasterkamp, R.J., Dooijes, D., Cuppen, E., Veldink, J.H. & van den Berg, L.H. (2010). FUS mutations in familial amyotrophic lateral sclerosis in the Netherlands. *Archives of neurology* **67**, 224–30.
- Gros-Louis, F., Larivière, R., Gowing, G., Laurent, S., Camu, W., Bouchard, J.-P., Meininger, V., Rouleau, G. a & Julien, J.-P. (2004). A frameshift deletion in peripherin

- gene associated with amyotrophic lateral sclerosis. *The Journal of biological chemistry* **279**, 45951–6.
- Guillemard, V., Ivanisevic, L., Garcia, A.G., Scholten, V., Lazo, O.M., Bronfman, F.C. & Saragovi, H.U. (2010). An agonistic mAb directed to the TrkC receptor juxtamembrane region defines a trophic hot spot and interactions with p75 coreceptors. *Developmental neurobiology* **70**, 150–64.
- Gurney, M., Cutting, F. & Zhai, P. (1996). Benefit of vitamin E, riluzole, and gababapentin in a transgenic model of familial amyotrophic lateral sclerosis. *Annals of neurology* **39**, 147–157.
- Gurney, M., Pu, H., Chiu, A., Dal Canto, M., Polchow, C., Alexander, D., Caliendo, J., Hentati, A., Kwon, Y., Deng, H., Chen, C., Zhai, P., Sufit, R. & Siddique, T. (1994). Motor neuron degeneration in mice that express a human Cu, Zn superoxide dismutase mutation. *Science* **264**, 1772–5.
- Gurney, M.E. (1997). The use of transgenic mouse models of amyotrophic lateral sclerosis in preclinical drug studies. In *Journal of the Neurological Sciences: S67–73*.
- Gurney, M.E., Fleck, T.J., Himes, C.S. & Hall, E.D. (1998). Riluzole preserves motor function in a transgenic model of familial amyotrophic lateral sclerosis. *Neurology* **50**, 62–66.
- Hadaczek, P., Eberling, J.L., Pivrotto, P., Bringas, J., Forsayeth, J. & Bankiewicz, K.S. (2010). Eight years of clinical improvement in MPTP-lesioned primates after gene therapy with AAV2-hAADC. *Molecular therapy : the journal of the American Society of Gene Therapy* **18**, 1458–61.
- Hai, T., Wolfgang, C., Marsee, D., Allen, A. & Sivaprasad, U. (1999). ATF3 and stress responses. *Gene expression* **7**, 321–35.
- Hallböök, F. (1999). Evolution of the vertebrate neurotrophin and Trk receptor gene families. *Current opinion in neurobiology* **9**, 616–21.
- Hamburger, V. (1934). The effects of wing bud extirpation on the development of the central nervous system in chick embryos. *Journal of Experimental Zoology* **68**, 449–494.
- Hamburger, V. & Levi-Montalcini, R. (1949). Proliferation, differentiation and degeneration in the spinal ganglia of the chick embryo under normal and experimental conditions. *The Journal of experimental zoology* **111**, 457–501.
- Hanzlikova, M., Ruponen, M., Galli, E., Rasmaja, A., Aseyev, V., Tenhu, H., Urtti, A. & Yliperttula, M. (2011). Mechanisms of polyethylenimine-mediated DNA delivery: free carrier helps to overcome the barrier of cell-surface glycosaminoglycans. *The Journal of Gene Medicine* **13**, 402–409.
- Hatzipetros, T., Bogdanik, L.P., Tassinari, V.R., Kidd, J.D., Moreno, A.J., Davis, C., Osborne, M., Austin, A., Vieira, F.G., Lutz, C. & Perrin, S. (2014). C57BL/6J congenic

- Prp-TDP43A315T mice develop progressive neurodegeneration in the myenteric plexus of the colon without exhibiting key features of ALS. *Brain research* **1584**, 59–72.
- Heiman-Patterson, T.D., Deitch, J.S., Blankenhorn, E.P., Erwin, K.L., Perreault, M.J., Alexander, B.K., Byers, N., Toman, I. & Alexander, G.M. (2005). Background and gender effects on survival in the TgN(SOD1-G93A)1Gur mouse model of ALS. *Journal of the neurological sciences* **236**, 1–7.
- Hempstead, B.L., Martin-Zanca, D., Kaplan, D.R., Parada, L.F. & Chao, M. V. (1991). High-affinity NGF binding requires coexpression of the trk proto-oncogene and the low-affinity NGF receptor. *Nature* **350**, 678–683.
- Henderson, C.E., Camu, W., Mettling, C., Gouin, A., Poulsen, K., Karihaloo, M., Rullamas, J., Evans, T., McMahon, S.B. & Armanini, M.P. (1993). Neurotrophins promote motor neuron survival and are present in embryonic limb bud. *Nature* **363**, 266–270.
- Henderson, C.E., Phillips, H.S., Pollock, R.A., Davies, A.M., Lemeulle, C., Armanini, M., Simpson, L.C., Moffet, B. & Vandlen, R.A. (1994). Factor for GDNF : Potent Survival Present in Peripheral Motoneurons Muscle. *Science* **266**, 1992–1995.
- Hengartner, M.O. (2000). The biochemistry of apoptosis. *Nature* **407**, 770–6.
- Henneman, E., Somjen, G. & Carpenter, D.O. (1964). Functional Significance of Cell Size in Spinal Motoneurons. *Journal of Neurophysiology* **28**, 560–580.
- Herron, L.R. & Miles, G.B. (2012). Gender-specific perturbations in modulatory inputs to motoneurons in a mouse model of amyotrophic lateral sclerosis. *Neuroscience* **226**, 313–23.
- Herrup, K. & Shooter, E.M. (1973). Properties of the beta nerve growth factor receptor of avian dorsal root ganglia. *Proceedings of the National Academy of Sciences of the United States of America* **70**, 3884–8.
- Higgins, C.M.J., Jung, C., Ding, H. & Xu, Z. (2002). Mutant Cu, Zn superoxide dismutase that causes motoneuron degeneration is present in mitochondria in the CNS. *The Journal of neuroscience : the official journal of the Society for Neuroscience* **22**, RC215.
- Hitomi, J., Katayama, T., Eguchi, Y., Kudo, T., Taniguchi, M., Koyama, Y., Manabe, T., Yamagishi, S., Bando, Y., Imaizumi, K., Tsujimoto, Y. & Tohyama, M. (2004). Involvement of caspase-4 in endoplasmic reticulum stress-induced apoptosis and Abeta-induced cell death. *The Journal of cell biology* **165**, 347–56.
- Holzbaun, E.L.F. (2004). Motor neurons rely on motor proteins. *Trends in cell biology* **14**, 233–40.
- Hu, B., Yip, H.K. & So, K.F. (1998). Localization of p75 neurotrophin receptor in the retina of the adult SD rat: an immunocytochemical study at light and electron microscopic levels. *Glia* **24**, 187–97.

- Hu, W.W., Syu, W.J., Chen, W.Y., Ruaan, R.C., Cheng, Y.C., Chien, C.C., Li, C., Chung, C.A. & Tsao, C.W. (2012). Use of biotinylated chitosan for substrate-mediated gene delivery. *Bioconjugate Chemistry* **23**, 1587–1599.
- Huang, A., Noga, B., Carr, P., Fedirchuk, B. & Jordan, L. (2000). Spinal cholinergic neurons activated during locomotion: localization and electrophysiological characterization. *Journal of Neurophysiology* **83**, 3537–3547.
- Huang, E.J. & Reichardt, L.F. (2003). Trk receptors: roles in neuronal signal transduction. *Annual review of biochemistry* **72**, 609–42.
- Huang, H.-N., Li, T.-L., Chan, Y.-L., Chen, C.-L. & Wu, C.-J. (2009). Transdermal immunization with low-pressure-gene-gun mediated chitosan-based DNA vaccines against Japanese encephalitis virus. *Biomaterials* **30**, 6017–6025.
- Ince, P., Stout, N., Shaw, P., Slade, J., Hunziker, W., Heizmann, C.W. & Baimbridge, K.G. (1993). Parvalbumin and calbindin D-28k in the human motor system and in motor neuron disease. *Neuropathology and applied neurobiology* **19**, 291–299.
- Ince, P.G., Highley, J.R., Kirby, J., Wharton, S.B., Takahashi, H., Strong, M.J. & Shaw, P.J. (2011). Molecular pathology and genetic advances in amyotrophic lateral sclerosis: An emerging molecular pathway and the significance of glial pathology. *Acta Neuropathologica*.
- Ip, N.Y., Ibáñez, C.F., Nye, S.H., McClain, J., Jones, P.F., Gies, D.R., Belluscio, L., Le Beau, M.M., Espinosa, R. & Squinto, S.P. (1992). Mammalian neurotrophin-4: structure, chromosomal localization, tissue distribution, and receptor specificity. *Proceedings of the National Academy of Sciences of the United States of America* **89**, 3060–3064.
- Itaka, K., Harada, A., Yamasaki, Y., Nakamura, K., Kawaguchi, H. & Kataoka, K. (2004). In situ single cell observation by fluorescence resonance energy transfer reveals fast intracytoplasmic delivery and easy release of plasmid DNA complexed with linear polyethylenimine. *The journal of gene medicine* **6**, 76–84.
- Itoh, N., Yonehara, S., Ishii, A., Yonehara, M., Mizushima, S., Sameshima, M., Hase, A., Seto, Y. & Nagata, S. (1991). The polypeptide encoded by the cDNA for human cell surface antigen Fas can mediate apoptosis. *Cell* **66**, 233–43.
- Jaarsma, D., Rognoni, F., van Duijn, W., Verspaget, H.W., Haasdijk, E.D. & Holstege, J.C. (2001). CuZn superoxide dismutase (SOD1) accumulates in vacuolated mitochondria in transgenic mice expressing amyotrophic lateral sclerosis-linked SOD1 mutations. *Acta neuropathologica* **102**, 293–305.
- Je, H.S., Yang, F., Ji, Y., Potluri, S., Fu, X.-Q., Luo, Z.-G., Nagappan, G., Chan, J.P., Hempstead, B., Son, Y.-J. & Lu, B. (2013). ProBDNF and mature BDNF as punishment and reward signals for synapse elimination at mouse neuromuscular junctions. *The Journal of neuroscience* **33**, 9957–62.

- Jing, S., Tapley, P. & Barbacid, M. (1992). Nerve growth factor mediates signal transduction through trk homodimer receptors. *Neuron* **9**, 1067–1079.
- Jing, S., Wen, D., Yu, Y., Holst, P.L., Luo, Y., Fang, M., Tamir, R., Antonio, L., Hu, Z., Cupples, R., Louis, J.C., Hu, S., Altmann, B.W. & Fox, G.M. (1996). GDNF-induced activation of the Ret protein tyrosine kinase is mediated by GDNFR- β , a novel receptor for GDNF. *Cell* **85**, 1113–1124.
- Johnson, B.S., Snead, D., Lee, J.J., McCaffery, J.M., Shorter, J. & Gitler, A.D. (2009). TDP-43 is intrinsically aggregation-prone, and amyotrophic lateral sclerosis-linked mutations accelerate aggregation and increase toxicity. *The Journal of biological chemistry* **284**, 20329–39.
- Johnson, D., Lanahan, A., Buck, C.R., Sehgal, A., Morgan, C., Mercer, E., Bothwell, M. & Chao, M. (1986). Expression and structure of the human NGF receptor. *Cell* **47**, 545–54.
- Johnson, J.O., Mandrioli, J., Benatar, M., Abramzon, Y., Van Deerlin, V.M., Trojanowski, J.Q., Gibbs, J.R., Brunetti, M., Gronka, S., Wu, J., Ding, J., McCluskey, L., Martinez-Lage, M., Falcone, D., Hernandez, D.G., Arepalli, S., Chong, S., Schymick, J.C., Rothstein, J., Landi, F., Wang, Y.-D., Calvo, A., Mora, G., Sabatelli, M., Monsurro, M.R., Battistini, S., Salvi, F., Spataro, R., Sola, P., Borghero, G., Galassi, G., Scholz, S.W., Taylor, J.P., Restagno, G., Chiò, A. & Traynor, B.J. (2010). Exome sequencing reveals VCP mutations as a cause of familial ALS. *Neuron* **68**, 857–64.
- Johnson, J.O., Pioro, E.P., Boehringer, A., Chia, R., Feit, H., Renton, A.E., Pliner, H. a, Abramzon, Y., Marangi, G., Winborn, B.J., Gibbs, J.R., Nalls, M. a, Morgan, S., Shoai, M., Hardy, J., Pittman, A., Orrell, R.W., Malaspina, A., Sidle, K.C., Fratta, P., Harms, M.B., Baloh, R.H., Pestronk, A., Weihl, C.C., Rogaeva, E., Zinman, L., Drory, V.E., Borghero, G., Mora, G., Calvo, A., Rothstein, J.D., Drepper, C., Sendtner, M., Singleton, A.B., Taylor, J.P., Cookson, M.R., Restagno, G., Sabatelli, M., Bowser, R., Chiò, A. & Traynor, B.J. (2014). Mutations in the Matrin 3 gene cause familial amyotrophic lateral sclerosis. *Nature neuroscience* **17**, 664–6.
- Johnston, J.A., Dalton, M.J., Gurney, M.E. & Kopito, R.R. (2000). Formation of high molecular weight complexes of mutant Cu, Zn-superoxide dismutase in a mouse model for familial amyotrophic lateral sclerosis. *Proceedings of the National Academy of Sciences of the United States of America* **97**, 12571–6.
- Jung, K.-M., Tan, S., Landman, N., Petrova, K., Murray, S., Lewis, R., Kim, P.K., Kim, D.S., Ryu, S.H., Chao, M. V & Kim, T.-W. (2003). Regulated intramembrane proteolysis of the p75 neurotrophin receptor modulates its association with the TrkA receptor. *The Journal of biological chemistry* **278**, 42161–9.
- Kabashi, E., Agar, J.N., Taylor, D.M., Minotti, S. & Durham, H.D. (2004). Focal dysfunction of the proteasome: a pathogenic factor in a mouse model of amyotrophic lateral sclerosis. *Journal of neurochemistry* **89**, 1325–35.

- Kai, E. & Ochiya, T. (2004). A method for oral DNA delivery with N-acetylated chitosan. *Pharmaceutical research* **21**, 838–43.
- Kanning, K., Kaplan, A. & Henderson, C. (2010). Motor neuron diversity in development and disease. *Annual review of neuroscience* **33**, 409–440.
- Kanning, K.C., Hudson, M., Amieux, P.S., Wiley, J.C., Bothwell, M. & Schecterson, L.C. (2003). Proteolytic processing of the p75 neurotrophin receptor and two homologs generates C-terminal fragments with signaling capability. *The Journal of neuroscience : the official journal of the Society for Neuroscience* **23**, 5425–5436.
- Kaplan, D.R., Hempstead, B.L., Martin-Zanca, D., Chao, M. V & Parada, L.F. (1991). The trk proto-oncogene product: a signal transducing receptor for nerve growth factor. *Science (New York, N.Y.)* **252**, 554–558.
- Kaplan, D.R. & Miller, F.D. (2000). Neurotrophin signal transduction in the nervous system. *Current opinion in neurobiology* **10**, 381–91.
- Karpati, G. (2010). *Disorders of Voluntary Muscle*. 8th edn. Cambridge University: Cambridge University Press.
- Kaspar, B.K., Lladó, J., Sherkat, N., Rothstein, J.D. & Gage, F.H. (2003). Retrograde viral delivery of IGF-1 prolongs survival in a mouse ALS model. *Science (New York, N.Y.)* **301**, 839–842.
- Kato, S. (2008). Amyotrophic lateral sclerosis models and human neuropathology: similarities and differences. *Acta neuropathologica* **115**, 97–114.
- Kaufman, R.J. (2002). Orchestrating the unfolded protein response in health and disease. *Journal of Clinical Investigation* **110**, 1389–1398.
- Kenchappa, R.S., Tep, C., Korade, Z., Urra, S., Bronfman, F.C., Yoon, S.O. & Carter, B.D. (2010). p75 neurotrophin receptor-mediated apoptosis in sympathetic neurons involves a biphasic activation of JNK and up-regulation of tumor necrosis factor-alpha-converting enzyme/ADAM17. *The Journal of biological chemistry* **285**, 20358–68.
- Kenchappa, R.S., Zampieri, N., Chao, M. V, Barker, P. a, Teng, H.K., Hempstead, B.L. & Carter, B.D. (2006). Ligand-dependent cleavage of the P75 neurotrophin receptor is necessary for NRIF nuclear translocation and apoptosis in sympathetic neurons. *Neuron* **50**, 219–32.
- Kerkhoff, H., Jennekens, F., Troost, D. & Veldman, H. (1991). Nerve growth factor receptor immunostaining in the spinal cord and peripheral nerves in amyotrophic lateral sclerosis. *Acta neuropathologica* **81**, 649–656.
- Khodorova, A., Nicol, G.D. & Strichartz, G. (2013). The p75NTR signaling cascade mediates mechanical hyperalgesia induced by nerve growth factor injected into the rat hind paw. *Neuroscience* **254**, 312–323.

- Kiernan, M.C., Vucic, S., Cheah, B.C., Turner, M.R., Eisen, A., Hardiman, O., Burrell, J.R. & Zoing, M.C. (2011). Amyotrophic lateral sclerosis. *Lancet* **377**, 942–55.
- Kirchheis, R., Kichler, A., Wallner, G., Kursa, M., Ogris, M., Felzmann, T., Buchberger, M. & Wagner, E. (1997). Coupling of cell-binding ligands to polyethylenimine for targeted gene delivery. *Gene therapy* **4**, 409–418.
- Kirchheis, R., Wightman, L. & Wagner, E. (2001). Design and gene delivery activity of modified polyethylenimines. *Advanced drug delivery reviews* **53**, 341–58.
- Kitamura, K., Fujiyoshi, K., Yamane, J., Toyota, F., Hikishima, K., Nomura, T., Funakoshi, H., Nakamura, T., Aoki, M., Toyama, Y., Okano, H. & Nakamura, M. (2011). Human Hepatocyte Growth Factor Promotes Functional Recovery in Primates after Spinal Cord Injury. *PLoS ONE* **6**, e27706.
- Klein, R., Jing, S., Nanduri, V., O'Rourke, E. & Barbacid, M. (1991a). The trk proto-oncogene encodes a receptor for nerve growth factor. *Cell* **65**, 189–197.
- Klein, R., Nanduri, V., Jing, S. & Lamballe, F. (1991b). The trkB tyrosine protein kinase is a receptor for brain-derived neurotrophic factor and neurotrophin-3. *Cell* **66**.
- Klein, R., Parada, L.F., Coulier, F. & Barbacid, M. (1989). trkB, a novel tyrosine protein kinase receptor expressed during mouse neural development. *The EMBO journal* **8**, 3701–3709.
- Klein, R.L., Muir, D., King, M.A., Peel, A.L., Zolotukhin, S., Möller, J.C., Krüttgen, A., Heymach, J. V, Muzyczka, N. & Meyer, E.M. (1999). Long-term actions of vector-derived nerve growth factor or brain-derived neurotrophic factor on choline acetyltransferase and Trk receptor levels in the adult rat basal forebrain. *Neuroscience* **90**, 815–21.
- Konishi, M., Kawamoto, K., Izumikawa, M., Kuriyama, H. & Yamashita, T. (2008). Gene transfer into guinea pig cochlea using adeno-associated virus vectors. *The journal of gene medicine* **10**, 610–618.
- Kriz, J., Gowing, G. & Julien, J.-P. (2003). Efficient three-drug cocktail for disease induced by mutant superoxide dismutase. *Annals of neurology* **53**, 429–36.
- Kustikova, O., Brugman, M. & Baum, C. (2010). The genomic risk of somatic gene therapy. *Seminars in cancer biology* **20**, 269–78.
- Kwiatkowski, T.J., Bosco, D.A., Leclerc, A.L., Tamrazian, E., Vanderburg, C.R., Russ, C., Davis, A., Gilchrist, J., Kasarskis, E.J., Munsat, T., Valdmanis, P., Rouleau, G.A., Hosler, B.A., Cortelli, P., de Jong, P.J., Yoshinaga, Y., Haines, J.L., Pericak-Vance, M.A., Yan, J., Ticozzi, N., Siddique, T., McKenna-Yasek, D., Sapp, P.C., Horvitz, H.R., Landers, J.E. & Brown, R.H. (2009). Mutations in the FUS/TLS gene on chromosome 16 cause familial amyotrophic lateral sclerosis. *Science (New York, N.Y.)* **323**, 1205–8.
- Lacomblez, L., Bensimon, G., Meininger, V., Leigh, P. & Guillet, P. (1996). Dose-ranging

- study of riluzole in amyotrophic lateral sclerosis. *The Lancet* **347**, 1425–1431.
- Lagier-Tourenne, C., Polymenidou, M., Hutt, K.R., Vu, A.Q., Baughn, M., Huelga, S.C., Clutario, K.M., Ling, S.-C., Liang, T.Y., Mazur, C., Wancewicz, E., Kim, A.S., Watt, A., Freier, S., Hicks, G.G., Donohue, J.P., Shiue, L., Bennett, C.F., Ravits, J., Cleveland, D.W. & Yeo, G.W. (2012). Divergent roles of ALS-linked proteins FUS/TLS and TDP-43 intersect in processing long pre-mRNAs. *Nature neuroscience* **15**, 1488–97.
- Lalli, G. & Schiavo, G. (2002). Analysis of retrograde transport in motor neurons reveals common endocytic carriers for tetanus toxin and neurotrophin receptor p75NTR. *The Journal of cell biology* **156**, 233–9.
- Lam, A. & Dean, D. (2010). Progress and prospects: nuclear import of nonviral vectors. *Gene therapy* **17**, 439–447.
- Lamballe, F., Klein, R. & Barbacid, M. (1991). trkC, a new member of the trk family of tyrosine protein kinases, is a receptor for neurotrophin-3. *Cell* **66**, 967–979.
- Lange, A., Mills, R.E., Lange, C.J., Stewart, M., Devine, S.E. & Corbett, A.H. (2007). Classical nuclear localization signals: definition, function, and interaction with importin alpha. *The Journal of biological chemistry* **282**, 5101–5.
- Lebrun-Julien, F., Bertrand, M.J., De Backer, O., Stellwagen, D., Morales, C.R., Di Polo, A. & Barker, P.A. (2010). ProNGF induces TNFalpha-dependent death of retinal ganglion cells through a p75NTR non-cell-autonomous signaling pathway. *Proceedings of the National Academy of Sciences of the United States of America* **107**, 3817–3822.
- Lebrun-Julien, F., Morquette, B., Douillette, A., Saragovi, H.U. & Di Polo, A. (2009). Inhibition of p75NTR in glia potentiates TrkA-mediated survival of injured retinal ganglion cells. *Molecular and Cellular Neuroscience* **40**, 410–420.
- Lee, K.F., Li, E., Huber, L.J., Landis, S.C., Sharpe, A.H., Chao, M. V & Jaenisch, R. (1992). Targeted mutation of the gene encoding the low affinity NGF receptor p75 leads to deficits in the peripheral sensory nervous system. *Cell* **69**, 737–49.
- Lee, R., Kermani, P., Teng, K.K. & Hempstead, B.L. (2001). Regulation of cell survival by secreted proneurotrophins. *Science (New York, N.Y.)*.
- Lefebvre, S., Bürglen, L., Reboullet, S., Clermont, O., Burlet, P., Viollet, L., Benichou, B., Cruaud, C., Millasseau, P. & Zeviani, M. (1995). Identification and characterization of a spinal muscular atrophy-determining gene. *Cell* **80**, 155–165.
- Leigh, P.N., Whitwell, H., Garofalo, O., Buller, J., Swash, M., Martin, J.E., Gallo, J.-M., Weller, R.O. & Anderton, B.H. (1991). Ubiquitin-Immunoreactive Intraneuronal Inclusions in Amyotrophic Lateral Sclerosis. *Brain* **114**, 775–788.
- Lentz, T.B., Gray, S.J. & Samulski, R.J. (2012). Viral vectors for gene delivery to the central nervous system. *Neurobiology of Disease* **48**, 179–188.

- Levi-Montalcini, R. (1987). The nerve growth factor 35 years later. *Science (New York, N.Y.)* **237**, 1154–1162.
- Lewis, P. & Emerman, M. (1994). Passage through mitosis is required for oncoretroviruses but not for the human immunodeficiency virus. *Journal of virology* **68**, 510–516.
- Li, S., Rizzo, M.A., Bhattacharya, S. & Huang, L. (1998). Characterization of cationic lipid-protamine-DNA (LPD) complexes for intravenous gene delivery. *Gene therapy* **5**, 930–937.
- Li, W., Ochalski, P.A., Brimijoin, S., Jordan, L.M. & Nagy, J.I. (1995). C-terminals on motoneurons: electron microscope localization of cholinergic markers in adult rats and antibody-induced depletion in neonates. *Neuroscience* **65**, 879–91.
- Li, W. & Szoka, F.C. (2007). Lipid-based nanoparticles for nucleic acid delivery. *Pharmaceutical research* **24**, 438–49.
- Ling, S.-C., Polymenidou, M. & Cleveland, D.W. (2013). Converging mechanisms in ALS and FTD: disrupted RNA and protein homeostasis. *Neuron* **79**, 416–38.
- Litzinger, D.C., Brown, J.M., Wala, I., Kaufman, S.A., Farrell, C.L., Collins, D. & others. (1996). Fate of cationic liposomes and their complex with oligonucleotide in vivo. *Biochimica et Biophysica Acta (BBA)-Biomembranes* **1281**, 139–149.
- Liu-Yesucevitz, L., Bilgutay, A., Zhang, Y.-J., Vanderweyde, T., Vanderwyde, T., Citro, A., Mehta, T., Zaarur, N., McKee, A., Bowser, R., Sherman, M., Petrucelli, L. & Wolozin, B. (2010). Tar DNA binding protein-43 (TDP-43) associates with stress granules: analysis of cultured cells and pathological brain tissue. *PloS one* **5**, e13250.
- Lomen-Hoerth, C., Anderson, T. & Miller, B. (2002). The overlap of amyotrophic lateral sclerosis and frontotemporal dementia. *Neurology* **59**, 1077–9.
- Loureiro, J.A., Gomes, B., Fricker, G., Cardoso, I., Ribeiro, C.A., Gaiteiro, C., Coelho, M.A.N., Pereira, M.D.C. & Rocha, S. (2015). Dual ligand immunoliposomes for drug delivery to the brain. *Colloids and Surfaces B: Biointerfaces* **134**, 213–219.
- Lowe, J., Lennox, G., Jefferson, D., Morrell, K., McQuire, D., Gray, T., Landon, M., Doherty, F.J. & Mayer, R.J. (1988). A filamentous inclusion body within anterior horn neurones in motor neurone disease defined by immunocytochemical localisation of ubiquitin. *Neuroscience letters* **94**, 203–210.
- Lowry, K., Murray, S., McLean, C., Talman, P., Mathers, S., Lopes, E. & Cheema, S. (2001). A potential role for the p75 low-affinity neurotrophin receptor in spinal motor neuron degeneration in murine and human amyotrophic lateral sclerosis. *Amyotrophic lateral sclerosis and other motor neuron disorders* **2**, 127–34.
- Ludolph, A.C., Bendotti, C., Blaugrund, E., Chio, A., Greensmith, L., Loeffler, J.-P., Mead, R., Niessen, H.G., Petri, S., Pradat, P.-F., Robberecht, W., Ruegg, M., Schwalenstöcker, B., Stiller, D., van den Berg, L., Vieira, F. & von Horsten, S. (2010). Guidelines for

- preclinical animal research in ALS/MND: A consensus meeting. *Amyotrophic lateral sclerosis : official publication of the World Federation of Neurology Research Group on Motor Neuron Diseases* **11**, 38–45.
- Lynch, J., Behan, N. & Birkinshaw, C. (2007). Factors controlling particle size during nebulization of DNA-polycation complexes. *Journal of aerosol medicine : the official journal of the International Society for Aerosols in Medicine* **20**, 257–268.
- Mackenzie, I.R.A., Bigio, E.H., Ince, P.G., Geser, F., Neumann, M., Cairns, N.J., Kwong, L.K., Forman, M.S., Ravits, J., Stewart, H., Eisen, A., McClusky, L., Kretzschmar, H.A., Monoranu, C.M., Highley, J.R., Kirby, J., Siddique, T., Shaw, P.J., Lee, V.M.-Y. & Trojanowski, J.Q. (2007). Pathological TDP-43 distinguishes sporadic amyotrophic lateral sclerosis from amyotrophic lateral sclerosis with SOD1 mutations. *Annals of neurology* **61**, 427–34.
- Magrané, J., Cortez, C., Gan, W.-B. & Manfredi, G. (2014). Abnormal mitochondrial transport and morphology are common pathological denominators in SOD1 and TDP43 ALS mouse models. *Human molecular genetics* **23**, 1413–24.
- Magrané, J., Hervias, I., Henning, M.S., Damiano, M., Kawamata, H. & Manfredi, G. (2009). Mutant SOD1 in neuronal mitochondria causes toxicity and mitochondrial dynamics abnormalities. *Human molecular genetics* **18**, 4552–64.
- Majounie, E., Renton, A.E., Mok, K., Dopper, E.G., Waite, A., Rollinson, S., Chiò, A., Restagno, G., Nicolaou, N., Simon-Sanchez, J., van Swieten, J.C., Abramzon, Y., Johnson, J.O., Sendtner, M., Pamphlett, R., Orrell, R.W., Mead, S., Sidle, K.C., Houlden, H., Rohrer, J.D., Morrison, K.E., Pall, H., Talbot, K., Ansorge, O., Hernandez, D.G., Arepalli, S., Sabatelli, M., Mora, G., Corbo, M., Giannini, F., Calvo, A., Englund, E., Borghero, G., Floris, G.L., Remes, A.M., Laaksovirta, H., McCluskey, L., Trojanowski, J.Q., Van Deerlin, V.M., Schellenberg, G.D., Nalls, M. a, Drory, V.E., Lu, C.-S., Yeh, T.-H., Ishiura, H., Takahashi, Y., Tsuji, S., Le Ber, I., Brice, A., Drepper, C., Williams, N., Kirby, J., Shaw, P., Hardy, J., Tienari, P.J., Heutink, P., Morris, H.R., Pickering-Brown, S. & Traynor, B.J. (2012). Frequency of the C9orf72 hexanucleotide repeat expansion in patients with amyotrophic lateral sclerosis and frontotemporal dementia: a cross-sectional study. *Lancet neurology* **4422**, 1–8.
- Malek, A., Merkel, O., Fink, L., Czubyko, F., Kissel, T. & Aigner, A. (2009). In vivo pharmacokinetics, tissue distribution and underlying mechanisms of various PEI(-PEG)/siRNA complexes. *Toxicology and Applied Pharmacology* **236**, 97–108.
- Manjappa, A.S., Chaudhari, K.R., Venkataraju, M.P., Dantuluri, P., Nanda, B., Sidda, C., Sawant, K.K. & Ramachandra Murthy, R.S. (2011). Antibody derivatization and conjugation strategies: Application in preparation of stealth immunoliposome to target chemotherapeutics to tumor. *Journal of Controlled Release* **150**, 2–22.
- Martin, L., Liu, Z., Chen, K., Price, A., Pan, Y., Swaby, J. & Golden, W. (2007). Motor

- neuron degeneration in amyotrophic lateral sclerosis mutant superoxide dismutase-1 transgenic mice: Mechanisms of mitochondriopathy and cell death. *The Journal of comparative neurology* **500**, 20–46.
- Martin, S.J. & Green, D.R. (1995). Protease activation during apoptosis: death by a thousand cuts? *Cell* **82**, 349–352.
- Martin-zanca, D., Oskam, R., Mitra, G., Copeland, T. & Barbacid, M. (1989). Molecular and Biochemical Characterization of the Human trk Proto-Oncogene. *Molecular and Cellular Biology*.
- Maruyama, H., Morino, H., Ito, H., Izumi, Y., Kato, H., Watanabe, Y., Kinoshita, Y., Kamada, M., Nodera, H., Suzuki, H., Komure, O., Matsuura, S., Kobatake, K., Morimoto, N., Abe, K., Suzuki, N., Aoki, M., Kawata, A., Hirai, T., Kato, T., Ogasawara, K., Hirano, A., Takumi, T., Kusaka, H., Hagiwara, K., Kaji, R. & Kawakami, H. (2010). Mutations of optineurin in amyotrophic lateral sclerosis. *Nature* **465**, 223–6.
- Mattiazzi, M., D'Aurelio, M., Gajewski, C.D., Martushova, K., Kiaei, M., Beal, M.F. & Manfredi, G. (2002). Mutated human SOD1 causes dysfunction of oxidative phosphorylation in mitochondria of transgenic mice. *The Journal of biological chemistry* **277**, 29626–33.
- Matusica, D., Fenech, M.P., Rogers, M.L. & Rush, R.A. (2008). Characterization and use of the NSC-34 cell line for study of neurotrophin receptor trafficking. *Journal of Neuroscience Research* **86**, 553–565.
- McHanwell, S. & Biscoe, T.J. (1981). The sizes of motoneurons supplying hindlimb muscles in the mouse. *Proceedings of the Royal Society of London. Series B, Containing papers of a Biological character. Royal Society (Great Britain)* **213**, 201–216.
- McLean, J.W., Fox, E.A., Baluk, P., Bolton, P.B., Haskell, A., Pearlman, R., Thurston, G., Umemoto, E.Y. & McDonald, D.M. (1997). Organ-specific endothelial cell uptake of cationic liposome-DNA complexes in mice. *The American journal of physiology* **273**, H387–H404.
- McPhedran, A., Wuerker, R. & Henneman, E. (1965). Properties of motor units in a homogeneous red muscle (soleus) of the cat. *Journal of neurophysiology* **28**, 71–84.
- McPhedran, A.M., Wuerker, R.B. & Henneman, E. (1965). Properties of Motor Units in a Heterogeneous Pale Muscle (M. Gastrocnemius) of the Cat. *Journal of neurophysiology* **28**, 85–99.
- Meininger, V., Pradat, P.F., Corse, A., Al-Sarraj, S., Brooks, B.R., Caress, J.B., Cudkovicz, M., Kolb, S.J., Lange, D., Leigh, P.N., Meyer, T., Milleri, S., Morrison, K.E., Orrell, R.W., Peters, G., Rothstein, J.D., Shefner, J., Lavrov, A., Williams, N., Overend, P., Price, J., Bates, S., Bullman, J., Krull, D., Berges, A., Abila, B., Meno-Tetang, G. & Wurthner, J. (2014). Safety, pharmacokinetic, and functional effects of the Nogo-A

- monoclonal antibody in amyotrophic lateral sclerosis: A randomized, first-in-human clinical trial. *PLoS ONE* **9**.
- Meyerowitz, J., Parker, S.J., Vella, L.J., Ng, D.C.H., Price, K.A., Liddell, J.R., Caragounis, A., Li, Q.-X., Masters, C.L., Nonaka, T., Hasegawa, M., Bogoyevitch, M.A., Kanninen, K.M., Crouch, P.J. & White, A.R. (2011). C-Jun N-terminal kinase controls TDP-43 accumulation in stress granules induced by oxidative stress. *Molecular neurodegeneration* **6**, 57.
- Miles, G.B., Hartley, R., Todd, A.J. & Brownstone, R.M. (2007). Spinal cholinergic interneurons regulate the excitability of motoneurons during locomotion. *Proceedings of the National Academy of Sciences of the United States of America* **104**, 2448–53.
- Miller, L., Leor, J. & Rubinsky, B. (2005). Cancer cells ablation with irreversible electroporation. *Technology in cancer research & treatment* **4**, 699–705.
- Miller, R.G., Jackson, C.E., Kasarskis, E.J., England, J.D., Forshev, D., Johnston, W., Kalra, S., Katz, J.S., Mitsumoto, H., Rosenfeld, J., Shoesmith, C., Strong, M.J. & Woolley, S.C. (2009). Practice Parameter update: The care of the patient with amyotrophic lateral sclerosis: Drug, nutritional, and respiratory therapies (an evidence-based review): Report of the Quality Standards Subcommittee of the American Academy of Neurology. *Neurology* **73**, 2134.
- Miller, R.G., Mitchell, J.D. & Moore, D.H. (2012). Riluzole for amyotrophic lateral sclerosis (ALS)/ motor neuron disease (MND) (Review). *Cochrane Database of Systematic Reviews*.
- Minciacchi, D., Kassa, R.M., Del Tongo, C., Mariotti, R. & Bentivoglio, M. (2009). Voronoi-based spatial analysis reveals selective interneuron changes in the cortex of FALS mice. *Experimental neurology* **215**, 77–86.
- Mintzer, M.A. & Simanek, E.E. (2008). Nonviral Vectors for Gene Delivery. *Chemical Reviews* **109**, 259–302.
- Mischel, P.S., Smith, S.G., Vining, E.R., Valletta, J.S., Mobley, W.C. & Reichardt, L.F. (2001). The extracellular domain of p75^{NTR} is necessary to inhibit neurotrophin-3 signaling through TrkA. *The Journal of biological chemistry* **276**, 11294–301.
- Mishra, S., Webster, P. & Davis, M.E. (2004). PEGylation significantly affects cellular uptake and intracellular trafficking of non-viral gene delivery particles. *European journal of cell biology* **83**, 97–111.
- Mislick, K.A. & Baldeschwieler, J.D. (1996). Evidence for the role of proteoglycans in cation-mediated gene transfer. *Proceedings of the National Academy of Sciences of the United States of America* **93**, 12349–12354.
- Mitchell, J., Paul, P., Chen, H.-J., Morris, A., Payling, M., Falchi, M., Habgood, J., Panoutsou, S., Winkler, S., Tisato, V., Hajitou, A., Smith, B., Vance, C., Shaw, C.,

- Mazarakis, N.D. & de Bellerocche, J. (2010). Familial amyotrophic lateral sclerosis is associated with a mutation in D-amino acid oxidase. *Proceedings of the National Academy of Sciences of the United States of America* **107**, 7556–61.
- Mitsumoto, H. & Rabkin, J.G. (2007). Palliative care for patients with amyotrophic lateral sclerosis: “prepare for the worst and hope for the best”. *JAMA : the journal of the American Medical Association* **298**, 207–216.
- Mizuno, Y., Amari, M., Takatama, M., Aizawa, H., Mihara, B. & Okamoto, K. (2006). Transferrin localizes in Bunina bodies in amyotrophic lateral sclerosis. *Acta neuropathologica* **112**, 597–603.
- Moghimi, S.M., Symonds, P., Murray, J.C., Hunter, A.C., Debska, G. & Szewczyk, A. (2005). A two-stage poly(ethylenimine)-mediated cytotoxicity: Implications for gene transfer/therapy. *Molecular Therapy* **11**, 990–995.
- Mohajeri, M.H., Figlewicz, D.A. & Bohn, M.C. (1998). Selective loss of alpha motoneurons innervating the medial gastrocnemius muscle in a mouse model of amyotrophic lateral sclerosis. *Experimental neurology* **150**, 329–36.
- Moles, E., Urbán, P., Jiménez-Díaz, M.B., Viera-Morilla, S., Angulo-Barturen, I., Busquets, M.A. & Fernández-Busquets, X. (2015). Immunoliposome-mediated drug delivery to Plasmodium-infected and non-infected red blood cells as a dual therapeutic/prophylactic antimalarial strategy. *Journal of Controlled Release* **210**, 217–229.
- Morille, M., Passirani, C., Vonarbourg, A., Clavreul, A. & Benoit, J.-P. (2008). Progress in developing cationic vectors for non-viral systemic gene therapy against cancer. *Biomaterials* **29**, 3477–96.
- Morrall, N., O’Neal, W., Rice, K., Leland, M., Kaplan, J., Piedra, P.A., Zhou, H., Parks, R.J., Velji, R., Aguilar-Córdova, E., Wadsworth, S., Graham, F.L., Kochanek, S., Carey, K.D. & Beaudet, A.L. (1999). Administration of helper-dependent adenoviral vectors and sequential delivery of different vector serotype for long-term liver-directed gene transfer in baboons. *Proceedings of the National Academy of Sciences of the United States of America* **96**, 12816–21.
- Morris, M.C., Chaloin, L., Heitz, F. & Divita, G. (2000). Translocating peptides and proteins and their use for gene delivery. *Current opinion in biotechnology* **11**, 461–6.
- Mufson, E.J. & Kordower, J.H. (1992). Cortical neurons express nerve growth factor receptors in advanced age and Alzheimer disease. *Proceedings of the National Academy of Sciences of the United States of America* **89**, 569–73.
- Mukai, J., Hachiya, T., Shoji-Hoshino, S., Kimura, M.T., Nadano, D., Suvanto, P., Hanaoka, T., Li, Y., Irie, S., Greene, L.A. & Sato, T.A. (2000). NADE, a p75NTR-associated cell death executor, is involved in signal transduction mediated by the common neurotrophin receptor p75NTR. *The Journal of biological chemistry* **275**, 17566–70.

- Münch, C., Sedlmeier, R., Meyer, T., Homberg, V., Sperfeld, A.D., Kurt, A., Prudlo, J., Peraus, G., Hanemann, C.O., Stumm, G. & Ludolph, A.C. (2004). Point mutations of the p150 subunit of dynactin (DCTN1) gene in ALS. *Neurology* **63**, 724–726.
- Nagao, M., Misawa, H., Kato, S. & Hirai, S. (1998). Loss of cholinergic synapses on the spinal motor neurons of amyotrophic lateral sclerosis. *Journal of neuropathology and experimental neurology* **57**, 329–333.
- Nagy, J.I., Yamamoto, T. & Jordan, L.M. (1993). Evidence for the cholinergic nature of C-terminals associated with subsurface cisterns in alpha-motoneurons of rat. *Synapse (New York, N.Y.)* **15**, 17–32.
- Nakagawa, T., Zhu, H., Morishima, N., Li, E., Xu, J., Yankner, B.A. & Yuan, J. (2000). Caspase-12 mediates endoplasmic-reticulum-specific apoptosis and cytotoxicity by amyloid-beta. *Nature* **403**, 98–103.
- Nakazawa, T., Nakazawa, C., Matsubara, A., Noda, K., Hisatomi, T., She, H., Michaud, N., Hafezi-Moghadam, A., Miller, J.W. & Benowitz, L.I. (2006). Tumor necrosis factor-alpha mediates oligodendrocyte death and delayed retinal ganglion cell loss in a mouse model of glaucoma. *The Journal of neuroscience : the official journal of the Society for Neuroscience* **26**, 12633–12641.
- Nardo, G., Iennaco, R., Fusi, N., Heath, P.R., Marino, M., Trolese, M.C., Ferraiuolo, L., Lawrence, N., Shaw, P.J. & Bendotti, C. (2013). Transcriptomic indices of fast and slow disease progression in two mouse models of amyotrophic lateral sclerosis. *Brain* **136**, 3305–3332.
- Nelson, A.L. (2010). Antibody fragments: Hope and hype. *mAbs* **2**, 77–83.
- Neumann, E., Schaefer-Ridder, M. & Wang, Y. (1982). Gene transfer into mouse lymphoma cells by electroporation in high electric fields. *The EMBO* **1**, 841–845.
- Neumann, M., Sampathu, D.M., Kwong, L.K., Truax, A.C., Micsenyi, M.C., Chou, T.T., Bruce, J., Schuck, T., Grossman, M., Clark, C.M., McCluskey, L.F., Miller, B.L., Masliah, E., Mackenzie, I.R., Feldman, H., Feiden, W., Kretschmar, H.A., Trojanowski, J.Q. & Lee, V.M.-Y. (2006). Ubiquitinated TDP-43 in frontotemporal lobar degeneration and amyotrophic lateral sclerosis. *Science (New York, N.Y.)* **314**, 130–3.
- Nishimura, A.L., Mitne-Neto, M., Silva, H.C.A., Richieri-Costa, A., Middleton, S., Cascio, D., Kok, F., Oliveira, J.R.M., Gillingwater, T., Webb, J., Skehel, P. & Zatz, M. (2004). A mutation in the vesicle-trafficking protein VAPB causes late-onset spinal muscular atrophy and amyotrophic lateral sclerosis. *American journal of human genetics* **75**, 822–31.
- Ogris, M., Brunner, S., Schüller, S., Kircheis, R. & Wagner, E. (1999). PEGylated DNA/transferrin-PEI complexes: reduced interaction with blood components, extended circulation in blood and potential for systemic gene delivery. *Gene therapy* **6**, 595–605.

- Okamoto, K., Hirai, S., Amari, M., Watanabe, M. & Sakurai, A. (1993). Bunina bodies in amyotrophic lateral sclerosis immunostained with rabbit anti-cystatin C serum. *Neuroscience Letters* **162**, 125–128.
- Okamoto, K., Mizuno, Y. & Fujita, Y. (2008). Bunina bodies in amyotrophic lateral sclerosis. *Neuropathology : official journal of the Japanese Society of Neuropathology* **28**, 109–115.
- Okura, Y., Arimoto, H., Tanuma, N., Matsumoto, K., Nakamura, T., Yamashima, T., Miyazawa, T. & Matsumoto, Y. (1999). Analysis of neurotrophic effects of hepatocyte growth factor in the adult hypoglossal nerve axotomy model. *The European journal of neuroscience* **11**, 4139–44.
- Opanasopit, P., Nishikawa, M. & Hashida, M. (2002). Factors affecting drug and gene delivery: effects of interaction with blood components. *Critical reviews in therapeutic drug carrier systems* **19**, 191–233.
- Opanasopit, P., Rojanarata, T., Apirakaramwong, A., Ngawhirunpat, T. & Ruktanonchai, U. (2009). Nuclear localization signal peptides enhance transfection efficiency of chitosan/DNA complexes. *International journal of pharmaceutics* **382**, 291–5.
- Oyanagi, K., Ikuta, F. & Horikawa, Y. (1989). Evidence for sequential degeneration of the neurons in the intermediate zone of the spinal cord in amyotrophic lateral sclerosis: a topographic and quantitative investigation. *Acta neuropathologica* **77**, 343–9.
- Pamphlett, R., Luquin, N., McLean, C., Jew, S.K. & Adams, L. (2009). TDP-43 neuropathology is similar in sporadic amyotrophic lateral sclerosis with or without TDP-43 mutations. *Neuropathology and applied neurobiology* **35**, 222–5.
- Panté, N. & Kann, M. (2002). Nuclear pore complex is able to transport macromolecules with diameters of ~ 39 nm. *Molecular biology of the cell* **13**, 425–434.
- Pardridge, W.M. (2006). Molecular Trojan horses for blood-brain barrier drug delivery. *Current opinion in pharmacology* **6**, 494–500.
- Parker, S.J., Meyerowitz, J., James, J.L., Liddell, J.R., Crouch, P.J., Kanninen, K.M. & White, A.R. (2012). Endogenous TDP-43 localized to stress granules can subsequently form protein aggregates. *Neurochemistry International* **60**, 415–424.
- Parkinson, N., Ince, P.G., Smith, M.O., Highley, R., Skibinski, G., Andersen, P.M., Morrison, K.E., Pall, H.S., Hardiman, O., Collinge, J., Shaw, P.J. & Fisher, E.M.C. (2006). ALS phenotypes with mutations in CHMP2B (charged multivesicular body protein 2B). *Neurology* **67**, 1074–7.
- Peñar, M., Cassina, P., Vargas, M.R., Castellanos, R., Viera, L., Beckman, J.S., Estévez, A.G. & Barbeito, L. (2004). Astrocytic production of nerve growth factor in motor neuron apoptosis: implications for amyotrophic lateral sclerosis. *Journal of neurochemistry* **89**, 464–73.

- Pérez-Martínez, F.C., Guerra, J., Posadas, I. & Ceña, V. (2011). Barriers to non-viral vector-mediated gene delivery in the nervous system. *Pharmaceutical Research* **28**, 1843–1858.
- Perlson, E., Jeong, G.-B., Ross, J.L., Dixit, R., Wallace, K.E., Kalb, R.G. & Holzbaur, E.L.F. (2009). A switch in retrograde signaling from survival to stress in rapid-onset neurodegeneration. *The Journal of neuroscience : the official journal of the Society for Neuroscience* **29**, 9903–17.
- Perrin, S. (2014). Preclinical research: Make mouse studies work. *Nature* **507**, 423–425.
- Peviani, M., Caron, I., Pizzasegola, C., Gensano, F., Tortarolo, M. & Bendotti, C. (2010). Unraveling the complexity of amyotrophic lateral sclerosis: recent advances from the transgenic mutant SOD1 mice. *CNS & neurological disorders drug targets* **9**, 491–503.
- Plaitakis, A. & Caroscio, J.T. (1987). Abnormal glutamate metabolism in amyotrophic lateral sclerosis. *Annals of neurology* **22**, 575–9.
- Plank, C., Mechtler, K. & Jr, F.S. (1996). Activation of the complement system by synthetic DNA complexes: a potential barrier for intravenous gene delivery. *Human Gene* **1446**, 1437–1446.
- Pullen, A.H. & Athanasiou, D. (2009). Increase in presynaptic territory of C-terminals on lumbar motoneurons of G93A SOD1 mice during disease progression. *European Journal of Neuroscience* **29**, 551–561.
- Rabizadeh, S., Oh, J., Zhong, L.T., Yang, J., Bitler, C.M., Butcher, L.L. & Bredesen, D.E. (1993). Induction of apoptosis by the low-affinity NGF receptor. *Science (New York, N.Y.)* **261**, 345–8.
- Ralph, G.S., Radcliffe, P.A., Day, D.M., Carthy, J.M., Leroux, M.A., Lee, D.C.P., Wong, L.-F., Bilsland, L.G., Greensmith, L., Kingsman, S.M., Mitrophanous, K.A., Mazarakis, N.D. & Azzouz, M. (2005). Silencing mutant SOD1 using RNAi protects against neurodegeneration and extends survival in an ALS model. *Nature medicine* **11**, 429–33.
- Raoul, C., Abbas-Terki, T., Bensadoun, J.-C., Guillot, S., Haase, G., Szulc, J., Henderson, C.E. & Aebischer, P. (2005). Lentiviral-mediated silencing of SOD1 through RNA interference retards disease onset and progression in a mouse model of ALS. *Nature medicine* **11**, 423–8.
- Ravits, J.M. & La Spada, A.R. (2009). ALS motor phenotype heterogeneity, focality, and spread: deconstructing motor neuron degeneration. *Neurology* **73**, 805–811.
- Reaume, A.G., Elliott, J.L., Hoffman, E.K., Kowall, N.W., Ferrante, R.J., Siwek, D.F., Wilcox, H.M., Flood, D.G., Beal, M.F., Brown, R.H., Scott, R.W. & Snider, W.D. (1996). Motor neurons in Cu/Zn superoxide dismutase-deficient mice develop normally but exhibit enhanced cell death after axonal injury. *Nature genetics* **13**, 43–47.
- Rende, M., Giambanco, I., Buratta, M. & Tonali, P. (1995). Axotomy induces a different

modulation of both low-affinity nerve growth factor receptor and choline acetyltransferase between adult rat spinal and brainstem motoneurons. *The Journal of comparative neurology* **363**, 249–63.

- Renton, A.E.E., Majounie, E., Waite, A., Simón-Sánchez, J., Rollinson, S., Gibbs, J.R.R., Schymick, J.C.C., Laaksovirta, H., van Swieten, J.C., Myllykangas, L., Kalimo, H., Paetau, A., Abramzon, Y., Remes, A.M.M., Kaganovich, A., Scholz, S.W.W., Duckworth, J., Ding, J., Harmer, D.W.W., Hernandez, D.G.G., Johnson, J.O.O., Mok, K., Ryten, M., Trabzuni, D., Guerreiro, R.J.J., Orrell, R.W.W., Neal, J., Murray, A., Pearson, J., Jansen, I.E.E., Sondervan, D., Seelaar, H., Blake, D., Young, K., Halliwell, N., Callister, J.B.B., Toulson, G., Richardson, A., Gerhard, A., Snowden, J., Mann, D., Neary, D., Nalls, M.A. a, Peuralinna, T., Jansson, L., Isoviita, V.-M., Kaivorinne, A.-L., Hölttä-Vuori, M., Ikonen, E., Sulkava, R., Benatar, M., Wu, J., Chiò, A., Restagno, G., Borghero, G., Sabatelli, M., Heckerman, D., Rogaeva, E., Zinman, L., Rothstein, J.D.D., Sendtner, M., Drepper, C., Eichler, E.E.E., Alkan, C., Abdullaev, Z., Pack, S.D.D., Dutra, A., Pak, E., Hardy, J., Singleton, A., Williams, N.M.M., Heutink, P., Pickering-Brown, S., Morris, H.R.R., Tienari, P.J.J., Traynor, B.J.J. & van Swieten, J.C. (2011). A Hexanucleotide Repeat Expansion in C9ORF72 Is the Cause of Chromosome 9p21-Linked ALS-FTD. *Neuron* **72**, 257–268.
- Rezaie, T., Child, A., Hitchings, R., Brice, G., Miller, L., Coca-Prados, M., Héon, E., Krupin, T., Ritch, R., Kreutzer, D., Crick, R.P. & Sarfarazi, M. (2002). Adult-onset primary open-angle glaucoma caused by mutations in optineurin. *Science (New York, N.Y.)* **295**, 1077–1079.
- Robberecht, W. & Philips, T. (2013). The changing scene of amyotrophic lateral sclerosis. *Nature reviews. Neuroscience* **14**, 248–64.
- Rodriguez-Tebar, A., Dechant, G. & Barde, Y.A. (1990). Binding of brain-derived neurotrophic factor to the nerve growth factor receptor. *Neuron* **4**, 487–492.
- Rogers, M. & Rush, R. (2012). Non-viral gene therapy for neurological diseases, with an emphasis on targeted gene delivery. *Journal of Controlled Release* **157**, 183–189.
- Rogers, M.-L., Atmosukarto, I., Berhanu, D.A., Matusica, D., Macardle, P. & Rush, R.A. (2006). Functional monoclonal antibodies to p75 neurotrophin receptor raised in knockout mice. *Journal of neuroscience methods* **158**, 109–20.
- Rogers, M.-L., Smith, K.S., Matusica, D., Fenech, M., Hoffman, L., Rush, R. a & Voelcker, N.H. (2014). Non-viral gene therapy that targets motor neurons in vivo. *Frontiers in Molecular Neuroscience* **7**, 1–12.
- Rooney, J., Byrne, S., Heverin, M., Tobin, K., Dick, A., Donaghy, C. & Hardiman, O. (2014). A multidisciplinary clinic approach improves survival in ALS: a comparative study of ALS in Ireland and Northern Ireland. *Journal of Neurology, Neurosurgery & Psychiatry* 1–6.

- Rosen, D.R., Siddique, T., Patterson, D., Figlewicz, D.A., Sapp, P., Hentati, A., Donaldson, D., Goto, J., O'Regan, J.P. & Deng, H.X. (1993). Mutations in Cu/Zn superoxide dismutase gene are associated with familial amyotrophic lateral sclerosis. *Nature* **362**, 59–62.
- Rothstein, J.D., Tsai, G., Kuncl, R.W., Clawson, L., Cornblath, D.R., Drachman, D.B., Pestronk, a, Stauch, B.L. & Coyle, J.T. (1990). Abnormal excitatory amino acid metabolism in amyotrophic lateral sclerosis. *Annals of neurology* **28**, 18–25.
- Roux, P.P. & Barker, P.A. (2002). Neurotrophin signaling through the p75 neurotrophin receptor. *Progress in Neurobiology* **67**, 203–233.
- Roux, P.P., Bhakar, A.L., Kennedy, T.E. & Barker, P.A. (2001). The p75 neurotrophin receptor activates Akt (protein kinase B) through a phosphatidylinositol 3-kinase-dependent pathway. *The Journal of biological chemistry* **276**, 23097–104.
- Rutherford, A.C., Traer, C., Wassmer, T., Pattni, K., Bujny, M. V, Carlton, J.G., Stenmark, H. & Cullen, P.J. (2006). The mammalian phosphatidylinositol 3-phosphate 5-kinase (PIKfyve) regulates endosome-to-TGN retrograde transport. *Journal of cell science* **119**, 3944–3957.
- Rutherford, N.J., Zhang, Y.-J., Baker, M., Gass, J.M., Finch, N.A., Xu, Y.-F., Stewart, H., Kelley, B.J., Kuntz, K., Crook, R.J.P., Sreedharan, J., Vance, C., Sorenson, E., Lippa, C., Bigio, E.H., Geschwind, D.H., Knopman, D.S., Mitsumoto, H., Petersen, R.C., Cashman, N.R., Hutton, M., Shaw, C.E., Boylan, K.B., Boeve, B., Graff-Radford, N.R., Wszolek, Z.K., Caselli, R.J., Dickson, D.W., Mackenzie, I.R., Petrucelli, L. & Rademakers, R. (2008). Novel mutations in TARDBP (TDP-43) in patients with familial amyotrophic lateral sclerosis. *PLoS genetics* **4**, e1000193.
- Rydén, M. & Ibáñez, C.F. (1996). Binding of neurotrophin-3 to p75LNGFR, TrkA, and TrkB mediated by a single functional epitope distinct from that recognized by TrkC. *Journal of Biological Chemistry* **271**, 5623–5627.
- Saito, M., Tomonaga, M. & Narabayashi, H. (1978). Histochemical study of the muscle spindles in parkinsonism, motor neuron disease and myasthenia. An examination of the pathological fusimotor endings by the acetylcholinesterase technic. *Journal of neurology* **219**, 261–71.
- Salehi, A.H., Roux, P.P., Kubu, C.J., Zeindler, C., Bhakar, A., Tannis, L.L., Verdi, J.M. & Barker, P.A. (2000). NRAGE, a novel MAGE protein, interacts with the p75 neurotrophin receptor and facilitates nerve growth factor-dependent apoptosis. *Neuron* **27**, 279–88.
- Sasabe, J., Chiba, T., Yamada, M., Okamoto, K., Nishimoto, I., Matsuoka, M. & Aiso, S. (2007). D-serine is a key determinant of glutamate toxicity in amyotrophic lateral sclerosis. *The EMBO journal* **26**, 4149–59.
- Saunders, N.R., Joakim Ek, C. & Dziegielewska, K.M. (2009). The neonatal blood-brain

- barrier is functionally effective, and immaturity does not explain differential targeting of AAV9. *Nature biotechnology* **27**, 804–805.
- Saxena, S., Howe, C.L., Cosgaya, J.M., Hu, M., Weis, J. & Krüttgen, A. (2004). Differences in the surface binding and endocytosis of neurotrophins by p75NTR. *Molecular and cellular neurosciences* **26**, 292–307.
- von Schack, D., Casademunt, E., Schweigreiter, R., Meyer, M., Bibel, M. & Dechant, G. (2001). Complete ablation of the neurotrophin receptor p75NTR causes defects both in the nervous and the vascular system. *Nature neuroscience* **4**, 977–8.
- Scherer, F., Anton, M., Schillinger, U., Henke, J., Bergemann, C., Kruger, A., Gansbacher, B. & Plank, C. (2002). Magnetofection: enhancing and targeting gene delivery by magnetic force in vitro and in vivo. *Gene therapy* **9**, 102–109.
- Schiavo, G., Matteoli, M. & Montecucco, C. (2000). Neurotoxins affecting neuroexocytosis. *Physiological reviews* **80**, 717–766.
- Schneider, R. & Schweiger, M. (1991). A novel modular mosaic of cell adhesion motifs in the extracellular domains of the neurogenic trk and trkB tyrosine kinase receptors. *Oncogene* **6**, 1807–1811.
- Schuster, L., Seifert, O., Vollmer, S., Kontermann, R.E., Schlosshauer, B. & Hartmann, H. (2015). Immunoliposomes for Targeted Delivery of an Antifibrotic Drug. *Molecular Pharmaceutics*.
- Schweigreiter, R. (2006). The dual nature of neurotrophins. *BioEssays* **28**, 583–594.
- Scott, S., Kranz, J.E., Cole, J., Lincecum, J.M., Thompson, K., Kelly, N., Bostrom, A., Theodoss, J., Al-Nakhala, B.M., Vieira, F.G., Ramasubbu, J. & Heywood, J.A. (2008). Design, power, and interpretation of studies in the standard murine model of ALS. *Amyotrophic lateral sclerosis : official publication of the World Federation of Neurology Research Group on Motor Neuron Diseases* **9**, 4–15.
- Sebert, M.E. & Shooter, E.M. (1993). Expression of mRNA for neurotrophic factors and their receptors in the rat dorsal root ganglion and sciatic nerve following nerve injury. *Journal of Neuroscience Research* **36**, 357–367.
- Secret, E., Smith, K., Dubljevic, V., Moore, E., Macardle, P., Delalat, B., Rogers, M.L., Johns, T.G., Durand, J.O., Cunin, F. & Voelcker, N.H. (2013). Antibody-Functionalized Porous Silicon Nanoparticles for Vectorization of Hydrophobic Drugs. *Advanced Healthcare Materials* **2**, 718–727.
- Sedel, F., Béchade, C. & Triller, A. (1999). Nerve growth factor (NGF) induces motoneuron apoptosis in rat embryonic spinal cord in vitro. *The European journal of neuroscience* **11**, 3904–12.
- Seeburger, J.L., Tarras, S., Natter, H. & Springer, J.E. (1993). Spinal cord motoneurons express p75NGFR and p145trkB mRNA in amyotrophic lateral sclerosis. *Brain research*

621, 111–5.

- Seiffers, R., Zhang, J., Matthews, J.C., Chen, A., Tamrazian, E., Babaniyi, O., Selig, M., Hynynen, M., Woolf, C.J. & Brown, R.H. (2014). ATF3 expression improves motor function in the ALS mouse model by promoting motor neuron survival and retaining muscle innervation. *Proceedings of the National Academy of Sciences of the United States of America* **111**, 1622–7.
- Shan, X., Chiang, P.-M., Price, D.L. & Wong, P.C. (2010). Altered distributions of Gemini of coiled bodies and mitochondria in motor neurons of TDP-43 transgenic mice. *Proceedings of the National Academy of Sciences of the United States of America* **107**, 16325–30.
- Sharma, V.K., Thomas, M. & Klibanov, A.M. (2005). Mechanistic studies on aggregation of polyethylenimine-DNA complexes and its prevention. *Biotechnology and bioengineering* **90**, 614–20.
- Shepherd, S.R., Chataway, T., Schultz, D.W., Rush, R.A. & Rogers, M.-L. (2014). The extracellular domain of neurotrophin receptor p75 as a candidate biomarker for amyotrophic lateral sclerosis. *PloS one* **9**, e87398.
- Shi, C., Cao, H., He, W., Gao, F., Liu, Y. & Yin, L. (2015). Novel drug delivery liposomes targeted with a fully human anti-VEGF165 monoclonal antibody show superior antitumor efficacy in vivo. *Biomedicine & Pharmacotherapy* **73**, 48–57.
- Shim, M.S. & Kwon, Y.J. (2009). Controlled cytoplasmic and nuclear localization of plasmid DNA and siRNA by differentially tailored polyethylenimine. *Journal of controlled release : official journal of the Controlled Release Society* **133**, 206–13.
- Shneider, N. a, Brown, M.N., Smith, C.A., Pickel, J. & Alvarez, F.J. (2009). Gamma motor neurons express distinct genetic markers at birth and require muscle spindle-derived GDNF for postnatal survival. *Neural development* **4**, 42.
- Skaper, S.D. (2008). The biology of neurotrophins, signalling pathways, and functional peptide mimetics of neurotrophins and their receptors. *CNS & neurological disorders drug targets* **7**, 46–62.
- Skaper, S.D. (2012). Neurotrophic Factors. In *Methods in Molecular Biology*, Methods in Molecular Biology: 1–12. Skaper, S.D. (Ed). . Totowa, NJ: Humana Press.
- Skibinski, G., Parkinson, N.J., Brown, J.M., Chakrabarti, L., Lloyd, S.L., Hummerich, H., Nielsen, J.E., Hodges, J.R., Spillantini, M.G., Thusgaard, T., Brandner, S., Brun, A., Rossor, M.N., Gade, A., Johannsen, P., Sørensen, S.A., Gydesen, S., Fisher, E.M.C. & Collinge, J. (2005). Mutations in the endosomal ESCRTIII-complex subunit CHMP2B in frontotemporal dementia. *Nature genetics* **37**, 806–8.
- Smith, C., Farrah, T. & Goodwin, R. (1994). The TNF receptor superfamily of cellular and viral proteins: activation, costimulation, and death. *Cell* **76**, 959–962.

- Snow, R., Turnbull, J., da Silva, S., Jiang, F. & Tarnopolsky, M. (2003). Creatine supplementation and riluzole treatment provide similar beneficial effects in copper, zinc superoxide dismutase (G93A) transgenic mice. *Neuroscience* **119**, 661–667.
- Snyder, S.L. & Sobocinski, P.Z. (1975). An improved 2,4,6-trinitrobenzenesulfonic acid method for the determination of amines. *Analytical biochemistry* **64**, 284–288.
- Sobreviela, T., Clary, D.O., Reichardt, L.F., Brandabur, M.M., Kordower, J.H. & Mufson, E.J. (1994). TrkA-immunoreactive profiles in the central nervous system: Colocalization with neurons containing p75 nerve growth factor receptor, choline acetyltransferase, and serotonin. *Journal of Comparative Neurology* **350**, 587–611.
- Soilu-Hänninen, M., Ekert, P., Bucci, T., Syroid, D., Bartlett, P.F. & Kilpatrick, T.J. (1999). Nerve growth factor signaling through p75 induces apoptosis in Schwann cells via a Bcl-2-independent pathway. *The Journal of neuroscience : the official journal of the Society for Neuroscience* **19**, 4828–38.
- Soo, K.Y., Atkin, J.D., Farg, M., Walker, A.K., Horne, M.K. & Nagley, P. (2012). Bim links ER stress and apoptosis in cells expressing mutant SOD1 associated with amyotrophic lateral sclerosis. *PloS one* **7**, e35413.
- Soppet, D., Escandon, E., Maragos, J., Middlemas, D.S., Reid, S.W., Blair, J., Burton, L.E., Stanton, B.R., Kaplan, D.R., Hunter, T., Nikolics, K. & Parada, L.F. (1991). The neurotrophic factors brain-derived neurotrophic factor and neurotrophin-3 are ligands for the trkB tyrosine kinase receptor. *Cell* **65**, 895–903.
- Spataro, R., Lo Re, M., Piccoli, T., Piccoli, F. & La Bella, V. (2010). Causes and place of death in Italian patients with amyotrophic lateral sclerosis. *Acta neurologica Scandinavica* **122**, 217–23.
- Spencer, P.S., Nunn, P.B., Hugon, J., Ludolph, a. & Roy, D.N. (1986). Motorneurone disease on Guam: Possible role of a food neurotoxin. *Lancet* **1**, 965.
- Squinto, S.P., Stitt, T.N., Aldrich, T.H., Davis, S., Bianco, S.M., Radziejewski, C., Glass, D.J., Masiakowski, P., Furth, M.E. & Valenzuela, D.M. (1991). trkB encodes a functional receptor for brain-derived neurotrophic factor and neurotrophin-3 but not nerve growth factor. *Cell* **65**, 885–93.
- Sreedharan, J., Blair, I.P., Tripathi, V.B., Hu, X., Vance, C., Rogelj, B., Ackerley, S., Durnall, J.C., Williams, K.L., Buratti, E., Baralle, F., de Bellerocche, J., Mitchell, J.D., Leigh, P.N., Al-Chalabi, A., Miller, C.C., Nicholson, G. & Shaw, C.E. (2008). TDP-43 mutations in familial and sporadic amyotrophic lateral sclerosis. *Science (New York, N.Y.)* **319**, 1668–72.
- Stephens, B., Guilloff, R.J., Navarrete, R., Newman, P., Nikhar, N. & Lewis, P. (2006). Widespread loss of neuronal populations in the spinal ventral horn in sporadic motor neuron disease. A morphometric study. *Journal of the neurological sciences* **244**, 41–58.

- Stephens, R.M. (1997). Autophosphorylation of Activation Loop Tyrosines Regulates Signaling by the TRK Nerve Growth Factor Receptor. *Journal of Biological Chemistry* **272**, 10957–10967.
- Stifani, N. (2014). Motor neurons and the generation of spinal motor neuron diversity. *Frontiers in Cellular Neuroscience* **8**, 293.
- Stockel, K., Schwab, M. & Thoenen, H. (1975). Comparison between the retrograde axonal transport of nerve growth factor and tetanus toxin in motor, sensory and adrenergic neurons. *Brain research* **99**, 1–16.
- Sturtz, L. a, Diekert, K., Jensen, L.T., Lill, R. & Culotta, V.C. (2001). A fraction of yeast Cu,Zn-superoxide dismutase and its metallochaperone, CCS, localize to the intermembrane space of mitochondria. A physiological role for SOD1 in guarding against mitochondrial oxidative damage. *The Journal of biological chemistry* **276**, 38084–9.
- Sun, W., Funakoshi, H. & Nakamura, T. (2002). Overexpression of HGF retards disease progression and prolongs life span in a transgenic mouse model of ALS. *The Journal of neuroscience : the official journal of the Society for Neuroscience* **22**, 6537–48.
- Suzie, H.P. & Davis, M.E. (2002). Development of a nonviral gene delivery vehicle for systemic application. *Bioconjugate Chemistry* **13**, 630–639.
- Swarup, V., Phaneuf, D., Dupré, N., Petri, S., Strong, M., Kriz, J. & Julien, J.-P. (2011). Deregulation of TDP-43 in amyotrophic lateral sclerosis triggers nuclear factor κB-mediated pathogenic pathways. *The Journal of experimental medicine* **208**, 2429–2447.
- Swash, M. & Fox, K.P. (1974). The pathology of the human muscle spindle: effect of denervation. *Journal of the neurological sciences* **22**, 1–24.
- Swash, M., Leader, M., Brown, A. & Swettenham, K.W. (1986). Focal loss of anterior horn cells in the cervical cord in motor neuron disease. *Brain* **109** (Pt 5, 939–952.
- Takahashi, M. (2001). The GDNF/RET signaling pathway and human diseases. *Cytokine & growth factor reviews* **12**, 361–73.
- Tateishi, T., Hokonohara, T., Yamasaki, R., Miura, S., Kikuchi, H., Iwaki, A., Tashiro, H., Furuya, H., Nagara, Y., Ohyagi, Y., Nukina, N., Iwaki, T., Fukumaki, Y. & Kira, J.I. (2010). Multiple system degeneration with basophilic inclusions in Japanese ALS patients with FUS mutation. *Acta Neuropathologica* **119**, 355–364.
- Terao, S., Sobue, G., Hashizume, Y., Mitsuma, T. & Takahashi, A. (1994). Disease-specific patterns of neuronal loss in the spinal ventral horn in amyotrophic lateral sclerosis, multiple system atrophy and X-linked recessive bulbospinal neuronopathy, with special reference to the loss of small neurons in the intermediate zone. *Journal of neurology* **241**, 196–203.
- Theiler, K. (1972). The house mouse. Development and normal stages from fertilization to 4

weeks of age. *Teratology* **9**, 168.

- Towne, C., Raoul, C., Schneider, B.L. & Aebischer, P. (2008). Systemic AAV6 delivery mediating RNA interference against SOD1: neuromuscular transduction does not alter disease progression in fALS mice. *Molecular therapy : the journal of the American Society of Gene Therapy* **16**, 1018–25.
- Towne, C., Setola, V., Schneider, B.L. & Aebischer, P. (2010). Neuroprotection by gene therapy targeting mutant SOD1 in individual pools of motor neurons does not translate into therapeutic benefit in fALS mice. *Molecular therapy : the journal of the American Society of Gene Therapy* **19**, 274–83.
- Trupp, M., Arenas, E., Fainzilber, M., Nilsson, A.S., Sieber, B.A., Grigoriou, M., Kilkenny, C., Salazar-Grueso, E., Pachnis, V. & Arumäe, U. (1996). Functional receptor for GDNF encoded by the c-ret proto-oncogene. *Nature* **381**, 785–789.
- Trusolino, L. & Comoglio, P.M. (2002). Scatter-factor and semaphorin receptors: cell signalling for invasive growth. *Nature reviews. Cancer* **2**, 289–300.
- Tsujino, H., Kondo, E., Fukuoka, T., Dai, Y., Tokunaga, a, Miki, K., Yonenobu, K., Ochi, T. & Noguchi, K. (2000). Activating transcription factor 3 (ATF3) induction by axotomy in sensory and motoneurons: A novel neuronal marker of nerve injury. *Molecular and cellular neurosciences* **15**, 170–82.
- Tuffereau, C., Bénéjean, J., Blondel, D., Kieffer, B. & Flamand, a. (1998). Low-affinity nerve-growth factor receptor (P75NTR) can serve as a receptor for rabies virus. *The EMBO journal* **17**, 7250–9.
- Turner, B.J., Murray, S.S., Piccenna, L.G., Lopes, E.C., Kilpatrick, T.J. & Cheema, S.S. (2004). Effect of p75 neurotrophin receptor antagonist on disease progression in transgenic amyotrophic lateral sclerosis mice. *Journal of neuroscience research* **78**, 193–9.
- Turner, B.J., Parkinson, N.J., Davies, K.E. & Talbot, K. (2009). Survival motor neuron deficiency enhances progression in an amyotrophic lateral sclerosis mouse model. *Neurobiology of disease* **34**, 511–7.
- Turner, B.J. & Talbot, K. (2008). Transgenics, toxicity and therapeutics in rodent models of mutant SOD1-mediated familial ALS. *Progress in neurobiology* **85**, 94–134.
- Turner, M.R., Parton, M.J., Shaw, C.E., Leigh, P.N. & Al-Chalabi, A. (2003). Prolonged survival in motor neuron disease: a descriptive study of the King's database 1990-2002. *Journal of neurology, neurosurgery, and psychiatry* **74**, 995–997.
- Tyc, F. & Vrbová, G. (2007). Modification of motoneuron size after partial denervation in neonatal rats. *Archives italiennes de biologie* **145**, 337–44.
- Ultsch, M.H., Wiesmann, C., Simmons, L.C., Henrich, J., Yang, M., Reilly, D., Bass, S.H. & de Vos, a M. (1999). Crystal structures of the neurotrophin-binding domain of TrkA,

- TrkB and TrkC. *Journal of molecular biology* **290**, 149–59.
- Underwood, C.K., Reid, K., May, L.M., Bartlett, P.F. & Coulson, E.J. (2008). Palmitoylation of the C-terminal fragment of p75(NTR) regulates death signaling and is required for subsequent cleavage by gamma-secretase. *Molecular and cellular neurosciences* **37**, 346–58.
- Urano, F., Wang, X., Bertolotti, A., Zhang, Y., Chung, P., Harding, H.P. & Ron, D. (2000). Coupling of stress in the ER to activation of JNK protein kinases by transmembrane protein kinase IRE1. *Science (New York, N.Y.)* **287**, 664–666.
- Urushitani, M., Kurisu, J., Tsukita, K. & Takahashi, R. (2002). Proteasomal inhibition by misfolded mutant superoxide dismutase 1 induces selective motor neuron death in familial amyotrophic lateral sclerosis. *Journal of Neurochemistry* **83**, 1030–1042.
- Urushitani, M., Tomoki, Nakamizo, Inoue, R., Sawada, H., Kihara, T., Honda, K., Akaike, A. & Shimohama, S. (2001). N-methyl-D-aspartate receptor-mediated mitochondrial Ca²⁺ overload in acute excitotoxic motor neuron death: A mechanism distinct from chronic neurotoxicity after Ca²⁺ influx. *Journal of Neuroscience Research* **63**, 377–387.
- Vance, C., Rogelj, B. & Hortobágyi, T. (2009). Mutations in FUS, an RNA processing protein, cause familial amyotrophic lateral sclerosis type 6. *Science* **323**, 1208–1211.
- Vande Velde, C., Miller, T.M., Cashman, N.R. & Cleveland, D.W. (2008). Selective association of misfolded ALS-linked mutant SOD1 with the cytoplasmic face of mitochondria. *Proceedings of the National Academy of Sciences of the United States of America* **105**, 4022–7.
- Vinsant, S., Mansfield, C., Jimenez-Moreno, R., Del Gaizo Moore, V., Yoshikawa, M., Hampton, T.G., Prevette, D., Caress, J., Oppenheim, R.W. & Milligan, C. (2013). Characterization of early pathogenesis in the SOD1(G93A) mouse model of ALS: part II, results and discussion. *Brain and behavior* **3**, 431–57.
- Vitetta, E.S., Krolick, K.A., Miyama-Inaba, M., Cushley, W. & Uhr, J.W. (1983). Immunotoxins: a new approach to cancer therapy. *Science (New York, N.Y.)* **219**, 644–50.
- Vlug, A.S., Teuling, E., Haasdijk, E.D., French, P., Hoogenraad, C.C. & Jaarsma, D. (2005). ATF3 expression precedes death of spinal motoneurons in amyotrophic lateral sclerosis-SOD1 transgenic mice and correlates with c-Jun phosphorylation, CHOP expression, somato-dendritic ubiquitination and Golgi fragmentation. *The European journal of neuroscience* **22**, 1881–94.
- De Vos, K.J., Chapman, A.L., Tennant, M.E., Manser, C., Tudor, E.L., Lau, K.-F., Brownlees, J., Ackerley, S., Shaw, P.J., McLoughlin, D.M., Shaw, C.E., Leigh, P.N., Miller, C.C.J. & Grierson, A.J. (2007). Familial amyotrophic lateral sclerosis-linked SOD1 mutants perturb fast axonal transport to reduce axonal mitochondria content. *Human molecular genetics* **16**, 2720–8.

- Waibel, S., Reuter, A., Malessa, S., Blaugrund, E. & Ludolph, A.C. (2004). Rasagiline alone and in combination with riluzole prolongs survival in an ALS mouse model. *Journal of neurology* **251**, 1080–4.
- Wang, L.-J., Lu, Y.-Y., Muramatsu, S., Ikeguchi, K., Fujimoto, K., Okada, T., Mizukami, H., Matsushita, T., Hanazono, Y., Kume, A., Nagatsu, T., Ozawa, K. & Nakano, I. (2002). Neuroprotective effects of glial cell line-derived neurotrophic factor mediated by an adeno-associated virus vector in a transgenic animal model of amyotrophic lateral sclerosis. *The Journal of neuroscience : the official journal of the Society for Neuroscience* **22**, 6920–8.
- Wang, W., Li, L., Lin, W.-L., Dickson, D.W., Petrucelli, L., Zhang, T. & Wang, X. (2013). The ALS disease-associated mutant TDP-43 impairs mitochondrial dynamics and function in motor neurons. *Human molecular genetics* **22**, 4706–19.
- Ward, C.M., Read, M.L. & Seymour, L.W. (2001). Systemic circulation of poly(L-lysine)/DNA vectors is influenced by polycation molecular weight and type of DNA: Differential circulation in mice and rats and the implications for human gene therapy. *Blood* **97**, 2221–2229.
- Watanabe, M., Dykes-Hoberg, M., Culotta, V.C., Price, D.L., Wong, P.C. & Rothstein, J.D. (2001). Histological evidence of protein aggregation in mutant SOD1 transgenic mice and in amyotrophic lateral sclerosis neural tissues. *Neurobiology of disease* **8**, 933–41.
- Waterman-storer, C.M., Karki, S. & Holzbaur, E.L.F. (1995). The p150Glued component of the dynactin complex binds to both microtubules and the actin-related protein centractin (Arp-1) **92**, 1634–1638.
- Watts, G.D.J., Wymer, J., Kovach, M.J., Mehta, S.G., Mumm, S., Darvish, D., Pestronk, A., Whyte, M.P. & Kimonis, V.E. (2004). Inclusion body myopathy associated with Paget disease of bone and frontotemporal dementia is caused by mutant valosin-containing protein. *Nature genetics* **36**, 377–81.
- Wegorzewska, I., Bell, S., Cairns, N.J., Miller, T.M. & Baloh, R.H. (2009). TDP-43 mutant transgenic mice develop features of ALS and frontotemporal lobar degeneration. *Proceedings of the National Academy of Sciences of the United States of America* **106**, 18809–14.
- Weinmann, O., Schnell, L., Ghosh, A., Montani, L., Wiessner, C., Wannier, T., Rouiller, E., Mir, A. & Schwab, M.E. (2006). Intrathecally infused antibodies against Nogo-A penetrate the CNS and downregulate the endogenous neurite growth inhibitor Nogo-A. *Molecular and Cellular Neuroscience* **32**, 161–173.
- Weisiger, R.A. & Fridovich, I. (1973). Superoxide Dismutase : ORGANELLE Dismutase. *The Journal of biological chemistry* **248**, 3582–3592.
- Wells, D.J. (2004). Gene therapy progress and prospects: electroporation and other physical methods. *Gene therapy* **11**, 1363–9.

- van Welsem, M.E., Hogenhuis, J.A., Meininger, V., Metsaars, W.P., Hauw, J.-J. & Seilhean, D. (2002). The relationship between Bunina bodies, skein-like inclusions and neuronal loss in amyotrophic lateral sclerosis. *Acta neuropathologica* **103**, 583–9.
- Weskamp, G., Schlöndorff, J., Lum, L., Becherer, J.D., Kim, T.-W., Saftig, P., Hartmann, D., Murphy, G. & Blobel, C.P. (2004). Evidence for a critical role of the tumor necrosis factor alpha convertase (TACE) in ectodomain shedding of the p75 neurotrophin receptor (p75NTR). *The Journal of biological chemistry* **279**, 4241–9.
- Wiese, S., Herrmann, T., Drepper, C., Jablonka, S., Funk, N., Klausmeyer, A., Rogers, M.-L., Rush, R. & Sendtner, M. (2010). Isolation and enrichment of embryonic mouse motoneurons from the lumbar spinal cord of individual mouse embryos. *Nature Protocols* **5**, 31–38.
- Wiese, S., Metzger, F., Holtmann, B. & Sendtner, M. (1999). The role of p75NTR in modulating neurotrophin survival effects in developing motoneurons. *The European journal of neuroscience* **11**, 1668–76.
- Williams, K.L., Warraich, S.T., Yang, S., Solski, J.A., Fernando, R., Rouleau, G.A., Nicholson, G.A. & Blair, I.P. (2012). UBQLN2/ubiquilin 2 mutation and pathology in familial amyotrophic lateral sclerosis. *Neurobiology of Aging* **33**, 2527.e3–10.
- Witts, E.C., Zagoraiou, L. & Miles, G.B. (2014). Anatomy and function of cholinergic C bouton inputs to motor neurons. *Journal of Anatomy*.
- Won, Y.-W., Lim, K.S. & Kim, Y.-H. (2011). Intracellular organelle-targeted non-viral gene delivery systems. *Journal of controlled release* **152**, 99–109.
- Wong, P.C., Pardo, C.A., Borchelt, D.R., Lee, M.K., Copeland, N.G., Jenkins, N. a, Sisodia, S.S., Cleveland, D.W. & Price, D.L. (1995). An adverse property of a familial ALS-linked SOD1 mutation causes motor neuron disease characterized by vacuolar degeneration of mitochondria. *Neuron* **14**, 1105–1116.
- Woods, N.-B., Bottero, V., Schmidt, M., von Kalle, C. & Verma, I.M. (2006). Gene therapy: therapeutic gene causing lymphoma. *Nature* **440**, 1123.
- Wooley, C.M., Sher, R.B., Kale, A., Frankel, W.N., Cox, G.A. & Seburn, K.L. (2005). Gait analysis detects early changes in transgenic SOD1(G93A) mice. *Muscle & nerve* **32**, 43–50.
- Wright, D.E. & Snider, W.D. (1995). Neurotrophin receptor mRNA expression defines distinct populations of neurons in rat dorsal root ganglia. *The Journal of comparative neurology* **351**, 329–38.
- Wu, C., Fallini, C., Ticozzi, N. & Keagle, P. (2012). Mutations in the profilin 1 gene cause familial amyotrophic lateral sclerosis. *Nature* **488**, 499–503.
- Wu, G.Y. & Wu, C.H. (1987). Receptor-mediated in vitro gene transformation by a soluble DNA carrier system. *The Journal of biological chemistry* **262**, 4429–32.

- Wu, T.-L. & Ertl, H.C.J. (2009). Immune barriers to successful gene therapy. *Trends in molecular medicine* **15**, 32–9.
- Xia, X., Zhou, H., Huang, Y. & Xu, Z. (2006). Allele-specific RNAi selectively silences mutant SOD1 and achieves significant therapeutic benefit in vivo. *Neurobiology of disease* **23**, 578–86.
- Xu, Y.-F., Gendron, T.F., Zhang, Y.-J., Lin, W.-L., D'Alton, S., Sheng, H., Casey, M.C., Tong, J., Knight, J., Yu, X., Rademakers, R., Boylan, K., Hutton, M., McGowan, E., Dickson, D.W., Lewis, J. & Petrucelli, L. (2010). Wild-type human TDP-43 expression causes TDP-43 phosphorylation, mitochondrial aggregation, motor deficits, and early mortality in transgenic mice. *The Journal of neuroscience : the official journal of the Society for Neuroscience* **30**, 10851–9.
- Yan, H. & Chao, M. V. (1991). Disruption of cysteine-rich repeats of the p75 nerve growth factor receptor leads to loss of ligand binding. *The Journal of biological chemistry* **266**, 12099–104.
- Yan, Q. & Johnson, E.M. (1987). A quantitative study of the developmental expression of nerve growth factor (NGF) receptor in rats. *Developmental biology* **121**, 139–148.
- Yan, Q. & Johnson, E.M. (1988). An immunohistochemical study of the nerve growth factor receptor in developing rats. *The Journal of Neuroscience* **8**, 3481–98.
- Yeo, T.T., Chua-Couzens, J., Butcher, L.L., Bredesen, D.E., Cooper, J.D., Valletta, J.S., Mobley, W.C. & Longo, F.M. (1997). Absence of p75NTR causes increased basal forebrain cholinergic neuron size, choline acetyltransferase activity, and target innervation. *The Journal of neuroscience : the official journal of the Society for Neuroscience* **17**, 7594–7605.
- Yokota, T., Milenic, D.E., Whitlow, M. & Schlom, J. (1992). Rapid tumor penetration of a single-chain Fv and comparison with other immunoglobulin forms. *Cancer Research* **52**, 3402–3408.
- Yoon, S.O., Casaccia-Bonnel, P., Carter, B. & Chao, M. V. (1998). Competitive signaling between TrkA and p75 nerve growth factor receptors determines cell survival. *The Journal of neuroscience : the official journal of the Society for Neuroscience* **18**, 3273–81.
- Yu, H., Yang, M., Wang, Y., Xiao, R. & Zhou, X.F. (2012). P75NTR is mainly responsible for A β toxicity but not for its internalization: A primary study. *Neurological Sciences* **33**, 1043–1050.
- Zagoraiou, L., Akay, T., Martin, J.F., Brownstone, R.M., Jessell, T.M. & Miles, G.B. (2009). A cluster of cholinergic premotor interneurons modulates mouse locomotor activity. *Neuron* **64**, 645–62.
- Zeira, E., Manevitch, A., Khatchaturians, A., Pappo, O., Hyam, E., Darash-Yahana, M.,

- Tavor, E., Honigman, A., Lewis, A. & Galun, E. (2003). Femtosecond infrared laser - An efficient and safe in vivo gene delivery system for prolonged expression. *Molecular Therapy* **8**, 342–350.
- Zhang, G., Budker, V., Williams, P., Subbotin, V. & Wolff, J.A. (2001). Efficient expression of naked dna delivered intraarterially to limb muscles of nonhuman primates. *Human gene therapy* **12**, 427–38.
- Zhang, G., Gao, X., Song, Y.K., Vollmer, R., Stolz, D.B., Gasiorowski, J.Z., Dean, D. & Liu, D. (2004). Hydroporation as the mechanism of hydrodynamic delivery. *Gene therapy* **11**, 675–82.
- Zhang, K.Y., Yang, S., Warraich, S.T. & Blair, I.P. (2014). Ubiquitin 2: a component of the ubiquitin-proteasome system with an emerging role in neurodegeneration. *The international journal of biochemistry & cell biology* **50**, 123–6.
- Zhang, Y. & Pardridge, W.M. (2009). Near complete rescue of experimental Parkinson's disease with intravenous, non-viral GDNF gene therapy. *Pharmaceutical research* **26**, 1059–63.
- Zheng, C., Juhls, C., Oswald, D., Sack, F., Westfehling, I., Wittig, B., Babiuk, L.A. & van Drunen Littel-van den Hurk, S. (2006). Effect of different nuclear localization sequences on the immune responses induced by a MIDGE vector encoding bovine herpesvirus-1 glycoprotein D. *Vaccine* **24**, 4625–9.
- Zufferey, R., Dull, T., Mandel, R.J., Bukovsky, A., Quiroz, D., Naldini, L. & Trono, D. (1998). Self-inactivating lentivirus vector for safe and efficient in vivo gene delivery. *Journal of virology* **72**, 9873–80.